The Dissertation Committee for Gookyoung Heo Certifies that this is the approved version of the following dissertation:

CONDENSED CHEMICAL MECHANISMS AND THEIR IMPACT ON RADICAL SOURCES AND SINKS IN HOUSTON

Committee:

David T. Allen, Supervisor

Elena McDonald-Buller, Co-Supervisor

Richard L. Corsi

Danny D. Reible

Gary T. Rochelle

CONDENSED CHEMICAL MECHANISMS AND THEIR IMPACT ON RADICAL SOURCES AND SINKS IN HOUSTON

by

Gookyoung Heo, B.S.; M.C.P.

Dissertation

Presented to the Faculty of the Graduate School of

The University of Texas at Austin

in Partial Fulfillment

of the Requirements

for the Degree of

Doctor of Philosophy

The University of Texas at Austin

August 2009

Dedication

To my family, friends, and teachers.

Acknowledgements

I am deeply grateful to my advisor, Dr. David T. Allen, for making this dissertation possible through his continuous support and guidance. I sincerely thank my co-supervisor, Dr. Elena McDonald-Buller, and other committee members, Dr. Richard Corsi, Dr. Danny Reible and Dr. Gary Rochelle, who provided me with insightful comments. Many thanks to Dr. Greg Yarwood, Dr. Gary Z. Whitten and Dr. William P. L. Carter for their teachings on the development and evaluation of chemical mechanisms used in air quality models. I also thank the excellent staff and great colleagues at the Center for Energy and Environmental Resources.

I would like to acknowledge the warm support of Rev. Roslyn Hogan and other church members at the University Christian Church where I have learned a lot about beautiful ways of living. I also thank taxpayers who intentionally and unintentionally supported my Ph.D. studies. Lastly, I thank my father and mother, my wife and my first son for their support, love and cooperation.

CONDENSED CHEMICAL MECHANISMS AND THEIR IMPACT ON RADICAL SOURCES AND SINKS IN HOUSTON

Publication No._____

Gookyoung Heo, Ph.D.

The University of Texas at Austin, 2009

Supervisor: David T. Allen

Co-Supervisor: Elena McDonald-Buller

Free radicals play a critical role in the formation of tropospheric air pollution, but current condensed chemical mechanisms used in gridded photochemical models under-predict total radical concentrations. This dissertation evaluates three hypotheses regarding radical sources and sinks using environmental chamber data and ambient data from southeast Texas. The first hypothesis, that aromatics chemistry is under-represented as a radical source in condensed chemical mechanisms, was evaluated mainly by using environmental chamber simulations and in part by using ambient simulations. Results indicate that improved characterization of aromatics chemistry in condensed chemical mechanisms will lead to more rapid and extensive free radical formation. The second hypothesis, that alkene reactions are under-represented as a radical source in condensed chemical mechanisms, was also evaluated using chamber data and TexAQS-2000 data. Results indicate that the methods used in mechanism condensation lead to lower estimates of free radical production than detailed, compound specific models.

The third hypothesis, chlorine emissions and chemistry as a radical source, was also evaluated in a series of sensitivity analyses with various levels of molecular chlorine emissions. Results imply that incorporating chlorine chemistry in condensed chemical mechanisms is expected to lead to more accurate modeling of OH, HO_2 and O_3, particularly for the southeast Texas region where relatively large chlorine emissions occur from various anthropogenic sources of molecular chlorine. The relative magnitudes of these radical sources (aromatics, alkenes, and molecular chlorine) in southeast Texas were also compared using box modeling with TexAQS-2000 data. Results indicate that the relative importance of these three types of radical sources depends on the strengths of their corresponding emissions.

Table of Contents

List of Tables xi

List of Figures xiii

Chapter 1: Introduction 1

1.1. Radical Chemistry in the Atmosphere 1

1.2. Summary of Major Air Quality Study Campaigns in Texas Relevant to Radical Chemistry 4

1.3. Strategies and Structure of This Study 6

1.4. References 8

Chapter 2: Combining Environmental Chamber Simulation and Ambient Simulation for Studying Chemical Mechanisms 11

2.1. Introduction 11

2.2. Environmental Chamber Simulation for Mechanism Evaluation 12

2.3. Ambient Simulation for Mechanism Evaluation 20

2.4. Summary 28

2.5. References 29

Chapter 3: Aromatics Chemistry as a Sink and Source of Radicals 35

3.1. Introduction 35

3.2. Toluene Oxidation Mechanisms 37

3.3. Environmental Chamber Simulation for Toluene Mechanism Evaluation 42

3.4. Overall Performance of CB05-Base and CB05-UNClite in Chamber Simulations 48

3.5. Summary and Recommendations 64

3.6. Further Information Available 65

3.7. Acknowledgements 66

3.8. References 66

Chapter 4: Alkene Chemistry as a Source of Radicals 72

4.1. Introduction 72

4.2. Data and Methods 79

4.3. Results and Discussion 83
4.4. Summary 95
4.5. Acknowledgements 96
4.6. References 96

Chapter 5: Sources of Free Radicals: An intercomparison of aromatic, alkene, and molecular chlorine sources in southeast Texas 102
5.1. Introduction 102
5.2. Data and Methods 108
5.3. Simulation Results 111
5.4. Summary 124
5.5. References 125

Chapter 6: Summary and Recommendations 129
6.1. Key Findings 129
6.2. Recommendations 132
6.3. References 134

Appendix A: Further Information for Chapter 3 135
A1. Simulations with the Ua, Ub and Dinitro Mechanisms 135
A2. Implementation of the Five Versions of CB05: CB05-Base, CB05-Ua, CB05-Ub, CB05-UNClite and CB05-Dinitro 143
A3. Auxiliary Mechanisms Used in Environmental Chamber Simulations160
A4. Box Modeling Results with CB05-Base and CB05-UNClite 181

Appendix B: Further Information for Chapter 4 185
B1. Graphical Representation of Major Pathways Leading to Radical Formation in the Ozonolysis of 1-Alkenes 186
B2. Listings of Explicit Reactions of 18 Additional Alkenes Added to the Fixed Version of SAPRC-07 (SAPRC07B.RXN) 187
B3. Implementation of the Reaction of 1-Butene and O_3 for the Mechanisms Listed in Table 4-9 194
B4. Additional Information Regarding Box Model Simulations 197

Appendix C: Further Information for Chapter 5 199

Appendix C1. Modification of CB05 to Incorporate the Chlorine Mechanism of Tanaka et al. (2003a).....200

Appendix C2. Modification of SAPRC-07 to Incorporate Chlorine Chemistry 202

Bibliography 207

Vita 223

List of Tables

Table 1-1. Sources, sinks, and propagation reactions related to OH and HO_2 radicals (Ehhalt, 1999; Finlayson-Pitts and Pitts, 2000; Clemitshaw, 2003). 3

Table 2-1. An overview of environmental chambers at UNC, UCR and TVA used for mechanism evaluation. 14

Table 2-2. Measured species relevant to HOx with measurement techniques, time resolution and detection limits, and accuracies during TexAQS-2000. 23

Table 2-3. Hydrocarbons measured by the three GC systems and PTR-MS system during TexAQS-2000. 24

Table 2-4. A summary of TexAQS-2000 data used in selecting cases for testing the three hypotheses. 27

Table 3-1. Overview of two CB05 toluene mechanisms. 41

Table 3-2. Comparison of reactions involving the bicyclic peroxy radical (TO_2) between Base and UNClite[a] 42

Table 3-3. Four classes of toluene experiments and standards applied to classification of toluene experiments. 46

Table 3-4. 7 toluene experiments of the outdoor UNC gas-phase chamber in the Morpho dataset[a] 46

Table 3-5. 31 non-blacklight toluene experiments of UCR chambers in the SAPRC dataset[a] 47

Table 3-6. Summary of the overall performance and characteristics of CB05-Base and CB05-UNClite against the chamber experiments in simulating Max(O_3), Max($\Delta(O_3$-NO)), and NOx crossover times. 63

Table 3-7. Summary of the overall performance and characteristics of CB05-Base and CB05-UNClite against the chamber experiments in simulating cresol concentrations, radical sources and NOx sinks. 64

Table 4-1. Summary of concentrations of 18 alkenes measured at La Porte during the TexAQS-2000 study (Jobson et al., 2004; Kuster et al., 2004)[a]. 73

Table 4-2. Representation of alkenes in SAPRC-07 (Carter, 2009)[a]. 74

Table 4-3. Relative contributions of each alkene to OLE1 and OLE2 based on measurements during the TexAQS-2000 study and comparison with the composition used in constructing the fixed-version SAPRC-07. 76

Table 4-4. Rate constants towards OH and O_3 of alkenes, and OH yields of alkene-O_3 reactions at 298 K and 1 atm. 77

Table 4-5. List of alkene-NOx chamber experiments used in this study: 18 experiments for non-propene OLE1 and OLE2 alkenes and 24 chamber experiments for propene. 81

Table 4-6. Summary of Max(O_3) performance of the three versions of SAPRC-07 for the 18 chamber experiments in Table 4-5. 84

Table 4-7. Summary of Max(O_3) performance of the three versions of SAPRC-07 for 24 propene-NOx experiments of UCR's EPA chamber. 87

Table 4-8. Summary of Max(OH) and Max(HO_2) simulated by the three versions of SAPRC-07 for 24 propene-NOx experiments of UCR's EPA chamber 87

Table 4-9. List of reaction parameters varied in the mechanisms used in simulating 1-butene-NOx chamber experiments[a]. 88

Table 5-1. Reaction rates of organic compounds measured at the La Porte site (units of k: $cm^3molecule^{-1}sec^{-1}$)* 106

Table A-1. Five versions of CB05 mechanisms evaluated by chamber simulations. 137

Table A-2. Comparison of three toluene reactions between CB05-Base, CB05-Ua and CB05-Ub.[a] 137

Table A-3. Comparison of 10 toluene reactions between CB05-Base, CB05-UNClite, CB05-Dinitro. 138

Table A-4. Additional 16 reactions in CB05-UNClite and 4 reactions in CB05-Dinitro related to toluene oxidation. 139

Table A-5. Summary of the overall performance and characteristics of each CB05 mechanism against the 38 chamber experiments in simulating Max(O_3), Max(Δ(O_3-NO)), NOx crossover, cresol yield, radical sources and NOx sinks.[a] . 141

Table A-6. A summary of auxiliary mechanism reactions actually used for 31 toluene experiments in the SAPRC dataset.* 167

Table A-7. Reaction rate parameters in the auxiliary mechanism used for 12 low-NOx toluene experiments in the SAPRC dataset. 168

Table A-8. Reaction rate parameters in the auxiliary mechanism used for 11 mid-NOx toluene experiments in the SAPRC dataset. 169

Table A-9. Reaction rate parameters in the auxiliary mechanism used for 5 high-NOx and 3 low O_3/NOx toluene experiments in the SAPRC dataset. 170

Table A-10. Split factors and initial concentrations for the LaPorte2000 case ([VOC]/[NOx] = 10 ppmC/ppm at start). 182

Table B-1. Initial concentrations of hydrocarbons and inorganics used in box modeling[a] 197

Table B-2. Meteorological conditions used in box modeling[a] 198

List of Figures

Figure 1-1. Major photochemical reactions involving HOx radicals (Seinfeld and Pandis, 1998; Finlayson-Pitts and Pitts, 2000). 1

Figure 1-2. OH and HO_2 measurements on August 25, 2000 during TexAQS-2000**.**..... 5

Figure 3-1. Under-predictions of ozone formation and NOx depletion rates by CB-IV and CB05 against a low-NOx environmental chamber experiment, EPA210A: (a) O_3, (b) NO, (c) NO_2. 37

Figure 3-2. Toluene oxidation pathways leading to major products such as cresols and dicarbonyls. (Calvert et al., 2002; Atkinson and Arey, 2003; Andino et al., 1996; Suh et al., 2003 and 2006; Hu et al., 2007; Arey et al., 2009)..... 39

Figure 3-3. Comparison of maximum ozone simulated by CB05-UNClite with measurements: (a) low-NOx, (b) mid-NOx, (c) high-NOx, (d) low O_3/NOx. 50

Figure 3-4. Comparison of maximum $\Delta(O_3\text{-NO})$ simulated by CB05-UNClite with measurements..... 51

Figure 3-5. Comparison of NO, NO_2, toluene and O_3 simulated by CB05-UNClite against measurements: (a) EPA210A, (b) AU0183R, (c) EC340, (d) OTC299B. .. 52

Figure 3-6. Comparison of NOx crossover times simulated by CB05-UNClite against measurements for UCR experiments (a) and for UNC experiments (b)..... 54

Figure 3-7. Comparison of cresol concentrations simulated by CB05-UNClite against measurements of 6 experiments..... 56

Figure 3-8. Comparison of OH and HO_2 simulated by CB05-UNClite with measurements (a), and major pathways contributing to radical formation (b) for Experiment EPA210A. 59

Figure 3-9. Comparison of NOx and NOz species simulated by CB05-UNClite against measurements: (a) EPA210A, (b) EPA210B. 61

Figure 4-1. Comparison of Max(O_3) simulated by three versions of SAPRC-07 for 18 experiments for 1-alkenes. 84

Figure 4-2. Comparison of concentrations simulated by three versions of SAPRC-07 for 24 propene-NOx experiments of UCR's EPA chamber: (a) Max(O_3), (b) Max(OH), (c) Max(HO_2). 86

Figure 4-3. Comparison of O_3 simulated by various formulations for reaction 1-butene + O_3 in SAPRC-07 against measurements of Experiment ITC927. 89

Figure 4-4. Comparisons of simulated OH, HO_2 and O_3 between the Fixed and Extended versions of SAPRC-07 for the case of August 25, 2000 at La Porte: (a) OH and HO_2, (b) O_3. 92

Figure 4-5. Comparison of sources of new radicals and HCHO between the Fixed and Extended versions of SAPRC-07 for the case of August 25, 2000 at La Porte: (a) sources of new radicals, (b) sources of HCHO. 93

Figure 4-6. Comparison of simulated OH, HO_2 and O_3 between the various versions of SAPRC-07 for the case of August 25, 2000 at La Porte: (a) OH and HO_2, (b) O_3. 95

Figure 5-1. OH and Cl reactivities on August 25, 2000 based on measured data during the TexAQS-2000 study. 103

Figure 5-2. Isoprene (ISOP), methyl vinyl ketone (MVK), methacrolein (MACR) and CMBO on August 25, 2000 110

Figure 5-3. Effects of injected chlorine (Cl_2) at 7:30 CST on August 25, 2000 on modeled OH concentrations in chemical mechanisms: (a) SAPRC-07F, (b) SAPRC-07E, (c) CB05-Base, (d) CB05-UNClite. 113

Figure 5-4. Effects of injected chlorine (Cl_2) at 7:30 CST on August 25, 2000 on modeled HO_2 concentrations in chemical mechanisms: (a) SAPRC-07F, (b) SAPRC-07E, (c) CB05-Base, (d) CB05-UNClite. 114

Figure 5-5. Effects of injected chlorine (Cl_2) at 7:30 CST on August 25, 2000 on modeled O_3 concentrations in chemical mechanisms: (a) SAPRC-07F, (b) SAPRC-07E, (c) CB05-Base, (d) CB05-UNClite. 115

Figure 5-6. Effects of injected chlorine (Cl_2) at 7:30 CST on August 25, 2000 on modeled CMBO concentrations in chemical mechanisms: (a) SAPRC-07F, (b) SAPRC-07E, (c) CB05-Base, (d) CB05-UNClite. 116

Figure 5-7. Effects of injected chlorine (Cl_2) at 7:30 CST on August 25, 2000 on modeled NO concentrations in chemical mechanisms: (a) SAPRC-07F, (b) SAPRC-07E, (c) CB05-Base, (d) CB05-UNClite. 117

Figure 5-8. Effects of injected chlorine (Cl_2) at 7:30 CST on August 25, 2000 on modeled HCHO concentrations in chemical mechanisms: (a) SAPRC-07F, (b) SAPRC-07E, (c) CB05-Base, (d) CB05-UNClite. 118

Figure 5-9. Comparison of effects of chlorine emissions and using different lumping strategies for alkenes in SAPRC-07 on (a) OH, (b) HO_2, (c) O_3 for the case of August 25, 2000. 121

Figure 5-10. Comparison of effects of chlorine emissions and using different toluene mechanisms in CB05 on (a) OH, (b) HO_2, (c) O_3 for the case of August 25, 2000. 122

Figure 5-11. Effect of using different toluene mechanisms in CB05 at different initial concentrations of toluene on (a) OH, (b) HO_2, (c) O_3 for the case of August 25, 2000 for the case of August 25, 2000. 123

Figure 5-12. Effects of using different toluene mechanisms in CB05 at different initial concentrations of toluene on (a) NO and (b) NOx for the case of August 25, 2000. 124

Figure A-1. Comparison of O_3, NO, NO_2 simulated by CB05-Base and CB05-UNClite for LaPorte2000 cases where [VOC]/[NOx]t=t0 (ppmC/ppm) = 10 (left), 15 (right). 183

Figure A-2. Comparison of O_3 concentrations simulated by CB05-Base and CB05-UNClite for the 39-City Average case. 183

Figure B-1. Major pathways leading to radical formation in the ozonolysis of 1-alkenes. 186

Chapter 1: Introduction

1.1. Radical Chemistry in the Atmosphere

Free radicals drive photochemical reactions leading to formation of air pollutants such as ozone (O_3) and secondary aerosols while oxidizing organic compounds in the air (Ehhalt, 1999; Finlayson-Pitts and Pitts, 1997; Meng et al., 1997). Ozone formation reactions in the lower troposphere proceed through free radical mechanisms, and the dominant free radical species are the hydroxyl radical, the hydroperoxy radical, the alkoxy radical, and the alkyl peroxy radical (OH, HO_2, RO, RO_2, respectively; HOx = OH + HO_2, ROx = HOx + RO_2 (+ RO), collectively). HO_2 and RO_2 are generated in the oxidation of hydrocarbons (RH) by OH. In turn, HO_2 and RO_2 convert NO into NO_2 without consumption of O_3, and the subsequent photolysis of this NO_2 leads to net O_3 formation. OH molecules are regenerated by NO directly from HO_2 and indirectly from RO_2. These interconversions of odd hydrogen radicals (HOx) constitute the radical propagation cycle which oxidizes hydrocarbons and creates ozone (Figure 1-1).

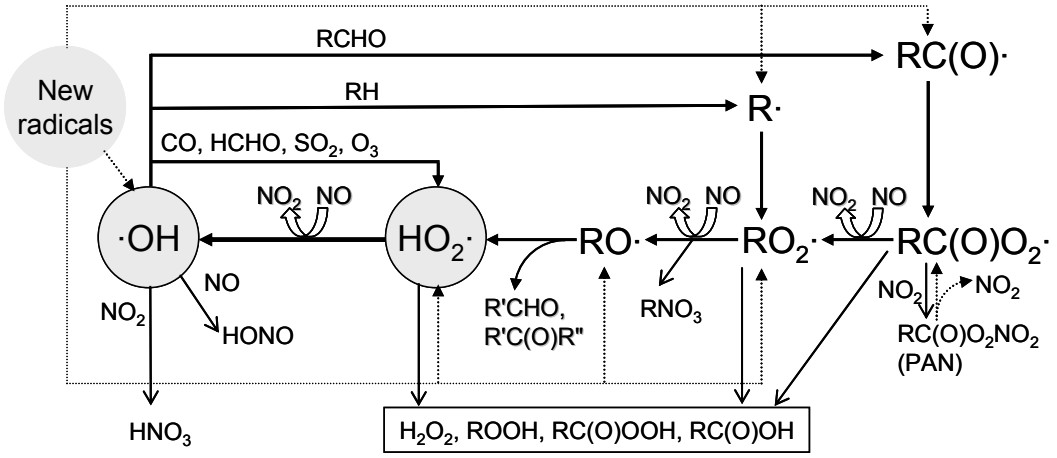

Figure 1-1. Major photochemical reactions involving HOx radicals (Seinfeld and Pandis, 1998; Finlayson-Pitts and Pitts, 2000).

Understanding these free radical chemistries and free radical sources and sinks is important in developing air quality policies for reducing concentrations of air pollutants (Figure 1-1; Ehhalt, 1999; Jenkin and Clemitshaw, 2000; Clemitshaw, 2003). Sources of HOx include photolytic sources and non-photolytic sources. Photolytic sources are active only during daytime hours; however, non-photolytic sources can act as HOx sources during both daytime and nighttime hours. Radical-generating photolysis reactions of O_3, formaldehyde (HCHO) and dicarbonyl compounds (e.g., glyoxal ($(CHO)_2$) and methylglyoxal ($CH_3C(O)CHO$)) are well-known photolytic HOx sources (Finlayson-Pitts and Pitts, 2000; Calvert et al., 2002). On the other hand, alkene oxidation by ozone and nitrate (NO_3) and thermal decomposition of peroxycarboxylic nitric anhydrides (PANs; commonly referred to by peroxyacyl nitrates) are non-photolytic HOx sources (Paulson and Orlando, 1996; Carter et al., 1981). Reactions forming nitric acid (HNO_3), hydrogen peroxide (H_2O_2), alkyl nitrates (RNO_3) and PANs are major HOx sinks that consume HOx radicals but do not regenerate HOx radicals via interconversions of OH, HO_2 and RO_2 (Figure 1-1). HONO formation is also a HOx sink during nighttime though nighttime HONO is a reservoir of OH which releases OH via photolysis after sunrise (Carter et al., 1981; Platt et al., 1980). Major HOx sources and sinks are listed in Table 1-1.

OH and HO_2 concentrations are determined by the balance of their sources and sinks. The OH concentration ([OH]) can be expressed as follows when sinks and sources are at balance:

$$P - L \cdot [OH] = 0;$$

$$[OH] = P/L$$

where P is the rate of OH production and L is the OH destruction frequency, the sum of products of their net OH destruction factor (y, whose value is usually 1.0 if there is no

regeneration of OH in the reaction), rate constant towards OH (k_{OH}) and concentration of each reactant, $\sum_i y_i \cdot k_{OH}^i \cdot [compound_i]$.

The HO_2 concentration ($[HO_2]$) can be described in the same way. Thus, whether [OH] or $[HO_2]$ will increase or decrease after some time is controlled by changes in the ratio of their production rate to their destruction frequency (P/L). In regard to OH, OH sources such as photolysis of HONO and O_3 and the reaction of HO_2 and NO constitute the major sources (P), and OH sinks such as NO_2 and hydrocarbons of various reactivities are the major loss terms (L, in units of 1/time).

Table 1-1. Sources, sinks, and propagation reactions related to OH and HO_2 radicals (Ehhalt, 1999; Finlayson-Pitts and Pitts, 2000; Clemitshaw, 2003).

Generated radical(s)	Initiation reaction (source)
OH	$O_3 + h\nu \rightarrow O(^1D) + O_2$; $O(^1D) + H_2O \rightarrow 2OH$
OH	$HONO + h\nu \rightarrow OH + NO$
HO_2	$HCHO + h\nu \rightarrow 2HO_2 + CO$
HO_2, RO_2	$RCHO + h\nu \rightarrow RO_2 + HO_2 + CO$
$RC(O)O_2$	$PAN \rightarrow RC(O)O_2 + NO_2$
OH, HO_2, RO_2	alkene + $O_3 \rightarrow$ a*OH + b*HO_2 + c*RO_2 + other products
RO_2	$Cl + RH \rightarrow RO_2$ + other products
Removed radical(s)	**Termination reaction (sink)**
OH	$OH + NO_2 \rightarrow HNO_3$
OH	$OH + NO \rightarrow HONO$
OH	$OH + HONO \rightarrow NO_2 + H_2O$
OH, HO_2	$OH + HO_2 \rightarrow H_2O + O_2$
HO_2	$HO_2 + HO_2 \rightarrow H_2O_2 + O_2$
HO_2, RO_2	$HO_2 + RO_2 \rightarrow ROOH + O_2$
HO_2, $RC(O)O_2$	$HO_2 + RC(O)O_2 \rightarrow RC(O)OOH + O_2$
$RC(O)O_2$	$RC(O)O_2 + NO_2 \rightarrow PAN$
RO_2, $RC(O)O_2$	$RO_2 + RC(O)O_2 \rightarrow RC(O)OH + RCHO + O_2$
RO_2	$RO_2 + NO \rightarrow RONO_2$
RO_2	$RO_2 + RO_2 \rightarrow ROH + RCHO + O_2$
RO_2	$RO_2 + RO_2 \rightarrow ROOR + O_2$

Type of conversion	Propagation reaction
OH to HO_2	$OH + O_3 \rightarrow HO_2 + O_2$
OH to HO_2	$OH + CO \rightarrow HO_2 + CO_2$
OH to HO_2	$OH + HCHO \rightarrow HO_2 + CO$
OH to HO_2	$OH + SO_2 \rightarrow HO_2 + SO_3$
OH to RO_2	$OH + RH (+ O_2) \rightarrow RO_2$
OH to $RC(O)O_2$	$OH + RCHO (+O_2) \rightarrow RC(O)O_2$
$RC(O)O_2$ to RO_2	$RC(O)O_2 + NO (+O_2) \rightarrow RO_2 + NO_2 (+CO_2)$
RO_2 to HO_2	$RO_2 + NO (+O_2) \rightarrow HO_2 + NO_2 +$ R'CHO (or R'C(O)R")
HO_2 to OH	$HO_2 + NO \rightarrow OH + NO_2$
HO_2 to OH	$HO_2 + O_3 \rightarrow OH + 2O_2$

Note: RO_2 is the alkyl peroxy radical, and $RC(O)O_2$ is the acyl peroxy radical that is also a peroxy radical (RO_2) containing the carbonyl group (C=O) adjacent to the –OO part.

1.2. SUMMARY OF MAJOR AIR QUALITY STUDY CAMPAIGNS IN TEXAS RELEVANT TO RADICAL CHEMISTRY

Two major air quality study campaigns carried out in Texas in 2000 and 2006 to clarify ozone formation in Houston, Texas, the Texas Air Quality Study 2000 (TexAQS-2000) and the Texas Air Quality Study II (TexAQS-2006), have suggested that OH radicals are under-predicted by our current chemical mechanisms for describing radical sinks and sources (Martinez et al, 2002; Rappenglück and Lefer, 2007; Chen et al., 2009; Figure 1-2).

During the TexAQS-2000 campaign, a suite of measurements, including OH and HO_2, relevant to radical sources and sinks was measured at the La Porte municipal airport (29.669N, 95.064W) 30 km southeast of downtown Houston, Texas (Martinez et al., 2002; www.utexas.edu/research/ceer/texaqs). The time series of the measured OH concentration showed vigorous fluctuations, which reflect their highly sensitive responses to changes in the atmospheric composition influenced by industrial emissions in and around Houston as well as common emissions such as mobile source emissions (Figure 1-2). Overall, however, OH and HO_2 radical concentrations in Houston were often

under-predicted by currently widely used chemical mechanisms such as the Carbon Bond 05 (CB05, Yarwood et al., 2005) relative to concentrations observed in TexAQS-2000 and 2006 (Figure 1-2; Chen et al., 2009). These under-predictions of OH and HO_2 are related to shortage in radical sources against radial sinks. Martinez et al. (2002) reported that OH formation processes other than O_3 photolysis and reaction of HO_2 with NO were necessary to increase the OH formation rate up to around 1 part per trillion (ppt) OH per second in order to match the OH destruction rate at the La Porte site during TexAQS-2000. Mao et al. (2009) also reported shortage in OH and HO_2 sources relative to HO and HO_2 sinks during TexAQS-2000. This dissertation will investigate radical sources and sinks and the radical chemistry which controls these radical concentrations in condensed chemical mechanisms, especially in early morning hours, and attempt to reduce the discrepancies between modeled and measured HOx during TexAQS-2000 and TexAQS-2006.

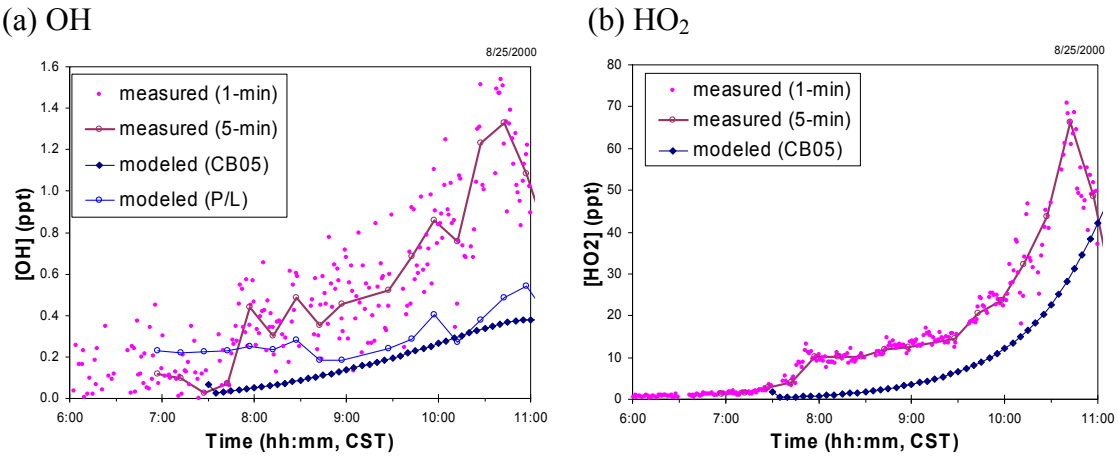

Figure 1-2. OH and HO_2 measurements on August 25, 2000 during TexAQS-2000.

Note: "modeled (CB05)" means the modeled OH or HO_2 by using the CB05 mechanism, and "modeled OH (P/L)" means the modeled OH calculated by dividing the production rate of OH from ozone photolysis and conversion of HO_2 by NO and O_3 (P) by the total OH loss frequency (L) as described earlier. Source of OH and HO_2 measurements: courtesy of Dr. Xinrong Ren (Ren, personal communication, 2008 and 2009).

Deficits in radical sources balancing against radical sinks were also observed in studies in other areas in the U.S. such as Nashville, Tennessee (Martinez et al., 2003) and New York City, New York (Ren et al., 2003). According to Martinez et al., (2003), the calculated OH production rate based on known OH-generating reactions, was less than the directly measured total OH loss rate by $(1–2)\times10^7$ molecules·cm^{-3}·s^{-1}, with relatively large uncertainty during the day and statistically significant at night. According to Ren et al. (2003), an additional OH production of 8.8×10^6 molecules·cm^{-3}·s^{-1} was needed to achieve an OH balance during nighttime, and OH production exceeded OH loss by $(1-4)\times10^7$ molecules·cm^{-3}·s^{-1} during 6:00 to 12:00 EDT. In both studies, additional OH sources of $\sim10^7$ molecules·cm^{-3}·s^{-1} other than known OH sources were required to have OH production and OH loss in balance. (Martinez et al., 2003; Ren et al., 2003; Kovacs et al., 2003).

1.3. STRATEGIES AND STRUCTURE OF THIS STUDY

Chemical mechanisms for air quality research and applications, including reactions that serve as radical sources and sinks, have been developed and tested traditionally by using environmental chamber data. This dissertation will examine environmental chamber data as well; however, as described later in this dissertation, there are critical shortcomings in using environmental chamber simulations alone for evaluating a chemical mechanism (Dodge, 2000; Faraji et al., 2007), especially free radical sources and sinks. Thus, both ambient data (from the Texas Air Quality Study) and environmental chamber data will be employed in this work.

Three hypotheses regarding radical sources and sinks will be examined using a combination of chamber data and ambient data:

- Aromatic emissions and chemistry significantly impact radical concentrations.

- Alkene emissions and chemistry significantly influence radical concentrations.
- Chlorine emissions and chemistry significantly influence radical concentrations.

These three hypotheses were selected, not because they represent the only significant issues associated with free radical sources and sinks, but because they are topics on which a significant amount of new data are available for evaluating the processes.

In Chapter 2, the general framework for evaluating the current condensed chemical mechanisms used in air quality models and for testing this study's hypotheses in describing the free radical chemistry will be presented. The necessity of using ambient data will be clarified by describing various limitations of environmental chamber simulations and the potential of using ambient data such as TexAQS-2000 measurements. Specific cases for testing this study's three hypotheses will be selected based on environmental chamber measurements and ambient measurements made during TexAQS-2000.

In Chapter 3, radical sources and sinks related to oxidation of aromatic compounds will be evaluated. Radical production via the reactions of aromatic ring fragmentation products will be examined. Radical sinks through formation of cresols and nitro-aromatics (e.g., nitro-cresols) will be studied as well.

In Chapter 4, alkene chemistry as a radical source will be tested. First, candidate alkene species will be selected; then, two types of contributions to radical production using condensed chemical mechanisms will be tested by using sensitivity simulations: direct radical formation by ozonolysis of alkenes and the strategies used in grouping the individual alkene chemistries into the reactions of a limited number of model species for alkenes in a condensed mechanism.

In Chapter 5, the relative impacts of aromatics chemistry and alkene chemistry on radical sources and sinks will be compared. These sources will also be compared to the impact of chlorine chemistry as a morning radical source. Chlorine atoms (Cl) have been suggested as an important radical source in coastal urban areas such as Houston, Texas where anthropogenic sources of Cl precursors co-exist with nearby natural sources (e.g., sea salts) (Chang et al., 2002, Osthoff, 2008). The impacts of these chemistries on radical sources and sinks will be quantitatively tested by using the case of August 25, 2000 at La Porte during TexAQS-2000.

Then, in Chapter 6, conclusions will be presented and modifications to existing chemical mechanisms and future work will be suggested.

1.4. REFERENCES

Calvert, J. G., Atkinson, R., Becker, K.H., Kamens, R.M., Seinfeld, J.H., Wallington, T.J., Yarwood, G., 2002. The Mechanisms of Atmospheric Oxidation of Aromatic Hydrocarbons, Oxford University Press, New York, 566p.

Carter, W. P. L., Winer, A. M., Pitts Jr., J. N., 1981. Effect of peroxy acetyl nitrate on the initiation of photochemical smog. Environmental Science & Technology 15(7), 831-834.

Chang, S., McDonald-Buller, E., Kimura, Y., Yarwood, G., Neece, J., Russell, M., Tanaka, P., Allen, D., 2002. Sensitivity of urban ozone formation to chlorine emission estimates. Atmospheric Environment 36, 4991-5003.

Chen, S., Ren, X., Mao, J., Chen, Z., Brune, W.H., Lefer, B., Rappenglück, B., Flynn, J., Olson, J., Crawford, J.H., 2009. A comparison of chemical mechanisms based on TRAMP-2006 field data, Atmospheric Environment (2009), doi: 10.1016/j.atmosenv.2009.05.027.

Clemitshaw, K. C., 2003. Hydroxyl Radical, in: Holton, J.R., Pyle, J.A., Curry, J.A., (Eds.), Encyclopedia of Atmospheric Sciences, Elsevier, Amsterdam, 2403-2411.

Dodge, M.C., 2000. Chemical oxidant mechanisms for air quality modeling: critical review. Atmospheric Environment 34, 2103-2130.

Ehhalt, D.H., 1999. Photooxidation of trace gases in the troposphere. Physical Chemistry Chemical Physics 1, 5401-5408.

Faraji, M., Heo, G., Kimura, Y., McDonald-Buller, E., Allen, D., Yarwood, G., Whitten, G., Carter, W. 2007. Comparison of the Carbon Bond and SAPRC photochemical mechanisms. Report to the Texas Commission on Environmental Quality, Work Order No. 582-04-65588-07, August, 2007.

Finlayson-Pitts, B.J., Pitts, J.N., 1997. Tropospheric air pollution: Ozone, airborne toxics, polycyclic aromatic hydrocarbons, and particles. Science 276 (May 16), 1045-1052.

Finlayson-Pitts, B.J., Pitts, J.N., 2000. Chemistry of the Upper and Lower Atmosphere: Theory, Experiments, and Applications, Academic Press, San Diego, 969p.

Jenkin, M.E., Clemitshaw, K.C., 2000. Ozone and other secondary photochemical pollutants: chemical processes governing their formation in the planetary boundary layer. Atmospheric Environment 34, 2499-2527.

Kovacs, T.A., Brune, W.H., Harder, H., Martinez, M., Simpas, J.B., Frost, G.J., Williams, E., Jobson, T., Stroud, C., Young, V., Fried, A., Wert, B., 2003. Direct measurements of urban OH reactivity during Nashville SOS in summer 1999. Journal of Environmental Monitoring 5, 68–74, doi:10.1039/b204339d.

Mao, J., Ren, X., Chen, S., Brune, W.H., Chen, Z., Martinez, M., Harder, H., Lefer, B., Rappenglück, Flynn, J., Leuchner, M., 2009. Atmospheric oxidation capacity in the summer of Houston 2006: Comparison with summer measurements in other metropolitan studies. Atmospheric Environment (2009), doi:10.1016/j.atmosenv.2009.01.013.

Martinez, M., Harder, H., DiCarlo, P., Brune, W.H., Hall, S.R., Shetter, R.E., Williams, E.J., Kuster, W., Jobson, B.T., 2002. OH and HO_2 concentrations, production and loss rates at the La Porte site during TexAQS 2000, Fourth Conference on Atmospheric Chemistry of the American Meteorological Society, Orlando, January 2002. (Available at http://ams.confex.com/ams/annual2002/techprogram/paper_32451.htm)

Martinez, M., Harder, H., Kovacs, T.A., Simpas, J.B., Bassis, J., Lesher, R., Brune, W.H., Frost, G.J., Williams, E.J., Stroud, C.A., Jobson, B.T., Roberts, J.M., Hall, S.R., Shetter, R.E., Wert, B., Fried, A., Alicke, B., Stutz, J., Young, V.L., White, A.B., Zamora, R.J., 2003. OH and HO_2 concentrations, sources, and loss rates during the Southern Oxidants Study in Nashiville, Tennessee, summer 1999. Journal of Geophysical Research 108(D19), 4617, doi:10.1029/2003JD003551.

Meng, Z., Dabdub, D., Seinfeld, J.H., 1997. Chemical coupling between atmospheric ozone and particulate matter. Science 277 (July 4), 116-119.

Osthoff, H.D., Roberts, J.M., Ravishankara, A.R., Williams, E.J., Lerner, B.M., Sommariva, R., Bates, T.S., Coffman, D., Quinn, P.K., Dibb, J.E., Stark, H., Burkholder, J.B., Talukdar, R.K., Meagher, J., Fehsenfeld, F.C., Brown, S.S., 2008. High levels of nitryl chloride in the polluted subtropical marine boundary layer. Nature Goescience 1, 324-328.

Paulson, S.E., Orlando, J.J., 1996. The reactions of ozone with alkenes: An important source of HOx in the boundary layer. Geophysical Research Letters 23, 3727-3730.

Platt, U., Perner, D., Harris, G.W., Winer, A.M., Pitts, J.N., Jr, 1980. Observations of nitrous acid in an urban atmosphere by differential optical absorption. Nature (London) 285, 312-314.

Rappenglück, B., Lefer, B., 2007. TRAMP data analysis and radical chemistry study, final report to Houston Advanced Research Center (HARC), TERC project H86, December 2007. (Available at http://files.harc.edu/Projects/AirQuality/Projects/H086/H086FinalReport.pdf)

Ren, X., 2008. Personal communication by email.

Ren, X., 2009. Personal communication by email.

Ren, X., Harder, H., Martinez, M., Lesher, R.L., Oliger, A., Simpas, J.B., Brune, W.H., Schwab, J.J., Demerjian, K.L., He, Y., Zhou, X., Gao, H., 2003. OH and HO_2 chemistry in the urban atmosphere of New York City. Atmospheric Environment 37, 3639-3651.

Seinfeld, J.H., Pandis, S.N., 1998. Atmospheric Chemistry and Physics: From Air Pollution to Climate Change, Wiley-Interscience, New York, 1326p.

Tanaka, P.L.; Riemer, D.D.; Chang, S.; Yarwood, G.; McDonald-Buller, E.C.; Apel, E.C.; Orlando, J.J.; Silva, P.J.; Jimenez, J.L.; Canagaratna, M.R.; Neece, J.D.; Mullins, C.B.; Allen, D.T., 2003. Direct evidence for chlorine-enhanced urban ozone formation in Houston, Texas. Atmospheric Environment 37, 1393-1400

Yarwood, G., Rao, S., Yocke, M., Whitten, G.Z., 2005. Updates to the Carbon Bond mechanism: CB05. Report to the U.S. Environmental Protection Agency, December 2005. (Available at http://www.camx.com/publ/pdfs/CB05_Final_Report_120805.pdf)

Chapter 2: Combining Environmental Chamber Simulation and Ambient Simulation for Studying Chemical Mechanisms

2.1. INTRODUCTION

Simulation of environmental chamber data has been used for decades to develop and evaluate chemical mechanisms for air quality modeling (Dodge, 2000; Gery et al., 1989; Carter and Lurmann, 1991; Carter, 2000 and 2009; Yarwood et al., 2005). Chamber data have the advantage of being produced under relatively well controlled environmental conditions, as compared to ambient data. However, chamber data also have limitations. Chamber radical sources, NOx (NO + NO_2) offgasing, and light conditions possibly very different from ambient conditions are very well-known artifacts of environmental chambers (Carter et al., 1982; Killus and Whitten, 1990; Dodge, 2000).

Using ambient data to evaluate chemical mechanisms also has strengths and limitations. In ambient simulations, uncertainties in emissions and meteorology can be substantial, however, there are no wall effects (e.g., offgasing of chamber materials) and the light conditions, by definition, are the target conditions to be simulated.

Thus, in this dissertation, both environmental chamber simulations and simulations of ambient conditions will be used to evaluate chemical mechanisms.

2.2. ENVIRONMENTAL CHAMBER SIMULATION FOR MECHANISM EVALUATION

2.2.1. Overview of Environmental Chamber Simulation

Simulation of environmental chamber data is useful in evaluating a chemical mechanism comprehensively or individual components of the entire chemical mechanism (Dodge, 2000). The overall procedure of the chamber simulation is briefly stated here; for details, refer to Carter and Lurmann (1991) and Carter (2000 and 2009).

First, chamber data appropriate for the purposes of evaluating the chemical mechanism should be obtained. Second, the chamber experiments should be evaluated for biases and uncertainties introduced by chamber artifacts. Characterizing chamber radical sources and NOx offgasing is usually the most important part of the chamber evaluation. In most cases, an auxiliary mechanism (commonly called "wall mechanism") is constructed to describe chamber-specific reactions separately from the reactions in the chemical mechanism to be evaluated. Parameters in the auxiliary mechanism are tuned by using direct measurements of those parameters or by modeling chamber characterization experiments such as CO-NOx and CO-air experiments (Carter et al., 2005). Third, the simulations are performed, and the chemical mechanism is evaluated by comparing measured and simulated quantities such as the maximum O_3 concentration ($Max(O_3)$) or the maximum amount of O_3 formation and NO oxidation ($Max(\Delta(O_3\text{-}NO))$) during the chamber simulation (Gery et al., 1989; Carter et al., 2000 and 2009; Yarwood et al., 2005). Using $Max(\Delta(O_3\text{-}NO))$ as a performance indicator has two advantages over using $Max(O_3)$. $\Delta(O_3\text{-}NO)$ quantifies the amount of NO oxidation by photochemical processes even when there is no significant O_3 production (Carter and Atkinson, 1987) and reduces the possibility of sampling error due to the reaction between O_3 and NO in the sampling line from inside the chamber reactor to the O_3 measuring

instrument. In this study, both Max(O_3) and Max($\Delta(O_3\text{-}NO)$), as well as other parameters, will be used as performance indicators.

2.2.2. Environmental Chamber Data

A relatively large number of chamber experiments have been performed in the U.S. In this work, data collected at various chambers at the University of North Carolina (UNC), the University of California at Riverside (UCR), and the Tennessee Valley Authority (TVA) will be used for mechanism evaluation (Dodge, 2000; Carter et al., 1995a; Carter, 2000 and 2009; Yarwood et al., 2005). Specifically, in this study, the chamber data produced at the UNC, UCR and TVA chambers listed in Table 2-1 will be used to evaluate radical chemistry.

William Carter and Gary Whitten, two developers of chemical mechanisms, the Statewide Air Pollution Research Center (SAPRC) mechanisms such as SAPRC-99 and SAPRC-07 (Carter, 2000 and 2009) and the Carbon Bond (CB) mechanisms such as CB-IV and CB05 (Gery et al., 1989; Yarwood et al., 2005), respectively, provided chamber simulation software and data for a mechanism comparison project (Faraji et al., 2007). In this study, those chamber datasets and mechanism evaluation software packages provided by Carter and Whitten will be referred to as the "SAPRC" dataset and the "Morpho" dataset, and the "SAPRC" software and the "Morpho" software, respectively. Morpho was developed at the University of North Carolina (UNC; Jeffries and Kessler, 1999) and has been used mainly in evaluating CB mechanisms with the UNC chamber data (Yarwood et al., 2005). The SAPRC software is the package of various programs for environmental simulations developed by William Carter (Carter, 2000 and 2009; http://www.engr.ucr.edu/~carter/SAPRC/files.htm). Thus, in this study, chamber

experiments will be selected from this large number of chamber experiments in the SAPRC and Morpho datasets, and simulated by using the SAPRC and Morpho software.

Table 2-1. An overview of environmental chambers at UNC, UCR and TVA used for mechanism evaluation.

Chamber	Chamber ID	Reactor type	Reactor volume (m^3)	Light source	Humidity (RH[a])	Operation period
Indoor chamber						
Evacuable Chamber at UCR	EC	single	~5.8	xenon arc	~50%	1975-84
Indoor Teflon Chamber at UCR	ITC	single	~6.4	blacklight	~50%	1982-86
Ernie's Teflon Chamber at UCR	ETC	single	~3.0	blacklight	dry (< 5%)	1989-93
Dividable Teflon Chamber at UCR	DTC	dual	~5.0 (X 2)	blacklight	dry (< 5%)	1993-99
Xenon arc Teflon Chamber at UCR	XTC	single	~5.0	xenon arc	dry (< 5%)	1993
CE-CERT Teflon Chamber at UCR	CTC (11-82[b])	single	~5.0	xenon arc	dry (< 5%)	1994-95
CE-CERT Teflon Chamber at UCR (rebuilt)	CTC (>82[b])	dual	~2.5 (X 2)	xenon arc	dry (< 5%)	1995-99
UCR EPA chamber	EPA	dual	~90 (X 2)	argon arc/ blacklight	dry (< 1%)	2003-present
TVA indoor chamber	TVA	single	~28	3 types including blacklight	~15%	1993-95
Outdoor chamber						
UNC outdoor gas-phase chamber	UNC[c]	dual	~150 (X 2)	sunlight	variable	1977-present
Outdoor Teflon Chamber at UCR	OTC	dual	~20 (X 2)	sunlight	dry (< 5%)	1992-93

a: relative humidity. **b**: run number of the chamber experiment. **c**: reconstructed twice according to http://airchem.sph.unc.edu/Research/Facilities/UNCChamber/default.htm. References: Dodge (2000), Carter (2000 and 2009), Carter et al. (2005).

2.2.3. Chamber Characterization

Characterizing the chamber conditions is required to properly simulate chamber data. Characterization of chamber run conditions includes describing the initial reactant concentrations, the light intensity and spectral distribution, temperature, humidity, and dilution inside the chamber reactor. Chamber effects under chamber run conditions include the release and removal of reactants such as radicals, O_3, NOx, HONO and HCHO by wall reactions and other chamber background effects (Carter and Lurmann, 1991; Dodge, 2000; Carter et al., 2005). Although there are still various uncertainties in chamber-dependent reactions, chamber effects need to be described in the auxiliary mechanism using currently available information for reducing errors and uncertainties in chamber simulations. Then, this auxiliary mechanism, a chamber dependent mechanism describing wall reactions and reactive contaminants, should be used in the chamber simulation together with the chamber light model characterizing the light conditions and the chemical mechanism to be tested.

2.2.3.1. Chamber effects of light conditions, reactant levels and humidity

Light conditions inside the environmental chamber are different than under the natural sunlight irradiation in the atmosphere to various degrees. Artificial lights at indoor chambers do not provide the same light intensity and spectral characteristics as sunlight. Even at outdoor chambers, the sunlight is modified while passing through the Teflon© film of the outdoor chamber reactor and being reflected inside the chamber reactor. Thus, characterizing the light conditions at an outdoor chamber is very difficult due to varying atmospheric conditions over the chamber as well as these modifications (Carter et al., 1995b; Dodge, 2000). Chamber light conditions different from sunlight-driven ambient light conditions raise at least two issues in evaluating chemical

mechanisms: "direct" modifications of photolytic reactions by changing the photolysis rate constants (j values) and "indirect" modifications of non-photolytic reactions by changing the concentrations of reactants participating in the reactions. Generally, for evaluating a chemical mechanism, we do not have to use chamber light conditions that are exactly the same as ambient light conditions. When well-characterized light conditions are used during the chamber simulation by constructing a light model, we can still legitimately evaluate the chemical mechanism (Carter et al., 1995b and 2005). However, with this type of evaluation, we might not see all the important features of the chemical mechanism that we could observe in the real atmosphere. For example, a blacklight as a chamber light source shows very different spectral characteristics from sunlight, especially in the longer wavelength region that significantly affects some features of the aromatics chemistry and NO_3 photolysis (Carter et al., 1995b and 2005).

The concentrations of volatile organic compounds (VOCs) and NOx injected into chambers are usually much higher than their typical ambient concentrations. The presence of chamber effects limits the lower-end concentrations of the test compounds or mixtures in the chamber because chamber effects will dominate the reactivity when an injection typical of ambient conditions (e.g., 1 ppb NOx and 5 ppb n-butane) is used. However, using high concentrations make some reactions more important than under ambient conditions. For example, high NOx leads to high $O(^3P)$ in the chamber reactor through photolysis of NO_2. In this case, reactions of some VOCs with $O(^3P)$ should be also added to the main chemical mechanism even if these reactions are expected to be negligible under most atmospheric conditions (Paulson et al., 1992; Calvert et al., 2000).

Using a low humidity ("dry" condition) in the chamber suppresses OH radical generation from O_3 photolysis and subsequent reaction of $O(^1D)$ and H_2O. The humidity levels used at most chambers in Table 2-1 are lower than typical ambient

humidity. For example, less than 5% relative humidity (< 5% RH) is far lower than under ambient conditions. However, as stated earlier, testing a chemical mechanism using chamber experiments carried out at a very low humidity level is also legitimate though the experiment may not test all the important characteristics of the chemical mechanism that would be important under ambient humidity conditions.

2.2.3.2. Chamber radical source and NOx offgasing

Chamber radical sources and NOx offgasing from the chamber walls have been identified as the most important chamber effects (Killus and Whitten, 1990; Carter and Lurmann, 1991; Dodge, 2000; Carter et al., 2005). The actual impacts of the chamber radical source and NOx offgasing depend on the chamber run conditions. When the reactivity of the compound or mixture injected into the chamber reactor becomes lower, chamber effects tend to dominate the total reactivity and evolution of the concentrations. For example, when a low reactivity compound such as CO or ethane is tested in the chamber or when the VOC/NOx ratio is relatively low, the impact of chamber-dependent radical sources dominates the time-concentration profiles of O_3 and radicals. When the injected NOx level is very low, the NOx offgasing will dominate the NOx concentration (Killus and Whitten, 1990; Carter et al., 2005; Carter, 2004 and 2009).

Chamber radical sources include initial HONO, offgasing of HONO, HCHO or other photolyzable species that can act as a radical source, and NOx offgasing can take any form of NOx; wall sources of NO, NO_2, or HONO can be easily converted into NOx (Carter et al., 1982 and 2005). In general, chamber radical sources and NOx offgasing are separately modeled in the auxiliary mechanism prepared for chamber simulations (e.g., Carter and Lurmann, 1991). However, Carter modified this approach later and used HONO offgasing for describing chamber radical sources and NOx offgasing in a

combined way based on the analysis that the required chamber-dependent radical production rate was nearly equal to the rate of NOx offgasing at UCR's EPA chamber (Carter et al., 2005; Carter, 2009).

Chamber studies in Europe also support this approach that uses HONO as both a radical source and NOx source (Rohrer et al., 2005; Zádor et al., 2006). Rohrer et al. (2005) measured HONO during chamber experiments of pure air, air-CO and air-NO_2 at the Simulation of Atmospheric PHotochemistry in a large Reaction chamber (SAPHIR) in Jülich, Germany, and found that HONO formation at SAPHIR occurred and was photo-enhanced during irradiation by sunlight. Zádor et al. (2006) measured HONO and HCHO at the European Photoreactor (EUPHORE) in Valencia, Spain to explain enhanced photo-oxidation at EUPHORE, and found the same result, that HONO was the major form of a chamber-dependent radical source and that HCHO offgasing was a minor radical source. However, in some chambers, such as the TVA chamber, HCHO offgasing also significantly contributed to the chamber-dependent radical generation (Simonaitis et al., 1997; Carter, 2004). Contaminants in the background air or other organic compounds released from the walls also lead to radical production, but their contribution is expected to be usually minor (Killus and Whitten, 1990; Carter et al., 2005; Carter, 2000 and 2009).

Chamber radical sources and NOx-offgasing directly influence radical chemistry. Thus, for studying the radical chemistry, we have to use chamber experiments which are expected to be influenced to a limited degree by chamber radical sources and NOx offgasing. For example, we cannot use many experiments in the SAPRC dataset to reliably study radical chemistry because the chamber effects and uncertainties in the chamber characterization dominate the chamber simulation. In this study, we will use chamber experiments whose chamber injections contain at least one compound as a direct

or indirect radical source and keep a reasonably high NOx level during the experiment to minimize the effect of the chamber-dependent radical source and NOx-offgasing.

2.2.4. Chamber Simulation for Studying Radical Chemistry

Direct measurements of OH and HO_2 radicals are not included in the currently available SAPRC and Morpho datasets except for some exceptional experiments though measuring OH and HO_2 at chambers is desirable to study chemical mechanisms using chamber experiments (Dodge, 2000). However, chamber simulations are still useful for clarifying uncertain features of a chemical mechanism in describing the radical chemistry. In this study, chamber simulations will be used extensively in testing aromatics chemistry as a radical sink and source, and will be used to a limited degree in testing other hypotheses that are suggested to resolve the model-measurement discrepancies in OH and HO_2 concentrations during TexAQS-2000 and TexAQS-2006 (Martinez et al, 2002; Rappenglück and Lefer, 2007, Chen et al., 2009): (1) alkene chemistry as a radical source, and (2) chlorine (Cl) emissions and chemistry as a radical source.

Alkene chemistry is relatively well-known and heavily tested against chamber data for simple terminal alkenes such as ethene and propene (Atkinson, 2000; Carter, 2007), and there is no adequate chamber data among the SAPRC and Morpho datasets for testing chlorine chemistry as a radical source. Thus, the focus will be on doing ambient simulations to test these hypotheses while still consulting the results of the recent chamber studies on alkene chemistry (Carter, 2004 and 2009; Yarwood et al., 2005; Faraji et al., 2007). In regard to aromatics chemistry, there are still various uncertainties in the mechanisms of oxidation reactions of aromatic compounds and their products (Atkinson et al., 2000; Calvert et al., 2002; Carter, 2004 and 2009; Bloss et al., 2005;

Gómez Alvarez et al., 2007). Thus, this work will concentrate on testing alternative mechanisms against chamber simulations.

2.3. AMBIENT SIMULATION FOR MECHANISM EVALUATION

The presence of chamber effects suggests that mechanism evaluation should be performed by using both chamber simulations and ambient simulations if ambient data are available for use in this combined approach. The two intensive air quality campaigns, TexAQS-2000 and TexAQS-2006, provide us with suites of data which might be very useful for mechanism evaluation. In this section, the general framework of evaluating chemical mechanisms by using ambient simulations will be described.

2.3.1. Overview of Ambient Simulations

Successful ambient simulations start with obtaining accurate ambient data as input data to the simulation model. These input data include atmospheric concentrations of major chemical species, meteorological data, and emissions (Seinfeld and Pandis, 1998; Russell and Dennis, 2000). However, ambient data are not in a form ready for use in the simulation model. In most cases, in addition to missing data and missing data points (for example, no available measurement of alkyl peroxy radicals (RO_2)), time stamps and averaging times are different between different types of measurements; for example, between the measurements of VOCs and the measurements of inorganic species such as O_3, NO, and NO_2. Thus, only after preparation of a model-ready dataset based on the raw ambient data, can ambient simulations with the selected chemical mechanism be performed for evaluating the chemical mechanism. In this study, the SAPRC software

will be used as a modeling tool, however, with settings for the "airshed" simulation instead of settings for the environmental chamber simulation (Carter, 2000 and 2009).

2.3.2. Ambient Data

In this study, TexAQS-2000 data will be used extensively and TexAQS-2006 data will not be used directly but referenced to a limited degree. The focus will be on stagnation events, when the importance of boundary conditions in the modeling and advection of chemical species is minimized.

Table 2-2 shows the major HOx-relevant species measured during TexAQS-2000 and the measurement techniques that were employed. OH and HO_2 radicals were measured by the Penn State ground-based tropospheric hydrogen oxides sensor (GTHOS) using laser-induced fluorescence (LIF) at low pressure (Martinez et al., 2002; Faloona et al., 2004). Differential optical absorption spectroscopy (DOAS) measurements also provide HONO and HCHO data (Stutz et al., 2004a,b), and HCHO measurements by a fluorometric detection method with the Hantzsch reaction (the condensation of HCHO with a β-ketoester in the presence of ammonia) at another site, HRM-3 (Houston Regional Monitoring network, EPA site 48-201-0803) located 24km NW from the La Porte site are also available (Dasgupta et al., 2005).

An important feature of chemical mechanisms in evaluating radical sources and sinks is the role of NO. Usually, the interconversion of HO_2 into OH via reaction with NO dominates OH production. For this reason, the sensitivity and accuracy of NO measurements are crucial as well as those of VOCs. VOCs both consume OH radicals and generate OH and HO_2 radicals; thus, the VOC measurements produced by three gas chromatography (GC) systems and a proton-transfer-reaction mass spectroscopy (PTR-MS) system for compounds listed in Table 2-3 will be used in this study. The three GC

systems used during the TexAQS-2000 study are a GC with a flame ionization detector (GC-FID), a GC with a quadrupole ion trap mass spectrometer (GC-ITMS), a GC with a linear quadrupole mass spectrometer (GC-QMS). For details, refer to Kuster et al., (2004) for the GC systems, and Karl et al. (2003) and Lindinger et al. (1998) for the PTR-MS system. In addition to basic meteorological data, photolysis frequencies were also measured by the National Oceanic and Atmospheric Administration (NOAA) using actinic flux spectroradiometry (Shetter and Muller, 1999). Brief descriptions of TexAQS-2006 data will be given where those data are referenced in subsequent chapters.

Table 2-2. Measured species relevant to HOx with measurement techniques, time resolution and detection limits, and accuracies during TexAQS-2000.

Measured species	Measurement technique[a]	Time resolution[b]	Detection limit	Accuracy[c]	References
inorganic					
O_3	chemiluminescence	1 min	1 ppb[d]	2%[d]	Williams et al., 2006
	UV absorption	1 min	1 ppb	2%	Williams et al., 2006
NO	chemiluminescence	1 min	5 ppt[d]	5%[d]	Thornton et al., 2003
NO_2	photolysis/ chemiluminescence	1 min	20 ppt[d]	7%[d]	Thornton et al., 2003
CO	-	1 min	-	-	-
SO_2	-	1 min	-	-	-
HONO	DOAS	variable	0.2 ppb[e]	6%[f]	Stutz et al., 2004a,b
HOx					
OH	LIF	1 min	0.012 ppt[g]	40% (at 2 σ)	Martinez et al., 2002, Faloona et al., 2004
HO_2	LIF	1 min	0.05 ppt[g]	40% (at 2 σ)	Martinez et al., 2002, Faloona et al., 2004
VOCs					
	GC-FID	5 min (15 min)	1-5 ppt	10%	Kuster et al.,2004
	GC-ITMS	10 min (1 hr)	1-10 ppt	20%	Jobson et al., 2004; Kuster et al., 2004
	GC-QMS	5 min (33 min)	1-10 ppt	10%	Riemer and Apel, 2001; Kuster et al., 2004
	PTR-MS	2-5 s (1 - 6 min)	20-100 ppt	20%	Karl et al., 2003; Kuster et al., 2004
HCHO[h]	DOAS[i]	variable (5-30 min)	1.6 ppb[e]	< 6%[f]	Dasgupta et al., 2005; Stutz et al., 2004b
	Hantzsch reaction/ fluorometry	3 min (~10 min)	70 ppt	-	Dasgupta et al., 2004; Li et al., 2004
PANs	GC/electron capture detection	30-60 s (15 min)	15 ppt	15-25%	Roberts et al., 2002, 2003

a: DOAS = differential optical absorption spectroscopy; LIF = laser-induced fluorescence; GC-FID = gas chromatography (GC) with a flame ionization detector; GC-ITMS = GC with a quadrupole ion trap mass spectrometer (MS); GC-QMS = GC with a linear quadrupole MS; PTR-MS = proton-transfer-reaction MS. **b**: numbers separately given in the parentheses are measurement intervals very different from their integration times. **c**: accuracies for VOCs and PANs depend on specific compounds measured. **d**: Geyer et al., 2003. **e**: Alicke et al., 2002. **f**: Alicke et al., 2003. **g**: Ren et al., 2003. **h**: HCHO was also measured by the PTR-MS. **i**: NO_3 was also measured by the DOAS (Geyer et al., 2003).

Table 2-3. Hydrocarbons measured by the three GC systems and PTR-MS system during TexAQS-2000.

Alkenes (19)		Alkanes (20)		Oxygenates (13)	
ethene	a	ethane	a	formaldehyde	d
tetrachloroethylene	b	methylchloroform	b	methanol	d
propene	a,d	propane	a	acetaladehyde	b,d
methylpropene	a	i-butane	a	propanal	b
1-butene	a	n-butane	a	acrolein	c
2-methyl-1-butene	a	2,2-dimethylbutane	a	methacrolein	c
3-methyl-1-butene	a	i-pentane	a,b	acetone	b,d
T-2-butene	a	n-pentane	a,b	MEK (2-butanone)	b
C-2-butene	a	2-methylpentane	b	MVK	c
2-methyl-2-butene	a,b	3-methylpentane	a,b	3-methyl-2-butanone	c
1-pentene	a,b	hexane	a,b	2-pentanone	c
T-2-pentene	a,b	2,2,4-trimethylpentane	b	3-pentanone	c
C-2-pentene	a,b	n-heptane	b	MTBE	c
cyclopentene	a	octane	b	Aromatics (10)	
1-hexene	b	nonane	b	benzene	b,c,d
1,3-butadiene	b,c	decane	b	toluene	b,c,d
isoprene	a,b,c,d	cyclopentane	b	ethylbenzene	b
α-pinene	b	methylcyclopentane	a,b	m/p-xylene	b
limonene	b	cyclohexane	b	o-xylene	b
Alkynes (3)		methylcyclohexane	b	styrene	b,d
acetylene	a	Cl markers (2)		1,2,4-trimethylbenzene	b
propyne	a	CMBO[e]	c	1,2,3-trimethylbenzene	b
1-butyne	a	CMBA[f]	c	1,3,5-trimethylbenzene	b
				(1-methylethyl)benzene	b

a: GC-FID, **b**: GC-ITMS , **c**: GC-QMS, **d**: PTR-MS, **e**: 1-chloro-3-methyl-3-butene-2-one, **f**: chloromethylbutenal.

2.3.3. Characterization of Ambient Data: Screening Ambient Data to Select Cases for Testing the Hypotheses

Three hypotheses will be investigated to explain the radical sinks and sources that lead to rapid increases in HOx in the morning at the La Porte site during the TexAQS-2000 study: (1) aromatics chemistry, (2) alkene chemistry, and (3) chlorine chemistry. The general strategies and the processes of selecting cases for testing the hypotheses will be described in this section.

2.3.3.1. Selection of modeling cases for testing three hypotheses

In selection of cases for testing the hypotheses, four criteria are applied in common: (1) the availability of measurements including major inorganic compounds (O_3, NO, NO_2, CO, SO_2) and hydrocarbons (typically abundant alkenes and alkanes: ethene, propene, ethane, propane, i-/n-butane, i-/n-pentane; most of these compounds were measured by the GC-FID); (2) the presence of abrupt increases in HOx which can be objectively confirmed by simultaneous presence of abrupt increases in NO_2/NO ratio; (3) the presence of relatively high ozone levels (e.g., above 80 ppb); (4) meteorological conditions of relatively low wind speeds in the morning. Criteria for selecting cases for each specific hypothesis are as follows.

Cl emissions and chemistry:

- Relatively high levels of Cl-markers (1-chloro-3-methyl-3-butene-2-one (CMBO) and chloromethylbutenal (CMBA)) in the morning
- Presence of a rapid ozone formation event
- Relatively high levels of alkanes and/or alcohols

Alkene chemistry:

- Relatively high concentrations of alkenes
- Relatively high HCHO concentrations

Aromatics chemistry:

- Relatively high concentrations of aromatics

Table 2-4 shows the detailed features of the TexAQS data used in the selection of test cases. CMBO and CMBA concentrations measured with the GC-QMS system and Cl-atom levels estimated by Riemer and Apel (2001) show August 25 and August 30 - 31, 2000 are possible candidates for testing the contribution of Cl chemistry to increasing HOx radicals. However, in the early morning of August 30, 2000, there was no clear steep increase in HOx.

Wind speeds were relatively slow on August 25 and September 5, 2000. In addition, hourly ozone levels above 100 ppb were detected on both days between 10:00 and 11:00 CST. Major alkenes and alkanes measured by the GC-FID system are available on all three days: August 25 and 31, September 5, 2000. However, measurements of NO are not available between 2:15 and 8:35 CST on August 31, 2000, and NO and NO_2 data are not available between 7:00 and 8:50 CST on September 5, 2000. On September 4, 2000, very steep increases in OH and HO_2 were detected (not shown); however, GC-FID data for major alkenes and alkanes and PTR-MS data for HCHO and CH_3OH are not available on this day. Thus, this interesting day is excluded from further analysis. Unfortunately for testing aromatics chemistry, no days recorded aromatics concentrations in the range of 15+ ppb toluene. Overall, morning hours of

August 25 and September 5, 2000 are best time windows for more detailed studies (Table 2-4). However, on September 5, 2000, measurements of both NO and NO_2 are missing between 7:00 and 8:50 CST (Table 2-4), which is a serious obstacle to using this date as a testing case. Thus, in this dissertation, only the date of August 25, 2000 is used as a case study.

Table 2-4. A summary of TexAQS-2000 data used in selecting cases for testing the three hypotheses.

Date	Missing measurements	Max (O_3) (ppb)	Presence of rapid changes in NO_2/NO ratio	Time window of non-zero CMBO or CMBA	Hypotheses to test
8/20	HOx (0:30-7:00, 10:30-13:00 CST)	74.1	-	5:02 - 10:05 CST	-
8/21	GC-FID data (until 7:10), GC-ITMS data (until 8:25)	122.4	6:30 - 8:00 CST	5:21 - 13:10	Cl
8/22	HOx (4:30-8:40, 10:45-12:00), GC-FID data (until 12:10)	68.1	-	4:34 - 9:39	-
8/23	-	83.8	7:15 - 8:00 (complex changes in NO)	7:10 - 10:34; no measurement until 7:10	Cl
8/24	OH (until 14:00), GC-FID data (until 7:40)	136.4	-	-	-
8/25	NO_2 (7:18-45, 12:18-22:45), NO (7:37-44)	136.3	7:30 - 8:00	6:06-8:23	Cl/alkene
8/26	no GC-FID data	80.4	-	-	-
8/27	-	68.4	-	no measurement	-
8/28	-	61.6	-	no measurement	-
8/29	HOx (9:45-11:55, 14:00-17:40), GC-FID data (until 8:40)	98.5	-	17:09-18:53; no measurment until 10:05	-
8/30	PTR-MS HCHO (until 13:25)	212.6	7:35-50, 9:30-40, 10:10-40 (unclear)	5:19 -14:47	Cl/alkene
8/31	NO_2 (2:15-8:36), GC-FID data (until 7:25)	198.9	7:30 - 8:40 (unclear); 9:50 - 10:05	7:24 -14:08	Cl/alkene
9/1	-	98.6	-	6:43 -10:08	Cl
9/2	-	133.5	-	-	-
9/3	-	125.0	-	-	-

9/4	no GC-FID data	116.7	-	-	-
9/5	NO and NO_2 (7:00-8:50), GC-FID data (until 7:10)	130.4	7:00 - 8:50 (unclear), 9:00-40	5:52-9:48	alkene/Cl
9/6	HOx (7:00-9:00), GC-FID data (8:45-11:00)	104.9	-	5:04-7:54	-
9/7	-	76.1	-	5:54-6:32	-
9/8	-	51.7	-	6:09-10:38	-
9/9	-	65.7	-	6:24-9:14	-
9/10	-	65.5	-	5:35-9:31	-
9/11	-	41.2	-	6:27-7:38	-

2.3.4. Ambient Simulation for Studying Radical Chemistry

Ambient simulations combined with chamber simulations are used in this dissertation to examine the consistency between observational data and free radical sources and sinks, for conditions relevant to the Texas Gulf Coast. The chemical mechanisms used in the analysis include SAPRC-07 as well as CB-05 (Carter, 2009; Yarwood et al., 2005; Faraji et al., 2007). The mechanisms are described in more detail in Chapter 3 and Chapter 4. Simulated concentrations will be compared with measured concentrations of OH, HO_2 and O_3, and sensitivity analyses such as investigating changes in radical sinks and sources in response to each hypothesis will be performed.

2.4. SUMMARY

In this chapter, a combined approach to mechanism evaluation, using both chamber simulations and ambient simulations was presented. In subsequent chapters, each of the hypotheses proposed in this study are described: aromatics chemistry (chapter 3), alkene chemistry (chapter 4), and chlorine chemistry (chapter 5).

2.5. REFERENCES

Alicke, B., Geyer, A., Hofzumahaus, A., Holland, F., Konrad, S., Pätz, H.W., Schäfer, J., Stutz, J., Volz-Thomas, A., Platt, U., 2003. OH formation by HONO photolysis during the BERLIOZ experiment. Journal of Geophysical Research 108(D4), 8247, doi:10.1029/2001JD000579.

Alicke, B., Platt, U., Stutz, J., 2002. Impact of nitrous acid photolysis on the total hydroxyl radical budget during the Limitation of Oxidant Production/Pianura Padana Produzione di Ozono study in Milan. Journal of Geophysical Research 107(D22), 8196, doi:10.1029/2000JD000075.

Atkinson, R., 2000. Atmospheric chemistry of VOCs and NOx. Atmospheric Environment 34, 2063-2101.

Bloss, C., Wagner, V., Bonzanini, A., Jenkin, M.E., Wirtz, K., Martin-Reviejo, M., Pilling, M.J., 2005. Evaluation of detailed aromatic mechanisms (MCMv3 and MCMv3.1) against environmental chamber data. Atmospheric Chemistry and Physics 5, 623-639. (http://www.atmos-chem-phys.net/5/623/2005/acp-5-623-2005.html)

Calvert, J. G., Atkinson, R., Becker, K.H., Kamens, R.M., Seinfeld, J.H., Wallington, T.J., Yarwood, G., 2002. The Mechanisms of Atmospheric Oxidation of Aromatic Hydrocarbons, Oxford University Press, New York, 566p.

Calvert, J. G., R. Atkinson, R., J. A. Kerr, J.A., S. Madronich, S., G. K. Moortgat, G.K., T. J. Wallington, T.J., Yarwood, G., 2000. The Mechanisms of Atmospheric Oxidation of Alkenes, Oxford University Press, New York, 552p.

Carter, W.P.L., 2000. Documentation of the SAPRC-99 chemical mechanism for VOC reactivity assessment, Report to the California Air Resources Board, Contracts 92-329 and 95-308, May 8. Available at http://www.cert.ucr.edu/~carter/absts.htm#saprc99.

Carter, W.P.L., 2004. Evaluation of a gas-phase atmospheric reaction mechanism for low NOx conditions. Final Report to California Air Resources Board Contract No. 01-305, May 5. Available at http://www.cert.ucr.edu/~carter/absts.htm#lnoxrpt.

Carter, W.P.L., 2009. Development of the SAPRC-07 chemical mechanism and updated ozone reactivity scales. Final Report to the California Air Resources Board Contract No. 03-318. Available at http://www.engr.ucr.edu/~carter/SAPRC/.

Carter, W.P.L., Atkinson, R., 1987. An experimental study of incremental hydrocarbon reactivity. Environmental Science & Technology 21, 670-679.

Carter, W.P.L., Atkinson, R., Winer, A.M., Pitts, J.N., 1982. Experimental investigation of chamber-dependent radical sources. International Journal of Chemical Kinetics 14, 1071-1103.

Carter, W.P.L., Cocker, D.R., Fitz, D.R., Malkina, I.L., Bumiller, K., Sauer, C.G., Pisano, J.T., Bufalino, C., and Song, C., 2005. A new environmental chamber for evaluation of gas-phase chemical mechanisms and secondary aerosol formation. Atmospheric Environment, 39, 7768-7788.

Carter, W.P.L., Luo, D., Malkina, I.L., Fitz, D., 1995a. The University of California, Riverside Environmental Chamber Data Base for Evaluating Oxidant Mechanism. Indoor Chamber Experiments through 1993. Report submitted to the U. S. Environmental Protection Agency, EPA/AREAL, Research Triangle Park, NC, March 20. Available at http://www.engr.ucr.edu/~carter/pubs/.

Carter, W.P.L., Luo, D., Malkina, I.L., Pierce, J.A., 1995b. Environmental chamber studies of atmospheric reactivities of volatile organic compounds. Effects of varying chamber and light source. Final Report to National Renewable Energy Laboratory, Contract XZ-2-12075, Coordinating Research Council, Inc., Project M-9, California Air Resources Board, Contract A032-0692, and South Coast Air Quality Management District, Contract C91323, March 26. Available at http://www.cert.ucr.edu/~carter/absts.htm#explrept.

Carter, W.P.L., Lurmann, F.W., 1991. Evaluation of a detailed gas-phase atmospheric reaction mechanism using environmental chamber data. Atmospheric Environmnet 25A, 2771-2806.

Carter, W.P.L., Pierce, J.A., Luo, D., Malkina, I.L., 1995. Environmental chamber study of maximum incremental reactivities of volatile organic compounds. Atmospheric Environment 29, 2499-2511.

Chen, S., Ren, X., Mao, J., Chen, Z., Brune, W.H., Lefer, B., Rappenglück, B., Flynn, J., Olson, J., Crawford, J.H., 2009. A comparison of chemical mechanisms based on TRAMP-2006 field data, Atmospheric Environment (2009), doi: 10.1016/j.atmosenv.2009.05.027.

Dasgupta, P.K., Li., J., Zhang, G., Luke, W.T., McClenny, W. A., Stutz, J., Fried, A., 2005. Summertime ambient formaldehyde in five U.S. metropolitan areas: Nashville, Atlanta, Houston, Philadelphia, and Tampa. Environmental Science & Technology 39, 4767-4783.

Dodge, M.C., 2000. Chemical oxidant mechanisms for air quality modeling: critical review. Atmospheric Environment 34, 2103-2130.

Faraji, M., Heo, G., Kimura, Y., McDonald-Buller, E., Allen, D., Yarwood, G., Whitten, G., Carter, W., 2007. Comparison of the Carbon Bond and SAPRC photochemical

mechanisms. Report to the Texas Commission on Environmental Quality, Work Order No. 582-04-65588-07, August, 2007.

Faloona, I.C., Tan, D., Lesher, R.L., Hazen, N.L., Frame, C.L., Simpas, J.B., Harder, H., Martinez,M., Di Carlo, P., Ren, X., Brune, W.H., 2004. A laser induced fluorescence instrument for detecting tropospheric OH and HO_2: characteristics and calibration. Journal of Atmospheric Chemistry 47, 139–167.

Gery, M.W., Whitten, G.Z., and Killus, J.P., Dodge, M.C., 1989. A photochemical kinetics mechanism for urban and regional scale computer modeling. Journal of Geophysical Research 94(D10), 12,925-12,956.

Geyer, A., Alike, B., Ackermann, R., Martinez, M., Harder, H., Brune, W., Di Carlo, P., Williams, E., Jobson, T., Hall, S., Shetter, R., Stutz, J., 2003. Direct observations of daytime NO_3: Implications for urban boundary layer chemistry. Journal of Geophysical Research 108(D12), 4368, doi:10.1029/2002JD002967.

Gómez Alvarez, E., Viidanoja, J., Muñoz, A., Wirtz, K., Hjorth, J., 2007. Experimental confirmation of the dicarbonyl route in the photo-oxidation of toluene and benzene. Environmental Science & Technology 41, 8362-8369.

Hess, G.D., Carnovale, F., Cope, M.E., Johnson, G.M., 1992. The evaluation of some photochemical smog reaction mechanisms - I. Initial composition effects. Atmospheric Environment 26A, 625-641.

Jeffries, H., Kessler, M., 1999. A User's Guide to MEval Solver Program for Morphoecule Mechanisms, a Part of Morpho, University of North Carolina, Chapel Hill, NC.

Jobson, B. T., Berkowitz, C. M., Kuster, W. C., Goldan, P. D., Williams, E. J., Fesenfeld, F. C., Apel, E. C., Karl, T., Lonneman, W. A., Riemer, D., 2004. Hydrocarbon source signatures in Houston, Texas: Influence of the petrochemical industry. Journal of Geophysical Research 109, D24305, doi:10.1029/2004JD004887.

Karl, T., Jobson, T., Kuster, W.C., Williams, E., Stutz, J., Shetter, R., Hall, S.R., Goldan, P., Fehsenfeld, F., W. Lindinger, W., 2003. Use of proton transfer-reaction mass spectrometry to characterize volatile organic compound sources at the La Porte super site during the Texas Air Quality Study. Journal of Geophysical Research 108(D16), 4508, doi:10.1029/2002JD003333.

Killus, J. P., Whitten, G. Z., 1990. Background reactivity in smog chambers. International Journal of Chemical Kinetics, 22, 547-575.

Kuster, W.C., Jobson, B.T., Karl, T., Riemer, D., Apel, E., Goldan, P.D., Fehsenfeld, F.C., 2004. Intercomparison of volatile organic carbon measurement techniques

and data at La Porte during the TexAQS2000 Air Quality study. Environmental Science & Technology, 38, 221-228.

Li, J., Dasgupta, P.K., Luke, W., 2004. Measurement of gaseous and aqueous trace formaldehyde: Revisiting the pentanedione reaction and field applications. Analytica Chimica Acta 531, 51-68.

Lindinger, W., Hansel, A., Jordan, A., 1998. On-line monitoring of volatile organic compounds at pptv levels by means of Proton-Transfer-Reaction Mass Spectrometry (PTR-MS): Medical applications, food control and environmental research. International Journal of Mass Spectrometry and Ion Processes, 173, 191-241.

Martinez, M., Harder, H., DiCarlo, P., Brune, W.H., Hall, S.R., Shetter, R.E., Williams, E.J., Kuster, W., Jobson, B.T., 2002. OH and HO_2 concentrations, production and loss rates at the La Porte site during TexAQS 2000, Fourth Conference on Atmospheric Chemistry of the American Meteorological Society, Orlando, January 2002. (Available at http://ams.confex.com/ams/annual2002/techprogram/paper_32451.htm)

Paulson, S.E., Flagan, R.C., Seinfeld, J.H., 1992. Atmospheric photo-oxidation of isoprene: part I. The hydroxyl radical and ground state atomic oxygen reactions. International Journal of Chemical Kinetics 24, 79–101.

Rappenglück, B., Lefer, B., 2007. TRAMP data analysis and radical chemistry study, final report to Houston Advanced Research Center (HARC), TERC project H86, December 2007. (Available at http://files.harc.edu/Projects/AirQuality/Projects/H086/H086FinalReport.pdf)

Ren, X., Harder, H., Martinez, M., Lesher, R.L., Oliger, A., Shirley, T., Adams, J., Simpas, J.B., Brune, W.H., 2003. HOx concentrations and OH reactivity observations during the PMTACS-NY 2001 campaign in New York City. Atmospheric Environment 37, 3627–3637.

Riemer, D. D.; Apel, E. C.,2001. Confirming the presence and extent of oxidation by Cl in the Houston, Texas urban area using specific isoprene oxidation products as tracers. Final report to the Texas Natural Resource Conservation Commission, Contract 582034743, University of Miami, FL. (Available at http://www.tceq.state.tx.us/assets/public/implementation/air/am/contracts/reports/oth/ConfirmingPresenceandExtentOfOxidationByCI.pdf)

Roberts, J. M., Flocke, F., Stroud, C.A., Hereid, D., Williams, E.J., Fehsenfeld, F.C., Brune, W., Martinez, M., Harder, H., 2002. Ground-based measurements of PANs during the 1999 Southern Oxidants Study Nashville intensive. Journal of Geophysical Research 107(D21), 4554, doi:10.1029/2001JD000947.

Roberts, J.M., Jobson, B.T., Kuster, W., Goldan, P., Murphy, P., Williams, E., Frost, G., Riemer, D., Apel, E., Stroud, C., Wiedinmyer, C., Fehsenfeld, F., 2003. An examination of the chemistry of peroxycarboxylic nitric anhydrides and related volatile organic compounds during Texas Air Quality Study 2000 using ground-based measurements. Journal of Geophysical Research 108(D16), 4495, doi:10.1029/2003JD003383.

Rohrer, F., Bohn, B., Brauers, T., Brüning, D., Johnen, F.-J., Wahner, A., Kleffmann, J., 2005. Characterisation of the photolytic HONO-source in the atmosphere simulation chamber SAPHIR. Atmospheric Chemistry and Physics 5, 2189–2201.

Russell, A., Dennis, R., 2000. NARSTO critical review of photochemical models and modeling. Atmospheric Environment 34, 2283-2324.

Ryerson, T.B., Trainer, M., Angevine, W.M., Brock, C.A., Dissly, R.W., Fehsenfeld, F.C., Frost, G.J., Goldan, P.D., Holloway, J.S., Hubler, G., Jakoubek, R.O., Kuster, W.C., Neuman, J.A., Nicks Jr., D. K., Parrish, D.D., Roberts, J.M., Sueper, D.T., Atlas, E.L., Donnelly, S.G., Flocke, F., Fried, A., Plotter, W.T., Schauffler, S., Stroud, V., Weinheimer, A.J., Wert, B.P., Wiedinmyer, C., 2003. Effect of petrochemical industrial emissions of reactive alkenes and NOx on tropospheric ozone formation in Houston, Texas. Journal of Geophysical Research 108(D8), 4249, doi:10.1029/2002JD003070.

Seinfeld, J.H., Pandis, S.N., 1998. Atmospheric Chemistry and Physics: From Air Pollution to Climate Change, Wiley-Interscience, New York, 1326p.

Shetter, R.E., Müller, M., 1999. Photolysis frequency measurements using actinic flux spectroradiometry during the PEM-Tropics mission: Instrumentation description and some results. Journal of Geophysical Research 104(D5), 5647-5661.

Simonaitis, R., Meagher, J., Bailey, E.M., 1997. Evaluation of the condensed Carbon Bond Mechanism against smog chamber data at low VOC and NOx Concentrations. Atmospheric Environment 31, 27–43.

Stutz, J., Alicke, B., Ackermann, R., Geyer, A., Wang, S., White, A.B., Williams, E.J., Spicer, C.W., Fast, J.D., 2004a. Relative humidity dependence of HONO chemistry in urban areas. Journal of Geophysical Research 109, D03307, doi:10.1029/2003JD004135.

Stutz, J., Alicke, B., Ackermann, R., Geyer, A., White, A., Williams, E., 2004b. Vertical profiles of NO_3, N_2O_5, O_3, and NOx in the nocturnal boundary layer: 1. Observations during the Texas Air Quality Study 2000, Journal of Geophysical Research 109, D12306, doi:10.1029/2003JD004209.

Wert, B.P., Trainer, M., Fried, A., Ryerson, T.B., Henry, B., Potter, W., Angevine, W.M., Atlas, E., Donnelly, S.G., Fehsenfeld, F.C., Frost, G.J., Goldan, P.D., Hansel, A.,

Holloway, J.S., Hubler, G., Kuster, W.C., Nicks Jr., D.K., Neuman, J.A., Parrish, D.D., Schauffler, S., Stutz, J., Sueper, D.T., Wiedinmyer, C., Wisthaler, A., 2003. Signatures of terminal alkene oxidation in airborne formaldehyde measurements during TexAQS 2000. Journal of Geophysical Research 108(D3), 4104, doi:10.1029/2002JD002502.

Whitten, G. Z., 1983. The chemistry of smog formation: A review of current knowledge. Environmental International 9, 447-463.

Williams, E.J., Fehsenfeld, F.C., Jobson, B.T., Kuster, W.C., Goldan, P.D., Stutz, J., McClenny, W.A., 2006. Comparison of Ultraviolet Absorbance, Chemiluminescence, and DOAS Instruments for Ambient Ozone Monitoring. Environmental Science & Technology 40(18), 5755 – 5762.

Yarwood, G., Rao, S., Yocke, M., Whitten, G.Z., 2005. Updates to the Carbon Bond mechanism: CB05, Report to the U.S. Environmental Protection Agency, December. (Available at http://www.camx.com/publ/pdfs/CB05_Final_Report_120805.pdf)

Zádor, J., Turányi, T., Wirtz, K., Pilling, M.J. (2006). Measurement and investigation of chamber radical sources in the European Photoreactor (EUPHORE). Journal of Atmospheric Chemistry 55, 147-166.

Chapter 3: Aromatics Chemistry as a Sink and Source of Radicals

This chapter is based on a manuscript submitted for publication in A*tmospheric Environment*., titled "Evaluation of Carbon Bond 05 (CB05) toluene oxidation mechanisms using environmental chamber simulations."

3.1. INTRODUCTION

Aromatic compounds such as toluene and xylenes are important in urban atmospheres due to their abundance and relatively high reactivities (Calvert et al., 2002). Toluene is emitted as part of automobile exhaust and from solvents, and is moderately reactive in the atmosphere (i.e., slightly less reactive towards the hydroxyl radical (OH) than ethene), but its reaction products such as dicarbonyls and cresols are more reactive than toluene itself (Calvert et al., 2002). Dicarbonyls such as glyoxal ($(CHO)_2$) and methylglyoxal ($CH_3C(O)CHO$) formed from toluene by fragmentation of the aromatic ring can act as a radical source (Calvert et al., 2002; Yu et al., 1997; Volkamer et al., 2001, 2005; Gómez Alvarez et al., 2007; Arey et al., 2009) although the fates of unsaturated γ-dicarbonyls such as 1,4-butendial ($CH(O)CH=CHCHO$) and 4-oxo-2-pentenal ($CH(O)CH=CHC(O)CH_3$) are still uncertain (Bierbach et al., 1994; Forstner et al., 1997; Liu et al., 1999; Tang and Zhu, 2005; Xiang et al., 2007). Relatively rapid NOx depletion is observed in the oxidation of toluene and its products (Killus and Whitten, 1982; Klotz et al., 1998). Cresols (mainly o-cresol) constitute nearly 20% of toluene products on a mass basis (Smith et al., 1998; Klotz et al., 1998), and rapidly react with NO_3 (Carter et al., 1981; Calvert et al., 2002). Thus, cresols and possibly other products of toluene oxidation could significantly deplete NOx and modulate NO/HO_2 ratios, and, as a result, could affect maximum ozone concentrations and fates of radicals.

Faraji et al. (2008) showed that two condensed mechanisms widely used in the United States, the Carbon Bond IV (CB-IV) and Statewide Air Pollution Research Center (SAPRC-99) mechanisms, lead to predictions of peak O_3 concentrations that differed by as much as 40 ppb for Houston, Texas; the NOx sensitivities of the two mechanisms also differed. Faraji et al. (2008) attributed these different model predictions to differences in the rate coefficient of reaction OH + NO_2 = HNO_3, production of aldehydes as radical sources, and chemistries of aromatics, especially mono-substituted aromatics such as toluene. Further analysis of CB-IV (the OTAG version developed in 1996; Gery et al., 1989; ENVIRON, 2008), SAPRC-99 (Carter, 2000) and CB05 (Yarwood et al., 2005) using chamber simulations indicates that CB05's descriptions of mono-substituted aromatic compounds retain differences with SAPRC-99 (Faraji et al., 2007; Figure 3-1).

In this study, simulations of environmental chamber data have been carried out (1) to re-evaluate the original toluene mechanism in CB05 (hereafter, referred to as "Base"), (2) to evaluate a new toluene mechanism proposed by Whitten et al. (2009) (hereafter, referred to as "UNClite") and (3) to compare the performance of CB05 with the UNClite toluene mechanism (CB05-UNClite) and that of CB05 with the Base toluene mechanism (CB05-Base) using chamber experiments produced at multiple environmental chambers, especially, low-NOx experiments where the NOx level is more relevant to ambient conditions. The performance of CB05-Base and CB05-UNClite will be evaluated using criteria such as maximum ozone concentrations, NOx crossover times, and cresol concentrations.

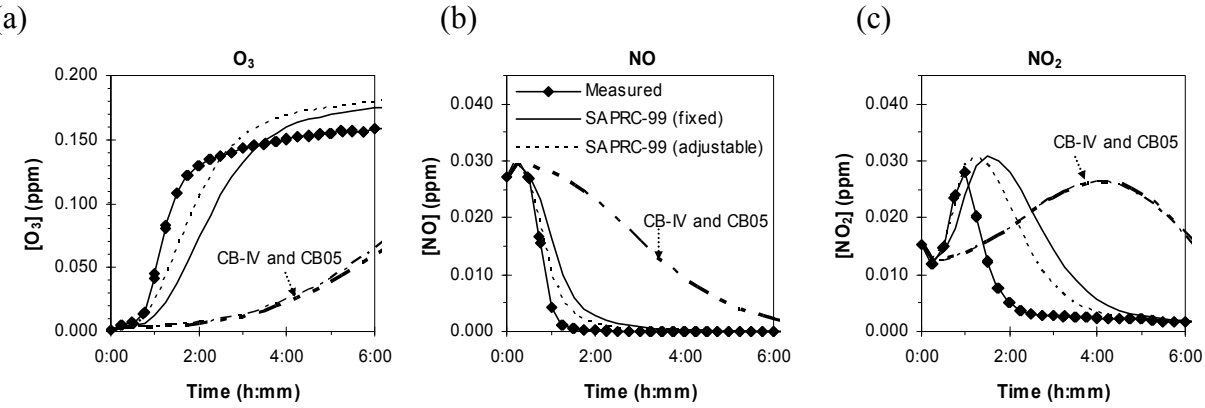

Figure 3-1. Under-predictions of ozone formation and NOx depletion rates by CB-IV and CB05 against a low-NOx environmental chamber experiment, EPA210A: (a) O_3, (b) NO, (c) NO_2.

Note: simulation results for the fixed and adjustable versions of SAPRC-99 (Carter, 2000) are also presented for comparison purposes.

3.2. TOLUENE OXIDATION MECHANISMS

3.2.1. Overview of Toluene Oxidation Mechanisms

Toluene is oxidized in the atmosphere mainly by OH as shown in Figure 3-2. The first step of the toluene oxidation is H-abstraction (~10%) or OH-addition forming OH-toluene adducts (~90%) (Perry et al., 1977; Markert and Pagsberg, 1993; Molina et al., 1999; Calvert et al., 2002, Atkinson and Arey, 2003), mostly at the ortho position (Kenley et al., 1981; Andino et al., 1996; Suh et al., 2002, Johnson et al., 2005, Andino and Vivier-Bunge, 2008). Under ambient conditions, the OH-toluene adducts further react with O_2 rather than decompose to reactants, OH and toluene (Perry et al., 1977; Suh et al., 2003); OH-toluene adducts may non-negligibly react with NO_2 when the NO_2 concentration is extremely high (~500 ppb level) such as in high-NOx chamber

experiments, but generally this pathway is not important under ambient conditions (Knispel et al., 1990; Bohn, 2001; Koch et al., 2007). Addition of O_2 to the aromatic ring results in aromatic peroxy radicals, OH-toluene-O_2 radicals (Molina et al., 1999; Bohn, 2001; Andino et al., 1996; Suh et al., 2003), and H-abstraction by O_2 results in ring-retaining products, cresols, with yield of ~20% (Klotz et al., 1998; Smith et al., 1998; Calvert et al., 2002). The aromatic peroxy radicals react primarily with O_2 rather than with NO, except when NO exists at concentrations of hundreds of ppb (Andino et al., 1996; Bohn, 2001), and cyclize to form bicyclic radicals as proposed by Darnall et al. (1979) by anchoring the terminal O of O-O to the aromatic ring (Andino et al., 1996; Suh et al., 2003; Figure 3-2). The aromatic bicyclic radicals further react with O_2 and form (secondary) aromatic peroxy radicals. Then, the aromatic peroxy radicals react with peroxy radicals (HO_2 or RO_2) or oxidize NO into NO_2 and form aromatic alkoxy radicals (Andino et al., 1996; Suh et al., 2003; Calvert et al., 2002).

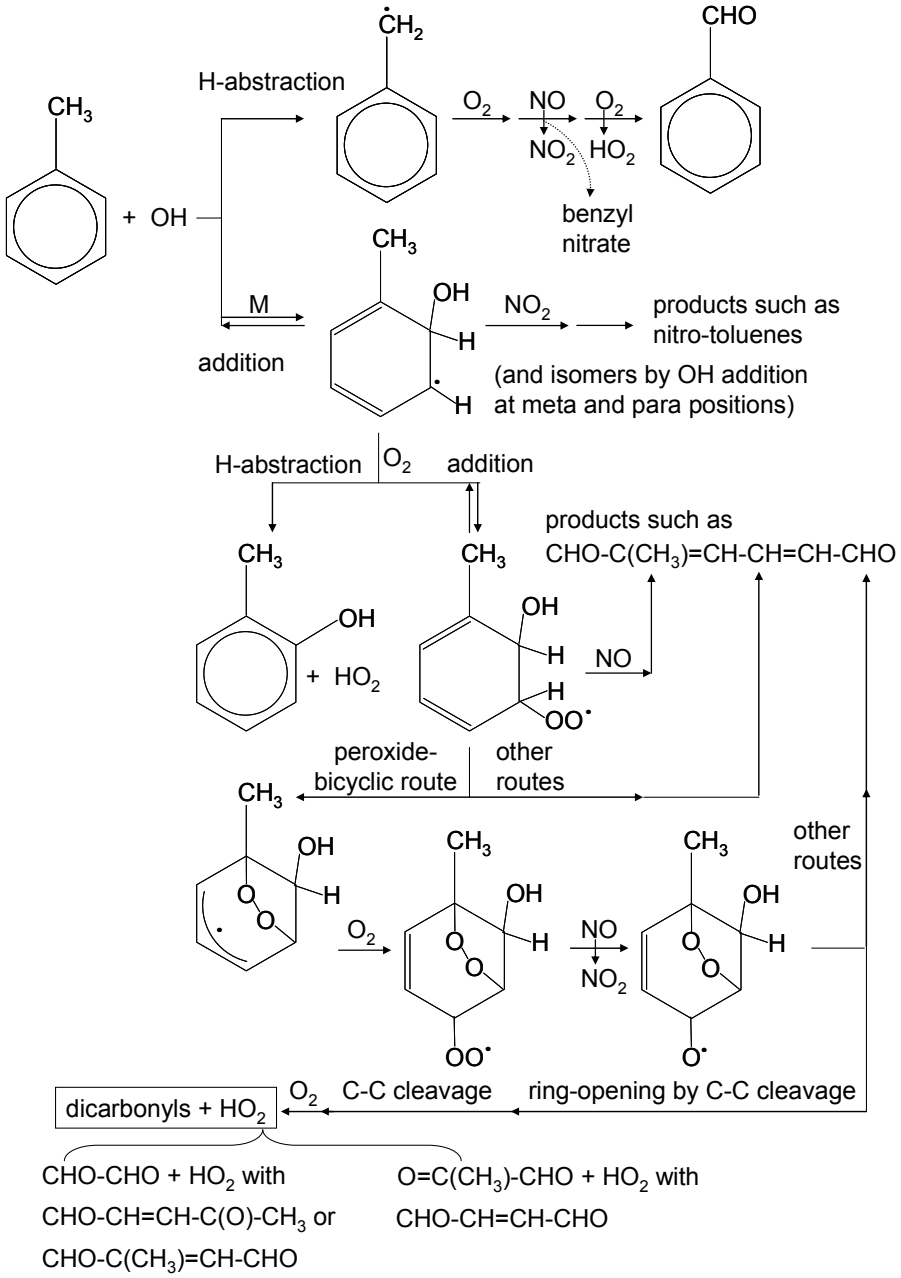

Figure 3-2. Toluene oxidation pathways leading to major products such as cresols and dicarbonyls. (Calvert et al., 2002; Atkinson and Arey, 2003; Andino et al., 1996; Suh et al., 2003 and 2006; Hu et al., 2007; Arey et al., 2009)

3.2.2. Proposed Toluene Oxidation Mechanism for Use in CB05

Toluene oxidation mechanisms used in condensed mechanisms, CB-IV, CB05, SAPRC-99 and SAPRC-07, are highly condensed descriptions of toluene oxidation processes initiated by OH in the atmosphere (Gery et al, 1989; Yarwood et al., 2005; Carter 2000 and 2009). Condensed chemical mechanisms such as CB and SAPRC mechanisms focus on accurate predictions of regulatory species such as O_3 while using a limited number of reactions to avoid too much computational burden in 3-dimensional grid modeling for air quality applications. Furthermore, due to various uncertainties in our current understanding of toluene chemistry (Calvert et al., 2002; Atkinson and Arey, 2003; Andino and Vivier-Bunge, 2008; Arey et al., 2009), the additional usefulness of using highly detailed and explicit toluene oxidation mechanisms with a large number of reactions is not clear, particularly from a regulatory perspective. Under this situation, CB and SAPRC mechanisms' approach has been viewed as a practical approach to describe toluene oxidation processes in gridded photochemical models, although more explicit chemical mechanisms such as the Master Chemical Mechanism (MCM, http://mcm.leeds.ac.uk/MCM, Bloss et al., 2005a,b) could provide more detailed information about the fates of air pollutants in the atmosphere.

However, as our understanding of toluene chemistry advances, these condensed mechanisms need updating of their descriptions of toluene oxidation so that the chemical mechanisms are compatible with our best knowledge of toluene chemistry based on both experimental and theoretical studies. In response to recent updates of toluene chemistry, a new CB05 toluene mechanism was proposed by Whitten et al. (2009) based on the detailed toluene oxidation mechanism of Hu et al. (2007). Table 3-1 provides an

overview of this new mechanism, UNClite. Detailed listings of the mechanisms are provided in Appendix A.

As shown in Table 3-2, a low-NOx switch that controls the fraction of peroxy radicals (TO_2) formed from toluene (TOL) that react with NO and HO_2 is added in the UNClite mechanism. The operation of this low-NOx switch depends on the NO/HO_2 ratio and was designed to promote the reaction of TO_2 with HO_2 resulting in radical termination, when the NO/HO_2 ratio becomes less than around 20; above a NO/HO_2 ratio of 20, most of TO_2 will react with NO and contribute to creating radicals and ozone. A lower cresol yield than the yield in Base is used in the new toluene mechanism based on Calvert et al. (2002). UNClite uses 16 additional reactions to more explicitly describe degradation of cresols and dicarbonyls than the Base mechanism. In short, the modifications to CB05's toluene mechanism described above are targeting a more consistent and accurate description of peroxy radical chemistry and NOx sinks relevant to the toluene oxidation and the distribution of the primary oxidation products including cresols and dicarbonyls.

Table 3-1. Overview of two CB05 toluene mechanisms.

Mechanism ID	Base	UNClite
Cresol yield[a]	0.36	0.18
TO_2 yield[a]	0.56	0.65
Benzaldehye yield[a]	0.08	0.10
Reaction $TO_2 + HO_2$	not used	used
OH formation	not used	0.072
Strong NOx sinks	cresols	cresols, γ-dicarbonyls[b]
Number of reactions dedicated to toluene oxidation	10 (156[c])	26 (172[c])
References	Gery et al, 1989; Yarwood et al., 2005	Hu et al., 2007; Calvert et al., 2002

[a]Yield in reaction toluene and OH (TOL + OH). [b]Acyl peroxy radicals derived from ring-opening products (OPEN) are modeled to form peroxyacyl nitrates (OPAN) in UNClite. [c]The total number of reactions in CB05 including the reactions dedicated to toluene oxidation.

Table 3-2. Comparison of reactions involving the bicyclic peroxy radical (TO_2) between Base and UNClite[a]

Mechanism ID	Reaction	Rate coefficient
	R128	
Base	TOL + OH = 0.56 TO_2 + 0.36 (CRES + HO_2) + 0.08 (XO_2 + HO_2)	1.8×10^{-12}·Exp(355/T)
UNClite	TOL + OH = **0.65** TO_2 + **0.18** (CRES + HO_2) + **0.10** (XO_2 + HO_2) + **0.072 OH**	1.8×10^{-12}·Exp(355/T)
	R129	
Base	TO_2 + NO = 0.9 (NO_2 + HO_2 + OPEN) + 0.1 NTR	8.10×10^{-12}
UNClite	TO_2 + NO = **0.86** (NO_2 + HO_2 + OPEN) + **0.520 MGLY + 0.336 (FORM + CO + HO_2)** + **0.004 HO_2 + 0.14** NTR	**2.7**$\times10^{-12}$**·Exp(360/T)**[b]
	R130	
Base	TO_2 = CRES + HO_2	4.2[c]
UNClite	TO_2 + **HO_2** = no product[d]	**1.9**$\times10^{-13}$**·Exp(1300/T)**

[a]Differences between the two toluene mechanisms are shown in bold. XO_2: operator for NO-to-NO_2 conversion by peroxy radicals without generating carbon-containing products; NTR: organic nitrates; OPEN: unsaturated γ-dicarbonyls derived from aromatics; FORM: formaldehyde. [b]2.7×10^{-12}·Exp(360/T) at T = 298 K is 9.04 cm^3·$molecule^{-1}$·sec^{-1} which is larger than 8.10×10^{-12} cm^3·$molecule^{-1}$·sec^{-1} by 12%. [c]The rate constant for this reaction is in sec^{-1} rather than in cm^3·$molecule^{-1}$·sec^{-1}. [d]Products were not assigned for this reaction by assuming the major products will go into the aerosol phase.

3.3. ENVIRONMENTAL CHAMBER SIMULATION FOR TOLUENE MECHANISM EVALUATION

3.3.1. Overview of Environmental Chamber Simulation

Simulations of environmental chamber experiments have been used for over 20 years in the development and evaluation of comprehensive chemical mechanisms for air quality applications (Dodge, 2000; Gery et al., 1989; Carter, 2000 and 2009; Yarwood et al., 2005). In comparison to ambient data, chamber data are produced under relatively well controlled environmental conditions and can examine a range of conditions that are

not frequently encountered in ambient observations; however, chamber data also have limitations including chamber artifacts such as chamber-dependent radical sources, NOx offgasing, and light conditions possibly very different from ambient conditions (Dodge, 2000). Chamber simulations are particularly useful in evaluating a chemical mechanism for individual chemical components, and the focus of this work will be on evaluating the chemistry of toluene. The overall procedure of the chamber simulation is briefly stated here; for details, refer to Chapter 2 or to Carter and Lurmann (1991) and Carter (2000 and 2009).

First, chamber data appropriate for the purposes of evaluating the chemical mechanism should be obtained. Second, the chamber experiments should be evaluated for biases and uncertainties introduced by chamber artifacts. Characterizing chamber radical sources and NOx offgasing is usually the most important part of the chamber evaluation. In most cases, an auxiliary mechanism (commonly called a "wall mechanism") is constructed to describe chamber-specific reactions separately from the reactions in the chemical mechanism to be evaluated. Parameters in the auxiliary mechanism are determined by using direct measurements of those parameters or by modeling chamber characterization experiments such as CO-NOx and CO-air experiments (Carter et al., 2005). Third, the chemical mechanism is evaluated by comparing measured and simulated quantities such as the maximum O_3 concentration ($Max(O_3)$) or the amount of O_3 formation and NO oxidation ($\Delta(O_3\text{-NO})$) during the chamber simulation (Gery et al., 1989; Carter et al., 2000 and 2009; Yarwood et al., 2005). Using $Max(\Delta(O_3\text{-NO}))$ as a performance indicator has two advantages over using $Max(O_3)$. $\Delta(O_3\text{-NO})$ quantifies the amount of NO oxidation by photochemical processes even when there is no significant O_3 production (Carter and Atkinson, 1987) and reduces the effect of possible sampling error due to the reaction between O_3 and NO

in the sampling line from inside the chamber reactor to the O_3 measuring instrument. Therefore, both Max(O_3) and Max(Δ(O_3-NO)) are used as performance indicators in this work.

3.3.2. Environmental Chamber Data

A relatively large number of chamber experiments have been performed in the U.S. at various locations, including the University of North Carolina (UNC), and the University of California at Riverside (UCR) (Dodge, 2000; Carter, 2000 and 2009; Yarwood et al., 2005). Using chamber data produced under various conditions at multiple chambers is recommended to minimize the impacts of run-to-run variability and chamber artifacts such as the chamber-dependent radical source and NOx offgasing (Carter and Lurmann, 1991; Dodge, 2000, Carter et al., 2005). Thus, in this work, toluene chamber experiments of multiple chambers at UNC and UCR listed in Table 2-1 were used to evaluate the toluene mechanisms.

Two differently formatted chamber datasets, "SAPRC" dataset and "Morpho" dataset, were used in this study. The SAPRC dataset includes chamber data produced at various chambers at UCR and has been used for evaluating SAPRC mechanisms using the SAPRC software (Carter, 2009). The SAPRC software is the package of various programs for environmental simulations developed by Carter (Carter, 2000 and 2009; http://www.engr.ucr.edu/~carter/SAPRC/files.htm). The Morpho dataset includes chamber data produced at the UNC outdoor gas-phase chamber and has been used for evaluating CB mechanisms using the Morpho software. Morpho was developed at UNC (Jeffries and Kessler, 1999) and has been used mainly in evaluating CB mechanisms with the UNC chamber data (Yarwood et al., 2005).

All chamber experiments where blacklight-type lights were used as a chamber light source were excluded in this study to avoid the risk of incorporating into the evaluation photolysis reactions that occur at different rates under blacklight compared to ambient conditions. Blacklights as a chamber light source show different spectral characteristics from sunlight in the longer wavelength region that significantly affects some features of the aromatics chemistry and NO_3 photolysis (Carter et al., 1995 and 2005). These differences can be taken into account in the model simulations if the quantum yields and adsorption cross sections of the relevant photolysis reactions are appropriately represented in the mechanism (Carter et al., 2005), but for some of the photoreactive aromatic products, these parameters are uncertain.

After excluding blacklight toluene experiments, 31 experiments of multiple UCR chambers and 7 experiments of the outdoor UNC gas-phase chamber, a total of 38 experiments, where toluene was injected as a single test organic compound, were classified into four categories listed in Table 3-3. The classification of experiments into the four categories, identified as low-NOx, mid-NOx, high-NOx and low O_3/NOx, was based on three criteria: (1) primary criterion: is $[NOx]_{t=0}$ equal to or less than 100 ppb (0.1 ppm); (2) secondary criterion: does the $[O_3]$ peak or plateau appear by around 3 hours since irradiation or since the initial production of ozone; (3) third criterion: is max $[O_3]$ to initial [NO] ratio is less than 0.6? The categorized experiments are summarized in Tables 3-4 and 3-5.

Table 3-3. Four classes of toluene experiments and standards applied to classification of toluene experiments.

Categories	Criteria applied
Low-NOx	initial [NOx] is equal to or less than 100 ppb (0.1 ppm)
Mid-NOx	[O_3] peak or plateau appears *by* around 180 minutes (3 hours) since irradiation or since initial production of ozone
High-NOx	[O_3] peak or plateau appears *after* around 3 hours since irradiation or since initial production of ozone, or [O_3] is still increasing at or near the end of the experiment
Low O_3/NOx	high NOx experiments whose max [O_3] to initial [NO] ratio is less than 0.6[a]

[a]The cut-off value of 0.6 was set to classify 3 high NOx UCR experiments in the SAPRC dataset as a separate class, "low O_3/NOx": CTC065, CTC079, OTC299B.

Table 3-4. 7 toluene experiments of the outdoor UNC gas-phase chamber in the Morpho dataset[a]

Exp. ID	Initial TOL (ppm)	Initial NOx (ppm)	Sunrise time (EDT)	VOC/NOx (ppmC/ppm)	Max (O_3) (ppm)	Max (NO) (ppm)	Max(O_3)/ Max(NO) (ppm/ppm)
Mid-NOx (6 experiments)							
AU0183R	0.655	0.395	6:25	11.6	0.458	0.351	1.31
AU1788R	0.704	0.361	6:37	13.8	0.461	0.292	1.58
AU3095B	1.000	0.618	6:47	11.3	0.545	0.530	1.03
AU1196R	0.995	0.333	6:33	20.9	0.333	0.290	1.15
ST2496B	1.911	0.638	7:07	21.0	0.593	0.575	1.03
AU2297R	1.444	0.633	6:41	16.0	0.634	0.557	1.14
Low O_3/NOx (1 experiment)							
ST1393B	0.273	0.322	6:58	5.9	0.157	0.285	0.55
Quality assurance (2 experiments)							
JN1379B[b]	0.451	0.443	6:00	13.3	0.756	0.363	2.08
JN1379R[b]	0.000	0.451	6:00	6.1	0.974	0.370	2.63

[a]Toluene (TOL) was the single test organic compound except for JN1379B and JN1379R, which were used for quality assurance. [b]In Experiment JN1379B (experiment in the Blue side of the UNC dual chamber on June 13, 1979), 0.908 ppm propene was also injected. In Experiment JN1379R (experiment in the Red side of the UNC dual chamber on June 13, 1979), 0.912 ppm propene was injected without injection of toluene.

Table 3-5. 31 non-blacklight toluene experiments of UCR chambers in the SAPRC dataset[a]

Exp. ID	Initial TOL (ppm)	Initial NOx (ppm)	Initial CO (ppm)	VOC/NOx (ppmC/ppm)	Max (O_3) (ppm)	Max (NO) (ppm)	Max(O_3)/ Max(NO) (ppm/ppm)
Low-NOx (12 experiments)							
EPA066B	0.061	0.005	0	85.1	0.058	0.004	13.26
EPA074A	0.151	0.024	0	44.0	0.124	0.024	5.19
EPA077A	0.152	0.023	0	47.3	0.122	0.023	5.37
EPA210A	0.262	0.042	0	43.5	0.159	0.031	5.21
EPA210B	0.263	0.093	0	19.8	0.231	0.066	3.52
EPA443A	0.170	0.031	0	37.9	0.127	0.030	4.28
EPA443B	0.365	0.099	0	25.8	0.224	0.070	3.21
EPA066A	0.055	0.004	24	101.5	0.097	0.003	33.44
EPA072A	0.155	0.014	25	76.4	0.149	0.014	10.57
EPA072B	0.155	0.015	27	70.4	0.159	0.016	10.26
EPA074B	0.157	0.027	45	41.3	0.261	0.026	9.92
EPA077B	0.165	0.026	50	44.3	0.275	0.026	10.66
Mid-NOx (11 experiments)							
CTC026	2.005	0.270	0	51.9	0.347	0.212	1.64
CTC034	2.214	0.524	0	29.6	0.467	0.372	1.26
CTC048	0.946	0.248	0	26.7	0.314	0.196	1.60
XTC106	1.915	0.245	0	54.6	0.395	0.216	1.83
EC264	1.156	0.440	0	18.4	0.417	0.387	1.08
EC266	1.196	0.440	0	19.0	0.404	0.388	1.04
EC271	1.146	0.215	0	37.4	0.294	0.185	1.59
EC273	0.587	0.112	0	36.8	0.214	0.096	2.23
EC293	1.071	0.487	0	15.4	0.771	0.398	1.05
OTC299A	1.218	0.509	0	16.8	0.611	0.389	1.57
OTC300B	0.509	0.224	0	15.9	0.421	0.186	2.27
High-NOx (5 experiments)							
EC269	0.566	0.485	0	8.2	0.316	0.410	0.77
EC270	0.576	0.466	0	9.0	0.367	0.404	0.91
EC327	0.573	0.492	0	8.2	0.375	0.386	0.97
EC340	0.537	0.493	0	7.6	0.343	0.399	0.86
OTC300A	0.513	0.521	0	6.9	0.381	0.442	0.86
Low O_3/NOx (3 experiments)							
CTC065	0.969	0.657	0	10.3	0.051	0.514	0.10
CTC079	0.504	0.256	0	13.8	0.125	0.215	0.58
OTC299B	0.509	0.502	0	7.1	0.214	0.382	0.56

[a]Toluene (TOL) was the only test VOC compound except for EC270 where 171 ppb HCHO (about 30% of 576 ppb toluene) was also injected in this experiment, EC270.

3.3.3. Environmental Chamber Simulations

Two versions of CB05, containing the Base mechanism or UNClite as their toluene mechanism (CB05-Base, CB05-UNClite), were evaluated against the 38 toluene chamber experiments. The auxiliary mechanisms adopted to simulate the chamber experiments are the same as wall mechanisms described in Carter (2009) and Faraji et al. (2007). In the Morpho software, only one auxiliary mechanism was applied to simulations of all 7 UNC chamber experiments selected. However, the sunrise times used in the simulations are different in each experiment. In the SAPRC software, multiple auxiliary mechanisms (approximately 10) originally developed by Carter for CB05-Base were applied to chamber simulations of the 31 UCR chamber experiments in the SAPRC dataset. For details of the auxiliary mechanisms and reaction parameters used in this work, refer to Appendix A.

3.4. Overall Performance of CB05-Base and CB05-UNClite in Chamber Simulations

This section will describe the overall performance of the two mechanisms, CB05-Base and CB05-UNClite while focusing on CB05-UNClite and using as criteria of performance, maximum ozone concentrations, maximum $\Delta(O_3\text{-NO})$, NOx crossover times, cresol concentrations, radical concentrations, and NOx sinks. The reasons for choosing these metrics and the performance of the mechanisms for each of these metrics are described in more detail in the subsections below. CB05-UNClite showed better performance than CB05-Base for most of the environmental chamber experiments used in this study.

3.4.1. Max(O_3) and Max($\Delta(O_3$-NO))

Max(O_3) and Max($\Delta(O_3$-NO)) were chosen as performance metrics because a primary goal of most condensed chemical mechanisms used in regional photochemical models is accurate prediction of maximum ozone concentrations. Max($\Delta(O_3$-NO)) provides a more accurate measure of total ozone production than Max(O_3) (Carter and Atkinson, 1987), so both metrics were used.

As shown in Figures. 3-3 and 3-4, CB05-Base consistently under-predicted Max(O_3) and Max($\Delta(O_3$-NO)) for most of the 38 chamber experiments, particularly, for low-NOx experiments (Figure 3-3a), and CB05-UNClite solved this under-prediction problem to some degree. The performance of each mechanism in simulating Max($\Delta(O_3$-NO)) was very similar to their performance in simulating Max(O_3).

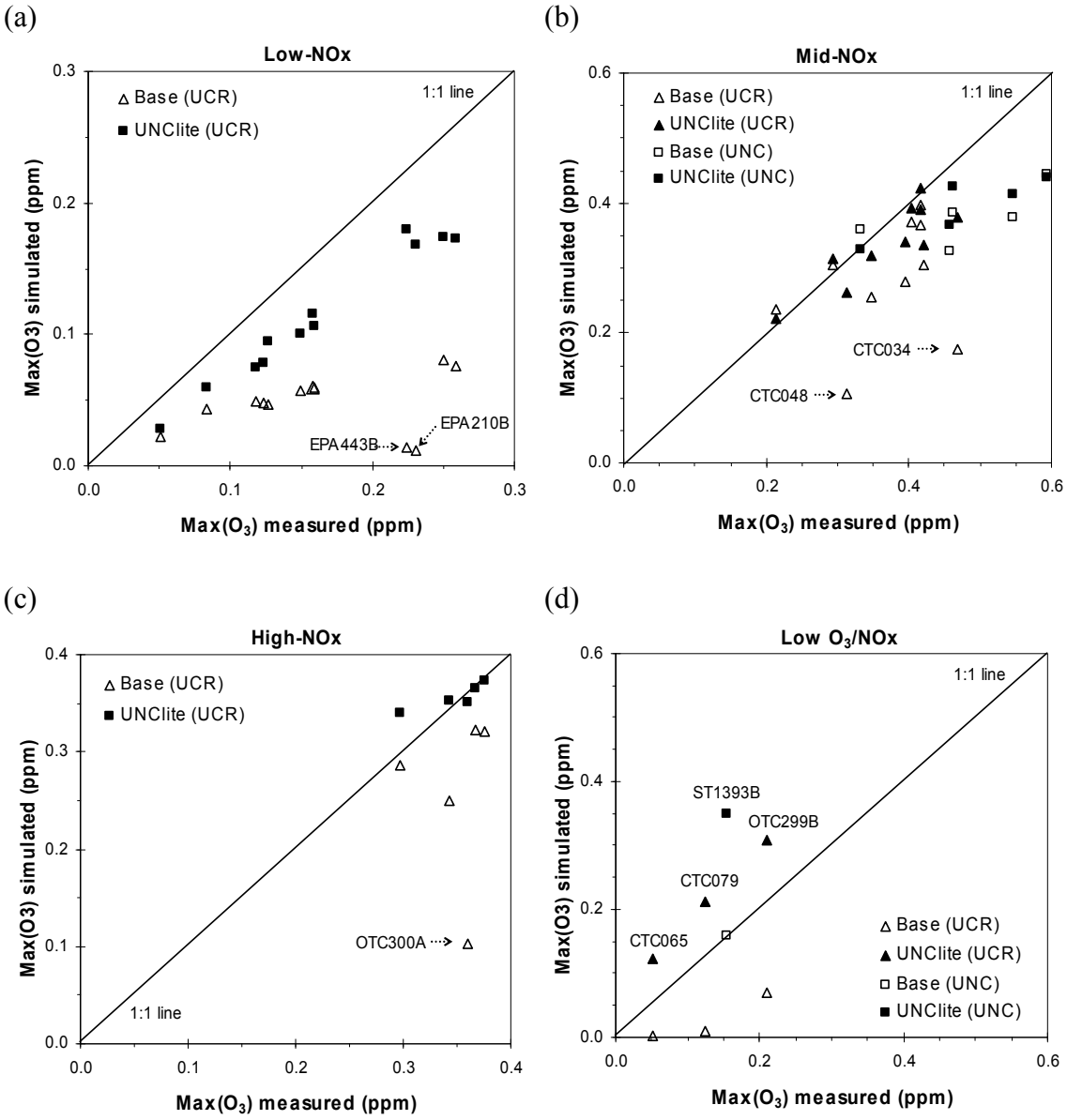

Figure 3-3. Comparison of maximum ozone simulated by CB05-UNClite with measurements: (a) low-NOx, (b) mid-NOx, (c) high-NOx, (d) low O_3/NOx.

Note: “UCR” and “UNC” in parentheses mean “UCR experiments simulated by the SAPRC software” and “UNC experiments simulated by the Morpho software”, respectively.

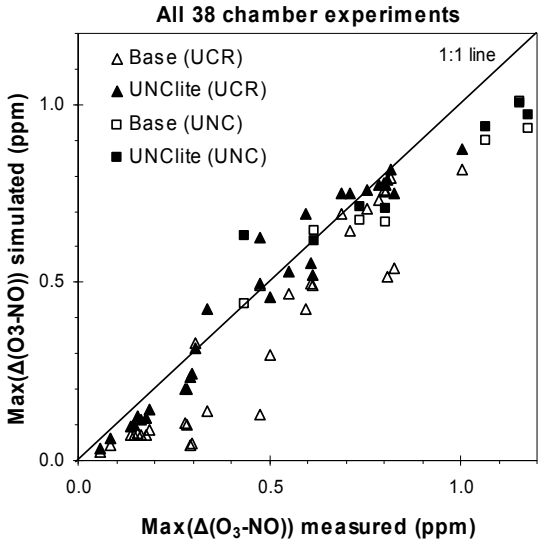

Figure 3-4. Comparison of maximum $\Delta(O_3\text{-NO})$ simulated by CB05-UNClite with measurements.

Note: "UCR" and "UNC" in parentheses mean "UCR experiments" and "UNC experiments", respectively. $\Delta(O_3\text{-NO}) = ([O_3]\text{-}[NO])_{t=t} - ([O_3]\text{-}[NO])_{t=0}$.

In Figure 3-5, time series of O_3, NO and NO_2 and toluene simulated by CB05-UNClite are presented for one representative experiment in each class defined in Table 3-3. For the low-NOx experiments (e.g., EPA210A), CB05-UNClite showed far better performance than CB05-Base. For the mid- and high-NOx experiments (e.g., AU0183R and EC340), CB05-UNClite started to increase O_3 earlier than CB05-Base and observation.

Neither CB05-Base nor CB05-UNClite predicted well Max(O_3) and Max($\Delta(O_3\text{-NO})$) for low O_3/NOx experiments. For example, CB05-UNClite over-predicted Max(O_3) for two of the four low O_3/NOx experiments by over 100%, and CB05-Base under-predicted Max(O_3) by over 65% for three experiments while CB05-Base simulated Max(O_3) relatively well for experiment ST1393B. CB05-UNClite simulated Max(O_3) better than CB05-Base for CTC079 and OTC299B (Figure 3-3d).

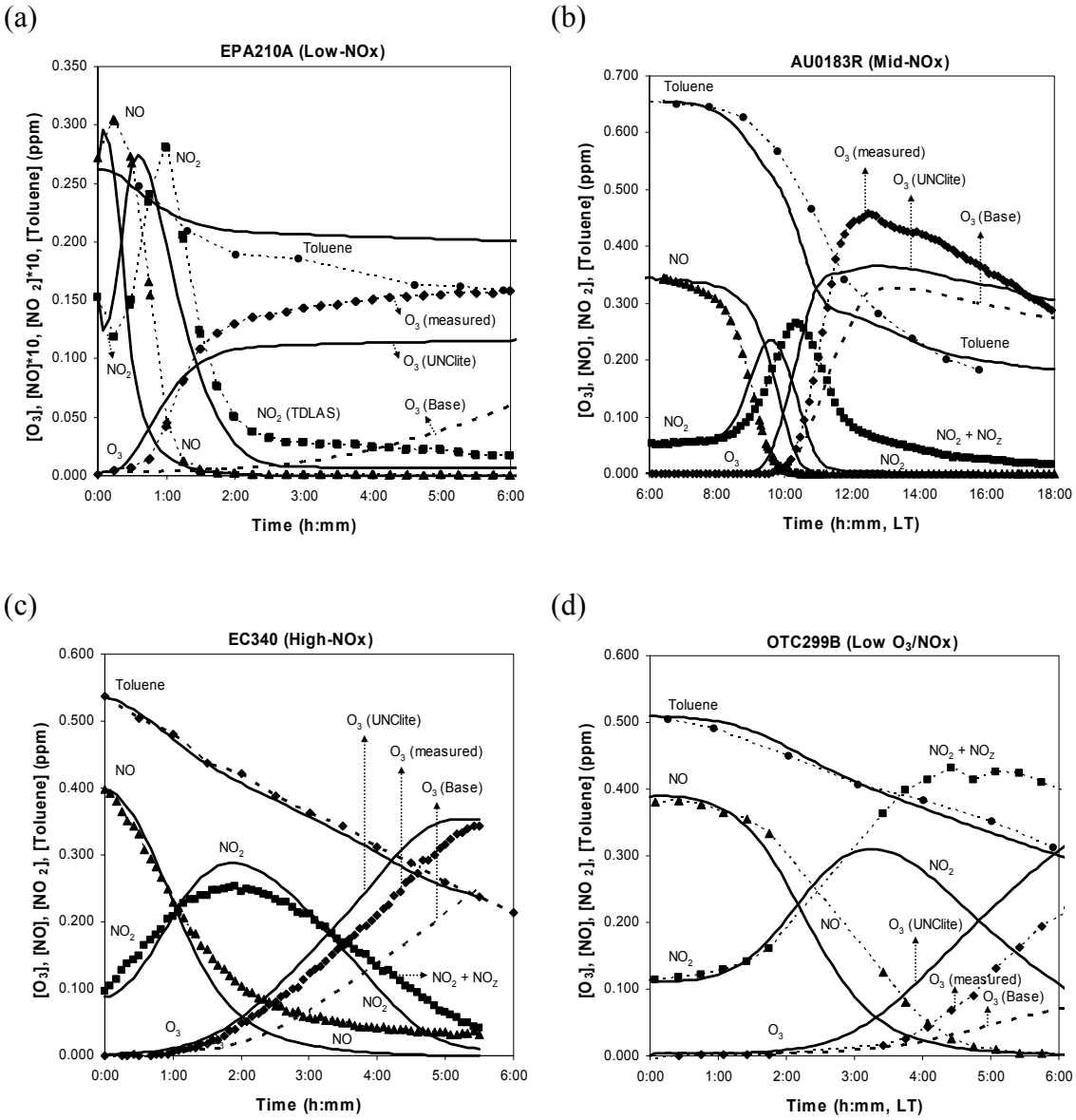

Figure 3-5. Comparison of NO, NO_2, toluene and O_3 simulated by CB05-UNClite against measurements: (a) EPA210A, (b) AU0183R, (c) EC340, (d) OTC299B.

Note: Dashed lines with symbols represent measured concentrations and solid lines represent modeled concentrations. For comparison, O_3 simulated by CB05-Base is also presented by broken lines without a symbol. NO_2 for EPA210A was measured by tunable diode laser absorption spectroscopy (TDLAS) instead of catalytic conversion of NO_2 into NO. For other experiments, AU0183R, EC340 and OTC299B, NO_2 concentrations were indirectly measured by conversion into NO, and contain interferences of NOx oxidation products (NOz, e.g., PAN and other organic nitrates).

Caution should be exercised in interpreting these results, because wall effects may be more important for experiments in the low O_3/NOx class, which tend to be sensitive to chamber radical sources. Uncertainties regarding chamber NOx offgasing may be non-negligible in the low NOx experiments at the lowest NOx levels, but sensitivity calculations where the NOx offgasing parameter in the wall mechanism was set to zero or increased by an order of magnitude indicated that the maximum O_3 levels were not significantly affected for the lowest NOx experiments.

3.4.2. NOx Crossover Times

Maximum O_3 and $\Delta(O_3\text{-NO})$ do not provide information on how fast ozone is formed and NO is oxidized in the chemical system. The NOx crossover time, when the NO_2 concentration becomes equal to the NO concentration, contains information on the rate of NO oxidation into NO_2 and accompanying O_3 formation. For this reason, the NOx crossover time was used along with $Max(O_3)$ and $Max(\Delta(O_3\text{-NO}))$ to evaluate the performance of the mechanisms.

CB05-UNClite partially fixed a problem of CB05-Base, slower O_3 production than observation; however, one caveat to this improvement is that the NOx crossovers predicted by CB05-UNClite tend to appear slightly earlier than observation (Figure 3-6). However, this problem of NOx crossovers earlier than observation is not as large as the problem of delayed NOx crossovers shown by CB05-Base for many UCR experiments (Figure 3-6a). For the UNC experiments, time lags in NOx crossover became larger with CB05-UNClite, but this problem is relatively moderate (Figure 3-6b).

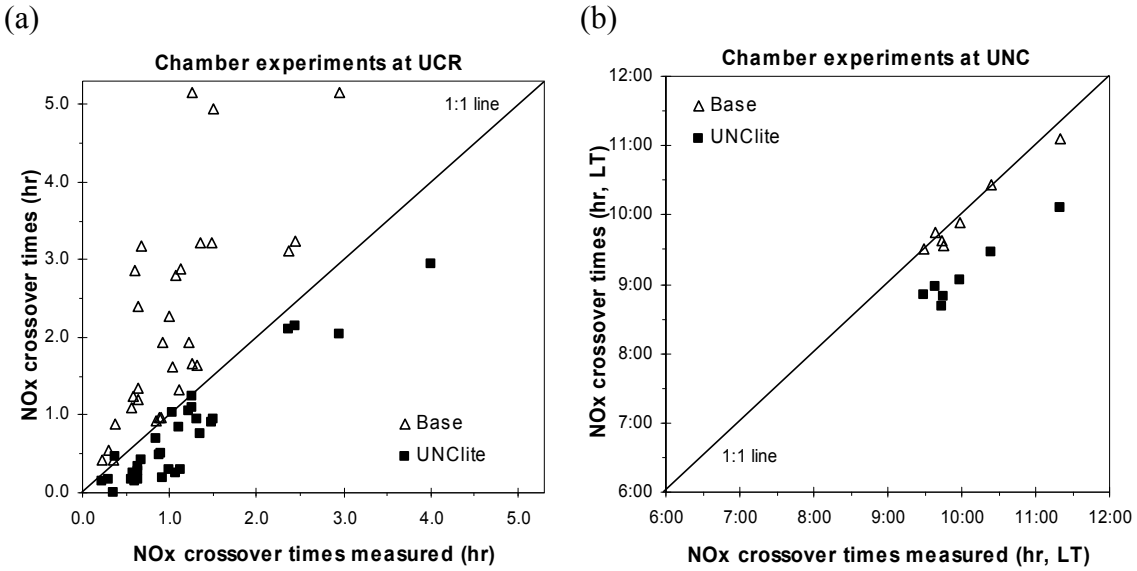

Figure 3-6. Comparison of NOx crossover times simulated by CB05-UNClite against measurements for UCR experiments (a) and for UNC experiments (b).

Note: NO_2 becomes equal to NO at the NOx crossover time.

3.4.3. Cresol Concentrations

Cresols are major ring-retaining products of toluene oxidation that can be relatively accurately measured, in comparison to ring-opening products which are highly reactive and difficult to measure (Calvert et al., 2002; Yu et al., 1997; Arey et al., 2009). Cresols and their oxidation products are also important NOx sinks in the toluene-NOx chemical system (Killus and Whitten, 1982; Klotz et al., 1998). Therefore, predicted cresol concentrations are also used as a metric to evaluate the performance of CB05-Base and CB05-UNClite.

The first-generation products of toluene oxidation by OH are classified into two groups: ring-opening products and ring-retaining products. Yields of dicarbonyl compounds such as glyoxal and 1,4-butenedial are over 50% of toluene oxidized, and the

overall yield of cresols, representative ring-retaining products, is about 18% of oxidized carbons of toluene (Calvert et al., 2002; Arey et al., 2009). Data for dicarbonyls are not available for the chamber experiments used. Therefore, this section presents comparisons of mechanism predictions and observations for the time-profile of cresols in toluene-NOx experiments to evaluate the cresol yield of the toluene + OH reaction.

As shown in Figure 3-7, the change in the cresol yield from 0.36 to 0.18 significantly improved the performance of CB05-UNClite in simulating cresols against 6 chamber experiments where cresol measurements are available. Thus, this change in the cresol yield is recommended to be implemented in the future versions of CB05 that explicitly include NOx sinks. The decrease in the cresol yield will result in more flux of toluene into the reactive "peroxide-bicyclic route" producing dicarbonyls (Andino et al., 1996; Volkamer et al., 2001, 2005; Suh et al., 2003, 2006; Bloss et al., 2005a,b; Gómez Alvarez et al., 2007; Arey et al., 2009), which is expected to contribute to solving the ozone under-prediction problem of CB05-Base (Figure 3-3).

It should be noted, however, that in CB05-Base, like CB-IV, the CRES model species might be thought of as representing not only cresols, but also other features of toluene oxidation processes such as formation of products less reactive than dicarbonyls and depletion of NOx in the toluene-NOx system (Gery et al., 1989).

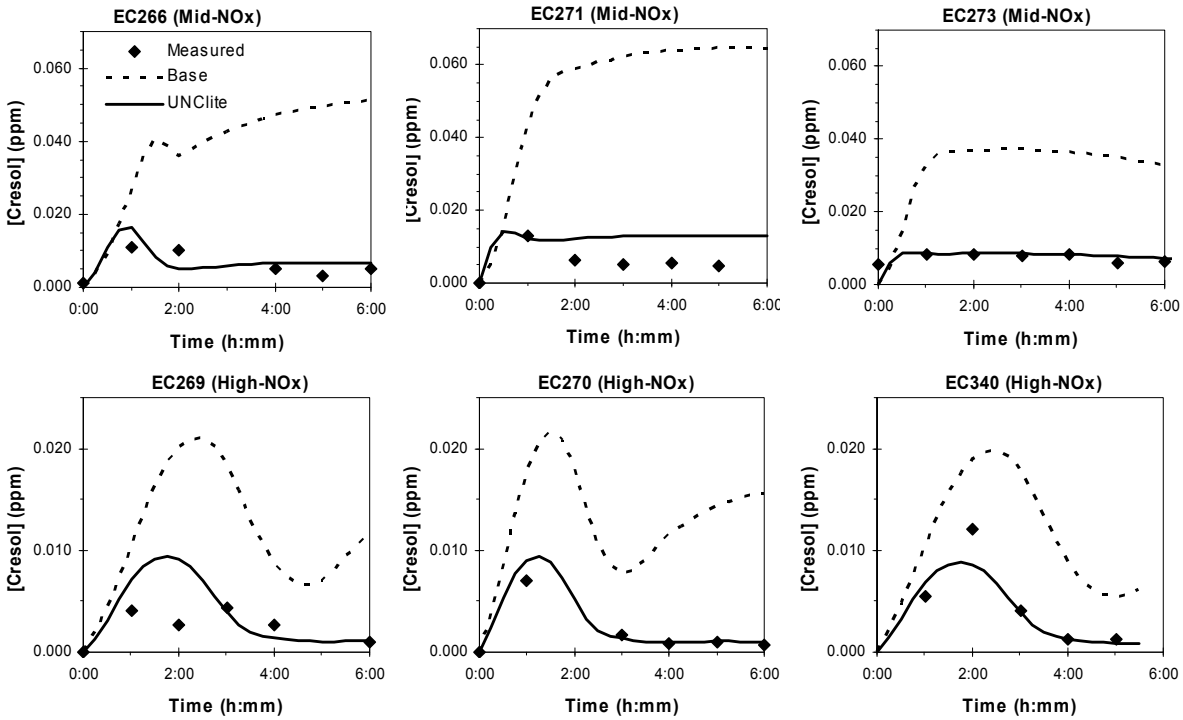

Figure 3-7. Comparison of cresol concentrations simulated by CB05-UNClite against measurements of 6 experiments.

3.4.4. Radical Concentrations

OH is the major initiator of oxidation of toluene and most of its products (Calvert et al., 2002). HO_2 and other radicals such as alkyl peroxy radicals (RO_2) are involved in net O_3 formation by oxidizing NO into NO_2 without consuming O_3. Therefore, OH and HO_2 concentrations are also used as performance metrics although OH and HO_2 measurements are available for only one experiment of the 38 experiments used in this study, EPA210A (http://www.engr.ucr.edu/~carter/SAPRC/files.htm; Xinrong Ren, personal communication, November 2008).

Under ambient conditions, typical NOx concentrations are well below 100 ppbv (0.1 ppmv). In this context, the low-NOx experiments of UCR's EPA chamber are valuable for testing the radical chemistry of the toluene mechanisms. In addition, the very low relative humidity in the EPA chamber suppresses OH formation by O_3 photolysis into O^1D and subsequent reaction of O^1D with H_2O. Thus, the low-NOx experiments listed in Table 3-5 provide a good opportunity to test radical sources involved in toluene oxidation. Radical concentrations are usually more important in the early stage of a chamber experiment than in the late stage because NOx is relatively abundant in the initial stage and OH and HO_2 radicals start to increase from negligible levels at the start of each chamber experiment. Thus, we will focus on radical sources in the early stage of each experiment rather than in the late stage when NOx availability is usually more important.

In comparison to CB05-Base, CB05-UNClite started to increase OH and HO_2 earlier. In experiment EPA210A where the initial NOx was about 40 ppb, CB05-UNClite started to increase OH and HO_2 rapidly and predicted a very steep OH peak (Figure 3-8a). Simulated HO_2 tended to increase later than simulated OH, which is caused by the rapid regeneration of OH by reaction of HO_2 and NO and the consequent delay in the increase in HO_2. OH and HO_2 simulated by CB05-UNClite are lower than observations: OH and HO_2 measured using laser induced fluorescence (LIF) by W. H. Brune's team (Ren et al., 2004, Faloona et al., 2004) and estimated OH using the decay rates of toluene derived from toluene data points shown in Figure 3-5a. The decay rates calculated from the toluene data are lower than the LIF OH measurements, but are still somewhat higher than the OH predicted by CB05-UNClite at the middle stage of the experiment.

To identify major contributors to radical formation causing rapid increases in OH shown in Figure 3-8a, a process analysis tool (Kimura and Allen, 2008) was used to calculate the net radical formation rates of each reaction in CB05-Base and CB05-UNClite. Those radical production rates were converted into OH production rates (in units of ppb OH/hr) by multiplying the corresponding propagation efficiency into OH of each peroxy radical (e.g, HO_2, $CH_3C(O)OO$). Reaction TO_2 + NO and photolysis of OPEN (γ-dicarbonyls) and MGLY (methylglyoxal) are the major radical sources in CB05-UNClite (Figure 3-8b) while OPEN formed via TO_2 is the largest contributor in CB05-Base in EPA210A (not shown).

In summary, the unsaturated γ-dicarbonyls (OPEN in CB05) formed by ring-opening in toluene oxidation are significant radical sources in both Base and UNClite although α-dicarbonyls, methylglyoxal and glyoxal (which is implicitly expressed as FORM + CO + HO_2 in CB05) are also significant radical sources. Therefore, OPEN (and MGLY in the case of CB05-UNClite) generated from TO_2 (the aromatic bicyclic peroxy radical) acted as a significant radical source in chamber simulations. Lowering the cresol yield (from 0.36 to 0.18) and increasing the TO_2 yield resulted in more radical sources (dicarbonyls) in CB05-UNClite during the early stage and contributed to solving the O_3 under-prediction problem through higher flux of toluene into the reactive "peroxide-bicylic" route.

(a)

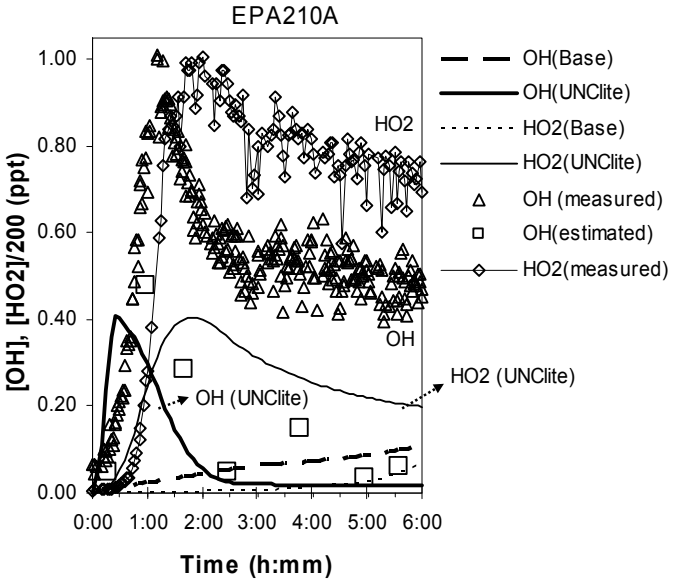

(b)

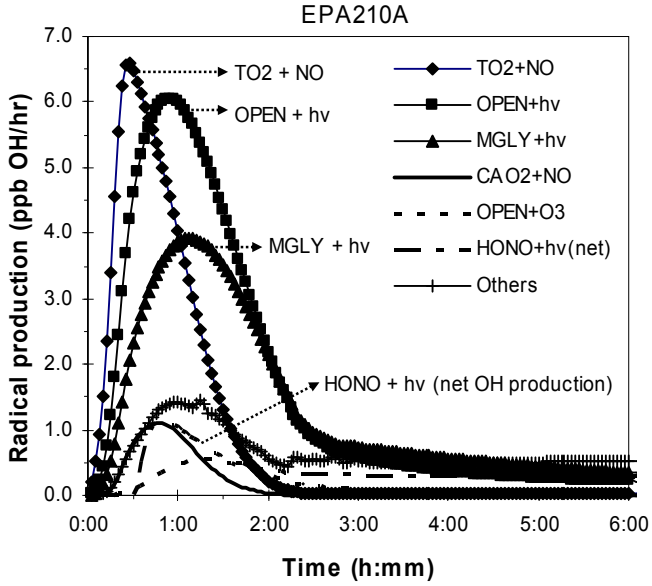

Figure 3-8. Comparison of OH and HO_2 simulated by CB05-UNClite with measurements (a), and major pathways contributing to radical formation (b) for Experiment EPA210A.

Note: "OH (measured)" is LIF-measured OH. "OH (estimated)" is derived from the decay rates of toluene.

3.4.5. NOx Sinks

In this section, NOx sinks in toluene oxidation are evaluated against very limited experimental data of NOx and NOz such as NO measured by chemiluminescence, NO_2 measured by tunable diode laser absorption spectroscopy (TDLAS), and HNO_3 measured by TDLAS and PAN by gas chromatography with luminol derivatization (GC-luminol) at the EPA chamber facility (Carter et al., 2005). Interferences of NOz species in indirect NO_2 measurements using catalytic conversion into NO, and lack of reliable speciated NOz measurements significantly limit evaluation efforts of NOx sinks simulated by a chemical mechanism (Dodge, 2000).

Based on NOx and NOz measurements of EPA210A and EPA210B for which relatively reliable NOx and NOz data are available, CB05-UNClite tends to under-predict HNO_3 and reasonably simulate PAN. There are two notable patterns: CB05-UNClite generates OPAN more than PAN (Figure 3-9), and starts to form NOz (NOy – NOx) species relatively earlier than CB05-Base (not shown).

The model slightly overpredicts PAN itself, but predicts that most of the peroxyacyl nitrates are formed from unsaturated γ-dicarbonyls (e.g., OPAN derived from OPEN, which is not measured). Liu et al. (1999) reported that unsaturated peroxyacyl nitrates formed from unsaturated acyl peroxy radicals seem to act as NOx reservoirs. Further studies on the fates of unsaturated γ-dicarbonyls under atmospherically relevant conditions are needed, and reliable measurements of speciated NOy are also necessary (if possible, both from chamber data and ambient data) to test if CB05-UNClite correctly calculates these NOz species such as OPAN and reasonably simulates NOx depletion.

(a)

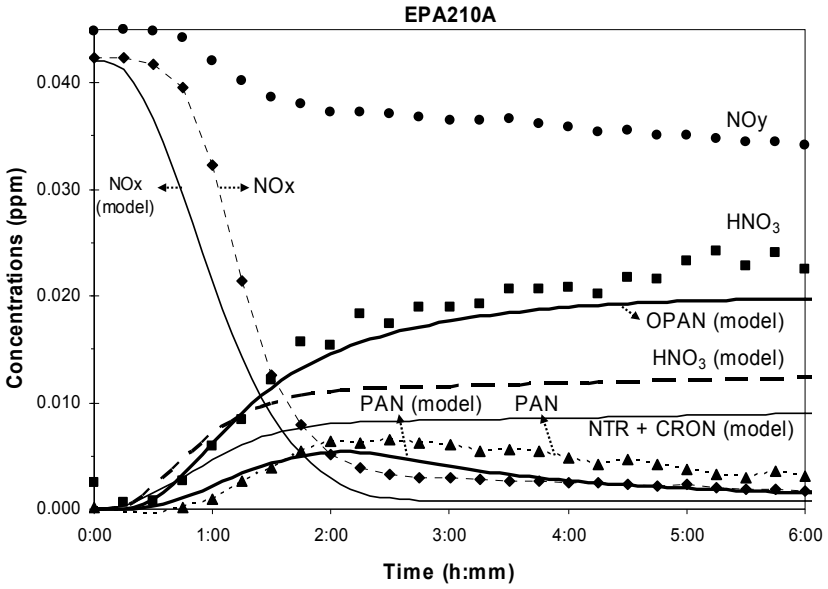

(b)

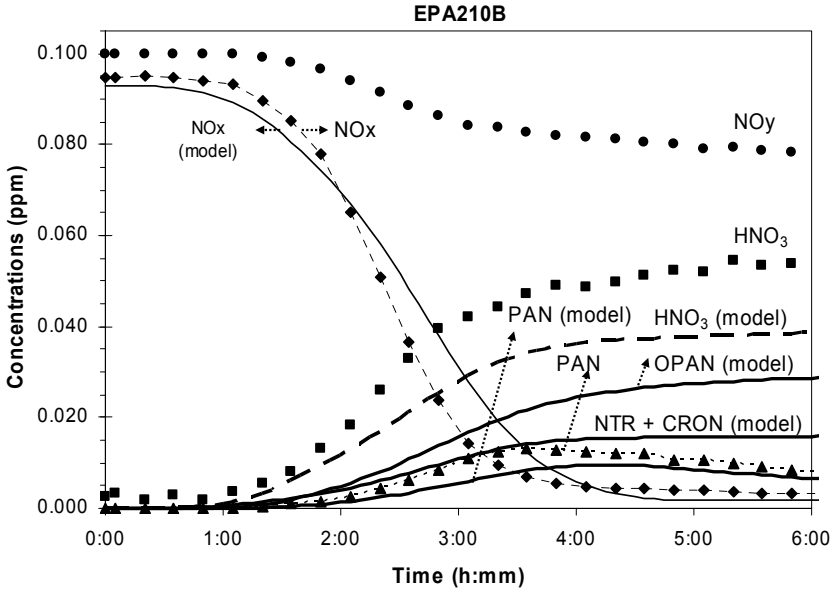

Figure 3-9. Comparison of NOx and NOz species simulated by CB05-UNClite against measurements: (a) EPA210A, (b) EPA210B.

Note: NOz = NOx oxidation products; NOy = NOx + NOz, the NOy measurements most probably include only part of HNO_3; OPAN = PAN-like compounds formed from acyl peroxy radicals originating from γ-dicarbonlyls.

3.4.5. Summary of Performance Characteristics

CB05-UNClite showed generally better performance than CB05-Base. The overall performance of the mechanisms in simulating Max(O_3), Max($\Delta(O_3$-NO)), and NOx crossover times is summarized in Table 3-6. CB05-Base showed two problems in simulating chamber experiments, especially the low-NOx experiments: (1) under-predictions of Max(O_3) and Max($\Delta(O_3$-NO)), (2) delays in NO oxidation and O_3 formation indicated by delayed NOx crossovers. CB05-UNClite mitigated the under-prediction problem of CB05-Base. None of the mechanisms simulated well the low O_3/NOx experiments. In regard to the poor performance of CB05-UNClite in simulating Max(O_3) and Max($\Delta(O_3$-NO)) against some low O_3/NOx experiments, caution should be exercised because of possible sensitivity to chamber radical sources. CB05-UNClite significantly improved simulations of NOx crossover times. NOx crossovers predicted by CB05-UNClite occurred somewhat earlier than measurements for many experiments; however, this problem is relatively minor in comparison to the problem of delayed initiation shown by CB05-Base.

Other performance characteristics such as cresol yields, major radical sources and NOx sinks are summarized in Table 3-7. OPEN produced through the reactive peroxide-bicyclic route, a model species in CB05 for representing ring-opening products of toluene oxidation, is a significant radical source. MGLY (methylglyoxal) is also a significant radical source in CB05-UNClite. In addition to formation of HNO_3, PAN and NTR (organic nitrates), NOx is also removed by formation of OPAN (peroxyacyl nitrates derived from OPEN) and CRON (nitro-cresols) in CB05-UNClite.

Table 3-6. Summary of the overall performance and characteristics of CB05-Base and CB05-UNClite against the chamber experiments in simulating Max(O_3), Max($\Delta(O_3\text{-NO})$), and NOx crossover times.

Mechanism	CB05-Base	CB05-UNClite
Max(O_3): model errors[a] [units: %]		
Low-NOx	-66.8 (14.0)	-31.2[b] (6.3)
Mid-NOx[c]	-22.6 (21.5)	-12.3 (11.3)
High-NOx	-25.7 (26.8)	2.7 (6.8)
Low O_3/NOx[d]	-62.2 (45.0)	95.4 (44.2)
Max($\Delta(O_3\text{-NO})$)[e]: model errors[a] [units: %]		
Low-NOx	-60.2 (12.4)	-27.7 (6.9)
Mid-NOx[c]	-13.0 (12.9)	-6.8 (6.6)
High-NOx[d]	-11.5 (14.3)	2.2 (4.9)
Low O_3/NOx	-40.0 (33.1)	29.7 (11.9)
NOx crossover times: model errors[f] [units: minutes]		
Low-NOx	99 (73)	-26 (14)
Mid-NOx[c,g]	28 (39)[g]	-32 (20)[g]
High-NOx	24 (16)	-10 (7)
Low O_3/NOx[d,h]	55 (74)[h]	-48 (28)[h]

[a]Model errors were calculated as (model – experimental)/experimental, and numbers are averages with standard deviations in parentheses. [b]Note the fact that CB05-UNClite simulated well the early stages of the low-NOx experiments. [c]For 11 UCR experiments in the SAPRC dataset and 6 UNC experiments in the Morpho dataset. [d]For 3 UCR experiments in the SAPRC dataset and 1 UNC experiment in the Morpho dataset. [e]$\Delta(O_3\text{-NO}) = ([O_3]\text{-}[NO])_{t=t} - ([O_3]\text{-}[NO])_{t=0}$. [f]Model errors were calculated as (model – experimental), and numbers in parentheses are standard deviations. [g]In terms of relative errors , 52.5% (56.4%) and -33.7% (22.5%) for CB05-Base and CB05-UNClite, respectively. [h]Experiment CTC065 was excluded in the calculations because CB05-Base could not simulate the NOx crossover by the end of the experiment.

Table 3-7. Summary of the overall performance and characteristics of CB05-Base and CB05-UNClite against the chamber experiments in simulating cresol concentrations, radical sources and NOx sinks.

Mechanism	CB05-Base	CB05-UNClite
Cresol concentrations	over-predict	reasonable
Major radical sources	OPEN formed from TO_2	OPEN, MGLY and TO_2[a]
Major NOx sinks	CRES[b]	CRES[b], OPEN[c]
NOx oxidation products by NOx sinks	PAN, NTR[d], HNO_3	PAN, NTR[d], HNO_3, OPAN[e], CRON[f]

[a]Unlike in CB05-Base, in CB05-UNClite, TO_2 + NO reaction is a net radical source (1.0 TO_2 is consumed and 1.2 HO_2 is formed) because glyoxal is expressed as (FORM + CO + HO_2) in the reaction. [b]CRES represents cresols in CB05. [c]Unsaturated γ-dicarbonyls (OPEN in CB05) deplete NOx by forming acyl peroxy radicals and corresponding peroxyacyl nitrates (OPAN in CB05). [d]Organic nitrates other than PAN-like compounds in CB05. [e]OPAN is a PAN-like species derived from OPEN. [f]CRON represents nitro-cresol compounds.

3.5. SUMMARY AND RECOMMENDATIONS

The current CB05 mechanism (CB05-Base) showed two under-prediction problems: Max(O_3), the rate of O_3 formation. CB05 with the newly proposed toluene mechanism (CB05-UNClite) showed better performance in simulating Max(O_3), Max(Δ(O_3-NO)) and the NOx crossover to various degrees. CB05-UNClite showed promising performance in simulating Max(O_3), the O_3 formation rate and NOx removal rate especially during the early stages of low-NOx experiments of UCR's EPA chamber. Lowering the cresol yield (from 0.36 to 0.18) resulted in better fits to cresol measurements and contributed to solving the O_3 under-prediction problem through more flux of toluene into the reactive "peroxide-bicylic" route. More radical sources (dicarbonlys) in CB05-UNClite during the early stage resulted in better fits to measured O_3 formation rates at the EPA chamber. More rapid NOx removal by extra NOx sinks such as formation of OPAN (PAN-like species originating from unsaturated γ-dicarbonyls) and CRON (nitro-cresols) in CB05-UNClite resulted in better simulations of

O_3 and NOx than CB05-Base. Further studies on radical sources and NOx sinks involved in toluene oxidation processes during the time window when wall effects are not dominant, if possible, under ambient conditions, are necessary.

The CB05 mechanism is currently being used in models for research and regulatory applications (Luecken et al., 2008; Faraji et al., 2007). Such models should be based on the best available science given the constraints of practicality and needs for condensation. Although significant uncertainties in toluene mechanisms remain and more research is needed, the toluene mechanism in CB05-UNClite represents a significant improvement over the toluene mechanism in the 2005 version CB05, being more chemically realistic and performing better simulating available chamber data.

3.6. FURTHER INFORMATION AVAILABLE

During the initial development of a new toluene mechanism for CB05, three toluene mechanisms (named "Ua (update a), "Ub (update b)", "Dinitro") were developed and tested. The reactions in these mechanisms and major evaluation results are available in Appendix A. Ua, Ub and Dinitro were eventually abandoned in favor of UNClite, which has been the focus of this Chapter.

Limited ambient simulations using a box model developed by Carter and briefly described in Chapter 2, indicated that using the UNClite mechanism in CB05 instead of the Base mechanism would most probably lead to increases in the ozone concentration (Heo et al., 2009). Box modeling results are available in Appendix A.

3.7. ACKNOWLEDGEMENTS

The work described in this Chapter was in part funded by the Texas Commission on Environmental Quality (TCEQ) through TCEQ Work Order No. 582-04-65588-07 and 582-07-84005-FY08-11. The authors thank Dr. Xinrong Ren for providing updated OH and HO_2 data for experiment EPA210A, and all investigators involved in measuring the chamber data of UCR and UNC used in this study.

3.8. REFERENCES

Andino, J. M., Smith, J. N., Flagan, R. C., Goddard III, W. A., and Seinfeld, J. H.: Mechanism of atmospheric photooxidation of aromatics: A theoretical study, Journal of Physical Chemistry 100, 10 967–10 980, 1996.

Andino J.M., Vivier-Bunge, A., 2008. Tropospheric chemistry of aromatic compounds emitted from anthropogenic sources. Advances in Quantum Chemistry: Applications of Theoretical Methods to Atmospheric Science 55, 297-310.

Arey, J., Obermeyer, G., Aschmann, S.M., Chattopadhyay, S., Cusick, R.D., Atkinson, R., 2009. Dicarbonyl products of the OH radical-initiated reaction of a series of aromatic hydrocarbons. Environmental Science & Technology 43, 683-689.

Atkinson, R., Arey, J., 2003. Atmospheric degradation of volatile organic compounds. Chemical Reviews 103, 4605-4638.

Bierbach, A., Barnes, I., Becker, K.H., Wiesen, E., 1994. Atmospheric chemistry of unsaturated carbonyls: Butendial, 4-oxo-2-pentenal, 3-hexene-2,5-dione, maleic anhydride, 3*H*-furan-2-one, and 5-methyl-3H-furan-2-one. Environmental Science & Technology 28, 715-729.

Bloss, C., Wagner, V., Bonzanini, A., Jenkin, M.E., Wirtz, K., Martin-Reviejo, M., Pilling, M.J., 2005a. Evaluation of detailed aromatic mechanisms (MCMv3 and MCMv3.1) against environmental chamber data. Atmospheric Chemistry and Physics 5, 623-639. (http://www.atmos-chem-phys.net/5/623/2005/acp-5-623-2005.pdf)

Bloss, C., Wagner, V., Jenkin, M.E., Volkamer, R., Bloss, W.J., Lee, J.D., Heard, D.E., Wirtz, K., Martin-Reviejo, M., Rea, G., Wenger, J.C., Pilling, M.J., 2005b. Developments of a detailed chemical mechanism (MCMv3.1) for the atmospheric oxidation of aromatic hydrocarbons. Atmospheric Chemistry and Physics 5, 641-664. (http://www.atmos-chem-phys.net/5/641/2005/acp-5-641-2005.pdf)

Bohn, B., 2001. Formation of peroxy radicals from OH-toluene adducts and O_2. Journal of Physical Chemistry A 105, 6092-6101.

Calvert, J. G., Atkinson, R., Becker, K.H., Kamens, R.M., Seinfeld, J.H., Wallington, T.J., Yarwood, G., 2002. The Mechanisms of Atmospheric Oxidation of Aromatic Hydrocarbons, Oxford University Press, New York, 566p.

Carter, W.P.L., 2000. Documentation of the SAPRC-99 chemical mechanism for VOC reactivity assessment, Report to the California Air Resources Board, Contracts 92-329 and 95-308. (http://www.engr.ucr.edu/~carter/absts.htm#saprc99)

Carter, W.P.L., 2004. Evaluation of a gas-phase atmospheric reaction mechanism for low NOx conditions. Final Report to California Air Resources Board Contract No. 01-305, May 5. (http://www.engr.ucr.edu/~carter/absts.htm#lnoxrpt).

Carter, W.P.L., 2009. Development of the SAPRC-07 chemical mechanism and updated ozone reactivity scales. Final Report to the California Air Resources Board Contract No. 03-318. (http://www.engr.ucr.edu/~carter/SAPRC/)

Carter, W.P.L., Atkinson, R., 1987. An experimental study of incremental hydrocarbon reactivity. Environmental Science & Technology 21, 670-679.

Carter, W.P.L., Cocker, D.R., Fitz, D.R., Malkina, I.L., Bumiller, K., Sauer, C.G., Pisano, J.T., Bufalino, C., and Song, C., 2005. A new environmental chamber for evaluation of gas-phase chemical mechanisms and secondary aerosol formation. Atmospheric Environment, 39, 7768-7788.

Carter, W.P.L., Luo, D., Malkina, I.L., Pierce, J.A., 1995. Environmental chamber studies of atmospheric reactivities of volatile organic compounds. Effects of varying chamber and light source. Final Report to National Renewable Energy Laboratory, Contract XZ-2-12075, Coordinating Research Council, Inc., Project M-9, California Air Resources Board, Contract A032-0692, and South Coast Air Quality Management District, Contract C91323, March 26. (http://www.engr.ucr.edu/~carter/absts.htm#explrept).

Carter, W.P.L., Lurmann, F.W., 1991. Evaluation of a detailed gas-phase atmospheric reaction mechanism using environmental chamber data. Atmospheric Environment 25A, 2771-2806.

Carter, W.P.L., Winer, A.M., Pitts, J.N., 1981. Major atmospheric sink for phenol and the cresols: Reaction with the nitrate radical. Environmental Science & Technology 15(7), 829-831.

Darnall, K.R., Atkinson, R., Pitts, J.N., 1979. Observation of biacetyl from the reaction of OH radicals with o-xylene. Evidence for ring cleavage. Journal of Physical Chemistry 83(15), 1943-1946.

Dodge, M.C., 2000. Chemical oxidant mechanisms for air quality modeling: critical review. Atmospheric Environment 34, 2103-2130.

ENVIRON, 2008. Comprehensive Air Quality Model with Extensions (CAMx) User's Guide, Version 4.50, http://www.camx.com/files/CAMxUsersGuide_v4.5.pdf.

Faloona, I.C., Tan, D., Lesher, R.L., Hazen, N.L., Frame, C.L., Simpas, J.B., Harder, H., Martinez,M., Di Carlo, P., Ren, X., Brune, W.H., 2004. A laser induced fluorescence instrument for detecting tropospheric OH and HO_2: characteristics and calibration. Journal of Atmospheric Chemistry 47, 139–167.

Faraji, M., Heo, G., Kimura, Y., McDonald-Buller, E., Allen, D., Yarwood, G., Whitten, G., Carter, W. 2007. Comparison of the Carbon Bond and SAPRC photochemical mechanisms. Report to the Texas Commission on Environmental Quality, Work Order No. 582-04-65588-07.

Faraji, M., Kimura, Y., McDonald-Buller, E., Allen, D., 2008. Comparison of the carbon bond and SAPRC photochemical mechanisms under conditions relevant to southeast Texas. Atmospheric Environment 42, 5821-5836.

Forstner, H.J.L., Flagan, R.C., Seinfeld, J.H., 1997. Secondary organic aerosol from the photooxidation of aromatic hydrocarbons: Molecular composition. Environmental Science & Technology 31, 1345-1358.

Gery, M.W., Whitten, G.Z., and Killus, J.P., Dodge, M.C., 1989. A photochemical kinetics mechanism for urban and regional scale computer modeling. Journal of Geophysical Research 94(D10), 12,925-12,956.

Gómez Alvarez, E., Viidanoja, J., Muñoz, A., Wirtz, K., Hjorth, J., 2007. Experimental confirmation of the dicarbonyl route in the photo-oxidation of toluene and benzene. Environmental Science & Technology 41, 8362-8369.

Heo, G., Kimura, Y., McDonald-Buller, E., Allen, D.T., Yarwood, G., Whitten, G.Z., 2009. Evaluation of a new toluene mechanism for Carbon Bond 05 using environmental chamber data and ambient data. Presented at the 102nd Annual Conference of the Air and Waste Management Association, June 16-19, 2009, Detroit, MI. (Abstract of this paper (Paper AB-2b.154) is available at http://www.conferencearchives.com/awma/2009/abstracts/AB-2b.154_a.html).

Hu, D., Tolocka, M., Li, Q., Kamens, R.M., 2007. A kinetic mechanism for predicting secondary organic aerosol formation from toluene oxidation in the presence of NOx and natural sunlight. Atmospheric Environment 41, 6478–6496

Jeffries, H., Kessler, M., 1999. A User's Guide to MEval Solver Program for Morphoecule Mechanisms, a Part of Morpho, University of North Carolina,

Chapel Hill, NC. (A short description on Morpho is available at http://airchem.sph.unc.edu/Research/Products/Software/Morpho/default.htm.)

Johnson, D., Raoult, S., Lesclaux, R., Krasnoperov, L.N., 2005. UV absorption spectra of methyl-substituted hydroxyl-cyclohexadienyl radicals in the gas phase. Journal of Photochemistry and Photobiology A: Chemistry 176, 98-106.

Kenley, R.A., Davenport, J.E., Hendry, D.G., 1981. Products and pathways for the reaction of OH with aromatic hydrocarbons. Journal of Physical Chemistry 85(19), 2740-2746.

Killus, J.P., Whitten, G.Z., 1982. A mechanism describing the photochemical oxidation of toluene in smog. Atmospheric Environment 16(8), 1973-1988.

Kimura, Y., Allen, D.T., 2008. Application of mechanism-independent photochemical cycles analysis tool (pyIrr) to evaluate the effect of changes in temperature, isoprene concentrations and insolation on regional photochemistry using CB05, SAPRC99 and SAPRC07 mechanisms. Presented at the second International Conference on Atmospheric Chemical Mechanisms, University of California at Davis, December 10 – 12, 2008.

Klotz, B.G., Bierbach, A., Barnes, I., Becker, K.H., 1995. Kinetic and mechanistic study of atmospheric chemistry of muconaldehydes. Environmental Science & Technology 29, 2322-2332.

Klotz, B., Sørensen, S., Barnes, I., Becker, K.H., Etzkorn, T., Volkamer, R., Platt, U., Wirtz, K., Martín-Reviejo, M., 1998. Atmospheric oxidation of toluene in a large-volume outdoor photoreactor: In situ determination of ring-retaining product yields. Journal of Physical Chemistry A 102, 10289-10299.

Knispel, R., Koch, R., Siese, M., Zetzsch, C., 1990. Adduct formation of OH radicals with benzene, toluene, and phenol and consecutive reactions of the adducts with NOx and O_2. Berichte Der Bunsen-Gesellschaft-Physical Chemistry Chemical Physics 94(11), 1375-1379.

Koch, R., Knispel, R., Elend, M., Siese, M., Zetzsch, C., 2007. Consecutive reactions of aromatic-OH adducts with NO, NO_2 and O_2: benzene, naphthalene, toluene, m- and p-xylene, hexamethylbenzene, phenol, m-cresol and aniline. Atmospheric Chemistry and Physics 7, 2057-2071. (http://www.atmos-chem-phys.net/7/2057/2007/)

Liu, X., Jeffries, H.E., Sexton, K.G., 1999. Atmospheric photochemical degradation of 1,4-unsaturated dicarbonyls. Environmental Science & Technology 33, 4212-4220.

Luecken, D.J., Phillips, S., Sarwar, G., Jang, C., 2008. Effects of using the CB05 vs. SAPRC99 vs. CB4 chemical mechanism on model predictions: Ozone and gas-phase photochemical precursor concentrations. Atmospheric Environment 42, 5805-5820.

Markert, F., Pagsberg, P., 1993. UV spectra and kinetics of radicals produced in the gas phase reactions of Cl, F and OH with toluene. Chemical Physics Letters 209, 445-454.

Molina, M.J., Zhang, R., Broekhuizen, K., Lei, W., Navarro, R., Molina, L.T., 1999. Journal of American Chemical Society 121, 10,225-10,226.

Perry, R.A., Atkinson, R., Pitts, J.N., 1977. Kinetics and mechanism of the gas phase reaction of hydroxyl radicals with aromatic hydrocarbons over the temperature range 296-473 K. Journal of Physical Chemistry 81(4), 296-304.

Ren, X., 2008. Personal communication via email, November 2008.

Ren, X., Mao, J., Kang, E., Metcalf, A.R., Mitchell, M., Lesher, R.L., Shirley, T., Brune, W.H., Carter, W.P., Tonnesen, G., Chien, C., Fitz, D., Malkina, I., Sauer, C., Bumiller, K., Bufalino, C., 2004. Behavior of the hydroxyl and hydroperoxy radicals in a smog chamber study, EOS Trans. AGU, 85(47), Fall Meet. Suppl., Abstract A53C-0908. (http://www.agu.org/meetings/fm04/fm04-sessions/fm04_A53C.html)

Smith, D.F., McIver, C.D., Kleindienst, T.E., 1998. Primary product distribution from the reaction of hydroxyl radicals with toluene at ppb NOx mixing ratios. Journal of Atmospheric Chemistry 30, 209-228.

Suh, I., Zhang, D., Zhang, R.Molina, L.T., Molina, M.J., 2002. Theoretical study of OH addition reaction to toluene. Chemical Physics Letters 364, 454-462.

Suh, I., Zhang, R., Molina, L.T., Molina, M.J., 2003. Oxidation mechanism of aromatic peroxy and bicyclic radicals from OH-toluene reactions. Journal of American Chemical Society 125, 12,655-12,665.

Suh, I., Zhao, J., Zhang, R., 2006. Unimolecular decomposition of aromatic bicylic alkoxy radicals and their acyclic radicals. Chemical Physics Letters 432, 313-320.

Tang, Y., Zhu, L., 2005. Photolysis of butenedial at 193, 248, 280, 308, 351, 400, and 450 nm. Chemical Physics Letters 409, 151-156.

Yu, J., Jeffries, H.E., Sexton, K.G., 1997. Atmospheric photooxidation of alkylbenzenes-I. Carbonyl product analyses. Atmospheric Environment 31(5), 2261-2280.

Volkamer, R., Platt, U., Wirtz, K., 2001. Primary and secondary glyoxal formation from aromatics: Experimental evidence for the bicycloalkyl-radical pathway from benzene, toluene, and p-xylene. Journal of Physical Chemistry A 105, 7865-7874.

Volkamer, R., Spietz, P., Burrows, J., Platt, U., 2005. High-resolution absorption cross-section of glyoxal in the UV-vis and IR spectral ranges. Journal of Photochemistry and Photobiology A: Chemistry 172, 35-46.

Whitten, G.Z., Heo, G., Kimura, Y., McDonald-Buller, E., Allen, D.T., Yarwood, G., 2009. A new condensed toluene mechanism for Carbon Bond. Submitted for publication in *Atmospheric Environment*.

Xiang, B., Zhu, L., Tang, Y., 2007. Photolysis of 4-oxo-2-pentenal in the 190-460 nm region. Journal of Physical Chemistry A 111(37), 9025-9033.

Yarwood, G., Rao, S., Yocke, M., Whitten, G.Z., 2005. Updates to the Carbon Bond mechanism: CB05. Report to the U.S. Environmental Protection Agency, December 2005. (http://www.camx.com/publ/pdfs/CB05_Final_Report_120805.pdf)

Chapter 4: Alkene Chemistry as a Source of Radicals

This chapter is based on a manuscript submitted for publication in A*tmospheric Environment*, titled "Modeling alkene chemistry using condensed mechanisms for conditions relevant to southeast Texas, USA."

4.1. INTRODUCTION

Alkenes are important in photochemical smog formation in southeast Texas due to their high emissions, especially from industrial sources in and around Houston (Ryerson et al., 2003; Wert et al., 2003; Daum et al., 2003, 2004; Murphy and Allen, 2005; Thomas et al., 2008) and their high reactivities (Calvert et al., 2000; Atkinson and Arey, 2003; Atkinson et al., 2006). In the atmosphere of southeast Texas, relatively high levels of alkenes were measured during two intensive air quality studies: the Texas Air Quality Study 2000 (TexAQS-2000) and the subsequent TexAQS-2006 campaign (Karl et al., 2003; Jobson et al., 2004; Gilman et al., 2009; Table 4-1). Among the alkenes, ethene (CH_2=CH_2) and propene (CH_2=CH_2CH_3) had the highest concentrations during both field campaigns (Jobson et al., 2004; Gilman, 2009; Table 4-1) and were found to be the dominant alkenes in terms of contribution to ozone formation in the greater Houston area (Ryerson et al., 2003; Wert et al., 2003; Daum et al., 2003, 2004).

Table 4-1. Summary of concentrations of 18 alkenes measured at La Porte during the TexAQS-2000 study (Jobson et al., 2004; Kuster et al., 2004)[a].

	Alkene	Average (ppb)	Median (ppb)	Maximum (ppb)	Standard deviation[b]	Measurement technique[c]
1	ethene	7.913	1.828	566.2	27.416	GC-FID
2	propene	2.717	0.450	111.3	7.635	GC-FID
3	1-butene	0.412	0.061	41.7	1.921	GC-FID
4	1-pentene	0.057	0.019	1.4	0.135	GC-FID
5	1-hexene	0.025	0.007	0.5	0.058	GC-ITMS
6	3-methyl-1-butene	0.025	0.008	0.6	0.055	GC-FID
7	2-methyl propene	0.145	0.055	3.0	0.272	GC-FID
8	2-methyl-1-butene	0.057	0.021	1.5	0.135	GC-FID
9	E-2-butene	0.037	0.010	1.2	0.094	GC-FID
10	Z-2-butene	0.033	0.010	0.9	0.082	GC-FID
11	E-2-pentene	0.053	0.014	1.7	0.141	GC-FID
12	Z-2-pentene	0.032	0.009	1.0	0.083	GC-FID
13	2-methyl-2-butene	0.046	0.019	1.7	0.109	GC-FID
14	cyclopentene	0.010	0.004	0.3	0.022	GC-FID
15	1,3-butadiene	0.305	0.087	16.7	1.143	GC-QMS
16	isoprene	0.288	0.182	28.9	0.886	GC-FID
17	α-pinene	0.022	0.010	0.2	0.033	GC-ITMS
18	limonene	0.007	0.004	0.1	0.013	GC-ITMS

[a]2,3-Dimethyl-2-butene, cyclohexene, and β-pinene were not measured during the TexAQS-2000 study. For details of measured alkene concentrations and measurement techniques, refer to Jobson et al. (2004) and Kuster et al. (2004), respectively. [b]Standard deviations in units of ppb, calculated with all available measurements during the TexAQS-2000 study. [c]GC-FID = gas chromatography (GC) with a flame ionization detector; GC-ITMS = GC with a quadrupole ion trap mass spectrometer (MS); GC-QMS = GC with a linear quadrupole MS.

Because of their high concentrations and reactivities, properly characterizing the chemistry of alkenes is important in understanding the formation of ozone and other photochemical air pollutants in Houston. In regional photochemical models used to predict the formation of ozone, alkene chemistry is represented in condensed, or lumped, photochemical mechanisms. Condensed photochemical mechanisms such as the Carbon Bond (CB) and the Statewide Air Pollution Research Center (SAPRC) mechanisms represent the reactions of alkenes with lumped rate parameters and product distributions designed to simulate the chemistry of alkenes with a limited number of reactions (Dodge,

2000; Gery et al., 1989; Yarwood et al., 2005; Carter, 2000, 2009). One method of grouping individual alkenes together into condensed reactions employs a lumped molecule approach, where alkene molecules of similar reactivity but different molecular weights or structures are grouped based on their reactivity. For example, in SAPRC-07, two model species, OLE1 and OLE2, represent all alkenes except ethene, isoprene and terpenes, as shown in Table 4-2 (Carter, 2009). Another approach to grouping alkenes into condensed reactions, employed by the Carbon Bond mechanism, breaks alkenes into different structural elements, namely, bond types (Whitten et al., 1980; Gery et al., 1989; Yarwood et al., 2005). For example, propene would be represented by one carbon double bond and one paraffinic carbon (1 OLE + 1 PAR in CB05), while 1-butene would be represented as one carbon double bond and two paraffinic carbons.

Table 4-2. Representation of alkenes in SAPRC-07 (Carter, 2009)[a].

OLE1[b]	OLE2[c]	TERP[d]	Explicitly represented
propene	2-methyl propene	α-pinene	ethene
1-butene	2-methyl-1-butene	β-pinene	isoprene
1-pentene	E-2-butene	*d*-limonene	
1-hexene	Z-2-butene	…	
3-methyl-1-butene	E-2-pentene		
…	Z-2-pentene		
	2-methyl-2-butene		
	2,3-dimethyl-2-butene		
	cyclopentene		
	cyclohexene		
	1,3-butadiene		
	…		

[a]Not all alkenes are listed in this table. [b]OLE1 is a model species in SAPRC-07 representing alkenes (other than ethene) with their OH reaction rate constant (k(OH)) less than 4.74×10^{-11} molecule^{-1}·cm^3·sec^{-1} (7.0×10^4 ppm^{-1} min^{-1}). [c]OLE2 is a model species in SAPRC-07 representing alkenes with their k(OH) equal to or higher than 4.74×10^{-11} molecule^{-1}·cm^3·sec^{-1}. [d]TERP is a model species for terpenes such as α- and β-pinene.

Both approaches to lumping employ approximations, and one of the goals of this Chapter is to examine the impact of those approximations on predictions of ozone concentrations in Houston, where the ambient distribution of alkenes is markedly different than in other urban areas (Table 4-3). One approximation that is encountered in lumped mechanisms is the chemical evolution of the lumped species. For example, in the lumped molecule approach used in SAPRC-07, where the reactions of two lumped species for alkenes (OLE1 and OLE2) represent reactions for nearly all alkenes, the overall reactivity of the lumped species decreases over time because the more reactive species in each lump disappear faster than the less reactive species. Some lumping strategies for alkenes in condensed mechanisms attempt to account for this chemical evolution of the lumps. For example, the adjustable-parameter version of SAPRC-07, which was evaluated against environmental chamber experiments (Carter, 2009), uses composition-dependent *variable* rate parameters and product distributions for the reactions of OLE1 and OLE2 with OH, O_3, NO_3 and O^3P; however, the fixed-parameter version of SAPRC-07, which is used in regional air quality models after further mechanism condensation, uses *fixed* rate parameters and product distributions derived from the composition of alkenes, as documented in Carter (2009). Thus, the fixed-parameter lumped mechanisms used in representing alkene reactions in Houston introduce two uncertainties. First, the fixed parameters may be based on an alkene mixture that is inappropriate for Houston (Table 4-3), and second, the chemical evolution of the lumped species in fixed parameter schemes may introduce errors due to differences in rate parameters of species within the lumped groups of OLE1 and OLE2 (Table 4-4). In this Chapter, the effects on predicted radical and ozone concentrations of lumping strategies for alkenes used in the fixed-parameter and adjustable-parameter versions of SAPRC-07 will be evaluated.

Table 4-3. Relative contributions of each alkene to OLE1 and OLE2 based on measurements during the TexAQS-2000 study and comparison with the composition used in constructing the fixed-version SAPRC-07.

Alkene	Contribution based on average concentrations (%)	Contribution based on median concentrations (%)	Average of urban areas[a] (%)
OLE1 alkene			
Propene	84	83	29
1-butene	13	11	12
1-pentene	2	3	11
1-hexene	1	1	24
3-methyl-1-butene	1	1	3
others	-[b]	-[b]	21
Sum	*100*	*100*	*100*
OLE2 alkene			
2-methyl propene	20	24	10
2-methyl-1-butene	8	9	8
E-2-butene	5	4	11
Z-2-butene	5	4	9
E-2-pentene	7	6	14
Z-2-pentene	4	4	14
2-methyl-2-butene	6	8	5
cyclopentene	1	2	-[c]
1,3-butadiene	42	38	6
others	-[b]	-[b]	23
Sum	*100*	*100*	*100*

[a]The average composition of alkenes for various cities in the United States was derived from analysis of ambient measurements in urban areas in the 1980s (Carter, 2009). [b]No data available. Contribution from alkenes grouped as "others" was assumed to be zero in calculating the relative contributions. [c]No data available for cyclopentene in Table 19 of Carter (2009).

Table 4-4. Rate constants towards OH and O_3 of alkenes, and OH yields of alkene-O_3 reactions at 298 K and 1 atm.

	Alkene	$k(OH)^a \times 10^{11}$	$k(O_3)^a \times 10^{17}$	Y_{OH} (Literature)[b]	Y_{OH} (SAPRC-07)[c]
-	ethene[d]	0.79[1]	0.16[1]	0.16[1]	0.16
-	isoprene[d]	10.0[1]	1.3[1]	0.25[1]	0.266
-	*OLE1*[e]	3.3[2]	1.1[2]	-	0.193
1	propene	2.9[1]	1.0[1]	0.34[1]	0.35
2	1-butene	3.1[3]	1.0[3]	0.29[4]	0.128
3	1-pentene	3.1[3]	1.1[3]	0.24[4]	0.128
4	1-hexene	3.7[3]	1.1[3]	0.18[4]	0.128
5	3-methyl-1-butene	3.2[3]	1.0[3]	0.29[i]	0.128
-	*OLE2*[f]	6.4[2]	12.4[2]	-	0.423
6	2-methyl propene	5.1[3]	1.1[3]	0.62[1]	0.72
7	2-methyl-1-butene	6.1[3]	1.4[3]	0.67[4]	0.72
8	E-2-butene	6.4[3]	19.0[3]	0.64[1]	0.54
9	Z-2-butene	5.6[3]	12.5[3]	0.33[1]	0.54
10	E-2-pentene	6.7[3]	16.0[3]	0.46[5]	0.318
11	Z-2-pentene	6.5[3]	13.0[3]	0.28[5]	0.318
12	2-methyl-2-butene	8.7[3]	40.3[3]	0.88[1]	0.862
13	2,3-dimethyl-2-butene	11.0[3]	113.0[3]	0.9[1]	1.0
14	cyclopentene	6.7[3]	57.0[3]	0.62[6]	0.095
15	cyclohexene	6.8[3]	8.1[3]	0.54[6]	0.095
16	1,3-butadiene	6.7[3]	0.63[3]	0.13[4]	0.08
-	*TERP*[g]	8.0[2]	7.0[2]	-	0.585
17	α-pinene	5.3[1]	9.0[1]	0.8[1]	0.728
[h]	β-pinene	7.4[3]	1.5[3]	0.24[7]	0.353
18	*d*-limonene	16.4[3]	21.0[3]	0.67[8]	0.729

[a]Units in molecule^{-1}·cm^3·s^{-1}. [b]Y_{OH} (Literature) is the OH yield reported in each reference. [c]Y_{OH} (SAPRC-07) is the OH yield in SAPRC-07 when each alkene is explicitly expressed as a separate species instead of a lumped species (e.g., PROPENE for propene) (Carter, 2009). [d]Explicitly represented in SAPRC-07, even in the Fixed version. [e]OLE1 is a model species in SAPRC-07 representing alkenes (other than ethene) with their OH reaction rate constant (k(OH)) less than 4.74×10^{-11} molecule^{-1}·cm^3·sec^{-1} (7.0×10^4 ppm^{-1} min^{-1}). [f]OLE2 is a model species in SAPRC-07 representing alkenes with their k(OH) equal to or higher than 4.74×10^{-11} molecule^{-1}·cm^3·sec^{-1}. [g]TERP is a model species for terpenes such as α- and β-pinene. [h]β-pinene was not measured during TexAQS-2000 and is not explicitly represented in the Extended version (SAPRC-07E). [i]Estimated by assuming the OH yield of 3-methyl-1-butne is the same as that of 1-butene.
References: 1. Atkinson et al., 2006; 2. Carter, 2009; 3. Atkinson and Arey, 2003; 4. Paulson et al., 1999; 5. Orzechowska and Paulson, 2002; 6. Fenske et al., 2000; 7. Rickard et al., 1999; 8. Aschmann et al., 2002.

A second, and related issue associated with alkene chemistry in Houston is the production of radicals from alkene-ozone reactions (Niki et al., 1987; Paulson et al., 1992; Atkinson et al., 1992; Atkinson et al., 1995; Donahue et al., 1998; Neeb and Moortgat, 1999; Paulson et al., 1999; Richard et al., 1999; Calvert et al., 2000; Siese et al., 2001; Kuwata et al., 2003, 2005; Atkinson et al., 2006; Johnson and Marston, 2008). Again, because alkene concentrations are relatively high in Houston, the production of radicals from ozonolysis may be a significant radical source, particularly at night (Paulson and Orlando, 1996; Ariya et al., 2000; Faloona et al., 2001; Heard et al., 2004; Goldstein et al., 2004), and predicted radical concentrations in Houston were often lower than concentrations observed in TexAQS-2000 and 2006 (Chen et al., 2009). During the TexAQS-2000 campaign, OH and HO_2 were measured at the La Porte municipal airport (29.669N, 95.064W) 30 km southeast of downtown Houston, Texas, and Martinez et al. (2002) reported that OH formation processes other than O_3 photolysis and reaction of HO_2 with NO were necessary to increase the OH formation rate up to around 1 part per trillion (ppt) OH per second in order to match the OH destruction rate. Daum et al. (2003) suggested that the high hydrocarbon reactivity dominated by low-molecular-weight alkenes (e.g., ethene, propene, butenes) not only provided hydrocarbon reactivity for O_3 formation but also contributed to radical production leading to rapid ozone formation rates of up to 140 parts per billion (ppb) O_3 per hour in the atmosphere of the greater Houston area.. New data on radical yields from alkene ozonolysis are emerging (Atkinson et al., 2006; Johnson and Marston, 2008), and introduction of new radical yields into condensed mechanisms may impact ozone and radical formation. This Chapter will examine the potential effect of using modified radical yields in alkene ozonolysis, particularly comparing the impacts of these modifications to changes in radical concentrations associated with changing the lumping strategies for alkenes.

4.2. DATA AND METHODS

To examine the impact of the lumping strategies and radical yields from ozonolysis, three versions of SAPRC-07 were compared to environmental chamber data produced at the University of California at Riverside (UCR) and ambient data obtained during the TexAQS-2000 study.

4.2.1. Representation of Alkenes in Three Versions of SAPRC-07

The three versions of SAPRC-07 used in this study were: the adjustable-parameter version (hereafter, referred to as "Adjustable" or "SAPRC-07A"), the fixed-parameter version (hereafter, "Fixed" or "SAPRC-07F"), and an extended version of SAPRC-07 (hereafter, "Extended" or "SAPRC-07E"). The adjustable and fixed mechanisms have been documented in Carter (2009); thus, they are only briefly described here. With SAPRC-07A, there are two options: alkenes can be represented explicitly as a separate species (e.g., propene as "propene") or lumped as a lumped model species (e.g., "propene as OLE1"). The former option is suitable for simulating environmental chamber experiments to evaluate mechanisms of individual compounds, and the latter option can be used for chamber simulations of experiments of complex mixtures and for box modeling with simulated ambient emissions (Carter, 2000, 2009). Even with the option of lumping into a limited number of model species, the reaction rate parameters and product distributions are adjusted in SAPRC-07A according to the hydrocarbon composition of the modeled air mixture. However, in SAPRC-07F, the reaction parameters are fixed for the pre-defined mixture used in deriving the fixed-parameter

version of SAPRC-07 described in Carter (2009), and all alkenes except ethene, isoprene (C_5H_8) and terpenes are speciated as OLE1 or OLE2.

Although SAPRC-07A with the option of lumping alkenes into a few model species is better at representing the changing air composition of alkenes with a limited number of reactions, incorporating this version into 3-dimensional air quality models requires further significant work. Thus, an extended version of SAPRC-07F, SAPRC-07E, was prepared for use in both chamber simulations and ambient simulations by incorporating explicit reactions for the first oxidation steps of 18 additional alkenes by the oxidants, OH, O_3, NO_3 and O^3P. In SAPRC-07E, all alkenes in Table 4-4, except β-pinene which was not measured during the TexAQS-2000 study, are explicitly represented (e.g., propene as "propene" instead of OLE1) based on the information in Appendix B-2 of Carter (2009). For details, refer to Appendix B of this work.

To evaluate the effect of radical yields from ozonolysis reactions on alkene chemistry in Houston, the yield data summarized in Table 4-4 were used. For several alkenes, there are obvious differences in the OH yield and rate constant of their ozonolysis reaction between SAPRC-07 and the recent evaluations and laboratory measurements (Table 4-4). Updated information on the OH yields and rate constants of 18 alkenes explicitly speciated in SAPRC-07E were used in sensitivity analyses.

4.2.2. Environmental Chamber Simulation

The effect of the alkene lumping modifications to the mechanisms was studied by running chamber simulations with the three versions of SAPRC-07 and comparing simulated OH, HO_2 and O_3 concentrations for the experiments listed in Table 4-5 where a single alkene was studied in presence of NOx (NO + NO_2). Most of the chamber experiments for alkenes other than propene were performed at UCR with relatively high

initial NOx concentrations (> 500 ppb) in the 1970s and 1980s (Carter et al., 1995; Carter, 2009). These experiments were supplemented by 24 recent chamber experiments for propene at UCR's EPA chamber (Carter et al., 2005). The wall mechanisms, chamber conditions, and software package for chamber simulations, originally prepared by Carter to develop and test SAPRC-07, were used without any change. For details, refer to Carter (2009).

Before using SAPRC-07E in simulations, SAPRC-07E, which has not previously been evaluated against chamber experiments, was compared with SAPRC-07A, which is the specific version of SAPRC-07 that was evaluated against thousands of chamber experiments (Carter, 2009). As described in Section 4.3.1, the Extended version (SAPRC-07E) and the Adjustable version (SAPRC-07A) showed nearly same Max(O_3) and time-concentration profiles of key species, such as O_3, OH and HO_2.

Table 4-5. List of alkene-NOx chamber experiments used in this study: 18 experiments for non-propene OLE1 and OLE2 alkenes and 24 chamber experiments for propene.

Test alkene	Run ID	$[Alkene]_o$ (ppm)	$[NOx]_o$ (ppm)	$[VOC]_o/[NOx]_o$ (ppmC/ppm)	Max(O_3)[a] (ppm)
1-butene	ITC927	1.063	0.538	7.9	0.651
	ITC930	2.792	0.526	21.3	0.725
	ITC935	2.862	1.088	10.5	0.879
	EC122	0.217	0.505	1.7	0.219
	EC123	0.404	0.510	3.2	0.505
	EC124	0.424	1.004	1.7	0.246
1-hexene	ITC929	0.844	0.519	9.8	0.299
	ITC931	1.706	0.512	20.0	0.610
	ITC934	1.613	1.069	9.0	0.382
2-methyl propene	DTC052B	0.543	0.297	7.3	0.723
	ITC694	1.013	0.500	8.1	0.893
E-2-butene	TVA063	0.025	0.020	5.1	0.097
	TVA064	0.024	0.040	2.4	0.095
	TVA065	0.024	0.041	2.4	0.100
	EC146	0.231	0.512	1.8	0.239
	EC147	0.417	0.962	1.7	0.154

	EC157	0.216	0.557	1.6	0.205
cyclohexene	EPA408B[b]	0.058	0.027	35.3	0.097
propene	EPA065A	0.052	0.024	6.5	0.153
	EPA065B	0.042	0.005	23.3	0.094
	EPA177A	0.320	0.010	91.8	0.105
	EPA177B	0.320	0.020	47.0	0.168
	EPA255A	0.331	0.027	36.8	0.204
	EPA255B	0.341	0.027	37.8	0.206
	EPA259A	0.410	0.015	80.6	0.102
	EPA259B	0.410	0.027	46.2	0.149
	EPA260A	0.431	0.029	44.9	0.198
	EPA260B	0.431	0.028	45.9	0.194
	EPA262A	0.416	0.027	46.7	0.186
	EPA280A	0.229	0.026	26.7	0.222
	EPA280B	0.235	0.026	26.8	0.154
	EPA281A	0.094	0.028	10.1	0.092
	EPA281B	0.095	0.028	10.3	0.189
	EPA329A	0.280	0.021	40.2	0.158
	EPA329B	0.331	0.027	37.1	0.187
	EPA341A	0.249	0.013	56.0	0.129
	EPA341B	0.249	0.013	55.3	0.133
	EPA348A	0.353	0.028	37.6	0.194
	EPA417A	0.300	0.028	32.7	0.211
	EPA417B	0.293	0.027	32.1	0.213
	EPA489A	0.303	0.027	34.3	0.148
	EPA489B	0.303	0.027	34.2	0.148

[a]Highest [O_3] measured by the end of each experiment. [b]n-butane (0.074), n-octane (0.022 ppm), ethene (0.014), propene (0.013), E-2-butene (0.014) were injected as well. Reference: Table C-1 of Carter (2009).

4.2.3. Box Modeling with the Fixed and Extended Versions of SAPRC-07

To characterize the effect of changes in alkene mechanisms under Houston conditions, simulations with a box model were performed using initial conditions in the morning of August 25, 2000 at the La Porte site. On this date, high concentrations of ethene and propene were measured and winds were relatively stagnant during the morning hours. The box model simulations were performed using the simulation software package developed by Carter (Carter, 2000 and 2009; http://www.engr.ucr.edu/~carter/SAPRC/files.htm). Simulations were done by using

measured inorganic and organic concentrations at around 7:30 CST as initial conditions, estimated temperatures, water vapor pressures and mixing heights based on measurements, and no additional emissions as described in Faraji et al. (2007). Additional information regarding the box model simulations is available in Appendix B.

4.3. RESULTS AND DISCUSSION

4.3.1. Comparison of Simulated O_3, OH and HO_2 Between the Three Versions of SAPRC-07 Under Chamber Conditions

Max(O_3) values simulated by the three versions of SAPRC-07 for the 18 chamber experiments for alkenes other than propene, listed in Table 4-5, are compared with measurements (Figure 4-1, Table 4-6). The Extended version (SAPRC-07E) and the Adjustable version (SAPRC-07A) showed nearly same Max(O_3) and time-concentration profiles of key species, such as O_3, OH and HO_2. The Adjustable and Extended versions showed better performance in simulating Max(O_3) than the Fixed version (SAPRC-07F) by reducing the mean error relative to the Fixed version, particularly for 1-butene and 1-hexene experiments (Table 4-6). The overall mean biases of all three mechanisms for all the 18 experiments were small, less than 5% relative to measurements; however, the overall standard deviation of the Fixed version was larger than those of the other two versions by a factor of 2 (Table 4-6).

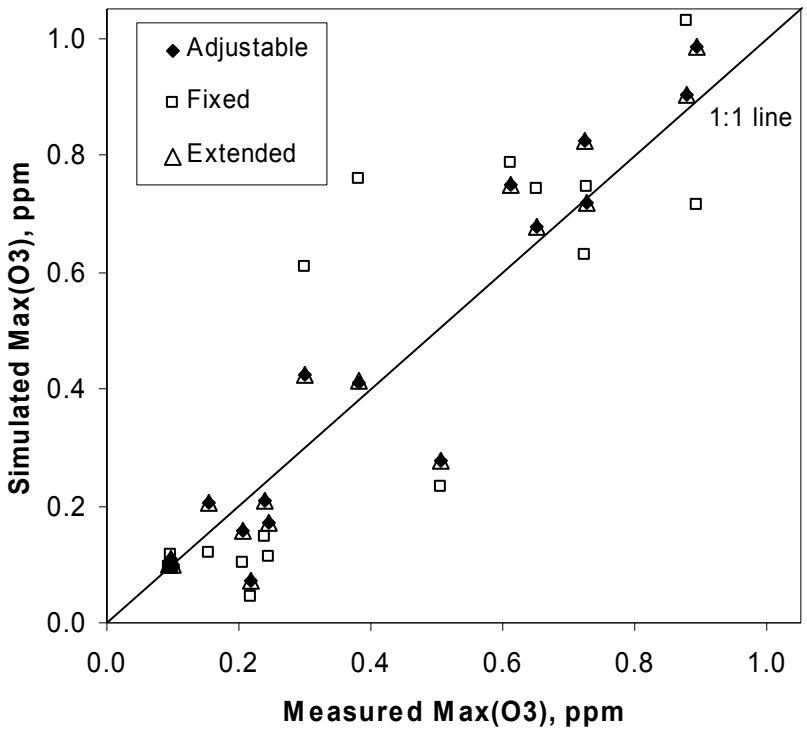

Figure 4-1. Comparison of Max(O_3) simulated by three versions of SAPRC-07 for 18 experiments for 1-alkenes.

Table 4-6. Summary of Max(O_3) performance of the three versions of SAPRC-07 for the 18 chamber experiments in Table 4-5.

Alkene	N[a]	Mean error[b] (standard deviation) [%]			Mean bias[c] (standard deviation) [%]		
		Adjustable	Fixed	Extended	Adjustable	Fixed	Extended
1-butene	6	25 (27)	37 (30)	25 (27)	-23 (30)	-26 (42)	-23 (30)
1-hexene	3	24 (17)	77 (42)	24 (17)	24 (17)	77 (42)	24 (17)
2-methyl propene	2	12 (3)	16 (5)	12 (3)	12 (3)	-16 (5)	12 (3)
E-2-butene	6	14 (12)	20 (20)	14 (12)	2 (20)	-18 (22)	2 (20)
cyclohexene	1	13 (-)	20 (-)	13 (-)	13 (-)	20 (-)	13 (-)
Overall	18	19 (18)	35 (32)	19 (18)	-1 (27)	-3 (48)	-1 (27)

[a]The number of experiments for each alkene. [b]Calculated as |model – experimental|/ experimental. [c]Calculated as (model – experimental)/experimental.

The effect of lumping strategies for alkenes in SAPRC-07F are more clearly presented in Figure 4-2 and Tables 4-7 and 4-8, which show simulated maximum concentrations for the 24 propene-NOx experiments of UCR's EPA chamber: the Adjustable and Extended versions give nearly same Max(O_3), Max(OH) and Max(HO_2) and perform better in simulating Max(O_3) than the Fixed version (Figure 4-2, Table 4-7), which is expected because propene is approximated by OLE1, a model species for multiple alkenes, in SAPRC-07F instead of a separate model species only for propene as in SAPRC-07A and SAPRC-07E. SAPRC-07F under-predicted Max(O_3) relative to measurements by about 25% (Table 4-7) and also simulated lower Max(OH) and Max(HO_2) relative to SAPRC-07A (and E) by about 50% and 35%, respectively (Figure 4-2, Table 4-8). These results imply that SAPRC-07F will under-estimate O_3 at least relative to a more explicit mechanism, SAPRC-07E, under ambient conditions when propene exists at high concentrations (e.g., tens of ppb) and dominates the OLE1 alkenes.

(a)

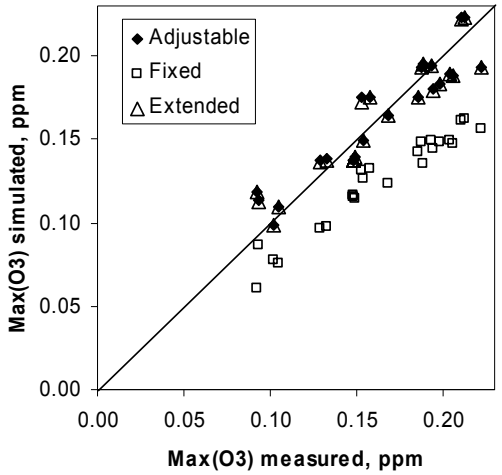

(b)

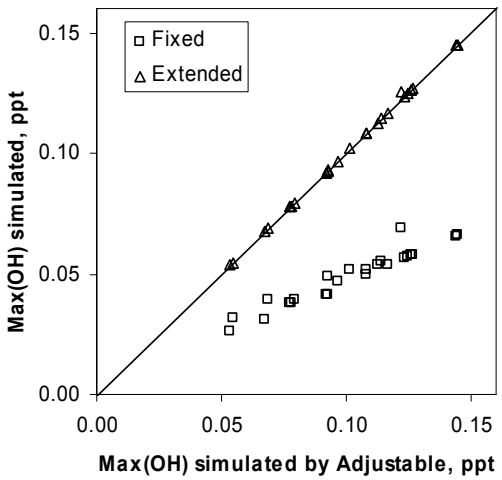

(c)

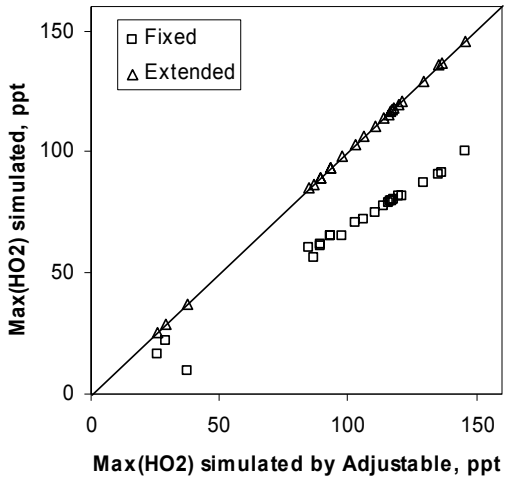

Figure 4-2. Comparison of concentrations simulated by three versions of SAPRC-07 for 24 propene-NOx experiments of UCR's EPA chamber: (a) Max(O_3), (b) Max(OH), (c) Max(HO_2).

For the propene + OH reaction, in SAPRC-07F, the HCHO and CH_3CHO yields are lower than in SAPRC-07E although the yield of higher aldehydes (RCHO) is greater than in SAPRC-07E (Carter, 2009). Furthermore, for the propene + O_3 reaction, the OH yield of SAPRC-07F is about 50% of that of SAPRC-07E (0.193 for OLE1 vs. 0.35 for propene; Table 4-4). Certainly, these different formulations to describe the oxidation of propene between SAPRC-07F and SAPRC-07A/E lead to different O_3, OH and HO_2 predictions. For further details of differences between SAPRC-07F and SAPRC-07A/E, refer to Carter (2009).

Table 4-7. Summary of Max(O_3) performance of the three versions of SAPRC-07 for 24 propene-NOx experiments of UCR's EPA chamber.

Mechanism	Mean error[a] (standard deviation) [%]	Mean bias[b] (standard deviation) [%]
Adjustable	7.7 (6.3)	1.2 (10.0)
Fixed	23.5 (5.6)	-23.5 (5.6)
Extended	7.6 (6.0)	1.0 (9.8)

[a]Calculated as |model – experimental|/experimental. [b]Calculated as (model – experimental)/experimental.

Table 4-8. Summary of Max(OH) and Max(HO_2) simulated by the three versions of SAPRC-07 for 24 propene-NOx experiments of UCR's EPA chamber

Mechanism	Mean ratio of Max(OH)[a] (standard deviation) [%]	Mean ratio of Max(HO_2)[b] (standard deviation) [%]
Fixed	48.7 (4.0)	66.5 (8.8)
Extended	100.2 (0.5)	99.8 (0.5)

[a]Calculated by averaging 24 ratios of Max(OH) simulated by each mechanism to Max(OH) simulated by the Adjustable version (SAPRC-07A) for the 24 experiments. [b]Calculated by averaging 24 ratios of Max(HO_2) simulated by each mechanism to Max(HO_2) simulated by the Adjustable version for the 24 experiments.

4.3.2. Testing Different Formulations for Reaction of O_3 with Unbranched Terminal Alkenes: 1-Butene Case Study

As documented in the last section, lumping strategies for alkenes used in condensed chemical mechanisms influence predicted radical formation from the ozonolysis of alkenes. To investigate the relative importance of lumping strategies, as opposed to reaction rate parameters, in influencing radical and O_3 production, different formulations for reaction of 1-butene with O_3, listed in Table 4-9, were evaluated.

Table 4-9. List of reaction parameters varied in the mechanisms used in simulating 1-butene-NOx chamber experiments[a].

Mechanism ID	OH yield[b]	Total radical yield[c]	α[d]	x[e]	y[f]	Radical formation from $[CH_3CH_2CHOO]^*$
SAPRC-07F	0.193	0.453	0.5	-	0.0	Not applicable because OLE1 + O_3 is used for 1-butene + O_3.
SAPRC-07A, SAPRC-07E	0.128	0.286	0.5	0.095	-	OH + CH_3CH_2 +CO (9.5%) and CH_3CH_2 + H + CO_2 (3.0%) as in SAPRC-07 (Carter, 2009)
X[1-butene + O_3 killed]	-	-	-	-	-	none; 1-butene + O_3 reaction was killed.
A1[alpha(0.5),OH(0.33)]	0.33	0.66	0.5	0.500	0.0	50% of $[CH_3CH_2CHOO]^*$ is syn and decomposed to OH + CO + CH_3CH_2
A2[alpha(0.5),OH(0.29)]	0.29	0.55	0.5	0.420	0.0	42% of $[CH_3CH_2CHOO]^*$ is decomposed to OH and CH_3CHCHO (methylated vinoxy radical) but no OH formation from CH_3CHCHO
A3[alpha(0.5),OH(0.16)]	0.16	0.32	0.5	0.160	0.0	same as in A2 but with 16%
B[alpha(0.5),OH(0.29)]	0.29	0.44	0.5	0.280	0.5	28% of $[CH_3CH_2CHOO]^*$ is decomposed to OH and CH_3CHCHO; 50% OH formation from CH_3CHCHO
C[alpha(0.65),OH(0.29)]	0.29	0.58	0.65	0.360	0.0	same as in A2 but with 36%
D[alpha(0.65),OH(0.29)]	0.29	0.486	0.65	0.288	0.25	28.8% of $[CH_3CH_2CHOO]^*$ is decomposed to OH and CH_3CHCHO; 25% OH formation from CH_3CHCHO

[a]Refer to Figure B-1 of Appendix B for a graphical description of the 1-butene + O_3 reaction and implementation of the 1-butne + O_3 reaction for each mechanism listed in this table. [b]Total OH yield from the 1-butene + O_3 reaction from $[CH_2OO]^*$ (0.16 OH per $[CH_2OO]^*$) and from $[CH_3CH_2CHOO]^*$. [c]Total radical yield for all types of radicals including OH and HO_2. [d]Branching ratio for $[CH_3CH_2CHOO]^*$ + HCHO. [e]Branching ratio for the OH-forming pathway of $[CH_3CH_2CHOO]^*$. [f]OH yield from the CH_3CHCHO radical.

The primary difference in direct radical formation from the ozonolysis of alkenes between the literature and SAPRC-07 exists in the yield of directly formed OH radicals (Y_{OH}) (Table 4-4). In SAPRC-07, the OH yields for 1-alkenes (except ethene and propene) and cycloalkenes are intentionally lowered relative to the corresponding literature values to make reasonable fits to environmental chamber measurements (Carter,

2009). OH yields in SAPRC-07 for reaction of O_3 with many unbranched terminal alkenes are about 50% of literature values (Table 4-4). For example, 1-butene shows a relatively large difference in the OH yield between SAPRC-07 and the literature (0.128 vs. 0.29 in Table 4-4); thus, several new formulations describing the reaction of 1-butene and O_3 were prepared for use in SAPRC-07E to explore the impact of various formulations of the reaction of O_3 with terminal alkenes (Table 4-9). Simulation results are shown in Figure 4-3, against a representative 1-butene-NOx experiment, ITC927, for which SAPRC-07A reasonably simulated O_3 and the initial 1-butene and NOx levels were relatively low among the available experiments for 1-butene (Table 4-5). OH and HO_2 measurements are not available for any of the chamber experiments used in this study; thus, comparison against O_3 measurements was made.

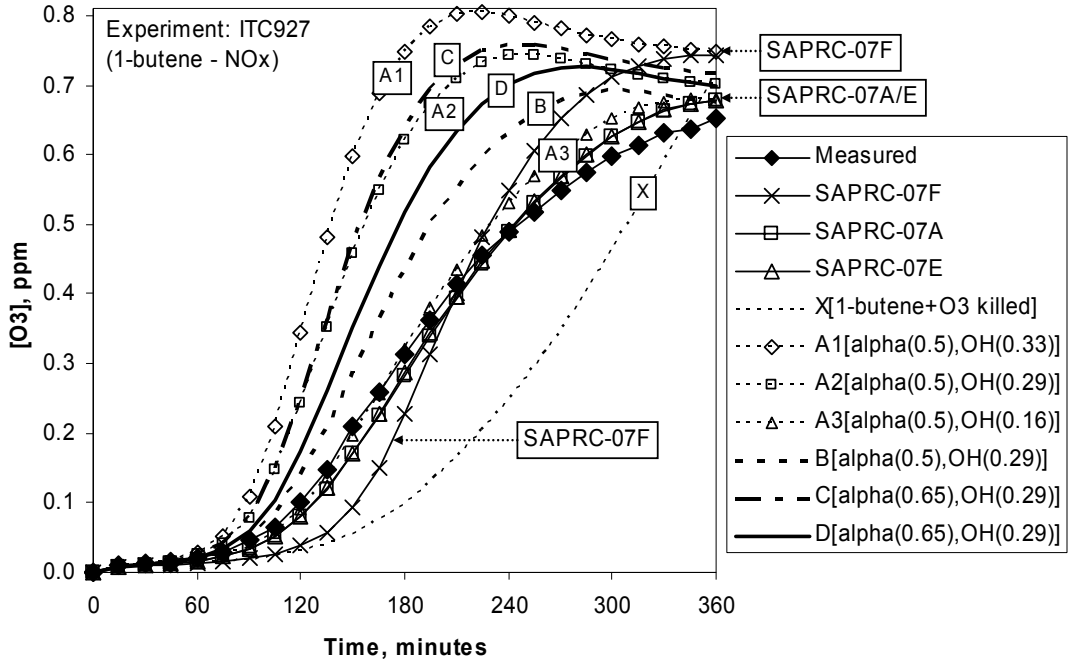

Figure 4-3. Comparison of O_3 simulated by various formulations for reaction 1-butene + O_3 in SAPRC-07 against measurements of Experiment ITC927.

As stated by Carter (2000, 2009), using an OH yield close to the literature value, 0.29, led to over-predictions of O_3, which is shown by formulations A1, A2 and C (Figure 4-3). However, formulation B where the overall OH yield is 0.29 but OH is also formed from 2-methyl vinoxy radicals ($CH_3HC=CHO$) with a yield of 0.5, shows promising performance even with the OH yield of 0.29 (Figure 4-3). This OH yield from the 2-methyl vinoxy radical, 0.5, is significantly larger than the theoretical prediction of Kuwata et al. (2005), of about 0.05. However, with formulation D where the OH yield from the 2-methyl vinoxy radical is reduced to 0.25, O_3 was over-predicted to a greater extent than with formation B.

Using intentionally lowered OH yields in SAPRC-07 for the ozonolysis of terminal alkenes such as 1-butene may contribute to reducing the OH yield from the propene-O_3 reaction when propene is lumped together with other terminal alkenes as in SAPRC-07F. Further studies on the fate of vinoxy radicals (XHC=CHO where X = alkyl or H) would help resolve the current discrepancies in OH yields for reaction of O_3 with 1-alkenes between SAPRC-07 and the literature and better represent radical formation from the ozonolysis of alkenes in the southeast Texas region.

4.3.3. Comparison of simulated OH, HO_2 and O_3 between the Fixed and Extended versions of SAPRC-07 under ambient conditions: A case study of August 25, 2000

To assess the impact of lumping strategies on predictions of ozone and radical concentrations under Houston conditions, box modeling simulations of August 25, 2000 were performed. This date was chosen because winds were largely stagnant and ethene and propene concentrations were high (Jobson et al., 2004). Using explicit reactions for first oxidation steps of alkenes increased simulated OH and HO_2 by up to 60 percent

(Figure 4-4a). These increased OH and HO_2 concentrations led to increased O_3 concentrations of up to about 15 ppb (Figure 4-4b) relative to O_3 simulated by the Fixed version (SAPRC-07F). Additional radical formation in the Extended version (SAPRC-07E) contributes to these increases in OH and HO_2. Mao et al. (2009) reported shortage in OH and HO_2 sources relative to HO and HO_2 sinks during TexAQS-2000. Thus, the direction of changes in OH and HO_2 is consistent with OH and HO_2 measurements.

HCHO photolysis was the dominant radical source in the morning of August 25, 2000 at La Porte (Figure 4-5a), due to relatively high HCHO concentrations in the Houston area (Wert et al., 2003; Dasgupta et al., 2005; Eom et al., 2008). On this morning, the dominant sources of secondary HCHO production were propene and ethene (Figure 4-5b) whose measured concentrations were 90 ppb and 103 ppb, respectively, at around 7:30 CST (Jobson et al., 2004), and propene also dominated alkenes classified as OLE1 in terms of OH and O_3 reactivities due to its high concentrations. However, as shown in Figure 4-5a, in the relatively early morning, e.g., between 7:30 (the model start time) and 8:00 CST, the direct radical formation from alkenes represented as OLE1 and OLE2 in SAPRC-07 is also relatively significant despite a HCHO concentration of over 20 ppb at 7:30 CST (Karl et al., 2003; Dasgupta et al., 2005). Alkenes expressed as OLE2 (OLE2 alkenes) existed at relatively low concentrations; however, their contribution to direct radical formation by their ozonolysis is significant in the early morning. For example, 1 ppb of 2-methyl-2-butene (dominant OLE2 species at 7:30) was predicted by SAPRC-07E to be comparable to 90 ppb of propene (dominant OLE1 species at 7:30) in terms of direct radical formation from reaction with O_3 (Figure 4-5a), due to the larger OH yield and rate constant ($k(O_3)$) of 2-methyl-2-butene compared to those of propene (Table 4-4).

(a)

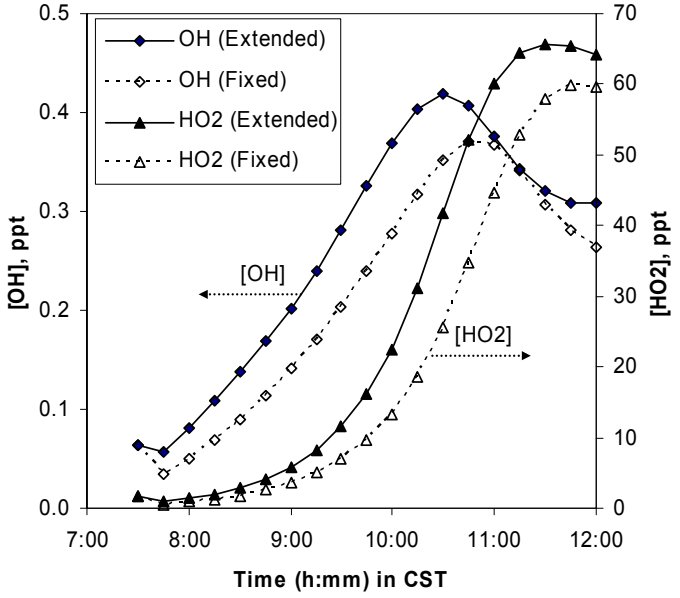

(b)

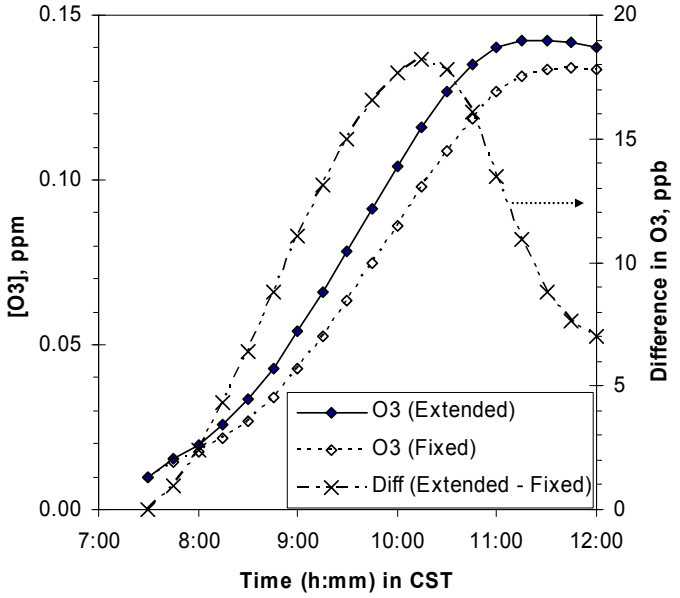

Figure 4-4. Comparisons of simulated OH, HO_2 and O_3 between the Fixed and Extended versions of SAPRC-07 for the case of August 25, 2000 at La Porte: (a) OH and HO_2, (b) O_3.

(a)

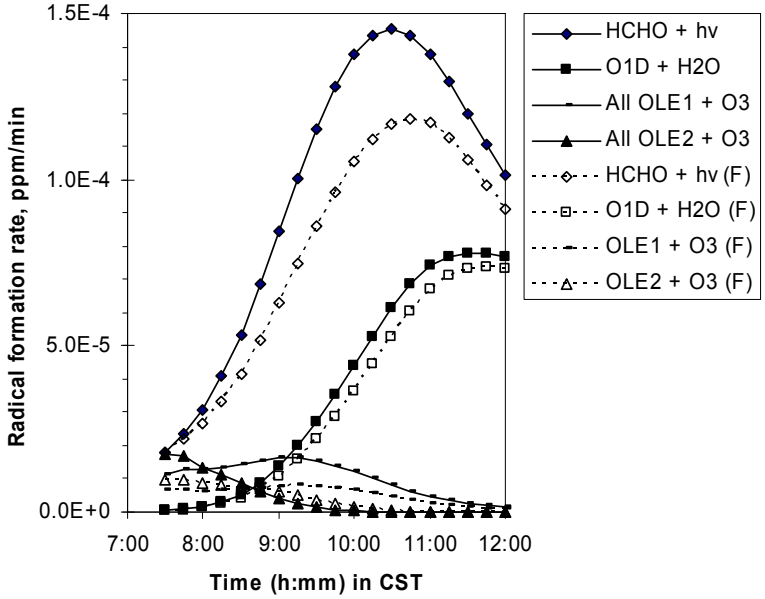

(b)

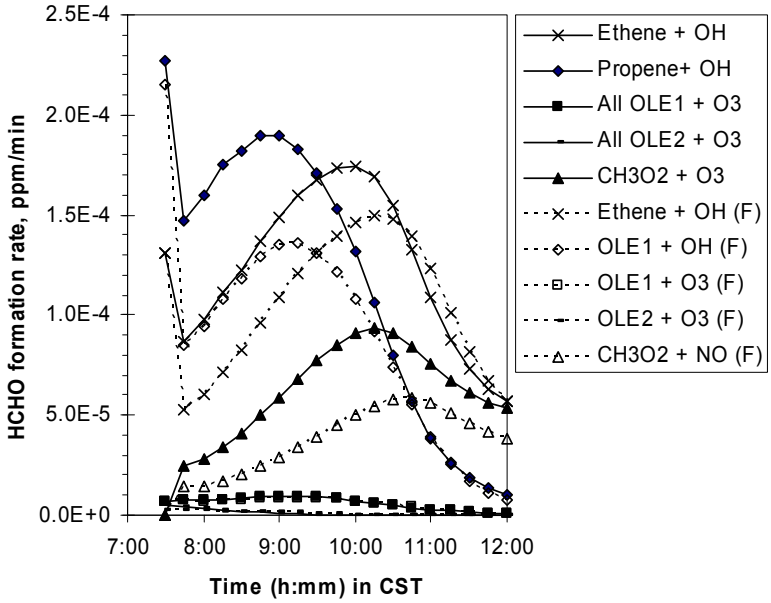

Figure 4-5. Comparison of sources of new radicals and HCHO between the Fixed and Extended versions of SAPRC-07 for the case of August 25, 2000 at La Porte: (a) sources of new radicals, (b) sources of HCHO.

Note: “All OLE1” and “All OLE2” means “all OLE1 alkenes” and “all OLE2 alkenes”, respectively.

Introducing a separate model species for propene to SAPRC-07F, and using the four reactions for propene used in SAPRC-07E resulted in nearly same OH, HO_2 and O_3 concentrations between SAPRC-07F and SAPRC-07E (Figure 4-6). Using updated rate parameters and product distributions for OLE1 and OLE2 also led to similar OH, HO_2 and O_3 between SAPRC-07F and SAPRC-07E when the OLE1 and OLE2 compositions in Table 4-3 based on the median concentrations were used in updating the OLE1 and OLE2 reactions of SAPRC-07F. These results indicate that providing accurate propene emissions into the model and using a separate model species for propene in chemical mechanisms improve performance in simulating OH, HO_2 and O_3 under ambient conditions influenced by industrial emissions in southeast Texas.

(a)

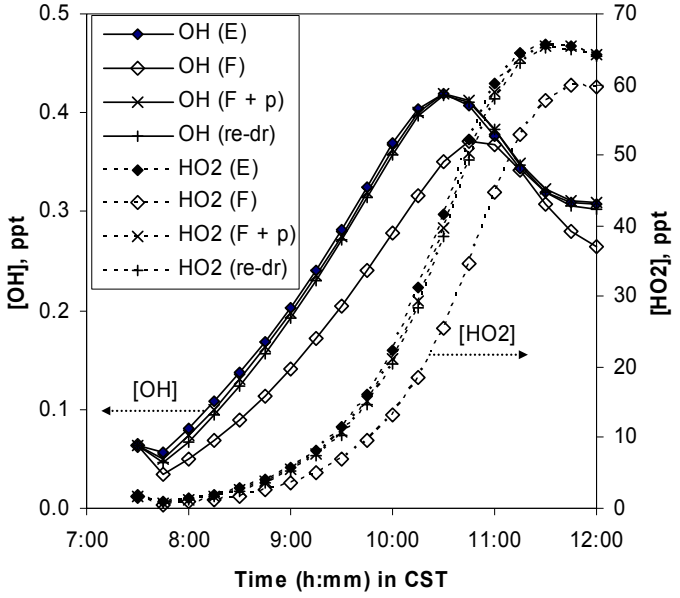

(b)

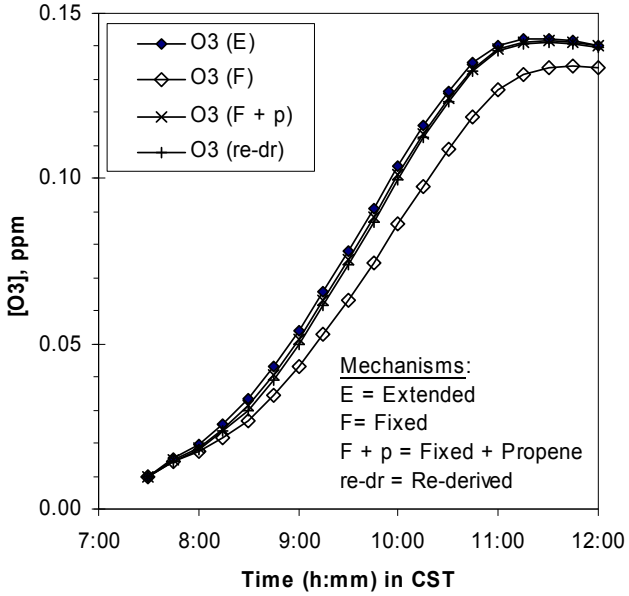

Figure 4-6. Comparison of simulated OH, HO_2 and O_3 between the various versions of SAPRC-07 for the case of August 25, 2000 at La Porte: (a) OH and HO_2, (b) O_3.

Note: "E", "F", 'F + p", and "re-dr" represent four mechanisms, namely, the Extended version, the original Fixed version, a modified Fixed version where propene is modeled separately, and a modified Fixed version with re-derived OLE1 and OLE2 reactions, respectively.

4.4. SUMMARY

The atmosphere of southeast Texas is frequently influenced by industrial emissions that lead to high alkene concentrations, especially for ethene and propene. Simulations under both chamber conditions and ambient conditions showed that the effect of the lumping strategies for alkenes in SAPRC-07 on modeled radical and ozone formation could be significant; if relatively reliable alkene concentration data are available, separately modeling individual alkenes (especially propene for southeast Texas) is recommended.

Caution must be exercised in un-lumping, however. Testing with different formulations of the 1-butene + O_3 reaction demonstrated that differences in OH yields between SAPRC-07 and the literature for reaction of O_3 with terminal alkenes could be reduced by incorporating OH formation from vinoxy radicals. However, incorporating these changes may necessitate additional reactions being added in condensed mechanisms. These results illustrate the complexity and interconnectedness in choices of stoichiometric parameters and the extent to which lumped mechanisms are un-lumped.

Currently available environmental chamber data for testing the oxidation mechanisms of alkenes except ethene and propene are very limited (Table 4-5). Further experimental studies (e.g, experimental studies on radical formation from alkenes in presence of NOx) are needed to include better descriptions of the reactions of terminal alkenes with O_3 in condensed mechanisms such as SAPRC-07 used in air quality models.

4.5. ACKNOWLEDGEMENTS

G. Heo thanks all investigators who contributed to producing the chamber data and ambient data and actually provided us with those data which were directly and indirectly used in this study, particularly, Thomas Karl for PTR-MS data, and Samuel Hall and Kurk Ullmann for actinic flux data measured during the TexAQS-2000 study.

4.6. REFERENCES

Aschmann, S.M., Arey, J., Atkinson, R., 2002. OH radical formation from the gas-phase reactions of O_3 with a series of terpenes. Atmospheric Environment 36, 4347-4355.

Atkinson, R., Aschmann, S.M., Arey, J., Shorees, B., 1992. Formation of OH radicals in the gas phase reactions of O_3 with a series of terpenes. Journal of Geophysical Research-Atmospheres 97(D5), 6065-6073.

Atkinson, R., Baulch, D.L., Cox, R.A., Crowley, J.N., Hampson, R.F., Hynes, R.G., Jenkin, M.E., Rossi, M.J., Troe, J., 2006. Evaluated kinetic and photochemical data for atmospheric chemistry: Volume II – gas phase reactions of organic species. Atmospheric Chemistry and Physics 6, 3625-4055. (http://www.atmos-chem-phys.net/6/3625/2006/)

Atkinson, R., Arey, J., 2003. Atmospheric degradation of volatile organic compounds. Chemical Reviews 103, 4605-4638.

Ariya, P.A., Sander, R., Crutzen, P.J., 2000. Significance of HOx and peroxides production due to alkene ozonolysis during fall and winter: A modeling study. Journal of Geophysical Research-Atmospheres 105(D14), 17,721-17,738.

Calvert, J. G., R. Atkinson, R., J. A. Kerr, J.A., S. Madronich, S., G. K. Moortgat, G.K., T. J. Wallington, T.J., Yarwood, G., 2000. The Mechanisms of Atmospheric Oxidation of Alkenes, Oxford University Press, New York, 552p.

Carter, W.P.L., 2000. Documentation of the SAPRC-99 chemical mechanism for VOC reactivity assessment, Report to the California Air Resources Board, Contracts 92-329 and 95-308, May 8. Available at http://www.cert.ucr.edu/~carter/absts.htm#saprc99.

Carter, W.P.L., 2009. Development of the SAPRC-07 chemical mechanism and updated ozone reactivity scales. Final Report to the California Air Resources Board Contract No. 03-318, March 20. Available at http://www.engr.ucr.edu/~carter/SAPRC/.

Carter, W.P.L., Cocker, D.R., Fitz, D.R., Malkina, I.L., Bumiller, K., Sauer, C.G., Pisano, J.T., Bufalino, C., and Song, C., 2005. A new environmental chamber for evaluation of gas-phase chemical mechanisms and secondary aerosol formation. Atmospheric Environment, 39, 7768-7788.

Carter, W.P.L., Luo, D., Malkina, I.L., Fitz, D., 1995. The University of California, Riverside Environmental Chamber Data Base for Evaluating Oxidant Mechanism. Indoor Chamber Experiments through 1993. Report submitted to the U. S. Environmental Protection Agency, EPA/AREAL, Research Triangle Park, NC, March 20. Available at http://www.engr.ucr.edu/~carter/pubs/.

Chen, S., Ren, X., Mao, J., Chen, Z., Brune, W.H., Lefer, B., Rappenglück, B., Flynn, J., Olson, J., Crawford, J.H., 2009. A comparison of chemical mechanisms based on TRAMP-2006 field data, Atmospheric Environment (2009), doi: 10.1016/j.atmosenv.2009.05.027.

Daum, P. H., Kleinman, L.I., Springston, S.R., Nunnermacker, L.J., Lee, Y.-N., Weinstein-Lloyd, J., Zheng, J., Berkowitz, C.M., 2003. A comparative study of O_3 formation in the Houston urban and industrial plumes during the 2000 Texas

Air Quality Study. Journal of Geophysical Research-Atmospheres 108(D23), 4715, doi:10.1029/2003JD003552.

Daum, P. H., Kleinman, L.I., Springston, S.R., Nunnermacker, L.J., Lee, Y.-N., Weinstein-Lloyd, J., Zheng, J., Berkowitz, C.M., 2003. Origin and properties of plumes of high ozone observed during the Texas 2000 Air Quality Study (TexAQS 2000). Journal of Geophysical Research-Atmospheres 109, D17306, doi:10.1029/2003JD004311.

Dasgupta, P.K., Li., J., Zhang, G., Luke, W.T., McClenny, W. A., Stutz, J., Fried, A., 2005. Summertime ambient formaldehyde in five U.S. metropolitan areas: Nashville, Atlanta, Houston, Philadelphia, and Tampa. Environmental Science & Technology 39, 4767-4783.

Dodge, M.C., 2000. Chemical oxidant mechanisms for air quality modeling: critical review. Atmospheric Environment 34, 2103-2130.

Donahue, N.M., Kroll, J.H., Anderson, J.G., Demerjian, K.L., 1998. Direct observation of OH production from the ozonolysis of olefins. Geophysical Research Letters 25(1), 59-62.

Eom, I.-Y., Li, Q., Li, J., Dasgupta, P.K., 2008. Robust hybrid flow analyzer for Formaldehyde. Environmental Science & Technology 42, 1221-1226.

Faloona, I., Tan, D., Brune, W., Hurst, J., Barket, D., Couch, T.L., Shepson, P., Apel, E., Riemer, D., Thornberry, T., Carroll, M.A., Sillman, S., Keeler, G.J., Sagady, J., Hooper, D., Paterson, K., 2001. Nighttime observations of anomalously high levels of hydroxyl radicals above a deciduous forest canopy. Journal of Geophysical Research-Atmospheres 106(D20), 24,315-24,333.

Faraji, M., Heo, G., Kimura, Y., McDonald-Buller, E., Allen, D., Yarwood, G., Whitten, G., Carter, W., 2007. Comparison of the Carbon Bond and SAPRC photochemical mechanisms. Report to the Texas Commission on Environmental Quality, Work Order No. 582-04-65588-07, August, 2007.

Fenske, J.D., Kuwata, K.T., Houk, K.N., Paulson, S.E., 2000. OH radical yields from the ozone reaction with cycloalkenes. Journal of Physical Chemistry A 1004, 7246-7254.

Gilman, J.B., Kuster, W.C., Goldan, P.D., Herndon, S.C., Zahniser, M.S., Tucker, S.C., Brewer, W.A., Lerner, B.M., Williams, E.J., Harley, R.A., Fehsenfeld, F.C., Warneke, C., de Gouw, J.A., 2009. Measurements of volatile organic compounds during the 2006 TexAQS/GoMACCS campaign: Industrial influences, regional characteristics, and diurnal dependencies of the OH reactivity. Journal of Geophysical Research-Atmospheres 114, D00F06, doi:10.1029/2008JD011525.

Goldstein, A.H., McKay, M., Kurpius, M.R., Schade, G.W., Lee, A., Holzinger, R., Rasmussen, R.A., 2004. Forest thinning experiment confirms ozone deposition to forest canopy is dominated by reaction with biogenic VOCs. Geophysical Research Letters 31, L22106, doi:10.1029/2004GL021259.

Heard, D.E., Carpenter, L.J., Creasey, D.J., Hopkins, J.R., Lee, J.D., Lewis, A.C., Pilling, M.J., Seakins, P.W., 2004. High levels of the hydroxyl radical in the winter urban troposphere. Geophysical Research Letters 31, L18112, doi:10.1029/2004GL020544.

Jobson, B. T., Berkowitz, C. M., Kuster, W. C., Goldan, P. D., Williams, E. J., Fesenfeld, F. C., Apel, E. C., Karl, T., Lonneman, W. A., Riemer, D., 2004. Hydrocarbon source signatures in Houston, Texas: Influence of the petrochemical industry. Journal of Geophysical Research-Atmospheres 109, D24305, doi:10.1029/2004JD004887.

Johnson, D., Marston, G., 2008. The gas-phase ozonolysis of unsaturated volatile organic compounds in the troposphere. Chemical Society Reviews 37, 699-716.

Karl, T., Jobson, T., Kuster, W.C., Williams, E., Stutz, J., Shetter, R., Hall, S.R., Goldan, P., Fehsenfeld, F., W. Lindinger, W., 2003. Use of proton transfer-reaction mass spectrometry to characterize volatile organic compound sources at the La Porte super site during the Texas Air Quality Study. Journal of Geophysical Research-Atmospheres 108(D16), 4508, doi:10.1029/2002JD003333.

Kuwata, K.T., Hasson, A.S., Dickinson, R.V., Peterson, E.B., Valin, L.C., 2005. Quantum chemical and master equation simulations of the oxidation and isomerization of vinoxy radicals. Journal of Physical Chemistry A 109, 2514-2524.

Kuwata, K.T., Templeton, K.L., Hasson, A.S., 2003. Computational studies of the chemistry of syn acetaldehyde oxide. Journal of Physical Chemistry A 107, 11,525-11,532.

Kuster, W.C., Jobson, B.T., Karl, T., Riemer, D., Apel, E., Goldan, P.D., Fehsenfeld, F.C., 2004. Intercomparison of volatile organic carbon measurement techniques and data at La Porte during the TexAQS2000 Air Quality study. Environmental Science & Technology, 38, 221-228.

Mao, J., Ren, X., Chen, S., Brune, W.H., Chen, Z., Martinez, M., Harder, H., Lefer, B., Rappenglück, Flynn, J., Leuchner, M., 2009. Atmospheric oxidation capacity in the summer of Houston 2006: Comparison with summer measurements in other metropolitan studies. Atmospheric Environment (2009), doi:10.1016/j.atmosenv.2009.01.013.

Martinez, M., Harder, H., DiCarlo, P., Brune, W.H., Hall, S.R., Shetter, R.E., Williams, E.J., Kuster, W., Jobson, B.T., 2002. OH and HO_2 concentrations, production and loss rates at the La Porte site during TexAQS 2000. Presented at the fourth Conference on Atmospheric Chemistry of the American Meteorological Society, Orlando, January 2002. Available at http://ams.confex.com/ams/annual2002/techprogram/paper_32451.htm.

Murphy, C. F., Allen, D.T., 2005. Hydrocarbon emissions from industrial release events in the Houston-Galveston area and their impact on ozone formation. Atmospheric Environment 39, 3785-3798.

Neeb, P., Moortgat, G.K., 1999. Formation of OH radicals in the gas-phase reaction of propene, isobutene, and isoprene with O_3: Yields and mechanistic implications. Journal of Physical Chemistry A 103, 9003-9012.

Niki, H., Maker, P.D., Savage, C.M., Breitenbach, L.P., Hurley, M.D., 1987. FTIR spectroscopic study of the mechanism for the gas-phase reaction between ozone and tetramethylethylene. Journal of Physical Chemistry 91, 941-946.

Orzechowska, G.E., Paulson, S.E., 2002. Production of OH radicals from the reactions of C_4-C_6 internal alkenes and styrenes with ozone in the gas phase. Atmospheric Environment 36, 571-581.

Paulson, S.E., Chung, M.Y., Hasson, A.S., 1999. OH radical formation from the gas-phase reaction of ozone with terminal alkenes and the relationship between structure and mechanism. Journal of Physical Chemistry A 103, 8125-8138.

Paulson, S.E., Flagan, R.C., Seinfeld, J.H., 1992. Atmospheric photooxidation of isoprene. 2. The ozone-isoprene reaction. International Journal of Chemical Kinetics 24(1), 103-125.

Paulson, S.E., Orlando, J.J., 1996. The reactions of ozone with alkenes: An important source of HOx in the boundary layer. Geophysical Research Letters 23, 3727-3730.

Rickard, A.R., Johnson, D., McGill, C.D., Marston, G., 1999. OH yields in the gas-phase reactions of ozone with alkenes. Journal of Physical Chemistry A 103, 7656–7664.

Ryerson, T.B., Trainer, M., Angevine, W.M., Brock, C.A., Dissly, R.W., Fehsenfeld, F.C., Frost, G.J., Goldan, P.D., Holloway, J.S., Hubler, G., Jakoubek, R.O., Kuster, W.C., Neuman, J.A., Nicks Jr., D. K., Parrish, D.D., Roberts, J.M., Sueper, D.T., Atlas, E.L., Donnelly, S.G., Flocke, F., Fried, A., Plotter, W.T., Schauffler, S., Stroud, V., Weinheimer, A.J., Wert, B.P., Wiedinmyer, C., 2003. Effect of petrochemical industrial emissions of reactive alkenes and NOx on

tropospheric ozone formation in Houston, Texas. Journal of Geophysical Research-Atmospheres 108(D8), 4249, doi:10.1029/2002JD003070.

Siese, M., Becker, K.H., Brockmann, K.J., Geiger, H., Hofzumahaus, A., Holland, F., Mihelcic, D., Wirtz, K., 2001. Direct measurement of OH radicals from ozonolysis of selected alkenes: A EUPHORE simulation chamber study. Environmental Science & Technology 35, 4660-4667.

Thomas, R., Smith, J., Jones, M., MacKay, J., Jarvie, J., 2008. Emissions modeling of specific highly reactive volatile organic compounds (HRVOC) in the Houston-Galveston-Brazoria ozone nonattainment area. Presented at the 17th Annual International Emission Inventory Conference: Inventory Evolution – Portal to Improved Air Quality, Portland, Oregon, June 2-5, 2008. Available at http://www.epa.gov/ttn/chief/conference/ei17/session6/thomas.pdf.

Wert, B.P., Trainer, M., Fried, A., Ryerson, T.B., Henry, B., Potter, W., Angevine, W.M., Atlas, E., Donnelly, S.G., Fehsenfeld, F.C., Frost, G.J., Goldan, P.D., Hansel, A., Holloway, J.S., Hubler, G., Kuster, W.C., Nicks Jr., D.K., Neuman, J.A., Parrish, D.D., Schauffler, S., Stutz, J., Sueper, D.T., Wiedinmyer, C., Wisthaler, A., 2003. Signatures of terminal alkene oxidation in airborne formaldehyde measurements during TexAQS 2000. Journal of Geophysical Research-Atmospheres 108(D3), 4104, doi:10.1029/2002JD002502.

Whitten, G.Z., Hogo, H., Killus, J.P., 1980. The carbon-bond mechanism: A condensed kinetic mechanism for photochemical smog. Environmental Science & Technology 14, 690-700.

Yarwood, G., Rao, S., Yocke, M., Whitten, G.Z., 2005. Updates to the Carbon Bond mechanism: CB05. Report to the U.S. Environmental Protection Agency, December. Available at http://www.camx.com/publ/pdfs/CB05_Final_Report_120805.pdf.

Chapter 5: Sources of Free Radicals: An intercomparison of aromatic, alkene, and molecular chlorine sources in southeast Texas

5.1. INTRODUCTION

Aromatics and alkenes act as radical sources as described in Chapter 3 and Chapter 4, respectively. Molecular chlorine (Cl_2) has also been identified as a radical source (Finlayson-Pitts and Pitts, 2000; Tanaka et al., 2000). In this Chapter, the relative magnitudes of these radical sources in southeast Texas will be compared using box modeling with TexAQS-2000 data. Before describing the box modeling, however, the reactions of reactive chlorine in urban atmospheres will be briefly described.

The dominant radical species associated with chlorine reactions in urban atmospheres is the chlorine atom, which is produced via the photolysis of molecular chlorine (Cl_2) or hypochlorous acid (HOCl). As described by Chang et al. (2002), the sources of Cl_2 and HOCl emissions that lead to atomic chlorine formation in Houston are direct emissions from industrial sources, and volatilization of industrial water treatment chemicals. Cl atoms are also heterogeneously generated from sea salts (Oum et al., 1998) and chloride-containing aerosols via $ClNO_2$ formation (Osthoff et al., 2008). These heterogeneous sources can generate significant amounts of atomic chlorine over large areas, but generally do not lead to the high localized concentrations of atomic chlorine that can be associated with industrial emissions.

Once formed in the atmosphere, chlorine (Cl) atoms react with most alkanes, alcohols and alkenes faster than OH radicals, typically by one or two orders (Table 5-1). Therefore, the total Cl reactivity is higher than the total OH reactivity (assuming equivalent radical concentrations) as shown in Figure 5-1 for August 25, 2000 at La Porte.

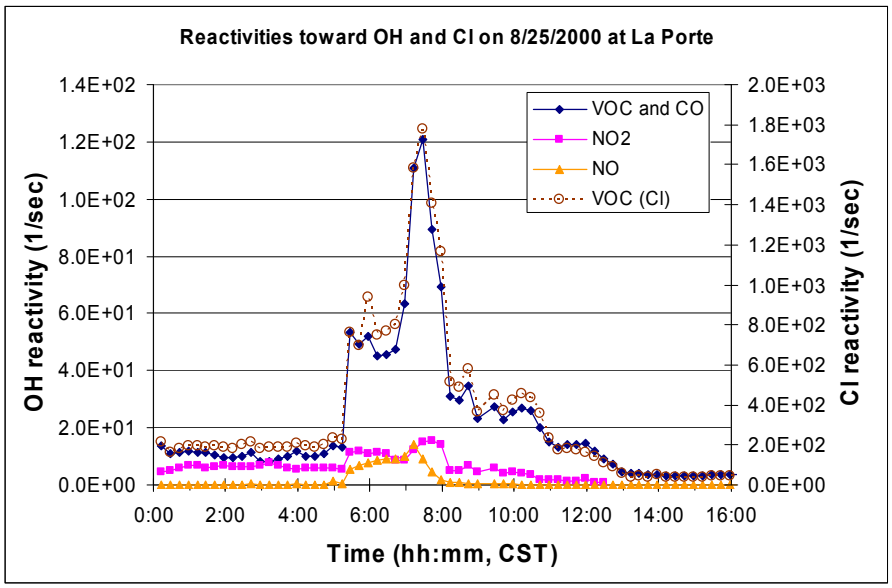

Figure 5-1. OH and Cl reactivities on August 25, 2000 based on measured data during the TexAQS-2000 study.

Note: Legends of VOC and CO, NO_2, and NO represent OH reactivities due to VOC and CO, NO_2, and NO, respectively.

In the lower troposphere, Cl atoms are commonly less abundant than OH radicals; however, in coastal urban areas where anthropogenic sources of Cl atoms such as industrial point sources, cooling towers and swimming pools also exist (Chang et al., 2002), chlorine atoms could play important roles in tropospheric chemistry while competing with OH for oxidation of organic compounds in the atmosphere (Hov, 1985; Tanaka et al., 2000). Even when Cl atoms cannot compete with OH radicals due to low availability, Cl atoms still have potential for accelerating the photochemical activities in the early morning by oxidizing hydrocarbons and supplying new OH and HO_2 (HOx) radicals without consumption of OH. At La Porte, a coastal urban area near Houston, Texas, where anthropogenic Cl sources exist nearby (Chang et al., 2002), Cl chemistry could compete with OH or increase OH to various degrees.

Measuring Cl-atom concentrations of typically well below ppt level is a technically difficult task (Finlayson-Pitts and Pitts, 2000). Therefore, atmospheric tracers that can be used for confirming the presence of Cl-atom chemistry have been studied in laboratories. 1-Chloro-3-methyl-3-butene-2-one (CMBO) and chloromethylbutenal (CMBA) including 4-chloro-3-methyl-2-butenal and 4-chloro-2-methyl-2-butenal are unique makers of Cl chemistry, which are produced by the reaction of isoprene by Cl atoms. When atomic chlorine reacts with 1,3-butadiene, 4-chlorocrotonaldehyde ((E)-4-chloro-2-butenal) and chloromethyl vinyl ketone (CMVK) serve as Cl markers (Ragains and Finlayson-Pitts, 1997; Nordmeyer et al., 1997; Wang and Finlayson-Pitts, 2000). In addition, 2-chloro-ethanal ($ClCH_2CHO$) and 1-chloro-2-propanone ($ClCH_2C(O)CH_3$) are major products of ethene ($CH_2=CH_2$) and propene ($CH_2=CH-CH_3$) reaction with Cl atoms (Yarwood et al., 1992; Orlando et al., 1998; Kukui and Le Bras, 2001; Orlando et al., 2003; Nakayama et al., 2007), and are suggested as markers of Cl chemistry (Orlando et al., 2003). The fractions of ethene and propene that react with Cl atoms and the fates of their products ($ClCH_2CHO$ and $ClCH_2C(O)CH_3$) in the ambient air are still uncertain though the oxidation of ethene and propene is expected to be dominated by OH under most ambient conditions .

Cl-chemistry markers, CMBO and CMBA, were detected at concentrations of up to 125 and 145 ppt, respectively, mostly in morning hours at the La Porte site during TexAQS-2000 (Riemer and Apel, 2001), which has confirmed the presence of Cl chemistry around the Houston Ship Channel area. Cl-atom concentration in the atmosphere of southeast Texas of up to (1-3) $\times$ 10^5 molecules/cm^3 was suggested by Riemer and Apel (2001) for the Houston area based on the CMBO and CMBA measurements during the TexAQS-2000. In addition, the enhancement of ozone formation by Cl chemistry has been demonstrated by smog chamber experiments using

captive ambient air (Tanaka et al, 2003a and 2003b). Cl chemistry enhances oxidation rates of relatively unreactive species such as methanol and ethane as well as relatively reactive alkenes such as ethene, propene, 1,3-butadiene and isoprene (Table 5-1). Thus, in the morning, when there are high emissions of organic compounds emitted from various sources and if Cl atoms are available in the air, the oxidation of these compounds by Cl radicals could supply significant HOx radicals.

Table 5-1. Reaction rates of organic compounds measured at the La Porte site (units of k: $cm^3 molecule^{-1} sec^{-1}$)*

	Organic compounds		k(OH)	$k(O_3)$	$k(NO_3)$	k(Cl)
	Alkenes					
1	Ethene	a	7.90E-12[1]	1.60E-18[1]	2.05E-16[2]	1.10E-10[1]
2	tetrachloroethylene	b	1.70E-13[3]	-	-	3.60E-11[3]
3	propene	a	2.90E-11[1]	1.00E-17[1]	9.50E-15[1]	2.70E-10[1]
4	methylpropene	a	5.14E-11[2]	1.13E-17[2]	3.44E-13[2]	3.40E-10[4]
5	1-butene	a	3.14E-11[2]	9.64E-18[2]	1.35E-14[2]	3.38E-10[4]
6	2-methyl-1-butene	a	6.10E-11[2]	1.40E-17[2]	-	3.58E-10[4]
7	3-methyl-1-butene	a	3.18E-11[2]	9.50E-18[2]	-	3.29E-10[4]
8	T-2-butene	a	6.40E-11[2]	1.90E-16[2]	3.90E-13[2]	3.31E-10[4]
9	C-2-butene	a	5.64E-11[2]	1.25E-16[2]	3.52E-13[2]	3.76E-10[4]
10	2-methyl-2-butene	a,b	8.69E-11[2]	4.03E-16[2]	9.37E-12[2]	3.95E-10[4]
11	1-pentene	a,b	3.14E-11[2]	1.06E-17[2]	1.50E-14[2]	3.97E-10[4]
12	T-2-pentene	a,b	6.70E-11[2]	1.60E-16[2]	-	-
13	C-2-pentene	a,b	6.50E-11[2]	1.30E-16[2]	-	-
14	cyclopentene	a	6.70E-11[2]	5.70E-16[2]	4.20E-13[2]	7.32E-10[4]
15	1-hexene	b	3.70E-11[2]	1.13E-17[2]	1.80E-14[2]	4.90E-10[6]
16	1,3-butadiene	b,c	6.66E-11[2]	6.30E-18[2]	1.00E-13[2]	4.20E-10[7]
17	isoprene	a,b,c	1.00E-10[1]	1.27E-17[1]	7.00E-13[1]	4.30E-10[8]
18	α-pinene	b	5.30E-11[1]	9.00E-17[1]	6.20E-12[1]	4.70E-10[9]
19	limonene	b	1.64E-10[2]	2.10E-16[2]	1.22E-11[2]	6.40E-10[9]
	Alkanes					
1	ethane	a	2.40E-13[1]	<1E-23[2]	< 1E-17[1]	5.90E-11[1]
2	methylchloroform	b	1.00E-14[3]	-	-	8.50E-15[3]
3	propane	a	1.10E-12[1]	<1E-23[2]	< 7E-17[1]	1.40E-10[1]
4	i-butane	a	2.12E-12[2]	<1E-23[2]	1.06E-16[2]	1.43E-10[6]
5	n-butane	a	2.36E-12[1]	<1E-23[2]	4.60E-17[1]	2.05E-10[1]
6	2,2-dimethylbutane	a	2.23E-12[2]	<1E-23[2]	-	
7	i-pentane	a,b	3.60E-12[2]	<1E-23[2]	1.62E-16[2]	2.20E-10[6]
8	n-pentane	a,b	3.80E-12[2]	<1E-23[2]	8.70E-17[2]	2.80E-10[6]
9	2-methylpentane	b	5.20E-12[2]	<1E-23[2]	1.80E-16[2]	2.90E-10[6]
10	3-methylpentane	a,b	5.20E-12[2]	<1E-23[2]	2.20E-16[2]	2.80E-10[6]
11	hexane	a,b	5.20E-12[2]	<1E-23[2]	1.10E-16[2]	3.40E-10[6]
12	2,2,4-trimethylpentane	b	3.34E-12[2]	<1E-23[2]	9.00E-17[2]	2.60E-10[6]
13	n-heptane	b	6.76E-12[2]	<1E-23[2]	1.50E-16[2]	3.90E-10[6]
14	octane	b	8.11E-12[2]	<1E-23[2]	1.90E-16[2]	4.60E-10[6]
15	nonane	b	9.70E-12[2]	<1E-23[2]	2.30E-16[2]	4.80E-106
16	decane	b	1.10E-11[2]	<1E-23[2]	2.80E-16[2]	5.50E-10[6]
17	cyclopentane	b	4.97E-12[2]	<1E-23[2]	-	3.05E-10[10]
18	methylcyclopentane	a,b	8.60E-12[2]	<1E-23[2]	-	2.82E-10[10]
19	cyclohexane	b	6.97E-12[2]	<1E-23[2]	1.40E-16[2]	3.50E-10[6]
20	methylcyclohexane	b	9.64E-12[2]	<1E-23[2]	-	3.90E-10[6]

	Oxygenates					
1	acetaladehyde	*b*	1.50E-11[1]	<1E-20[2]	2.70E-15[1]	8.00E-11[1]
2	propanal	*b*	2.00E-11[1]	<1E-20[2]	6.40E-15[1]	1.30E-10[1]
3	acrolein	*c*	2.40E-11[2]	-	1.10E-15[11]	1.80E-10[11]
4	methacrolein	*c*	2.90E-11[1]	1.20E-18[1]	3.40E-15[1]	2.40E-10[8]
5	acetone	*b*	1.70E-13[1]	<1E-20[2]	< 3E-17[1]	2.10E-12[1]
6	MEK (2-butanone)	*b*	1.22E-12[1]	<1E-20[2]	-	3.60E-11[1]
7	MVK	*c*	2.00E-11[2]	5.20E-18[1]	5.20E-18[1]	2.20E-10[8]
8	3-methyl-2-butanone	*c*	2.90E-12[2]	-	-	-
9	2-pentanone	*c*	4.40E-12[2]	<1E-20[2]	-	-
10	3-pentanone	*c*	2.00E-12[2]	<1E-20[2]	-	-
11	MTBE	*c*	2.94E-12[2]	-	-	-
	Aromatics					
1	benzene	*b,c*	1.22E-12[2]	<1E-20[2]	< 3E-17[2]	1.30E-16[12]
2	toluene	*b,c*	5.63E-12[2]	<1E-20[2]	7.00E-17[2]	6.20E-11[13]
3	ethylbenzene	*b*	7.00E-12[2]	<1E-20[2]	< 6E-16[2]	1.15E-10[5]
4	m- & p-xylene	*b*	23.1E-12[2] (m) 14.3E-12[2] (p)	<1E-20[2]	4.1E-16[2] (m) 5.0E-16[2] (p)	1.35E-10 [13](m) 1.44E-10[13](p)
5	o-xylene	*b*	1.36E-11[2]	<1E-20[2]	4.10E-16[2]	1.40E-10[13]
6	styrene	*b*	5.80E-11[2]	1.70E-17[2]	1.50E-12[2]	3.60E-10[14]
7	1,2,4-trimethylbenzene	*b*	3.25E-11[2]	<1E-20[2]	1.80E-15[2]	-
8	1,2,3-trimethylbenzene	*b*	3.27E-11[2]	<1E-20[2]	1.90E-15[2]	-
9	1,3,5-trimethylbenzene	*b*	5.67E-11[2]	<1E-20[2]	8.80E-16[2]	2.32E-10[13]
10	(1-methylethyl)benzene	*b*	6.30E-12[2]	<1E-20[2]	-	-
	Cl markers					
1	CMBO	*c*	-	-	-	-
2	CMBA	*c*	-	-	-	-
	Others*					
1	HCHO		8.50E-12[1]	-	5.60E-16[1]	7.20E-11[1]
2	CH_4		6.40E-15[1]	-	< 1E-18[1]	1.00E-13[1]
3	CH_3OH		9.00E-13[1]	-	1.30E-16[1]	5.50E-11[1]
4	C_2H_5OH		3.20E-12[1]	-	< 2E-15[1]	1.00E-10[1]

*Three measured alkynes, acetylene, propyne, and 1-butyne were excluded in this table due to their relatively low reactivities. HCHO and CH_3OH were measured by the PTR-MS (Proton-Transfer Reaction Mass Spectrometer) system (Karl et al., 2003), and CH_4 and $C2H_5OH$ were listed only for reference. [a]GC-FID (Gas chromatograph with a flame ionization detector). [b]GC-ITMS (GC with a quadrupole ion trap mass spectrometer detector). [c]GC-QMS (GC with a linear quadrupole mass spectrometer). For details, refer to Chapter 2 and Kuster et al. (2004).
1. Atkinson et al. (2006), **2**. Atkinson and Arey (2003), **3**. Sander et al. (2006), **4**. Ezell et al. (2002), **5**. Anderson et al. (2007a), **6**. Atkinson (1997), **7**. Ragains and Finlayson-Pitts (1997), **8**. Orlando et al. (2003), **9**. Finlayson-Pitts et al. (1999), **10**. Anderson et al. (2007b), **11**. Ullerstam et al. (2001), **12**. Sokolov et al. (1998), **13**. Wang et al. (2005), **14**. Shi and Bernhard (1997), **15**. Coquet and Aria (2000).

5.2. DATA AND METHODS

There are no chamber experiments relevant to testing Cl chemistry as a radical source in the chamber data described in Chapter 2. Therefore, box modeling with TexAQS-2000 data was used in this study.

5.2.1. Selection of a Modeling Case: August 25, 2000 at La Porte

The significance of this Cl chemistry depends on the chemical composition in the air as well as the availability of Cl atoms. For example, on August 25, 2000, methanol (CH_3OH), which more rapidly reacts with Cl atoms than with OH radicals, was detected at concentrations up to 300 ppb at around 6:00 CST at the La Porte site (Karl et al., 2003), and there were simultaneous rapid increases in OH, HO_2 and O_3 around 7:45 CST when ethene, propene, ethane and propane existed all above 20 ppb and non-zero CMBO and CMBA were detected (Jobson et al., 2004; Riemer and Apel, 2001; Figure 1-2 of Chapter 1).

Based on the TexAQS-2000 data summarized in Tables 2-2 to 2-4 of Chapter 2, the significance of Cl chemistry was tested using a case of the morning of August 25, 2000. Several levels of the initial concentration of Cl_2 at 7:30 CST ranging 0 ppb to 30 ppb were used in the sensitivity analyses using the SAPRC software for box modeling developed by Carter (Chapter 2).

5.2.2. Estimating Cl_2 Emissions for the Case of August 25, 2000 at La Porte

Measured concentrations of isoprene and CMBO were used to estimate the amount of Cl_2 emissions for the selected modeling case. The level of chlorine atoms and the magnitude of Cl_2 emissions were calculated as follows:

$\int_{t1}^{t2} y_{CMBO} \cdot k_{Cl} \cdot [isoprene] \cdot [Cl]$ = Change in [CMBO] between t_1 and t_2

when the CMBO concentration ([CMBO]) is dominated by the rate of CMBO formation rather than by the rate of CMBO degradation. y_{CMBO} is the yield of CMBO for the reaction of isoprene with the Cl atom.

When the average concentration of isoprene over the time interval, t_1 to t_2, is used, [Cl] can be approximated as follows: [Cl] $\approx$ ($[CBMO]_{t2} - [CMBO]_{t1}$) / {$y_{CMBO} \cdot k_{Cl} \cdot$ average [ISOP]$\cdot(t_2 - t_1)$}. If we assume that the photolysis of Cl_2 is the dominant source of Cl atoms and that the air mass is stagnant, the required amount of Cl_2 emissions in terms of the Cl_2 concentration ($[Cl_2]o$) can be calculated as follows: $[Cl_2]o$ = (Total Cl reactivity)$\cdot$[Cl]/{$2 \cdot j(Cl_2)$}, which is derived from the balance of Cl formation and destruction (P - L$\cdot$[Cl] = 0 where P is $2 \cdot j(Cl_2) \cdot [Cl_2]$; refer to Chapter 2 for calculation of L (the total Cl reactivity, or the loss frequency).

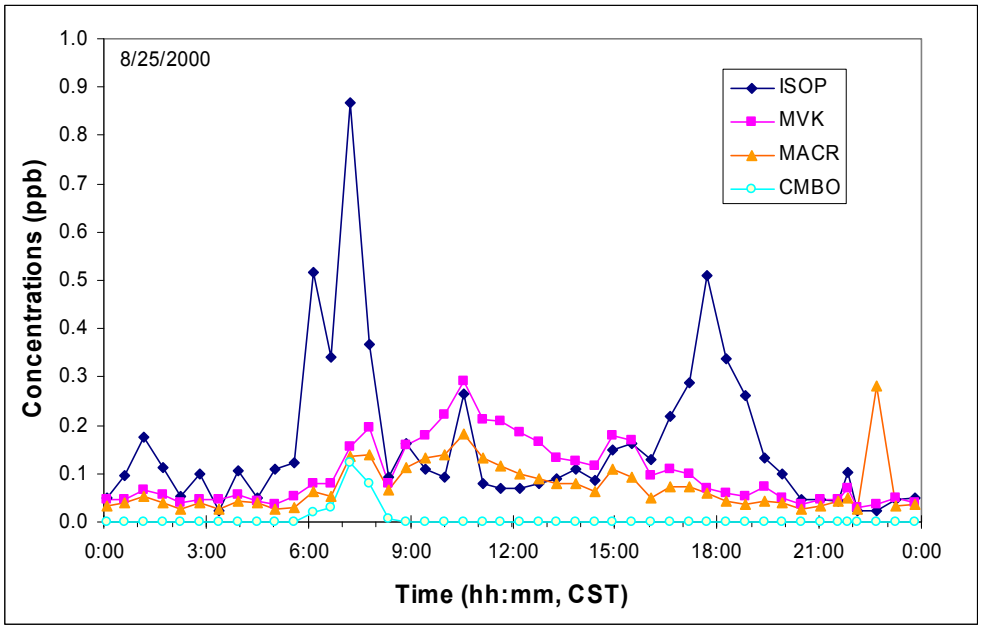

Figure 5-2. Isoprene (ISOP), methyl vinyl ketone (MVK), methacrolein (MACR) and CMBO on August 25, 2000

Note: Isoprene, methyl vinyl ketone and methacrolein and CMBO were measured for 5 minutes at intervals of 33 minutes by the GC-QMS system (Riemer and Apel, 2001; Kuster et al., 2004).

Using the CMBO yield of 0.28 (Tanaka et al., 2003a), the rate constant (k) of 10.6 $ppb^{-1} \cdot sec^{-1}$ (Orlando et al., 2003; Table 5-1), an average isoprene concentration of about 0.6 ppb and a change in [CMBO] of 0.09 ppb between 6:40 and 7:15 CST (Figure 5-2), [Cl] is estimated to be 0.025 ppt (assuming a pseudo-steady state for this short time period). With an average Cl loss frequency (L) of 1500 sec^{-1} (Figure 5-1), the required Cl_2 emissions as $[Cl_2]o$ is 22 ppb Cl_2 for the SAPRC-07 mechanism and 18 ppb Cl_2 for the CB05 mechanism because $j(Cl_2)$ in CB05 is higher than in SAPRC-07 at 7:30 CST, the model start time. Therefore, in this work, Cl_2 emissions were given as an instantaneous input of Cl_2 at 7:30 CST between 0 ppb and 30 ppb of Cl_2.

5.2.3. Chemical Mechanisms Used in Box Modeling

Four different chemical mechanisms were used: the two versions of CB05 (either with the Base toluene mechanism or the UNClite mechanism; refer to Chapter 3), and the Fixed and Extended versions of SAPRC-07 (Chapter 4). These four chemical mechanisms were used after being extended for chlorine chemistry by incorporating the chlorine mechanism of Tanaka et al. (2003) in CB05 and adding relevant reactions of chlorine atoms in SAPRC-07 (Carter, 2009). For details of modifications of CB05-Base (hereafter, also referred to as "CB05B"), CB05-UNClite (also referred to as "CB05U"), the Fixed SAPRC-07 (SAPRC-07F; also referred to as "S07F") and the Extended SAPRC-07 (SAPRC-07E; also referred to as "S07E"), refer to Appendix C. Note in particular, in SAPRC-07E, propene is separately modeled for its reactions with both OH and Cl (Appendix C).

5.3. SIMULATION RESULTS

5.3.1. Impacts of Chlorine Emissions on Radicals and Ozone

Results from sensitivity simulations of chlorine injections at the model start (7:30 CST) on August 25, 2000 show that Cl chemistry could increase concentrations of OH and HO_2, and accelerate the formation of O_3 (Figures 5-3, 5-4, 5-5). Although the estimated magnitude of Cl_2 emissions was around 20 ~ 25 ppb Cl_2, $[Cl_2]o$ above 10 ppb seems to be too much based on unreasonably large increases in O_3 in response to the injection of Cl_2 at 7:30 CST (Figure 5-5). Even using 30 ppb $[Cl_2]o$, modeled CBMO concentrations did not go higher than 7 ppt in any chemical mechanism used in this work (Figure 5-6). The measured peak CMBO concentration in this morning was 123 ppt around 7:15 CST, second highest measured CMBO concentration during the TexAQS-

2000 (Riemer and Apel, 2001); however, the initial condition of CMBO was set at 0 ppt because CMBO itself is an indicator of the reaction of isoprene with chlorine atoms but does not act as a major radical source or sink. The modeled peak CMBO concentrations in the four mechanisms ranging 1.5 ppt to 6.5 ppt in response to injection of Cl_2 between 5 ppb and 30 ppb (Figure 5-6) seem to be reasonably modeled when those values are compared to the 90th percentile value of CMBO measurements during the TexAQS-2000, 5 ppt (Riemer and Apel, 2001).

As shown in Figures 5-3 and 5-4, chlorine chemistry will increase OH and HO_2, and available Cl atoms will be consumed rapidly not only by isoprene but also by other reactive compounds when there are abundant hydrocarbons such as propane and propene and no continuous Cl-atom sources. Furthermore, isoprene is oxidized by both OH radicals and Cl atoms. When OH is high, methyl vinyl ketone (MVK) and metharcrolein (MACR) will dominate over CMBO in the distribution of isoprene oxidation products (Figure 5-2). Thus, CMBO formation will be favored under conditions when OH levels are relatively low at a given source strength of Cl atoms and when isoprene is abundant relative to other compounds reactive towards Cl. In other words, non-zero CMBO levels when other reactive compounds are abundant support that Cl chemistry is significant.

The impact of Cl_2 emissions on OH, HO_2 and O_3 can be explained by rapid reaction of Cl atoms with organic compounds including alkanes and alkenes. During oxidation of these organic compounds, peroxy radicals are generated and oxidize NO into NO_2, which is demonstrated by rapid decreases in NO (Figure 5-7). Cl atoms formed from Cl_2 also lead to increases in formaldehyde (HCHO), a photolytic radical source (Figure 5-8). Therefore, even though Cl atoms tend to have short lifetimes due to their high reactivity with atmospheric pollutants, products from oxidation by Cl atoms (e.g.,

peroxy radicals and HCHO) influence the evolution on OH, HO_2 and O_3 (Figure 5-3, 5-4, 5-5).

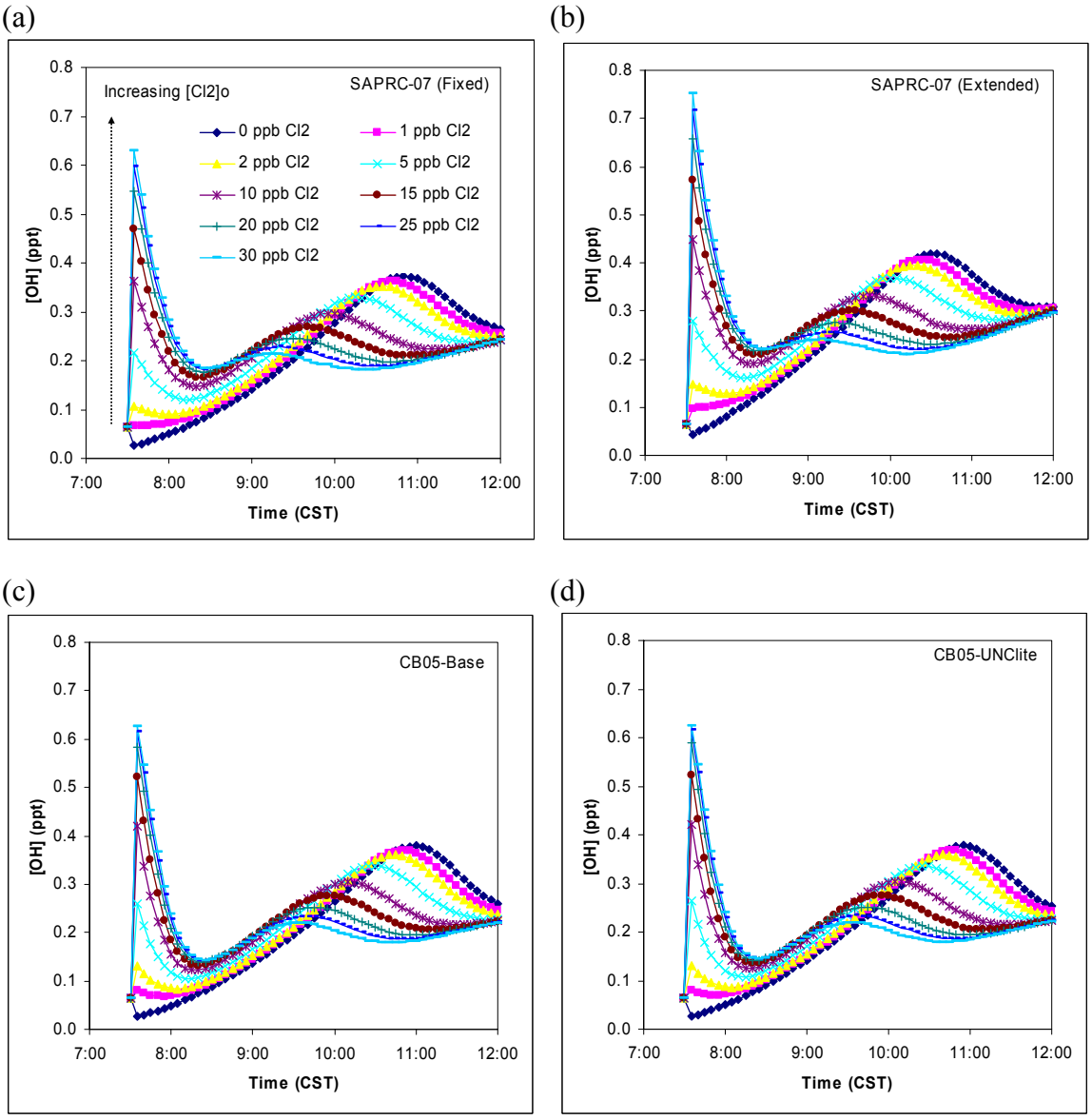

Figure 5-3. Effects of injected chlorine (Cl_2) at 7:30 CST on August 25, 2000 on modeled OH concentrations in chemical mechanisms: (a) SAPRC-07F, (b) SAPRC-07E, (c) CB05-Base, (d) CB05-UNClite.

Note: Box modeling was not intended to match modeled and measured concentrations.

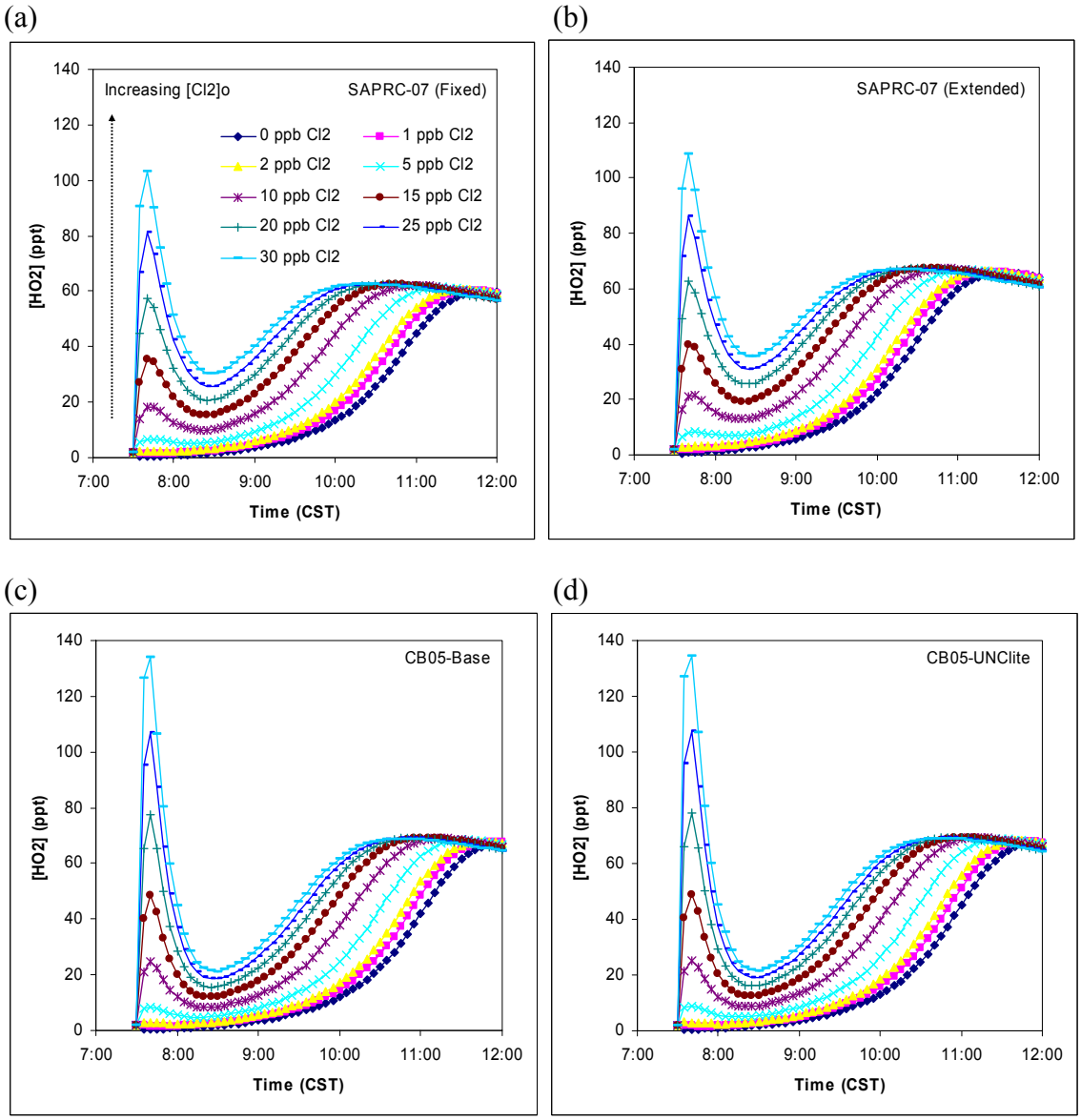

Figure 5-4. Effects of injected chlorine (Cl_2) at 7:30 CST on August 25, 2000 on modeled HO_2 concentrations in chemical mechanisms: (a) SAPRC-07F, (b) SAPRC-07E, (c) CB05-Base, (d) CB05-UNClite.

Note: Box modeling was not intended to match modeled and measured concentrations.

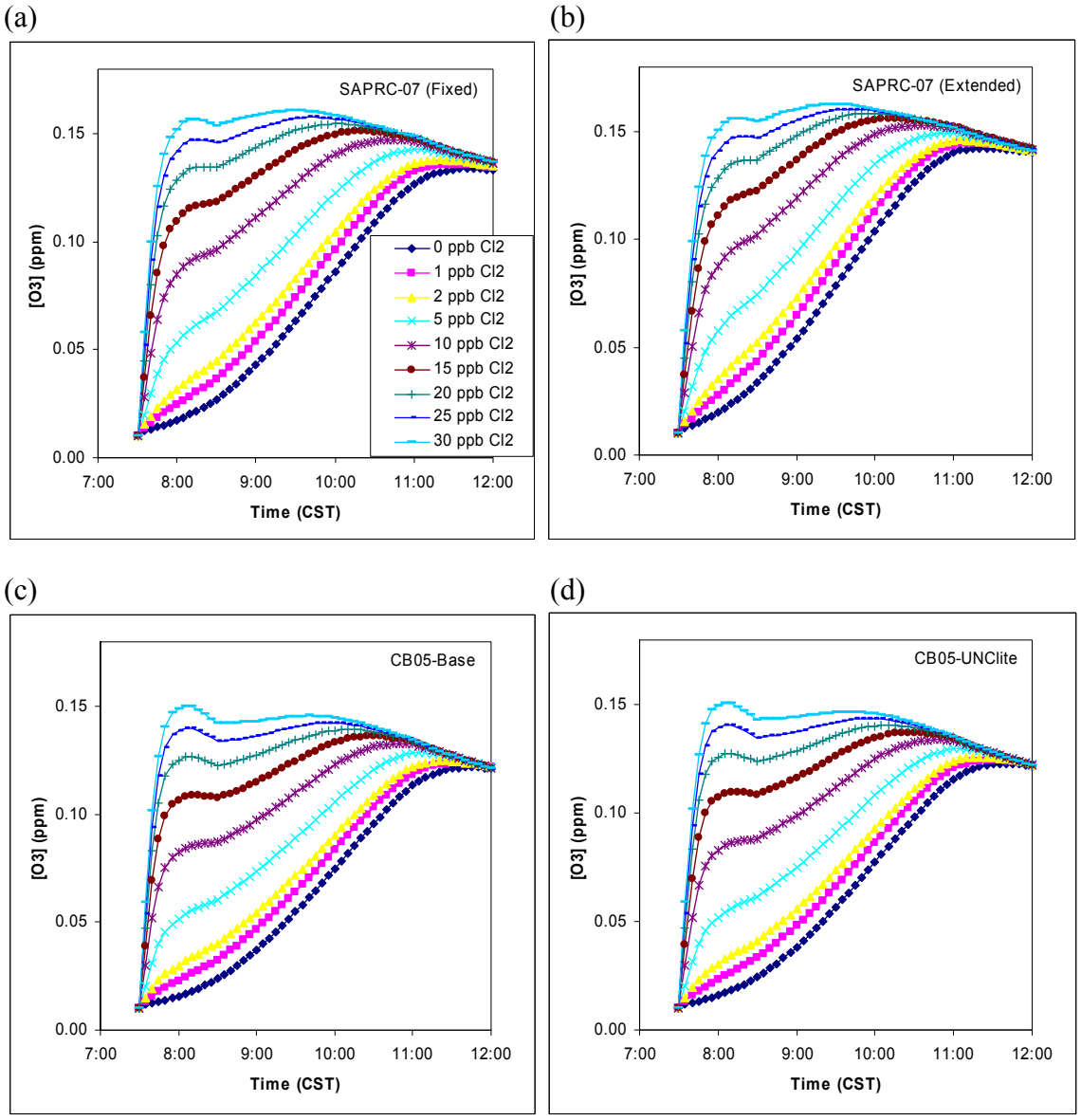

Figure 5-5. Effects of injected chlorine (Cl_2) at 7:30 CST on August 25, 2000 on modeled O_3 concentrations in chemical mechanisms: (a) SAPRC-07F, (b) SAPRC-07E, (c) CB05-Base, (d) CB05-UNClite.

Note: Box modeling was not intended to match modeled and measured concentrations.

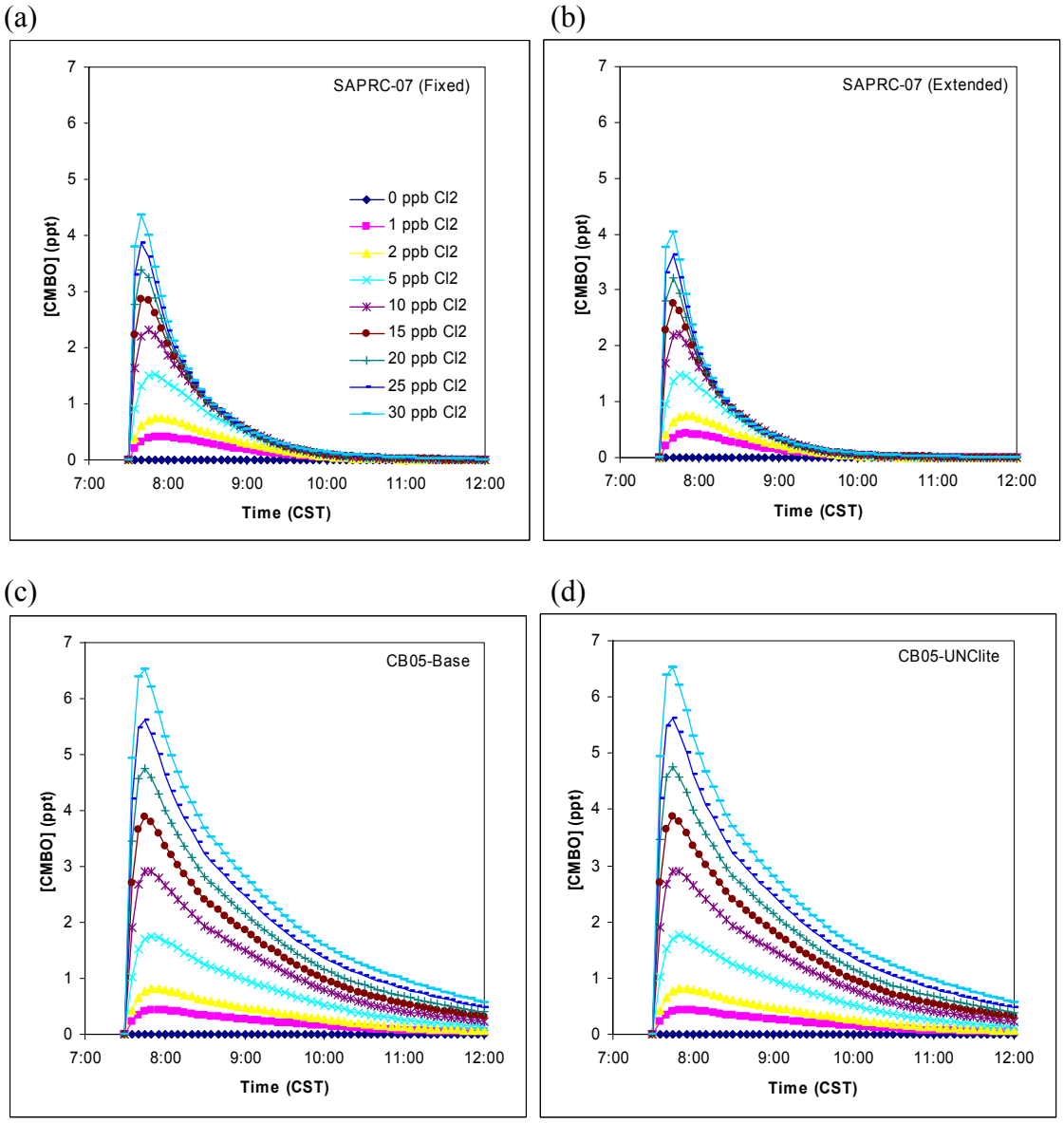

Figure 5-6. Effects of injected chlorine (Cl_2) at 7:30 CST on August 25, 2000 on modeled CMBO concentrations in chemical mechanisms: (a) SAPRC-07F, (b) SAPRC-07E, (c) CB05-Base, (d) CB05-UNClite.

Note: Box modeling was not intended to match modeled and measured concentrations.

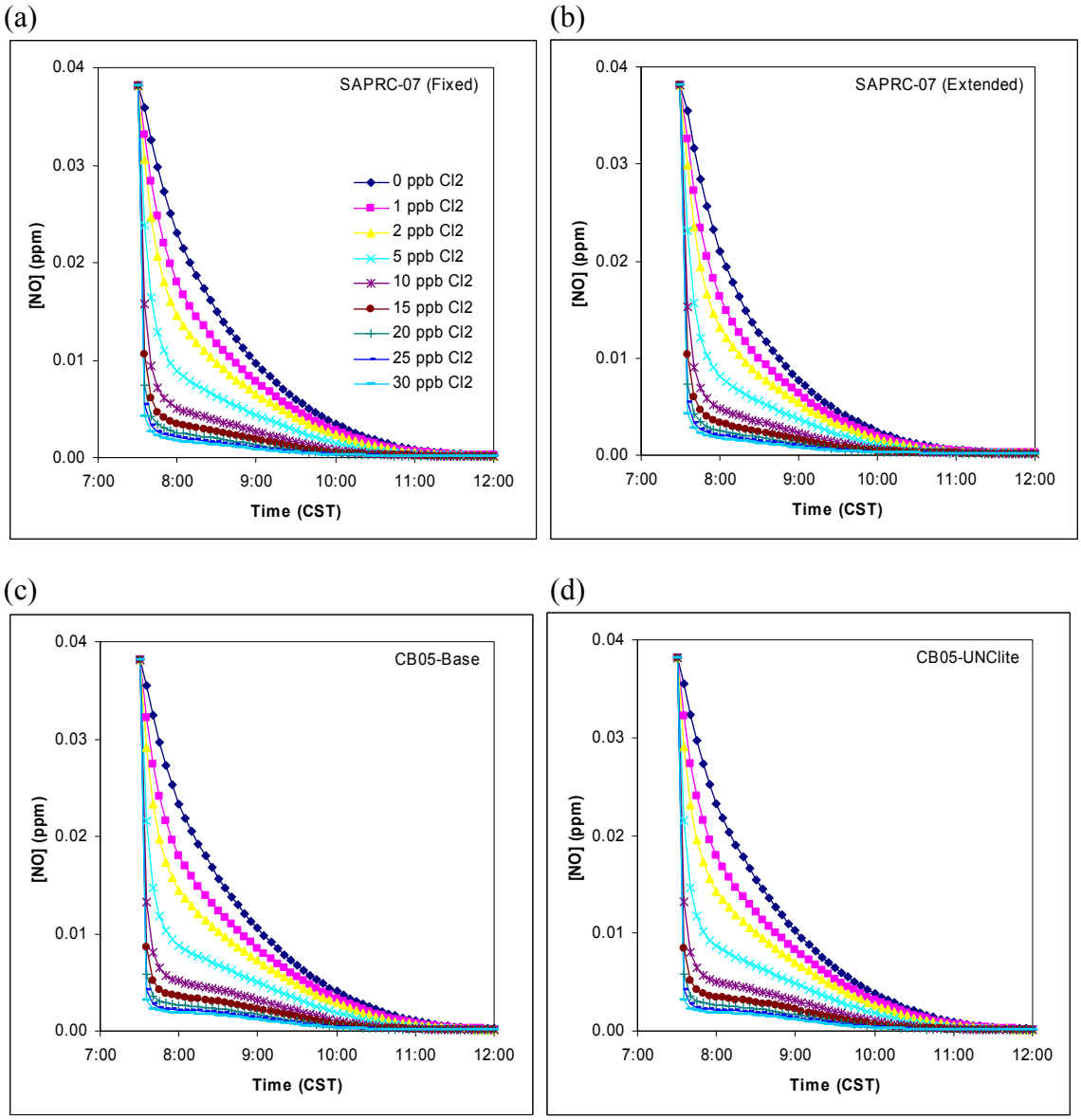

Figure 5-7. Effects of injected chlorine (Cl_2) at 7:30 CST on August 25, 2000 on modeled NO concentrations in chemical mechanisms: (a) SAPRC-07F, (b) SAPRC-07E, (c) CB05-Base, (d) CB05-UNClite.

Note: Box modeling was not intended to match modeled and measured concentrations.

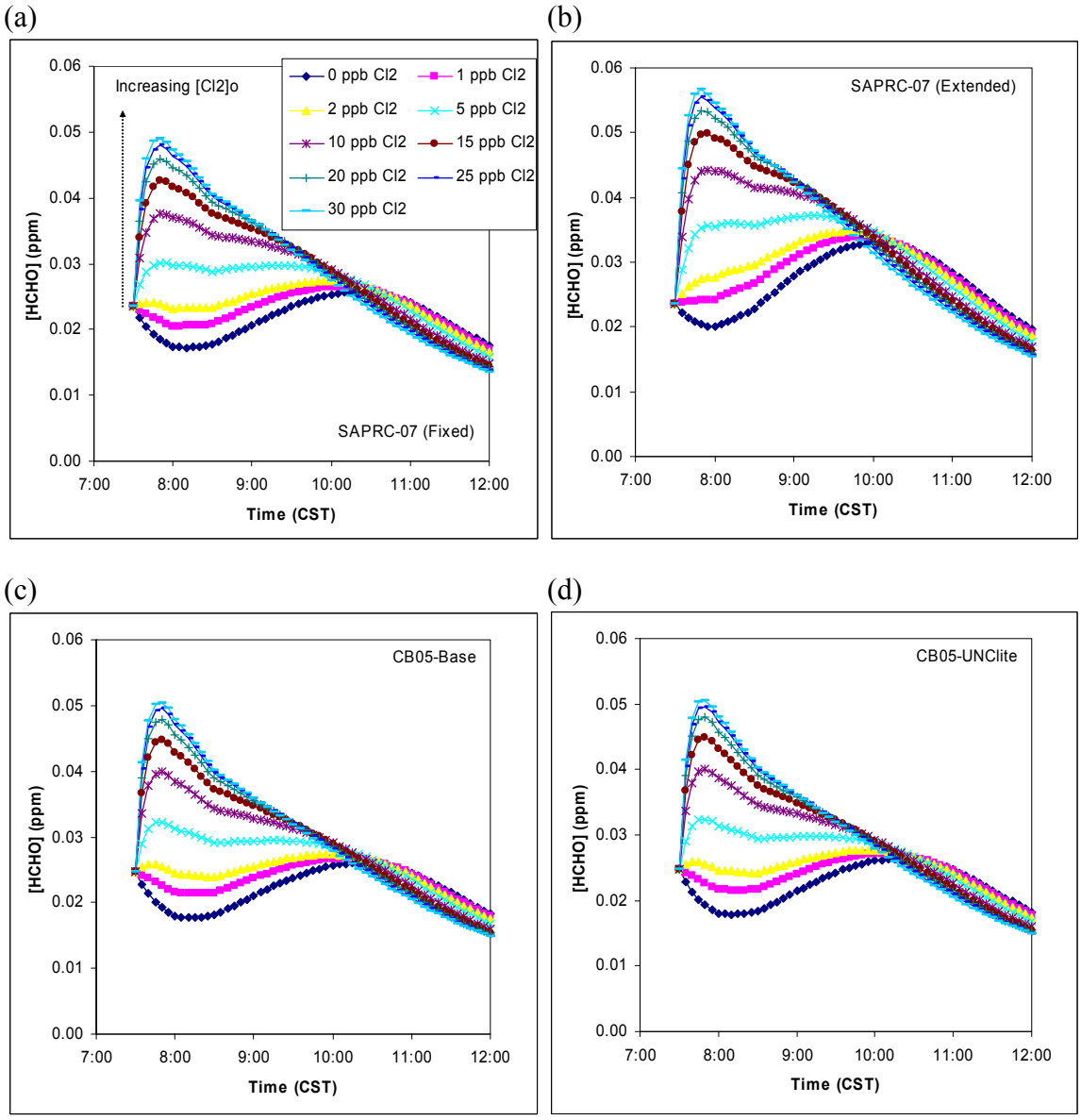

Figure 5-8. Effects of injected chlorine (Cl_2) at 7:30 CST on August 25, 2000 on modeled HCHO concentrations in chemical mechanisms: (a) SAPRC-07F, (b) SAPRC-07E, (c) CB05-Base, (d) CB05-UNClite.

Note: Box modeling was not intended to match modeled and measured concentrations.

5.3.2. Intercomparison of Effects of Aromatics, Alkenes and Molecular Chlorine Emissions on Radicals

Aromatics, alkenes and molecular chlorine contribute to radical formation. Thus, the impacts of these different radical sources were compared. Figures 5-3 to 5-5 are too complex to use for this purpose. Therefore, simplified figures are prepared (Figures 5-9 and 5-10). Overall, the relative importance of each radical source (aromatics, alkenes, molecular chlorine) depends on their emissions. As described in detail in Chapter 4, on the morning of August 25, 2000, at La Porte, alkenes (e.g., ethene and propene) were relatively high; however, the concentrations of toluene and xylenes were below 5 ppb (Jobson et al., 2004). Therefore, the effect on OH, HO_2 and O_3 of using different representations of alkenes in SAPRC-07 is larger than the effect of using different toluene mechanisms in CB05 (Figures 5-9 and 5-10).

The impact of using different lumping strategies for alkenes in SAPRC-07 is comparable to that of Cl_2 emissions equal to $[Cl_2]o$ of 1 ppb (compare the lines for S07E(0 ppb Cl_2) and S07F (1 ppb Cl_2) in Figure 5-9 where S07E and S07F represent the Extended version SAPRC-07 and the Fixed version SAPRC-07, respectively). Combination of separately modeling major alkenes (e.g., propene) and using molecular chlorine emissions results in even more increases in OH, HO_2, O_3 than just using molecular chlorine emissions (compare the lines for S07E (1 ppb Cl_2) and S07F (1 ppb Cl_2), and the lines for S07E (5 ppb Cl_2) and S07F (5 ppb Cl_2)).

The impact of using different toluene mechanisms in CB05 was simulated to be relatively small (Figure 5-10) due to low concentrations of toluene and xylenes in this morning. However, the actual impacts of these different contributors to radical formation in condensed chemical mechanisms such as SAPRC-07 and CB05 will depend on specific ambient conditions such as emissions. Therefore, changes in modeled OH,

HO_2 and O_3 concentrations in CB05 by increases in the initial concentration of toluene (TOL) ranging from 5 ppb to 100 ppb were compared with changes in OH, HO_2 and O_3 by chlorine emissions of 1 ppb Cl_2 (Figure 5-11). The magnitude of the impact of 15 ppb of toluene (TOL) on HO_2 is similar to that of 1 ppb [Cl_2] (Figure 5-11b). As the initial toluene concentration increases, the rate of NO oxidation and the rate of NOx depletion increase. However, NO oxidation is accelerated more strongly and quickly by Cl_2 emissions than using different lumping strategies for alkenes in SAPRC-07 (Figure 5-7a,b) and using a different toluene mechanism (UNClite) in CB05 (Figure 5-12a, Figure 5-7c,d).

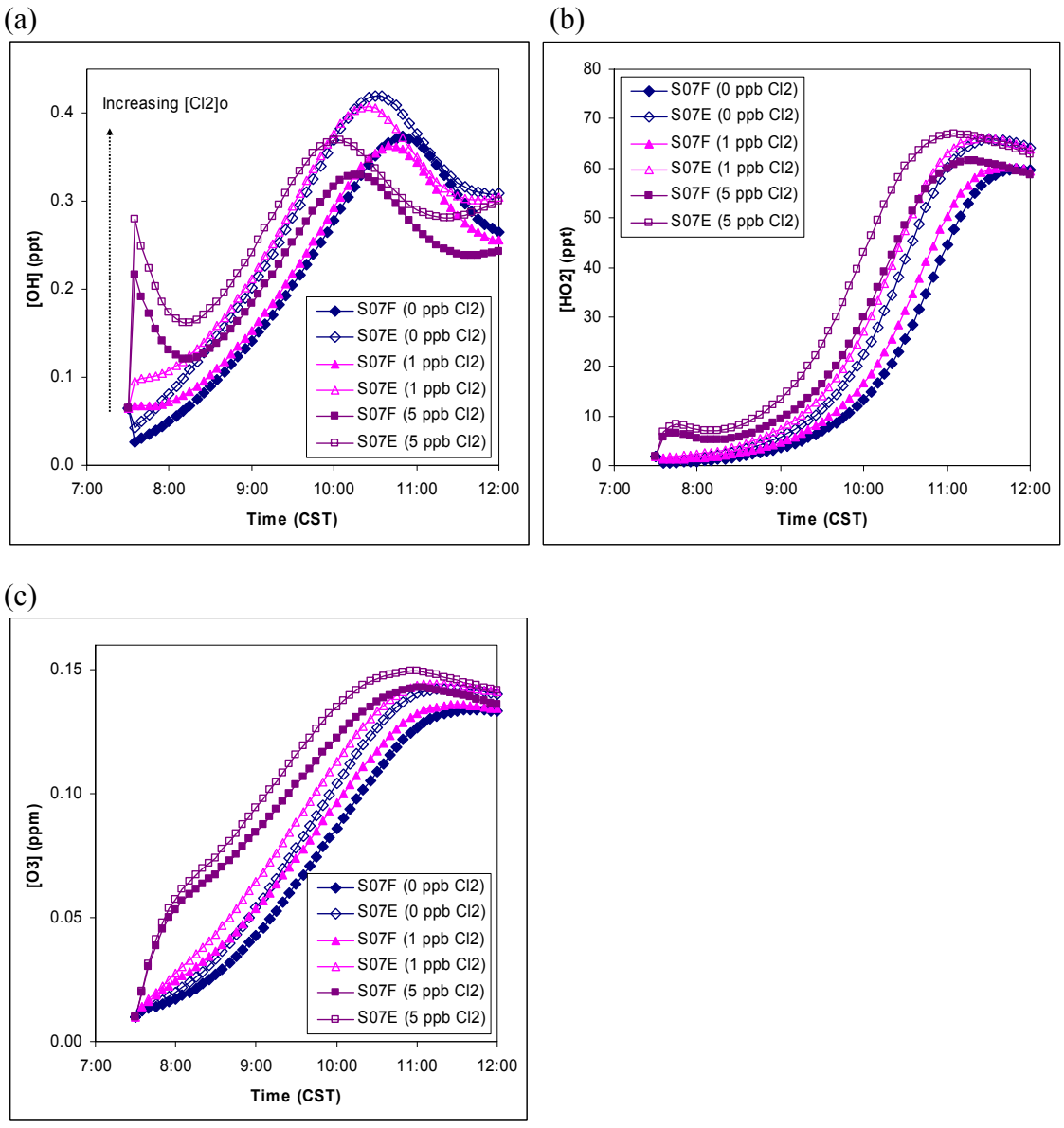

Figure 5-9. Comparison of effects of chlorine emissions and using different lumping strategies for alkenes in SAPRC-07 on (a) OH, (b) HO_2, (c) O_3 for the case of August 25, 2000.

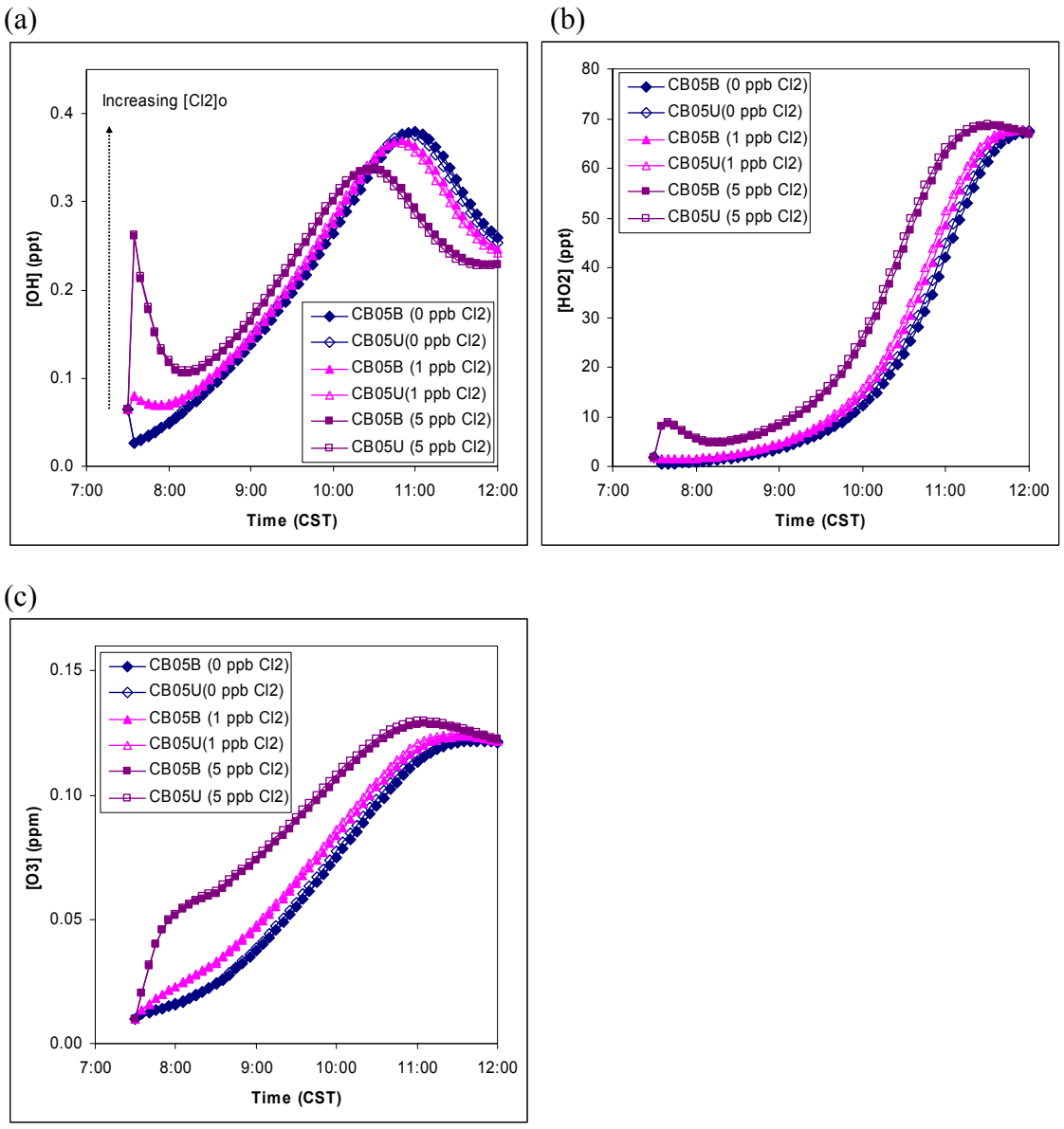

Figure 5-10. Comparison of effects of chlorine emissions and using different toluene mechanisms in CB05 on (a) OH, (b) HO_2, (c) O_3 for the case of August 25, 2000.

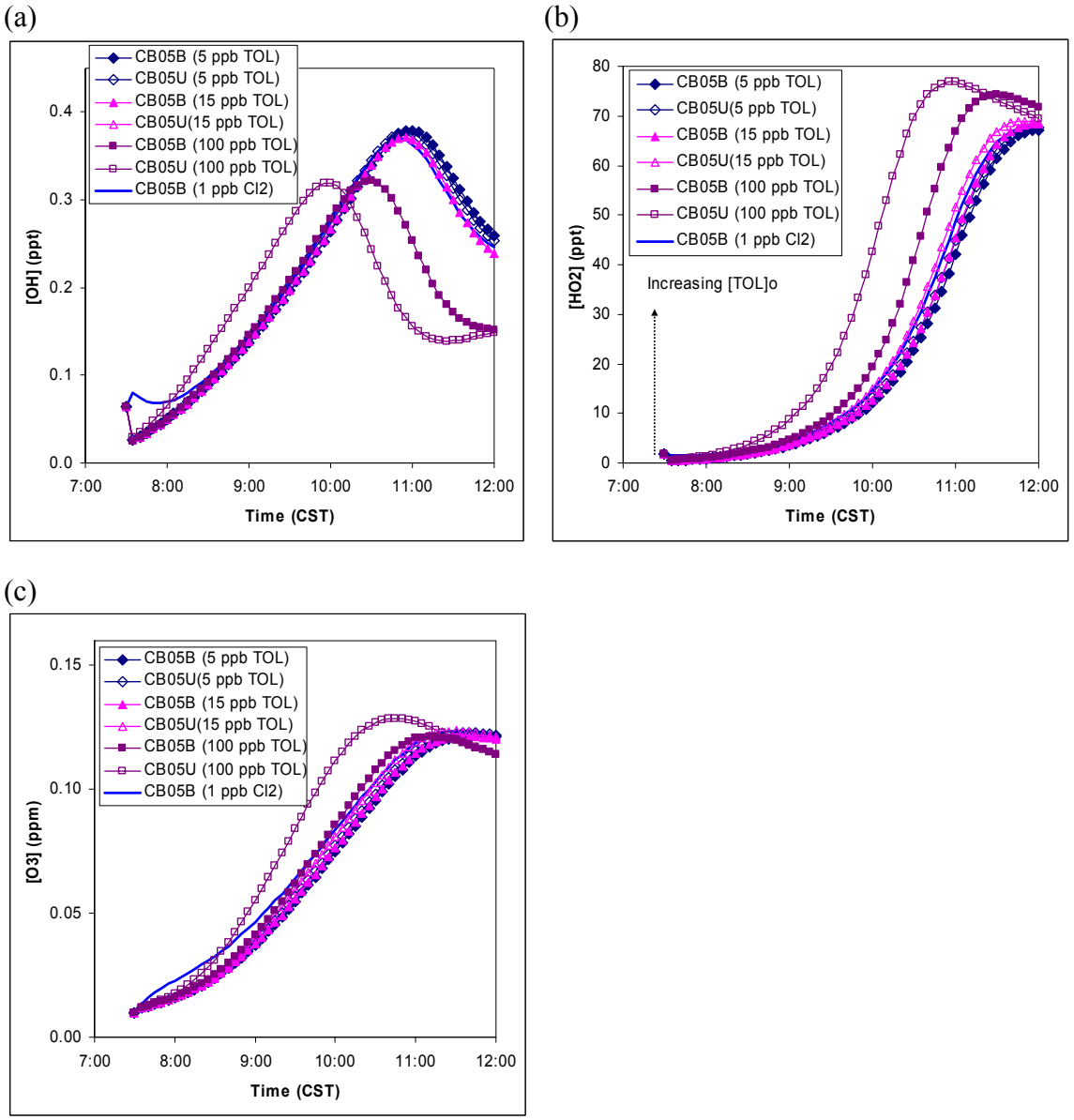

Figure 5-11. Effect of using different toluene mechanisms in CB05 at different initial concentrations of toluene on (a) OH, (b) HO_2, (c) O_3 for the case of August 25, 2000 for the case of August 25, 2000.

Note: For comparison with the effect of of chlorine emissions of 1 ppb Cl_2, the simulated OH, HO_2 and O_3 for $[Cl_2]o$ of 1 ppb are also presented in this Figure. CB05B and CB05U gave very similar OH, HO_2 and O_3 in response to 1 ppb of $[Cl_2]o$ (Figure 5-10).

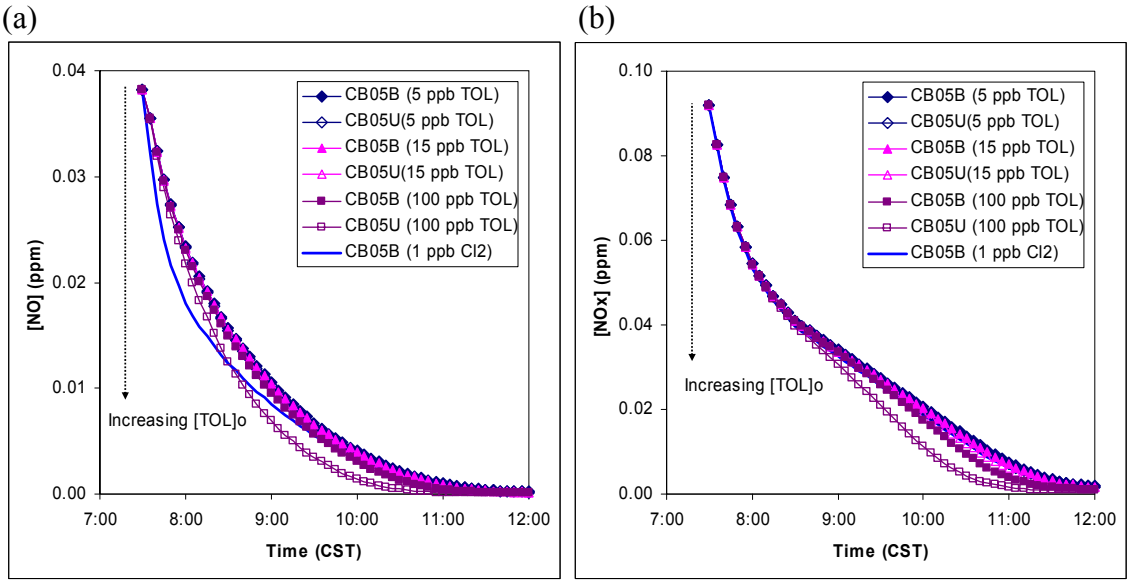

Figure 5-12. Effects of using different toluene mechanisms in CB05 at different initial concentrations of toluene on (a) NO and (b) NOx for the case of August 25, 2000.

5.4. SUMMARY

In this chapter, the potential of chlorine emissions and chlorine chemistry as a radical source was examined by sensitivity analyses using various levels of Cl_2 as a Cl-atom source. The box modeling results using a case of the morning of August 25, 2000 , showed that Cl emissions and Cl chemistry could accelerate the conversion rate of NO into NO_2, decrease NO rapidly, and increase the NO_2/NO ratio, OH, HO_2 and O_3, which was observed around 7:45 CST at the La Porte site during the TexAQS-2000 study.

The effects of (1) chlorine emissions and chemistry, (2) using different lumping strategies for alkenes, (3) using different toluene mechanisms on radicals and ozone were compared. The intercomparsion in this work indicates that the relative importance of

these three depends on the strengths of their corresponding emissions: (1) molecular chlorine emissions, (2) alkene emissions, (3) and aromatics emissions. Incorporating chlorine chemistry in condensed chemical mechanisms such as SAPRC-07 and CB05 seems to be at least as important as using better lumping strategies for alkenes and using a better description of aromatics chemistry, particularly for the greater Houston area where relatively high chlorine emissions (e.g., several ppb Cl_2) occur.

5.5. REFERENCES

Anderson, R.S., Huang, L., Iannone, R., Rudolph, J. 2007a. Laboratory measurements of the $^{12}C/^{13}C$ kinetic isotope effects in the gas-phase reactions of unsaturated hydrocarbons with Cl atoms at 298±3 K. Journal of Atmospheric Chemistry 56, 275-291.

Anderson, R.S., Huang, L., Iannone, R., Rudolph, J. 2007b. Measurements of the $^{12}C/^{13}C$ kinetic isotope effects in the gas-phase reactions of light alkanes with chlorine atoms. Journal of Physical Chemistry A 111, 495-504.

Atkinson, R., 1997. Gas-phase tropospheric chemistry of volatile organic compounds: 1. Alkanes and alkenes. Journal of Physical and Chemical Reference Data 26, 215-290.

Atkinson, R., Arey, J., 2003. Atmospheric degradation of volatile organic compounds. Chemical Reviews 103, 4605-4638.

Atkinson, R., Baulch, D.L., Cox, R.A., Crowley, J.N., Hampson, R.F., Hynes, R.G., Jenkin, M.E., Rossi, M.J., Troe, J., 2006. Evaluated kinetic and photochemical data for atmospheric chemistry: Volume II – gas phase reactions of organic species. Atmospheric Chemistry and Physics 6, 3625-4055. Available at http://www.atmos-chem-phys.net/6/3625/2006/acp-6-3625-2006.html.

Chang, S., McDonald-Buller, E., Kimura, Y., Yarwood, G., Neece, J., Russell, M., Tanaka, P., Allen, D., 2002. Sensitivity of urban ozone formation to chlorine emission estimates. Atmospheric Environment 36, 4991-5003.

Coquet, S., Ariya, P.A., 2000. Kinetics of the gas-phase reactions of Cl atom with selected C_2–C_5 unsaturated hydrocarbons at $283 < T < 323$ K. International Journal of Chemical Kinetics 32, 478-484.

Ezell, M.J., Wang, W., Ezell, A.A., Soskin, G., Finlayson-Pitts, B.J., 2002. Kinetics of reactions of chlorine atoms with a series of alkenes at 1 atm and 298 K: Structure and reactivity. Physical Chemistry Chemical Physics 4, 5813-5820.

Finlayson-Pitts, B. J., Keoshian, C.J., Buehler, B., Ezell, A.A., 1999. Kinetics of reaction of chlorine atoms with some biogenic organics. International Journal of Chemical Kinetics 31, 491-499.

Finlayson-Pitts, B.J., Pitts, J.N., 2000. Chemistry of the Upper and Lower Atmosphere: Theory, Experiments, and Applications, Academic Press, San Diego, 969p.

Hov, O., 1985. The effect of chlorine on the formation of photochemical oxidants in southern Telemark, Norway. Atmospheric Environment 19, 471–485.

Jobson, B. T., Berkowitz, C. M., Kuster, W. C., Goldan, P. D., Williams, E. J., Fesenfeld, F. C., Apel, E. C., Karl, T., Lonneman, W. A., Riemer, D., 2004. Hydrocarbon source signatures in Houston, Texas: Influence of the petrochemical industry. Journal of Geophysical Research 109, D24305, doi:10.1029/2004JD004887.

Karl, T., Jobson, T., Kuster, W.C., Williams, E., Stutz, J., Shetter, R., Hall, S.R., Goldan, P., Fehsenfeld, F., W. Lindinger, W., 2003. Use of proton transfer-reaction mass spectrometry to characterize volatile organic compound sources at the La Porte super site during the Texas Air Quality Study. Journal of Geophysical Research 108(D16), 4508, doi:10.1029/2002JD003333.

Kukui, A., Le Bras, G., 2001. Theoretical study of the thermal decomposition of several β-chloroalkoxy radicals. Physical Chemistry Chemical Physics 3, 175-178.

Kuster, W.C., Jobson, B.T., Karl, T., Riemer, D., Apel, E., Goldan, P.D., Fehsenfeld, F.C., 2004. Intercomparison of volatile organic carbon measurement techniques and data at La Porte during the TexAQS2000 Air Quality study. Environmental Science & Technology, 38, 221-228.

Nakayama, T., Takahashi, K., Matsumi, Y., Toft, A., Anderson, M.P.S., Nielsen, O.J., Waterland, R.L., Buck, R.C., Hurley, M.D., Wallington, T.J., 2007. Atmospheric chemistry of $CF_3CH=CH_2$ and $C_4F_9CH=CH_2$: Products of the gas-phase reactions with Cl atoms and OH radicals. Journal of Physical Chemistry A 111, 909-915.

Nordmeyer, T., W. Wang, M. L. Ragains, B. J. Finlayson-Pitts, C. W. Spicer, and R. A. Plastridge, 1997. Unique products of the reaction of isoprene with atomic chlorine: Potential markers of chlorine atom chemistry. Geophysical Research Letters 24(13), 1615-1618.

Orlando, J.J., Tyndall, G.S., Apel, E.C., Riemer, D.D., Paulson, S.E., 2003. Rate coefficients and mechanisms of the reaction of Cl-atoms with a series of

unsaturated hydrocarbons under atmospheric conditions. International Journal of Chemical Kinetics 35(8), 334-353.

Orlando, J.J., Tyndall, G.S., Bilde, M., Ferronato, C., Wallington, T.J., Vereecken, L., Peeters, J., 1998. Laboratory and theoretical study of the oxy radicals in the OH- and Cl-initiated oxidation of ethene. Journal of Physical Chemistry A 102, 8116-8123.

Osthoff, H.D., Roberts, J.M., Ravishankara, A.R., Williams, E.J., Lerner, B.M., Sommariva, R., Bates, T.S., Coffman, D., Quinn, P.K., Dibb, J.E., Stark, H., Burkholder, J.B., Talukdar, R.K., Meagher, J., Fehsenfeld, F.C., Brown, S.S., 2008. High levels of nitryl chloride in the polluted subtropical marine boundary layer. Nature Goescience 1, 324-328.

Oum, K.W., Lakin, M.J., DeHaan, D.O., Brauers, T., Finlayson-Pitts, B.J., 1998. Formation of molecular chlorine from the photolysis of ozone and aqueous sea-salt particles. Science 297, 74-77.

Ragains, M.L.; Finlayson-Pitts, B.J., 1997. Kinetics and mechanism of the reaction of Cl atoms with 2-methyl-1,3-butadiene (isoprene). Journal of Physical Chemistry A 101, 1509-1517.

Riemer, D. D.; Apel, E. C.,2001. Confirming the presence and extent of oxidation by Cl in the Houston, Texas urban area using specific isoprene oxidation products as tracers. Final report to the Texas Natural Resource Conservation Commission, Contract 582034743, University of Miami, FL. (Available at http://www.tceq.state.tx.us/assets/public/implementation/air/am/contracts/reports/oth/ConfirmingPresenceandExtentOfOxidationByCI.pdf)

Sander, S.P., Orkin, V.L., Kurylo, M.J., Golden, D.M., Huie, R.E., Kolb, C.E., Finlayson-Pitts, B.J., Molina, M.J., Friedl, R.R., Ravishankara, A.R., Moortgat, G. K., Keller-Rudek, H., Wine, P.H., 2006. Chemical Kinetics and Photochemical Data for Use in Atmospheric Studies, Evaluation Number 15. NASA Jet Propulsion Laboratory. February. Available at http://jpldataeval.jpl.nasa.gov/download.html.

Shi, J.C., Bernhard, M.J.,1997. Kinetic studies of Cl-atom reactions with selected aromatic compounds using the photochemical reactor-FTIR spectroscopy technique. International Journal of Chemical Kinetics 29, 349-358.

Sokolov, O.; Hurley, M. D.; Wallington, T. J.; Kaiser, E. W.; Platz, J.; Nielsen. O. J.; Berho, F.; Rayez, M.-T.; Lesclaux, R., 1998. Kinetics and mechanism of the gas-phase reaction of Cl atoms with benzene. Journal of Physical Chemistry A, 102, 10671-10681.

Tanaka, P.L., Oldfield, S., Neece, J.D., Mullins, C.B., Allen, D.T., 2000. Anthropogenic sources of chlorine and ozone formation in urban atmospheres. Environmental Science & Technology 34, 4470-4473.

Tanaka, P. L., D. T. Allen, and C. B. Mullins, 2003a. An environmental chamber investigation of chlorine-enhanced ozone formation in Houston, Texas. Journal of Geophysical Research 108(D18), 4576, doi:10.1029/2002JD003314.

Tanaka, P. L.; Riemer, D. D.; Chang, S.; Yarwood, G.; McDonald-Buller, E. C.; Apel, E. C.; Orlando, J. J.; Silva, P. J.; Jimenez, J. L.; Canagaratna, M. R.; Neece, J. D.; Mullins, C. B.; Allen, D. T., 2003b. Direct evidence for chlorine-enhanced urban ozone formation in Houston, Texas. Atmospheric Environment 37, 1393-1400.

Ullerstam, M., Evert Ljungström and Langer, S., 2000. Reactions of acrolein, crotonaldehyde and pivalaldehyde with Cl atoms: structure-activity relationship and comparison with OH and NO_3 reactions. Physical Chemistry Chemical Physics 3, 986-992.

Wang, L., Arey, J., Atkinson, R., 2005. Reactions of chlorine atoms with a series of aromatic hydrocarbons. Environmental Science & Technology 39, 5302-5310.

Wang, W., Finlayson-Pitts, B.J., 2000. 4-Chlorocrotonaldehyde as a unique chlorine-containing compound from the reaction of atomic chlorine with 1,3-butadiene in air at room temperature. Geophysical Research Letters 27(7), 947– 950.

Yarwood, G., Peng, N., Niki, H., 1992. FTIR spectroscopic study of the Cl-atom and Br-atom initiated oxidation of ethene. International Journal of Chemical Kinetics 24(4), 369-383.

Chapter 6: Summary and Recommendations

This dissertation examined three hypotheses regarding radical sources and sinks in southeast Texas by using both environmental chamber simulations and box modeling with ambient data. In Chapter 3, the first hypothesis, that radical production from aromatics is underestimated by current condensed mechanisms, was tested by evaluating a new toluene mechanism for the CB condensed mechanism named UNClite (Whitten et al., 2009). The mechanism was evaluated against 38 toluene-NOx environmental chamber experiments. In Chapter 4, the second hypothesis, that the mechanism condensation used for alkenes significantly impacts radical production, was examined. In addition, direct OH formation from the reaction of O_3 with alkenes was also studied using the reaction of 1-butene and O_3 as a case study. In Chapter 5, the third hypothesis, chlorine emissions and chemistry as a radical source, was investigated by carrying out box modeling with various strengths of Cl_2 emissions for a case of August 25, 2000 at La Porte, Texas. The relative magnitudes of these radical sources (alkenes, aromatics, and molecular chlorine) in southeast Texas were also compared using box modeling with TexAQS-2000 data. Key findings and recommendations are summarized below.

6.1. KEY FINDINGS

Aromatics chemistry:

- CB05 with the toluene mechanism in the 2005 version CB05 (CB05-Base) under-predicts O_3 concentrations especially under low-NOx chamber conditions.
- CB05-Base predicts rates of NO oxidation and O_3 formation slower than observation, especially under low-NOx chamber conditions.
- Radical sources are under-represented in CB05-Base.

- Descriptions of NOx sinks associated with toluene oxidation in CB05-Base (e.g., cresol formation with a yield of 0.36) are not consistent with our current understanding of toluene oxidation processes.
- The new toluene mechanism, UNClite, is more consistent with our current knowledge of toluene oxidation based on theoretical and experimental studies.
- A lower yield of cresols in UNClite, 0.18 instead of 0.36, is consistent with the literature and leads to better fits to cresol measurements in toluene-NOx experiments.
- Using a lower yield of cresols (0.18) and a higher yield for reactive ring-opening products (dicarbonyls) leads to more radical production through the reactive "bicyclic" route (Figure 3-2).
- Formation of peroxyacyl nitrates (PANs) from dicarbonyls is predicted to be a major NOx-depleting process.
- CB05-UNClite shows better performance in simulating maximum ozone concentrations, NOx crossovers, cresol yields, radical sources and NOx sinks than CB05-Base for most of toluene-NOx chamber experiments used.
- Using UNClite instead of the Base toluene mechanism leads to increased O_3 concentrations both under chamber conditions (Chapter 3) and simulated ambient conditions (Section A4 of Appendix A).

Alkene chemistry:

- How alkene reactions are represented in condensed chemical mechanisms as a limited number of model species (in short, lumping strategies for alkenes) could significantly influence predictions of radical and ozone concentrations.

- Separately modeling alkenes instead of lumping alkenes into reactions of a few model species for alkenes leads to generally better ozone predictions under chamber conditions.
- Representing propene (C_3H_6) separately in SAPRC-07 leads to higher OH, HO_2 and O_3 under both chamber conditions and simulated ambient conditions.
- The alkene composition used in deriving the reaction parameters for alkenes classified as OLE1 and OLE2 in SAPRC-07 is very different from the alkene composition based on TexAQS measurements (Table 4-3).
- Radical formation from reactive OLE2 alkenes (e.g., 2-methyl-2-butene) could be significant even at moderate concentrations such as 1 ppb, due to their relatively large rate constant towards O_3 ($k(O_3)$) and OH radical yields (Y_{OH}) in their ozonolysis.
- Incorporating OH radical formation from vinoxy radicals ($XHC=CHO^{\cdot}$ where X is alkyl or H) has potential to reduce the current discrepancies in OH yields for ozonolysis of terminal alkenes between the literature and SAPRC-07.

Chlorine emissions and chemistry:

- Anthropogenic chlorine upset emissions in early mornings could boost OH, HO_2 and O_3 concentrations in a short time.
- Increased OH and HO_2 concentrations initiated by chlorine atoms lead to fast conversion of NO into NO_2 and simultaneous increases in O_3.
- High time-resolution measurements of isoprene and CMBO can be used to estimate the concentration of chlorine atoms under some conditions.
- The relative importance of the impact on radicals and ozone of (1) using different toluene mechanisms described in Chapter 3, (2) using different lumping strategies

for alkenes described in Chapter 4 and (3) chlorine emissions and chemistry described in Chapter 5 depends on the strengths of their corresponding emissions: (1) aromatics emissions, (2) alkene emissions, (3) and molecular chlorine emissions.

- In addition to using better lumping strategies for alkenes and using a better description of aromatics chemistry, incorporating chlorine chemistry in condensed chemical mechanisms such as SAPRC-07 and CB05 is expected to lead to more accurate modeling of OH, HO_2 and O_3, particularly for the southeast Texas region where relatively large chlorine emissions occur from various anthropogenic sources of molecular chlorine.

6.2. RECOMMENDATIONS

- The newly developed toluene mechanism, UNClite, should be used in CB05, instead of the toluene mechanism in the 2005 version CB05.
- Further evaluation of the UNClite mechanism is needed because xylene chemistry in CB shares model species such as CRES (as a primary product) and OPEN (as a product of CRES) with the toluene mechanism. Impacts of the updated reactions of dicarbonyls (OPEN) and cresols (CRES) on xylene (XYL) performance should be studied although their effects should be moderate due to the moderate cresol yield (0.2) in reaction XYL + OH in CB05.
- Further evaluation of CB05-UNClite using gridded air quality models such as the Comprehensive Air Quality Model with extensions (CAMx) and the Community Multiscale Air Quality modeling system (CMAQ) should be followed.
- Radical sources and NOx sinks (e.g., dicarbonyls) involved in toluene oxidation processes should be further studied.

- The composition of an alkene mixture used in deriving the SAPRC-99 and SAPRC-07 mechanisms is based on measurements in the 1980s and needs to be updated especially for the southeast Texas region where industrial emissions of alkenes (e.g., ethene and propene) frequently influence its atmosphere.
- Separately modeling alkenes (especially propene) is recommended in photochemical modeling for the southeast Texas region including the greater Houston area whenever reliable emissions data for alkenes are available.
- Effects of lumping strategies for alkenes should be considered while evaluating impacts of highly reactive volatile organic compounds (HRVOCs) on ozone in the greater Houston area.
- OH formation from vinoxy radicals should be studied to provide better condensed reactions for reaction of O_3 with terminal alkenes and reduce the current discrepancies between SAPRC-07 and the literature.
- Further experimental studies (e.g, experimental studies on radical formation from alkenes in presence of NOx) are needed to include better descriptions of the reactions of terminal and internal alkenes with O_3 in condensed chemical mechanisms such as SAPRC-07 used for air quality applications.
- A publicly accessible database for tracking anthropogenic chlorine emissions would be helpful in modeling the impact of chlorine emissions and chlorine chemistry because the importance of chlorine emissions and chemistry primarily depends on chlorine emissions and their accurate representation in air quality modeling.
- Reliable methods other than using unique makers of chlorine chemistry such as CMBO and CMBA to estimate the level of chlorine atoms and the concentration of molecular chlorine should be studied. For example, concentrations of simple

alkanes (e.g., ethane and propane which react more rapidly with Cl atoms than OH radicals by an order of two) abundant in southeast Texas and their products from reaction with chlorine atoms (e.g, HCl) could be used.

6.3. REFERENCES

Whitten, G.Z., Heo, G., Kimura, Y., McDonald-Buller, E., Allen, D.T., Yarwood, G., 2009. A new condensed toluene mechanism for Carbon Bond. Submitted for publication in *Atmospheric Environment*.

Yarwood, G., Rao, S., Yocke, M., Whitten, G.Z., 2005. Updates to the Carbon Bond mechanism: CB05. Report to the U.S. Environmental Protection Agency, December 2005. (http://www.camx.com/publ/pdfs/CB05_Final_Report_120805.pdf)

Appendix A: Further Information for Chapter 3

This Appendix consists of four sections as follows:

- A1. Simulations with the Ua, Ub and Dinitro Mechanisms.
- A2. Implementation of the Five Versions of CB05: CB05-Base, CB05-Ua, CB05-Ub, CB05-UNClite and CB05-Dinitro.
- A3. Auxiliary Mechanisms Used in Environmental Chamber Simulations.
- A4. Box modeling results with CB05-Base and CB05-UNClite.

A1. SIMULATIONS WITH THE UA, UB AND DINITRO MECHANISMS

A1.1. Introduction: Ua, Ub and Dinitro Mechanisms

Two alternative CB05 toluene mechanisms were initially proposed by Greg Yarwood and Gary Whitten, and two additional mechanisms were proposed subsequently (Table A-1), based on recent studies (Calvert et al., 2002; Hu et al., 2007) and evaluation results of the first two toluene mechanisms. The first CB05 toluene mechanism initially proposed (Update A; called CB05-Ua hereafter) contains a low-NOx switch which controls the fractions of peroxy radicals (TO_2) formed from toluene (TOL) that are reacted with NO and HO_2. The operation of this low-NOx switch depends on the ratio of NO to HO_2 (NO/HO_2) and was designed to make TO_2 start to significantly react with HO_2 and result in radical termination when the NO/HO_2 ratio becomes less than around 20; above a NO/HO_2 ratio of 20, most of TO_2 will react with NO and contribute to creating radicals and ozone (Whitten, personal communication, June 2008). The second CB05 toluene mechanism proposed (Update B; called CB05-Ub hereafter) uses a lower yield of cresol (CRES) and higher yield of TO_2 in the reaction of TOL and OH than the

yields for CB05-Ua or the 2005 version CB05 (called CB05-Base in this report) by 0.18. The CB05-Ub does not have a low-NOx switch. Only three reactions (Reactions 128, 129 and 130) are different as described in Table A-2, and all other reactions are same in the three CB05 mechanisms. For a list of full reactions in CB05-Base, refer to Section A2.

Two additional versions of alternative CB05 toluene mechanisms were proposed by Greg Yarwood and Gary Whitten based on recent studies (Calvert et al., 2002; Hu et al., 2007) after initial evaluation of the two mechanisms, CB05-Ua and CB05-Ub. These two mechanisms involve more extensive modifications to the CB05-Base mechanism than CB05-Ua and CB05-Ub, and are referred to as CB05-UNClite and CB05-Dinitro (Table A-1). Features of these two more detailed mechanisms are summarized in Tables A-3 and A-4. In Table A-3, modifications for CB05-UNClite and CB05-Dinitro in 10 reactions of CB05-Base are listed; in Table A-4, newly added reactions are shown. CB05-UNClite describes the toluene chemistry more explicitly than CB05-Base, and contains 12 more reactions to describe toluene oxidation than CB05-Dinitro.

Major simulation results for CB05 with Ua, Ub and Dinitro are given below. For simulation results for CB05-UNClite, refer to Chapter 3.

Table A-1. Five versions of CB05 mechanisms evaluated by chamber simulations.

Mechanism ID	CB05-Base	CB05-Ua	CB05-Ub	CB05-UNClite	CB05-Dinitro
Cresol yield	0.36	0.36	0.18	0.18	0.18
TO_2 yield	0.56	0.56	0.74[a]	0.65[b]	0.74
Benzaldehye yield	0.08	0.08	0.08	0.10	0.08
Is reaction $TO_2 + HO_2$ used?	no	yes	no	yes	yes
Extra NOx sinks added?	-	no	no	yes	yes
Number of reactions modified	-	2	3	9	4
Number of extra reactions	-	0	0	+16	+4
Reference	Yarwood et al., 2005	Calvert et al., 2002	Calvert et al., 2002	Hu et al., 2007; Calvert et al., 2002	Hu et al., 2007

[a]0.74 = 0.56 + 0.18. [b]10% of 0.72 (= 0.74 – 0.02) goes into another minor route.

Table A-2. Comparison of three toluene reactions between CB05-Base, CB05-Ua and CB05-Ub.[a]

Mechanism ID	Reaction	Rate constant
	R128	
CB05-Base	TOL + OH = 0.56 TO_2 + 0.36 (CRES + HO_2) + 0.08 (XO_2 + HO_2)	1.8E-12·Exp(355/T)
CB05-Ua	TOL + OH = 0.56 TO_2 + 0.36 (CRES + HO_2) + 0.08 (XO_2 + HO_2)	1.8E-12·Exp(355/T)
CB05-Ub	TOL + OH = **0.74**[b] TO_2 + **0.18**[c] (CRES + HO_2) + 0.08 (XO_2 + HO_2)	1.8E-12·Exp(355/T)
	R129	
CB05-Base	TO_2 + NO = 0.9 (NO_2 + HO_2) + 0.9 OPEN + 0.1 NTR	8.10E-12
CB05-Ua	TO_2 + NO = 0.9 (NO_2 + HO_2) + 0.9 OPEN + 0.1 NTR	**2.7E-12·Exp(360/T)**[d]
CB05-Ub	TO_2 + NO = 0.9 (NO_2 + HO_2) + 0.9 OPEN + 0.1 NTR	**2.7E-12·Exp(360/T)**[d]
	R130	
CB05-Base	TO_2 = CRES + HO_2 (unimolecular reaction)	4.2[e]
CB05-Ua	**TO_2 + HO_2 = TO_2HO_2** (the product, TO_2HO_2, is unreactive)	**1.9E-13·Exp(1300/T)**
CB05-Ub	**TO_2 + HO_2 = TO_2HO_2**	**0**

[a]Differences between the two modified toluene mechanisms and CB05-Base are shown in bold.
[b]0.74 = 0.56 + 0.18. [c]0.18 = 0.36 - 0.18. [d]$2.7 \cdot 10^{-12}$·Exp(360/T) at T = 298 K is 9.04

cm^3/(molecule·sec) which is larger than $8.10 \cdot 10^{-12}$ cm^3/(molecule·sec) by 12%. [e]The rate constant for this reaction in CB05-Base is in 1/sec rather than in cm^3/(molecule·sec).

Table A-3. Comparison of 10 toluene reactions between CB05-Base, CB05-UNClite, CB05-Dinitro.

Rxn ID	Mechanism ID	Reaction[a]	Rate constant
R128	CB05-Base	TOL + OH = 0.56 TO_2 + 0.36 (CRES + HO_2) + 0.08 (XO_2 + HO_2)	1.8E-12·Exp(355/T)
	CB05-UNClite	TOL + OH = **0.65** TO_2 + **0.18** (CRES + HO_2) + **0.10** (XO_2 + HO_2) + **0.072 OH**	1.8E-12·Exp(355/T)
	CB05-Dinitro	TOL + OH = **0.74**[b] TO_2 + **0.18**[c] (CRES + HO_2) + 0.08 (XO_2 + HO_2)	1.8E-12·Exp(355/T)
R129	CB05-Base	TO_2 + NO = 0.9 (NO_2 + HO_2 + OPEN) + 0.1 NTR	8.1E-12
	CB05-UNClite	TO_2 + NO = **0.86** (NO_2 + HO_2 + OPEN) + **0.520 MGLY + 0.336 (FORM + CO + HO_2) + 0.004 HO_2 + 0.14** NTR	2.7E-12·Exp(360/T)[d]
	CB05-Dinitro	TO_2 + NO = 0.9 (NO_2 + HO_2 + OPEN) + 0.1 NTR	2.7E-12·Exp(360/T)[d]
R130	CB05-Base	TO_2 = CRES + HO_2 (unimolecular reaction)	4.2[e]
	CB05-UNClite CB05-Dinitro	**TO_2 + HO_2 =**	1.9E-13·Exp(1300/T)
R131	CB05-Base	CRES + OH = 0.4 CRO + 0.6 {0.5 (OPEN + XO_2 + HO_2) + 0.5 (XO_2 + HO_2)}	4.10E-11
	CB05-UNClite	CRES + OH = **0.06 CRO + 0.732 CAT1 + 0.06 (FORM + CO + HO_2) + 0.13 OPEN + 0.12 XO_2 + 0.06 XO_2N + 1.14 HO_2**	1.70E-12·Exp(950/T)
	CB05-Dinitro	CRES + OH = **0.8** CRO + **0.1** (OPEN + XO_2 + HO_2) + **0.1** (XO_2 + HO_2)	4.10E-11
R132	CB05-Base CB05-Dinitro	CRES + NO_3 = CRO + HNO_3	2.20E-11
	CB05-UNClite	CRES + NO_3 = **0.30** CRO + HNO_3 + **0.60 XO_2 + 0.48 ALDX + 0.24 (FORM + CO + HO_2) + 0.24 MGLY + 0.12 (OPEN + HO_2) + 0.10 XO_2N**	1.40E-11
R133	CB05-Base	CRO + NO_2 = NTR	1.40E-11
	CB05-UNClite CB05-Dinitro	CRO + NO_2 = **CRON**	2.10E-12
R134	CB05-Base CB05-UNClite CB05-Dinitro	CRO + HO_2 = CRES	5.50E-12
R135	CB05-Base CB05-Dinitro	OPEN = C_2O_3 + HO_2 + CO	9.0·j(FORM→HO_2)[e]
	CB05-UNClite	OPEN = **OPO_3** + HO_2 + CO	0.04·j(NO_2)[e]
R136	CB05-Base CB05-Dinitro	OPEN + OH = XO_2 + 2 CO + 2 HO_2 + C_2O_3 + FORM	3.00E-11

	CB05-UNClite	OPEN + OH = **0.6 OPO_3 + 0.4 CAO_2**	4.40E-11
R137	CB05-Base CB05-Dinitro	OPEN + O_3 = 0.03 ALDX + 0.62 **C_2O_3** + 0.70 FORM + 0.03 XO_2 + 0.69 CO + 0.08 OH + 0.76 HO_2 + 0.20 MGLY	5.4E-17·Exp(-500/T)
	CB05-UNClite	OPEN + O_3 = 0.03 ALDX + 0.62 **OPO_3** + 0.70 FORM + 0.03 XO_2 + 0.69 CO + 0.08 OH + 0.76 HO_2 + 0.20 MGLY	5.4E-17·Exp(-500/T)

[a]Differences between CB05-UNClite, CB05-Dinitro and CB05-Base are expressed in bold. [b]0.74 = 0.56 + 0.18. [c]0.18 = 0.36 - 0.18. **d**: $2.7 \cdot 10^{-12} \cdot Exp(360/T)$ at T = 298 K is 9.04 cm^3/(molecule·sec) which is larger than $8.10 \cdot 10^{-12}$ cm^3/(molecule·sec) by 12%. [e]The rate constant for this reaction is in 1/sec rather than in cm^3/(molecule·sec).

Table A-4. Additional 16 reactions in CB05-UNClite and 4 reactions in CB05-Dinitro related to toluene oxidation.

No.	Mechanism ID	Reaction	Rate constant
1	CB05-UNClite	CRON + OH = CRNO	1.53E-12
	CB05-Dinitro	CRON + OH = 0.80 CRNO + 0.1 (XO_2 + HO_2) + 0.10 (OPEN + XO_2 + HO_2)	1.53E-12
2	CB05-UNClite CB05-Dinitro	CRON + NO_3 = CRNO + HNO_3	3.80E-12
3	CB05-UNClite CB05-Dinitro	CRNO + NO_2 = 2.0 NTR	2.10E-12
4	CB05-Dinitro	CRNO + HO_2 = CRON	5.50E-12
5	CB05-UNClite	CRNO + O_3 = CRN_2	2.86E-13
6	CB05-UNClite	CRN_2 + NO = CRNO + NO_2	2.54E-12·Exp(360/T)
7	CB05-UNClite	CRN_2 + HO_2 = CRPX	2.40E-13·Exp(1300/T)
8	CB05-UNClite	CRPX = CRNO + OH	0.01·j(NO2)[a]
9	CB05-UNClite	CRPX + OH = CRN_2	1.90E-12·Exp(190/T)
10	CB05-UNClite	OPEN + NO_3 = OPO_3 + HNO_3	3.80E-12
11	CB05-UNClite	CAT1 + OH = CAO_2	7.00E-11
12	CB05-UNClite	CAT1 + NO_3 = CRO + HNO_3	1.70E-10
13	CB05-UNClite	CAO2 + NO = 0.86 NO_2 + 1.2 HO_2 + 0.344 FORM + 0.344 CO + 0.14 NTR	2.54E-12·Exp(360/T)
14	CB05-UNClite	CAO_2 + HO_2 = CRPX	2.40E-13·Exp(1300/T)
15	CB05-UNClite	OPO_3 + NO = NO_2 + XO_2 + HO_2 + ALDX	1.00E-11
16	CB05-UNClite	OPO_3 + NO_2 = OPAN	1.00E-11
17	CB05-UNClite	OPAN = OPO_3 + NO_2	1.00E-04[a]

[a]The rate constant for this reaction is in 1/sec rather than in cm^3/(molecule·sec).

A1.2. Summary of Performance: Max(O_3) and Max($\Delta(O_3\text{-NO})$), NOx Crossover Time, Cresol Yield, Radical Sources and NOx Sinks

CB05-Ua and CB05-Ub fixed the under-prediction problem to some degree; however, CB05-Ub showed another problem: over-predictions of Max(O_3) and Max($\Delta(O_3\text{-NO})$) for the mid- and high-NOx and low O_3/NOx classes. CB05-Dinitro also mitigated the under-prediction problem of CB05-Base. However, CB05-Dinitro over-predicted Max(O_3) and Max($\Delta(O_3\text{-NO})$) for the high-NOx class (Table A-5). None of the mechanisms simulated well the low O_3/NOx experiments, though CB05-UNClite showed better performance than any other mechanism in modeling Max(O_3) and Max($\Delta(O_3\text{-NO})$) for experiments CTC065, CTC079 and OTC299B (Figures 3-3 and 3-4).

CB05-Ua and CB05-Ub did not solve the problem of slow initiation of active ozone formation shown by CB05-Base for many chamber experiments in the low- and mid-NOx classes though the delays in NOx crossover were shortened (Table A-5). CB05-Dinitro also did not solve this slow initiation problem (Table A-5). However, CB05-UNClite significantly improved in simulating NOx crossover times (Table A-5). NOx crossovers predicted by CB05-UNC occurred somewhat earlier than measurements for many low- and mid-NOx experiments; however, this problem is relatively minor in comparison to the slow initiation problem shown by other mechanisms.

The performance of each toluene mechanism against the chamber experiments are summarized in Table A-5. CB05-UNClite showed generally best performance among the five versions of CB05 mechanisms. In regard to the poor performance of CB05-UNClite in simulating Max(O_3) and Max($\Delta(O_3\text{-NO})$) against the low O_3/NOx experiments, caution should be exercised because these low O_3/NOx experiments are relatively sensitive to chamber effects (e.g, chamber-dependent radical sources).

Major radical sources and NOx sinks are also listed in Table A-5. OPEN produced through the reactive peroxide-bicyclic route, a model species in CB05 for representing ring-cleavage products of toluene oxidation, is a significant radical source in all five mechanisms. MGLY (methylglyoxal) is also a significant radical source in CB05-UNClite. In addition to HNO_3, PAN and NTR (organic nitrates), OPAN and CRON are extra NOx sinks in CB05-UNClite.

Table A-5. Summary of the overall performance and characteristics of each CB05 mechanism against the 38 chamber experiments in simulating Max(O_3), Max($\Delta(O_3$-NO)), NOx crossover, cresol yield, radical sources and NOx sinks.[a]

Mechanism	CB05-Base	CB05-UNClite	CB05-Ua	CB05-Ub	CB05-Dinitro
Max(O_3)	under-predict	-		-	-
Low-NOx	-67% (14%)	-31%[f] (6%)	-35% (26%)	-13% (14%)	-22% (13%)
Mid-NOx	-23% (21%)	-12% (11%)	0% (16%)	30% (19%)	4% (15%)
High-NOx	-26% (27%)	3% (7%)	14% (36%)	66% (12%)	31% (9%)
Low O_3/NOx	-62% (45%)	95% (44%)	-24% (104%)	45% (142%)	19% (118%)
Max($\Delta(O_3$-NO))[b]	under-predict	-	-	-	-
Low-NOx	-60% (12%)	-28% (7%)	-31% (21%)	-13% (13%)	-20% (12%)
Mid-NOx	-13% (13%)	-7% (7%)	0% (9%)	18% (11%)	3% (9%)
High-NOx	-11% (14%)	2% (5%)	7% (18%)	32% (7%)	15% (4%)
Low O_3/NOx	-40% (33%)	30% (12%)	-24% (52%)	8% (61%)	-3% (54%)
NOx crossover	Delayed	earlier	delayed	Delayed	delayed
Low-NOx	191% (117%)	-59% (25%)	109% (74%)	86% (61%)	91% (61%)
Mid-NOx	53% (56%)	-34% (22%)	46% (53%)	29% (44%)	32% (45%)
High-NOx	30% (17%)	-13% (9%)	25% (17%)	5% (13%)	9% (13%)
Low O_3/NOx[c]	34% (40%)	-24% (10%)	28% (37%)	10% (28%)	13% (30%)
Cresol yield	over-predict	reasonable	over-predict	reasonable	reasonable
Radical sources[d]	OPEN formed from toluene via TO2	OPEN, MGLY and TO2[g]	OPEN formed from toluene via TO2	OPEN formed from toluene via TO2	OPEN formed from toluene via TO2
NOx sinks[e]	PAN, NTR, HNO3	PAN, NTR, HNO3, OPAN[h], CRON[i]	PAN, NTR, HNO3	PAN, NTR, HNO3	PAN, NTR, HNO3, CRON[j]

[a]For 12 low-NOx experiments, 17 mid-NOx experiments, 5 high NOx experiments and 4 low O_3/NOx experiments. Standard deviations associated with model errors ((model – experimental) /experimental) are included in the parentheses. [b]$\Delta(O_3\text{-NO}) = ([O_3]\text{-}[NO])_{t=t} - ([O_3]\text{-}[NO])_{t=0}$. [c]Experiment CTC065 was excluded in the calculations because CB05-Base could not simulate the NOx crossover by the end of the experiment. [d]Described only significant radical sources

relevant to toluene photo-oxiation. [e]Described only significant NOx sinks relevant to toluene photo-oxiation. [f]Note the fact that CB05-UNClite described the early stages of the low-NOx experiments generally best among the five CB05 mechanisms. [g]Unlike in CB05-Base or CB05-Dinitro, in CB05-UNClite, TO2 + NO reaction is a net radical source (1.0 TO2 is consumed and 1.2 HO2 is formed) because glyoxal (GLY) is experessed as FORM + CO + HO2 in that reaction. [h]OPAN is a PAN-like species derived from OPEN (ring-opening products of toluene oxidation). [i]CRON represents nitro-cresol compounds.

A2. IMPLEMENTATION OF THE FIVE VERSIONS OF CB05: CB05-BASE, CB05-UA, CB05-UB, CB05-UNCLITE AND CB05-DINITRO

A2.1. Implementation in the SAPRC Software

CB05-Base:

```
CB05 Mechanism
!CARBON BOND "PLUS" MECHANISM FOR CHAMBER SIMULATIONS.
!USES CB4PLUS BASE MECHANSIM WITH WALL EFFECTS AND TRACER RXNS ADDED
!
TEMP 300.0      ! added by GH to set the default simulation temperature
TREF 300.0      ! to set the reference temperature for uses in (T/Tref)^B.
! SPECIES IN THE MODEL
!
.ACT
= O3 + NO + NO2 + NO3 + N2O5 + HNO3 + HONO + PNA + OH + HO2 + H2O2 + SO2
= SULF + CO + PAR + ETH + OLE + IOLE + TOL + XYL + FORM + ALD2 + ALDX
= ETHA + MEOH + ETOH + ISOP + TERP + CRES + FACD + AACD + PAN + PANX
= NTR + MEPX + PACD + ROOH + ISPD + MGLY + OPEN + C2O3 + CXO3 + XO2 + MEO2
= XO2N + ROR
!
.STS
= O + O1D + HCO3 + CRO + TO2
!
.CON
HV      1.0
M       1.00E+6
O2      2.09E+5
H2O     2.00E+4
CH4     1.20
H2      0.0
!
!            UNREACTIVE SPECIES (OF VARIOUS NAMES) IGNORED.
.COE
NR        0.0
UNR       0.0
INERT 0.0
!
! *Note: CB05 with PNA active with Wall on version [Final: Aug 15, 2007]
!GH: replaced CB05.RXN with CB05_156.RXN
!@CB05_156.RXN !@CB05.RXN
!GH: replaced CB05_156.RXN with CB05Fix1.RXN [June 24, 2007]
!@CB05Fix1.RXN
!GH: replaced CB05Fix1.RXN with CB05Fix2.RXN [June 25, 2007]
!@CB05Fix2.RXN
!GH: replaced CB05Fix2.RXN with CB05Fix3.RXN [July 4, 2007]
!
!START: Include CB05 RXN FILE
!@CB05Fix3.RXN
! CB05 Mechanism
! CB4 Plus Mechanism
! Created from cb4plus.xls 15-Mar-2005 17:06
```

```
!
! Modification:
! Gookyoung Heo on 18 June 2007
! 1. Add reaction 156 (NO2 + ISOP -> Products) based on reaction 156 in
!       Morpho's CB05.rxn provided by Dr. Gary Whitten.
! 2. Changed primary photolysis filenames (excluding extension name, phf):
!       NO2 (1), O3O3P (8), O3O1D (9), NO3NO2 (14), NO3NO (15), HONO (25),
!       H2O2 (36), PNA (51), HNO3 (52), N2O5 (53), NTR (62), ROOH (64),
!       MEPX (71), FORMR (74), FORMS (75), ALD2 (86), PAN (90), PACD (96),
!       ALDX (101), PAN (90,105), MGLY (140), ACROX (*148 with factor of 3.6E-3)
!       cchor (#AAHV|#131), ispd (#IPHV|#173)
! 3. Updated photolysis constant expressions
! 1)        PF=NO2
! 8)        PF=O3O3P
! 9)        PF=O3O1D
! 14)       PF=NO3NO2
! 15)       PF=NO3NO
! 25)       PF=HONO
! 36)       PF=H2O2
! 51)       PF=PNA
! 52)       PF=HNO3
! 53)       PF=N2O5
! 62)       PF=NTR
! 64)       PF=ROOH
! 71)       PF=MEPX
! 74)       PF=FORMR
! 75)       PF=FORMS
! 86)       PF=ALD2
! 90)       PF=PAN
! 96)       PF=PACD
! 101)      PF=ALDX
! 105)      PF=PAN
! 135)      PF=FORMR QY=9.00e+0
! 140)      PF=MGLY
! 148)      PF=ACROX QY=3.60e-3
! Gookyoung Heo on 25 June 2007
! 1. Changed reaction rate parameters in Rxn 65.
!       Rxn 65: OH + CO -> HO2; K1 + K2[M]
!       rate paramters from (1.50e-13 3.68e-33) to (1.44E-13 3.43E-33)
! 2. Added "-PAR" in the product part in Rxn 118.
!       Rxn 118: O3 + OLE -> products.
!       *Minor change: changed #-1 PAR to #-1.0 PAR in Rxn 119.
! 3. Rxn 139: 1.80E-11 => 1.70E-11 (Gery et al. (1989), CB05 Final Report)
! 4. Changes in photolysis reactions
!       Rxn 71: Phot(MEPX, R71) = Phot(ROOH, R64)
!                       PF=MEPX => PF=ROOH
!       Rxn 96: Phot(PACD, R96) = 0.0*Phot(ROOH, R64) (CB05 Final Report)
!                       PF=PACD => PF=ROOH QY=0.00e+0
! *Notes
!       Rxn 148: Phot(ISPD, R148) = 0.0036*Phot(ACROLEIN (or ACROX))
!                         in Morpho and CB05 Final Report
!                         = Phot(ISPD, primary phot., R152 in mech. 6)
!                         in the mechanism 6's chemparam file according to Greg Yarwood.
!                         Thus, no change.
! GH on 3 July 2007 [References: CB05 final report]
! 1. Corrections of reaction rate constants
!       Rxn 137: 1.00e-17 => 5.40e-17
!       Rxn 142: -408.      => -407.6
! 2. Corrections of reaction products
!       Rxn 75:    FORM + HV = CO =>    CO + H2 !(Add H2)
```

```
!       Rxn 123: NO3 + ETH = NO2 + CH4 + CO => NO2 + XO2 + #2 FORM
!       Rxn 149: TERP + O = #0.15 ALDX + #0.51 PAR => #0.15 ALDX + #5.12 PAR
!       Rxn 150: TERP + OH = #0.75 HO2 + #1.25 XO2 + #0.25 XO2N +
!                                  #0.28 FORM + #0.47 ALDX
!                                => #0.75 HO2 + #1.25 XO2 + #0.25 XO2N +
!                                  #0.28 FORM + #0.47 ALDX + #1.66 PAR !(Add 1.66 PAR)
! *Notes: Possible additions of H2O in Rxns 26, 27, 29, 33, 37, 43.
!               Possilbe addition of CO2 in Rxn 65
!
.UNITS=EA:DEGK
.UNITS=PPM
.RXN
1)      PF=NO2                          ;NO2 + HV = NO + O
2)      6.00e-34 0. -2.40         ;O + O2 + M = O3 + M
3)      3.00e-12 1500.             ;O3 + NO = NO2
4)      5.60e-12 -180.             ;O + NO2 = NO
5)      FALLOFF                         ;O + NO2 = NO3
        2.50e-31 0. -1.80
        2.20e-11 0. -0.70
        0.60 1.0
6)      FALLOFF                         ;O + NO = NO2
        9.00e-32 0. -1.50
        3.00e-11 0.
        0.60 1.0
7)      1.20e-13 2450.             ;NO2 + O3 = NO3
8)      PF=O3O3P                        ;O3 + HV = O
9)      PF=O3O1D                        ;O3 + HV = O1D
10)     2.10e-11 -102.             ;O1D + M = O
11)     2.20e-10 0.                ;O1D + H2O = #2 OH
12)     1.70e-12 940.              ;O3 + OH = HO2
13)     1.00e-14 490.              ;O3 + HO2 = OH
14)     PF=NO3NO2                       ;NO3 + HV = NO2 + O
15)     PF=NO3NO                        ;NO3 + HV = NO
16)     1.50e-11 -170.             ;NO3 + NO = #2 NO2
17)     4.50e-14 1260.             ;NO3 + NO2 = NO + NO2
18)     FALLOFF                         ;NO3 + NO2 = N2O5
        2.00e-30 0. -4.40
        1.40e-12 0. -0.70
        0.60 1.0
19)     2.50e-22 0.                ;N2O5 + H2O = #2 HNO3
20)     1.80e-39 0.                ;N2O5 + H2O + H2O = #2 HNO3
21)     FALLOFF                         ;N2O5 = NO3 + NO2
        1.00e-03 11000. -3.50
        9.70e+14 11080. 0.10
        0.45 1.0
22)     3.30e-39 -530.             ;NO + NO + O2 = #2 NO2
23)     5.00e-40 0.                ;NO + NO2 + H2O = #2 HONO
24)     FALLOFF                         ;NO + OH = HONO
        7.00e-31 0. -2.60
        3.60e-11 0. -0.10
        0.60 1.0
25)     PF=HONO                         ;HONO + HV = NO + OH
26)     1.80e-11 390.              ;OH + HONO = NO2
27)     1.00e-20 0.                ;HONO + HONO = NO + NO2
28)     FALLOFF                         ;NO2 + OH = HNO3
        2.00e-30 0. -3.00
        2.50e-11 0.
        0.60 1.0
29)     K0+K3M/1+K3M/K2             ;OH + HNO3 = NO3
        2.40e-14 -460.
```

```
      2.70e-17 -2199.
      6.50e-34 -1335.
30)   3.50e-12 -250.          ;HO2 + NO = OH + NO2
31)   FALLOFF                 ;HO2 + NO2 = PNA
      1.80e-31 0. -3.20
      4.70e-12 0.
      0.60 1.0
32)   FALLOFF                 ;PNA = HO2 + NO2
      4.10e-05 10650.
      4.80e+15 11170.
      0.60 1.0
33)   1.30e-12 -380.          ;OH + PNA = NO2
34)   K1+K2[M]                ;HO2 + HO2 = H2O2
      2.30e-13 -600.
      1.70e-33 -1000.
35)   K1+K2[M]                ;HO2 + HO2 + H2O = H2O2
      3.22e-34 -2800.
      2.38e-54 -3200.
36)   PF=H2O2                 ;H2O2 + HV = #2 OH
37)   2.90e-12 160.           ;OH + H2O2 = HO2
38)   1.10e-10 0.            ;O1D + H2 = OH + HO2
39)   5.50e-12 2000.          ;OH + H2 = HO2
40)   2.20e-11 -120.          ;OH + O = HO2
41)   4.20e-12 240.           ;OH + OH = O
42)   FALLOFF                 ;OH + OH = H2O2
      6.90e-31 0. -1.00
      2.60e-11 0. 0.00
      0.60 1.0
43)   4.80e-11 -250.          ;OH + HO2 =
44)   3.00e-11 -200.          ;HO2 + O = OH
45)   1.40e-12 2000.          ;H2O2 + O = OH + HO2
46)   1.00e-11 0.             ;NO3 + O = NO2
47)   2.20e-11 0.             ;NO3 + OH = HO2 + NO2
48)   3.50e-12 0.             ;NO3 + HO2 = HNO3
49)   1.00e-17 0.             ;NO3 + O3 = NO2
50)   8.50e-13 2450.          ;NO3 + NO3 = #2 NO2
51)   PF=PNA                  ;PNA + HV = #0.61 HO2 + #0.61 NO2 + #0.39 OH +
                              #0.39 NO3
52)   PF=HNO3                 ;HNO3 + HV = OH + NO2
53)   PF=N2O5                 ;N2O5 + HV = NO2 + NO3
54)   2.60e-12 -365.          ;XO2 + NO = NO2
55)   2.60e-12 -365.          ;XO2N + NO = NTR
56)   7.50e-13 -700.          ;XO2 + HO2 = ROOH
57)   7.50e-13 -700.          ;XO2N + HO2 = ROOH
58)   6.80e-14 0.             ;XO2 + XO2 =
59)   6.80e-14 0.             ;XO2N + XO2N =
60)   6.80e-14 0.             ;XO2 + XO2N =
61)   5.90e-13 360.           ;NTR + OH = HNO3 + HO2 + #0.33 FORM + #0.33 ALD2 +
                              #0.33 ALDX + #-0.66 PAR
62)   PF=NTR                  ;NTR + HV = NO2 + HO2 + #0.33 FORM + #0.33 ALD2 +
                              #0.33 ALDX + #-0.66 PAR
63)   3.01e-12 -190.          ;ROOH + OH = XO2 + #0.5 ALD2 + #0.5 ALDX
64)   PF=ROOH                 ;ROOH + HV = OH + HO2 + #0.5 ALD2 + #0.5 ALDX
65)   K1+K2[M]                ;OH + CO = HO2
      1.44E-13 0.
      3.43E-33 0.
66)   2.45e-12 1775.          ;OH + CH4 = MEO2
67)   2.80e-12 -300.          ;MEO2 + NO = FORM + HO2 + NO2
68)   4.10e-13 -750.          ;MEO2 + HO2 = MEPX
69)   9.50e-14 -390.          ;MEO2 + MEO2 = #1.37 FORM + #0.74 HO2 + #0.63 MEOH
```

```
70)  3.80e-12 -200.          ;MEPX + OH = #0.7 MEO2 + #0.3 XO2 + #0.3 HO2
71)  PF=ROOH                 ;MEPX + HV = FORM + HO2 + OH
72)  7.30e-12 620.           ;MEOH + OH = FORM + HO2
73)  9.00e-12 0.             ;FORM + OH = HO2 + CO
74)  PF=FORMR                ;FORM + HV = #2 HO2 + CO
75)  PF=FORMS                ;FORM + HV = CO + H2
76)  3.40e-11 1600.          ;FORM + O = OH + HO2 + CO
77)  5.80e-16 0.             ;FORM + NO3 = HNO3 + HO2 + CO
78)  9.70e-15 -625.          ;FORM + HO2 = HCO3
79)  2.40e+12 7000.          ;HCO3 = FORM + HO2
80)  5.60e-12 0.             ;HCO3 + NO = FACD + NO2 + HO2
81)  5.60e-15 -2300.         ;HCO3 + HO2 = MEPX
82)  4.00e-13 0.             ;FACD + OH = HO2
83)  1.80e-11 1100.          ;ALD2 + O = C2O3 + OH
84)  5.60e-12 -270.          ;ALD2 + OH = C2O3
85)  1.40e-12 1900.          ;ALD2 + NO3 = C2O3 + HNO3
86)  PF=ALD2                 ;ALD2 + HV = MEO2 + CO + HO2
87)  8.10e-12 -270.          ;C2O3 + NO = MEO2 + NO2
88)  FALLOFF                 ;C2O3 + NO2 = PAN
      2.70e-28 0. -7.10
      1.20e-11 0. -0.90
      0.30 1.0
89)  FALLOFF                 ;PAN = C2O3 + NO2
      4.90e-03 12100.
      5.40e+16 13830.
      0.30 1.0
90)  PF=PAN                  ;PAN + HV = C2O3 + NO2
91)  4.30e-13 -1040.         ;C2O3 + HO2 = #0.8 PACD + #0.2 AACD + #0.2 O3
92)  2.00e-12 -500.          ;C2O3 + MEO2 = #0.9 MEO2 + #0.9 HO2 + FORM +
                                 #0.1 AACD
93)  4.40e-13 -1070.         ;C2O3 + XO2 = #0.9 MEO2 + #0.1 AACD
94)  2.90e-12 -500.          ;C2O3 + C2O3 = #2 MEO2
95)  4.00e-13 -200.          ;PACD + OH = C2O3
96)  PF=ROOH QY=0.00e+0      ;PACD + HV = MEO2 + OH
97)  4.00e-13 -200.          ;AACD + OH = MEO2
98)  1.30e-11 870.           ;ALDX + O = CXO3 + OH
99)  5.10e-12 -405.          ;ALDX + OH = CXO3
100) 6.50e-15 0.             ;ALDX + NO3 = CXO3 + HNO3
101) PF=ALDX                 ;ALDX + HV = MEO2 + CO + HO2
102) 6.70e-12 -340.          ;CXO3 + NO = ALD2 + NO2 + HO2 + XO2
103) FALLOFF                 ;CXO3 + NO2 = PANX
      2.70e-28 0. -7.10
      1.20e-11 0. -0.90
      0.30 1.0
104) FALLOFF                 ;PANX = CXO3 + NO2
      4.90e-03 12100.
      5.40e+16 13830.
      0.30 1.0
105) PF=PAN                  ;PANX + HV = CXO3 + NO2
106) 3.00e-13 0.             ;PANX + OH = ALD2 + NO2
107) 4.30e-13 -1040.         ;CXO3 + HO2 = #0.8 PACD + #0.2 AACD + #0.2 O3
108) 2.00e-12 -500.          ;CXO3 + MEO2 = #0.9 ALD2 + #0.9 XO2 + HO2 +
                                 #0.1 AACD + #0.1 FORM
109) 4.40e-13 -1070.         ;CXO3 + XO2 = #0.9 ALD2 + #0.1 AACD
110) 2.90e-12 -500.          ;CXO3 + CXO3 = #2 ALD2 + #2 XO2 + #2 HO2
111) 2.90e-12 -500.          ;CXO3 + C2O3 = MEO2 + XO2 + HO2 + ALD2
112) 8.10e-13 0.             ;PAR + OH = #0.87 XO2 + #0.13 XO2N + #0.11 HO2 +
                                 #0.06 ALD2 + #-0.11 PAR + #0.76 ROR + #0.05 ALDX
113) 1.00e+15 8000.          ;ROR = #0.96 XO2 + #0.6 ALD2 + #0.94 HO2 +
                                 #-2.1 PAR + #0.04 XO2N + #0.02 ROR + #0.5 ALDX
```

```
114)  1.60e+03 0.              ;ROR = HO2
115)  1.50e-11 0.              ;ROR + NO2 = NTR
116)  1.00e-11 280.            ;O + OLE = #0.2 ALD2 + #0.3 ALDX + #0.3 HO2 +
                                   #0.2 XO2 + #0.2 CO + #0.2 FORM + #0.01 XO2N +
                                   #0.2 PAR + #0.1 OH
117)  3.20e-11 0.              ;OH + OLE = #0.8 FORM + #0.33 ALD2 + #0.62 ALDX +
                                   #0.8 XO2 + #0.95 HO2 + #-0.7 PAR
118)  6.50e-15 1900.           ;O3 + OLE = #0.18 ALD2 + #0.74 FORM + #0.32 ALDX +
                                   #0.22 XO2 + #0.1 OH + #0.33 CO + #0.44 HO2 +
                                   #-1.0 PAR
119)  7.00e-13 2160.           ;NO3 + OLE = NO2 + FORM + #0.91 XO2 + #0.09 XO2N +
                                   #0.56 ALDX + #0.35 ALD2 + #-1.0 PAR
120)  1.04e-11 792.            ;O + ETH = FORM + #1.7 HO2 + CO + #0.7 XO2 +
                                   #0.3 OH
121)  FALLOFF                      ;OH + ETH = XO2 + #1.56 FORM + #0.22 ALDX + HO2
      1.00e-28 0. -0.80
      8.80e-12 0.
      0.60 1.0
122)  1.20e-14 2630.           ;O3 + ETH = FORM + #0.63 CO + #0.13 HO2 +
                                   #0.13 OH + #0.37 FACD
123)  3.30e-12 2880.           ;NO3 + ETH = NO2 + XO2 + #2 FORM
124)  2.30e-11 0.              ;IOLE + O = #1.24 ALD2 + #0.66 ALDX + #0.1 HO2 +
                                   #0.1 XO2 + #0.1 CO + #0.1 PAR
125)  1.00e-11 -550.           ;IOLE + OH = #1.3 ALD2 + #0.7 ALDX + HO2 + XO2
126)  8.40e-15 1100.           ;IOLE + O3 = #0.65 ALD2 + #0.35 ALDX + #0.25 FORM +
                                   #0.25 CO + #0.5 O + #0.5 OH + #0.5 HO2
127)  9.60e-13 270.            ;IOLE + NO3 = #1.18 ALD2 + #0.64 ALDX + HO2 + NO2
128)  1.80e-12 -355.           ;TOL + OH = #0.44 HO2 + #0.08 XO2 + #0.36 CRES +
                                   #0.56 TO2
129)  8.10e-12 0.              ;TO2 + NO = #0.9 NO2 + #0.9 HO2 + #0.9 OPEN +
                                   #0.1 NTR
130)  4.20e+00 0.              ;TO2 = CRES + HO2
131)  4.10e-11 0.              ;OH + CRES = #0.4 CRO + #0.6 XO2 + #0.6 HO2 +
                                   #0.3 OPEN
132)  2.20e-11 0.              ;CRES + NO3 = CRO + HNO3
133)  1.40e-11 0.              ;CRO + NO2 = NTR
134)  5.50e-12 0.              ;CRO + HO2 = CRES
135)  PF=FORMR QY=9.00e+0      ;OPEN + HV = C2O3 + HO2 + CO
136)  3.00e-11 0.              ;OPEN + OH = XO2 + #2 CO + #2 HO2 + C2O3 + FORM
137)  5.40e-17 500.            ;OPEN + O3 = #0.03 ALDX + #0.62 C2O3 + #0.7 FORM +
                                   #0.03 XO2 + #0.69 CO + #0.08 OH + #0.76 HO2 +
                                   #0.2 MGLY
138)  1.70e-11 -116.           ;OH + XYL = #0.7 HO2 + #0.5 XO2 + #0.2 CRES +
                                   #0.8 MGLY + #1.1 PAR + #0.3 TO2
139)  1.70e-11 0.              ;OH + MGLY = XO2 + C2O3
140)  PF=MGLY                      ;MGLY + HV = C2O3 + HO2 + CO
141)  3.60e-11 0.              ;O + ISOP = #0.75 ISPD + #0.5 FORM + #0.25 XO2 +
                                   #0.25 HO2 + #0.25 CXO3 + #0.25 PAR
142)  2.54e-11 -407.6          ;OH + ISOP = #0.912 ISPD + #0.629 FORM +
                                   #0.991 XO2 + #0.912 HO2 + #0.088 XO2N
143)  7.86e-15 1912.           ;O3 + ISOP = #0.65 ISPD + #0.6 FORM + #0.2 XO2 +
                                   #0.066 HO2 + #0.266 OH + #0.2 CXO3 + #0.15 ALDX +
                                   #0.35 PAR + #0.066 CO
144)  3.03e-12 448.            ;NO3 + ISOP = #0.2 ISPD + #0.8 NTR + XO2 +
                                   #0.8 HO2 + #0.2 NO2 + #0.8 ALDX + #2.4 PAR
145)  3.36e-11 0.              ;OH + ISPD = #1.565 PAR + #0.167 FORM +
                                   #0.713 XO2 + #0.503 HO2 + #0.334 CO +
                                   #0.168 MGLY + #0.252 ALD2 + #0.21 C2O3 +
                                   #0.25 CXO3 + #0.12 ALDX
146)  7.10e-18 0.              ;O3 + ISPD = #0.114 C2O3 + #0.15 FORM +
```

```
                                    #0.85 MGLY + #0.154 HO2 + #0.268 OH + #0.064 XO2 +
                                    #0.02 ALD2 + #0.36 PAR + #0.225 CO
147)   1.00e-15 0.              ;NO3 + ISPD = #0.357 ALDX + #0.282 FORM +
                                    #1.282 PAR + #0.925 HO2 + #0.643 CO + #0.85 NTR +
                                    #0.075 CXO3 + #0.075 XO2 + #0.15 HNO3
148)   PF=ACROX QY=3.60e-3      ;ISPD + HV = #0.333 CO + #0.067 ALD2 + #0.9 FORM +
                                    #0.832 PAR + #1.033 HO2 + #0.7 XO2 + #0.967 C2O3
149)   3.60e-11 0.              ;TERP + O = #0.15 ALDX + #5.12 PAR
150)   1.50e-11 -449.           ;TERP + OH = #0.75 HO2 + #1.25 XO2 + #0.25 XO2N +
                                    #0.28 FORM + #0.47 ALDX + #1.66 PAR
151)   1.20e-15 821.            ;TERP + O3 = #0.57 OH + #0.07 HO2 + #0.76 XO2 +
                                    #0.18 XO2N + #0.24 FORM + #0.001 CO + #7 PAR +
                                    #0.21 ALDX + #0.39 CXO3
152)   3.70e-12 -175.           ;TERP + NO3 = #0.47 NO2 + #0.28 HO2 + #1.03 XO2 +
                                    #0.25 XO2N + #0.47 ALDX + #0.53 NTR
153)   FALLOFF                    ;SO2 + OH = SULF + HO2
        3.00e-31 0. -3.30
        1.50e-12 0.
        0.60 1.0
154)   6.90e-12 230.            ;OH + ETOH = HO2 + #0.9 ALD2 + #0.05 ALDX +
                                    #0.1 FORM + #0.1 XO2
155)   8.70e-12 1070.           ;OH + ETHA = #0.991 ALD2 + #0.991 XO2 +
                                    #0.009 XO2N + HO2
156)   1.5E-19                  ;NO2    + ISOP = #0.80 {NTR + HO2} + #0.20 NO +
                                    XO2    + #0.80 ALDX + #2.40 PAR + #0.20 ISPD
.
!END: Include CB05 RXN FILE
!
! GH: replaced with a dummy wall-reaction file
@CB05WALL.RXN
!@dumwallh.rxn
@CB05TRAC.RXN
!
.DUM
HCHO
.INS INIT
"C FORM" = "C FORM"+"C HCHO"
.
.END
```

==========

CB05-Ua:

Note: The reactions other than R128, R129 and R130 are the same as in CB05-Base.

```
!B2. Proposed mechanism 1 (cresol yield of 0.36)
!           Start: Proposed update I (with CRES yield of 0.36)
128)   1.80e-12 -355.           ;TOL + OH = #0.44 HO2 + #0.08 XO2 + #0.36 CRES +
                                    #0.56 TO2
129)   2.70e-12 -360.           ;TO2 + NO = #0.9 NO2 + #0.9 HO2 + #0.9 OPEN +
                                    #0.1 NTR
130)   1.90e-13 -1300.          ;TO2 + HO2 = TO2HO2
!           End: Proposed update I (with CRES yield of 0.36)
```

==========

CB05-Ub:

Note: The reactions other than R128, R129 and R130 are the same as in CB05-Base.

```
!B3. Proposed mechanism 2 (cresol yield of 0.18)
!!          Start: Proposed update II (with CRES yield of 0.18)
128)   1.80e-12 -355.          ;TOL + OH = #0.26 HO2 + #0.08 XO2 + #0.18 CRES +
                                    #0.74 TO2
129)   2.70e-12 -360.          ;TO2 + NO = #0.9 NO2 + #0.9 HO2 + #0.9 OPEN +
                                    #0.1 NTR
130)   0.00e+00 -1300.         ;TO2 + HO2 = TO2HO2
```

==========

CB05-UNClite:

Note: The reactions of CB05-Base other than Reactions R128 – R137 are also used in CB05-UNClite and will not be repeated here.

```
!!          Start: Proposed mechanism: UNClite
TL1)   1.80E-12 -355.          ;TOL + OH = #0.28 HO2 + #0.10 XO2 + #0.18 CRES +
                                    #0.65 TO2 + #0.072 OH
TL2)   2.70E-12 -360.          ;TO2 + NO = #0.86 NO2 + #1.2 HO2 + #0.86 OPEN +
                                    #0.14 NTR + #0.52 MGLY + #0.336 FORM +
                                    #0.336 CO
TL3)   1.90E-13 -1300.         ;TO2 + HO2 =
TL4)   1.70E-12 -950.          ;OH + CRES = #0.060 CRO + #0.12 XO2 + #1.12 HO2 +
                                    #0.13 OPEN + #0.732 CAT1 + #0.06 CO +
                                    #0.06 XO2N + #0.06 FORM
TL5)   1.40E-11   0.           ;CRES + NO3 = #0.300 CRO + HNO3 + #0.600 XO2 +
                                    #0.360 HO2 + #0.48 ALDX + #0.24 FORM +
                                    #0.24 MGLY + #0.12 OPEN + #0.10 XO2N +
                                    #0.24 CO
TL6)   2.10E-12   0.           ;CRO + NO2 = CRON
TL7)   5.50E-12   0.           ;CRO + HO2 = CRES
TL8)   1.53E-12   0.           ;CRON + OH = CRNO
TL9)   3.80E-12   0.           ;CRON + NO3 = CRNO + HNO3
TL10) 2.10E-12   0.            ;CRNO + NO2 = #2.00 NTR
TL11) 2.86E-13   0.            ;CRNO + O3 = CRN2
TL12) 2.54E-12 -360.           ;CRN2 + NO = CRNO + NO2
TL13) 2.40E-13 -1300.          ;CRN2 + HO2 = CRPX
TL14) PF=NO2 QY=1.00E-2        ;CRPX + HV = CRNO + OH
! UNClite used 3.00E-12*Exp(190/T) instead of 1.9E-12*Exp(190/T)
! 3.00E-12*Exp(190/T) => 1.9E-12*Exp(190/T)
TL15) 1.90E-12 -190.           ;CRPX + OH = CRN2
TL16) PF=NO2 QY=4.00E-2        ;OPEN + HV = OPO3 + HO2 + CO
TL17) 4.40E-11 0.              ;OPEN + OH = #0.6 OPO3 + #0.4 CAO2
TL18) 5.40E-17 500.            ;OPEN + O3 = #0.03 ALDX + #0.62 OPO3 +
                                    #0.70 FORM + #0.76 HO2 + #0.69 CO +
                                    #0.20 MGLY + #0.08 OH + #0.03 XO2
TL19) 3.80E-12   0.            ;OPEN + NO3 = OPO3 + HNO3
! UNClite used 7.00E-11 instead of 6.98E-10; 7.00E-11 => 6.98E-10 (21 Aug 08)
! Return to 7.00E-11 according to Dr. Gary Z. Whitten's comment      (7 Sep 08)
TL20) 7.00E-11   0.            ;CAT1 + OH = CAO2
TL21) 1.70E-10   0.            ;CAT1 + NO3 = CRO + HNO3
TL22) 2.54E-12 -360.           ;CAO2 + NO = #0.86 NO2 + #1.2 HO2 +
                                    #0.344 FORM + #0.344 CO + #0.14 NTR
TL23) 2.40E-13 -1300.          ;CAO2 + HO2 = CRPX
! Add HO2 as a product in TL24 (7 Sep 08)
! OPO3 + NO = NO2 + XO2 + ALDX => OPO3 + NO = NO2 + XO2 + HO2 + ALDX (7 Sep 08)
```

```
TL24) 1.00E-11    0.              ;OPO3 + NO = NO2 + XO2 + HO2 + ALDX
TL25) 1.00E-11    0.              ;OPO3 + NO2 = OPAN
TL26) 1.00E-04    0.              ;OPAN = OPO3 + NO2
!!          END: Proposed mechanism: UNClite
```

==========

CB05-Dinitro:

Note: The reactions of CB05-Base other than Reactions R128 – R134 are also used in CB05-Dinitro and will not be repeated here.

```
!           Start: Proposed mechanism [Dinitro]
TL1)   1.80E-12 -355.          ;TOL + OH = #0.260 HO2 + #0.080 XO2 + #0.180 CRES +
                                   #0.740 TO2
TL2)   2.70E-12 -360.          ;TO2 + NO = #0.900 NO2 + #0.900 HO2 + #0.900 OPEN +
                                   #0.100 NTR
TL3)   1.90E-13 -1300.         ;TO2 + HO2 =
TL4)   4.10E-11 0.             ;OH + CRES = #0.800 CRO + #0.200 XO2 +
                                   #0.200 HO2 + #0.100 OPEN
TL5)   2.20E-11 0.             ;CRES + NO3 = CRO + HNO3
TL6)   2.10E-12 0.             ;CRO + NO2 = CRON
TL7)   5.50E-12 0.             ;CRO + HO2 = CRES
TL8)   1.53E-12 0.             ;CRON + OH = #0.800 CRNO + #0.200 XO2 +
                                   #0.200 HO2 + #0.100 OPEN
TL9)   3.80E-12 0.             ;CRON + NO3 = CRNO + HNO3
TL10) 2.10E-12 0.              ;CRNO + NO2 = #2.000 NTR
TL11) 5.50E-12 0.              ;CRNO + HO2 = CRON
!           End: Proposed mechanism [Dinitro]
```

A2.2. Implementation in the Morpho Software

CB05-Base:

```
// Carbon Bond 05 Principle Mechanism
//
// Description:
//     CB05 Mechanism for use in Chamber Modeling
//     UNITS = cm^3_molecule^-1_s^-1
//     Format = Morpho
//       Initial file on 06/06/05 by Gary Z. Whitten
//       Correction:
//          April 2007: Yosuke Kimura at CEER, UT-Austin
//                      R[I124]: changed species name from O to O3P
//          June & July 2007 : Gookyoung Heo at CEER, UT-Austin
//                             based on CB05 Final Report (Dec. 8, 2005) and
//                             e-mail response of Gary Z. Whitten and Greg Yarwood.
//                      R[I5]:      TROE(2.5E-31*T_300^-1.8,2.2E-11,b[M],0.7)
//                              => TROE(2.5E-31*T_300^-1.8,2.2E-11*T_300^-0.7,b[M],0.6)
//                      R[I35]: TROE(3.22E-34*EXP(2800./TK),2.38E-54*EXP(3200./TK),b[H2O],0.6)
//                              => (3.22E-34*EXP(2800./TK) + 2.38E-54*EXP(3200./TK)*b[M])
//                      R[I65]:    1.44E-13(1. + 0.586*Patm) => (1.44E-13 + 3.43E-33* b[M])
//                      R[I118]:    Add "+ s_p4*PAR" (-PAR) in the product part.
//                      R[I139]: 1.8E-11 => 1.7E-11 (Gery et al. (1989), CB05 Final Report)
//                      *Changes in photolysis reactions
//                      R[I71]: Phot(MEPX, R71) = Phot(ROOH, R64)
//                                j[MEPX_to_OH] => j[ROOH_to_OH]
//                      R[I96]: Phot(PACD, R96) = 0.0*Phot(ROOH, R64) (CB05 Final Report)
//                                j[PACD_to_OH] => 0.0E+0*j[ROOH_to_OH]
//                      R[I105]:Phot(PANX, R105) = Phot(PAN, R90)
//                                j[PANX_to_NO2] => j[PAN_to_NO2]
//                      R[I4]:    5.6E-12*EXP(-180.0/TK) => 5.6E-12*EXP(180.0/TK)
//                      *Notes
//                      R[I148]: Phot(ISPD, R148) = 0.0036*Phot(ACROLEIN (or ACROX))
//                                  in Morpho and CB05 Final Report
//                                    = Phot(ISPD, primary phot., R152 in mech. 6)
//                                  in the mechanism 6's chemparam file according to Greg Yarwood.
//                                  Thus, no change.
//                      Gary Z. Whitten added -M- and -hv- to clarify the types of reactions.
//
// Source:
//     Base mechanism from EPA project
//
//
//
//
//     Species ADDED for chamber simulations
//
//     NR              -- added as species to balance C on input
//
// Needed photolysis rates:
//     NO2_to_O3P
//     O3_to_O3P
//     O3_to_O1D
//     NO3_to_NO2
//     NO3_to_NO
//     HONO_to_OH
//     H2O2_to_OH
```

```
//      PNA_to_HO2
//      HNO3_to_OH
//      N2O5_to_NO2
//      NTR_to_NO2
//      ROOH_to_OH
//      MEPX_to_OH ! MEPX.CQY (MEPX.CQY = ROOH.CQY); not required.
//      FORM_to_HO2
//      FORM_to_H2
//      ALD2_to_HO2
//      PAN_to_NO2
//      PACD_to_OH ! PACD.CQY (Phot(PACD) = 0.0*Phot(ROOH)); not required.
//      ALDX_to_HO2
//      MGLY_to_HO2
//      ACRO_to_RO2
//

NAMES
  PhotoRateIDs += { NO2_to_O3P };

    R[I1] =              NO2              -hv-> NO    + O3P          @ j[NO2_to_O3P];
    R[I2] = O3P + O2 + M          ----> O3    + M              @ 6.0E-34*T_300^-2.4;
    R[I3] = O3    + NO             ----> NO2 + O2           @ 3.0E-12*EXP(-1500.0/TK);
    R[I4] = O3P + NO2              ----> NO    + O2           @ 5.6E-12*EXP(180.0/TK);
    R[I5] = O3P + NO2              -M--> NO3 + O2           @ TROE(2.5E-31*T_300^-1.8,
                                                                   2.2E-11*T_300^-0.7,
                                                                   b[M], 0.6);
    R[I6] = O3P + NO               -M--> NO2                  @ TROE(9.00E-32*T_300^-1.5,
                                                                   3.0E-11, b[M], 0.6);
    R[I7] = O3    + NO2            ----> NO3 + O2           @ 1.2E-13*EXP(-2450.0/TK);

NAMES
  PhotoRateIDs += { O3_to_O3P, O3_to_O1D, NO3_to_NO2, NO3_to_NO };

    R[I8] = O3                     -hv-> O3P + O2           @ j[O3_to_O3P] ;
    R[I9] = O3                     -hv-> O1D + O2           @ j[O3_to_O1D] ;
   R[I10] = O1D + M                ----> O3P + M            @ 2.1E-11*EXP( 102.0/TK) ;
   R[I11] = O1D + H2O              ----> 2.0*OH             @ 2.20E-10 ;
   R[I12] = O3    + OH             ----> HO2 + O2           @ 1.7E-12*EXP(-940.0/TK) ;
   R[I13] = O3    + HO2            ----> OH    + 2.0*O2     @ 1.0E-14*EXP(-490.0/TK) ;
   R[I14] =             NO3        -hv-> NO2 + O3P          @ j[NO3_to_NO2] ;
   R[I15] =             NO3        -hv-> NO    + O2         @ j[NO3_to_NO] ;
   R[I16] = NO3 + NO               ----> 2.0*NO2            @ 1.50E-11*EXP(170.0/TK) ;
   R[I17] = NO3 + NO2              ----> NO    + NO2 + O2 @ 4.50E-14*EXP(-1260.0/TK) ;
   R[I18] = NO3 + NO2              -M--> N2O5                 @ TROE(2.0E-30*T_300^-4.4,
                                                                   1.4E-12*T_300^-0.7,
                                                                   b[M], 0.6) ;
   R[I19]= N2O5 + H2O              ----> 2.0*HNO3           @ 2.5E-22 ;
   R[I20]= N2O5 + H2O + H2O        ----> 2.0*HNO3           @ 1.8E-39 ;
   R[I21]=              N2O5        -M--> NO3 + NO2 @ TROE(1.E-03*T_300^-3.5*EXP(-11000./TK),
                                                                 9.7E14*T_300^0.1*EXP(-11080./TK),
                                                                 b[M], 0.45) ;
   R[I22]= NO      + NO    + O2     ----> 2.0*NO2            @ 3.30E-39*EXP(530.0/TK) ;

NAMES
  PhotoRateIDs += { HONO_to_OH } ;

   R[I23] = NO      + NO2 + H2O ----> 2.0*HONO           @ 5.0E-40 ;
   R[I24] = OH      + NO            -M--> HONO             @ TROE(7.00E-31*T_300^-2.6,
                                                                   3.60E-11*T_300^-0.1,
                                                                   b[M], 0.6) ;
```

```
  R[I25] =              HONO          -hv-> OH    + NO           @ j[HONO_to_OH] ;
  R[I26] = OH     + HONO          ----> NO2 + H2O          @ 1.80E-11*EXP(-390.0/TK);
  R[I27] = HONO + HONO          ----> NO    + NO2 +H2O @ 1.0E-20 ;
  R[I28] = OH     + NO2         -M--> HNO3                 @ TROE(2.0E-30*T_300^-3.0,
                                                                  2.5E-11*T_300^-0.0,
                                                                  b[M], 0.6) ;
  R[I29] = OH     + HNO3        -M--> NO3 + H2O          @ 2.4E-14*EXP(460.0/TK) +
                                                              LMHW(6.5E-34*EXP(1335.0/TK),
                                                                 2.7E-17*EXP(2199.0/TK),
                                                                 b[M]) ;
  R[I30] = HO2    + NO          ----> OH    + NO2        @ 3.50E-12*EXP(250.0/TK) ;
  R[I31] = HO2    + NO2         -M--> PNA                  @ TROE(1.80E-31*T_300^-3.2,
                                                                  4.70E-12*T_300^-0.0,
                                                                  b[M], 0.6) ;
  R[I32] =              PNA           -M--> HO2 + NO2          @ TROE(4.1E-5*EXP(-10650./TK),
                                                                  4.8E15*EXP(-11170./TK),
                                                                  b[M], 0.6) ;
  R[I33] = OH     + PNA         ----> NO2 + H2O + O2 @ 1.30E-12*EXP(380.0/TK) ;

NAMES
  PhotoRateIDs += { H2O2_to_OH } ;

  R[I34] = HO2    + HO2         -M--> H2O2 + O2          @ ( 2.3E-13*EXP( 600.0/TK) +
                                                                 1.7E-33*EXP(1000.0/TK)* b[M]) ;
  R[I35] = HO2    + HO2 + H2O -M--> H2O2 + O2          @ (3.22E-34*EXP(2800./TK) +
                                                              2.38E-54*EXP(3200./TK)*b[M]);
  R[I36] =              H2O2          -hv-> 2.0*OH           @ j[H2O2_to_OH] ;
  R[I37] = OH     + H2O2          ----> HO2    + H2O       @ 2.90E-12*EXP(-160./TK) ;
  R[I38] = O1D    + H2            ----> OH     + HO2       @ 1.1E-10 ;
  R[I39] = OH     + H2            ----> HO2                @ 5.5E-12*EXP(-2000./TK) ;
  R[I40] = OH     + O3P           ----> HO2                @ 2.2E-11*EXP(    120./TK) ;
  R[I41] = OH     + OH            ----> O3P                @ 4.2E-12*EXP( -240./TK) ;
R[I42] = OH     + OH            -M--> H2O2                 @ TROE(6.9E-31*T_300^-1.0,
                                                                  2.6E-11*T_300^0.0,
                                      b[M], 0.6) ;
  R[I43] = OH     + HO2           ----> O2     + H2O       @ 4.8E-11*EXP(    250./TK) ;
  R[I44] = HO2    + O3P           ----> OH                 @ 3.0E-11*EXP(    200./TK) ;
  R[I45] = H2O2 + O3P           ----> OH     + HO2       @ 1.4E-12*EXP(-2000./TK) ;
  R[I46] = NO3    + O3P           ----> NO2                @ 1.0E-11 ;
  R[I47] = NO3    + OH            ----> HO2    + NO2       @ 2.2E-11 ;
  R[I48] = NO3    + HO2           ----> HNO3               @ 3.5E-12 ;
  R[I49] = NO3    + O3            ----> NO2                @ 1.0E-17 ;
  R[I50] = NO3    + NO3           ----> 2.0*NO2            @ 8.5E-13*EXP(-2450./TK) ;

NAMES
  PhotoRateIDs += { PNA_to_HO2, HNO3_to_OH, N2O5_to_NO2, NTR_to_NO2, ROOH_to_OH };
SCALARS
  const s_p0 = -0.66, s_p1 = -0.11, s_p2 = -2.1,
  s_p3 = -0.70, s_p4 = -1.0, kOPEN_R = 9.0;

  R[I51] = PNA                  -hv-> 0.610*HO2 + 0.610*NO2 +
                                      0.390*OH    + 0.390*NO3          @ j[PNA_to_HO2] ;
  R[I52] = HNO3                 -hv-> OH             + NO2           @ j[HNO3_to_OH] ;
  R[I53] = N2O5                 -hv-> NO2            + NO3           @ j[N2O5_to_NO2] ;
  R[I54] = XO2    + NO          ----> NO2                            @ 2.6E-12*EXP(365./TK) ;
  R[I55] = XO2N + NO            ----> NTR                            @ 2.6E-12*EXP(365./TK) ;
  R[I56] = XO2    + HO2         ----> ROOH                           @ 7.5E-13*EXP(700./TK) ;
  R[I57] = XO2N + HO2           ----> ROOH                           @ 7.5E-13*EXP(700./TK) ;
  R[I58] = XO2    + XO2         ---->                                @ 6.8E-14 ;
  R[I59] = XO2N + XO2N          ---->                                @ 6.8E-14 ;
```

```
 R[I60] = XO2    + XO2N          ---->                                          @ 6.8E-14 ;
 R[I61] = NTR    + OH            ----> HNO3 + HO2 + 0.33*FORM +
                                   0.33*ALD2 + 0.33*ALDX + s_p0*PAR            @ 5.9E-13*EXP(-360./TK) ;
 R[I62] = NTR                    -hv-> NO2    + HO2 + 0.33*FORM +
                                   0.33*ALD2 + 0.33*ALDX + s_p0*PAR            @ j[NTR_to_NO2] ;
 R[I63] = ROOH + OH              ----> XO2    + 0.50*ALD2 + 0.50*ALDX          @ 3.01E-12*EXP(190./TK) ;
 R[I64] = ROOH                   -hv-> OH     + HO2          + 0.50*ALD2 +
                                   0.50*ALDX                                   @ j[ROOH_to_OH] ;
 R[I65] = OH + CO                -M--> HO2    + CO2                            @ (1.44E-13 + 3.43E-33* b[M]) ;

// ORGANIC CHEMISTRY ================================================

 R[I66] = OH     + CH4           ----> MEO2                                    @ 2.45E-12*EXP(-1775./TK);
 R[I67] = MEO2 + NO              ----> FORM + HO2    + NO2                      @ 2.8E-12*EXP(300./TK) ;
 R[I68] = MEO2 + HO2             ----> MEPX                                    @ 4.1E-13*EXP(750./TK) ;
 R[I69] = MEO2 + MEO2             ----> 1.37*FORM     + 0.74*HO2 +
                                         0.63*MEOH                             @ 9.5E-14*EXP(390./TK) ;
 R[I70] = MEPX + OH              ----> 0.70*MEO2     + 0.30*XO2 +
                                         0.30*HO2                              @ 3.8E-12*EXP(200./TK) ;

NAMES
 PhotoRateIDs += { MEPX_to_OH, FORM_to_HO2, FORM_to_H2 };

 R[I71] = MEPX                   -hv-> FORM    + HO2    + OH                    @ j[ROOH_to_OH];
 R[I72] = MEOH + OH               ----> FORM    + HO2                          @ 7.3E-12*EXP( -620./TK) ;
 R[I73] = FORM + OH              ----> HO2     + CO                           @ 9.0E-12 ;
 R[I74] = FORM                   -hv-> 2.00*HO2 + CO                          @ j[FORM_to_HO2] ;
 R[I75] = FORM                   -hv-> CO       + H2                          @ j[FORM_to_H2] ;
 R[I76] = FORM + O3P             ----> OH       +     HO2    +    CO           @ 3.4E-11*EXP(-1600./TK) ;
 R[I77] = FORM + NO3             ----> HNO3     +     HO2    +    CO            @ 5.8E-16 ;
 R[I78] = FORM + HO2             ----> HCO3                                    @ 9.7E-15*EXP(    625./TK) ;
 R[I79] = HCO3                   ----> FORM    + HO2                          @ 2.4E+12*EXP(-7000./TK) ;
 R[I80] = HCO3 + NO              ----> FACD    + NO2       + HO2              @ 5.6E-12 ;
 R[I81] = HCO3 + HO2             ----> MEPX                                    @ 5.6E-15*EXP( 2300./TK) ;
 R[I82] = FACD + OH              ----> HO2                                     @ 4.0E-13 ;
 R[I83] = ALD2 + O3P             ----> C2O3    + OH                           @ 1.8E-11*EXP(-1100./TK) ;
 R[I84] = ALD2 + OH              ----> C2O3                                    @ 5.6E-12*EXP(    270./TK) ;
 R[I85] = ALD2 + NO3             ----> C2O3    + HNO3                         @ 1.4E-12*EXP(-1900./TK) ;

NAMES
 PhotoRateIDs += { ALD2_to_HO2, PAN_to_NO2 };

 R[I86] = ALD2                   -hv-> MEO2    + CO    + HO2                   @ j[ALD2_to_HO2] ;
 R[I87] = C2O3 + NO              ----> NO2     + MEO2                         @ 8.1E-12*EXP(270./TK) ;
 R[I88] = C2O3 + NO2             -M--> PAN                                    @ TROE(2.7E-28*T_300^-7.1,
                                                                                     1.2E-11*T_300^-0.9,
                                                                                     b[M], 0.3) ;
 R[I89]=          PAN             -M--> C2O3    + NO2                        @ TROE(4.9E-3*EXP(-12100./TK),
                                                                                   5.4E16*EXP(-13830./TK),
                                                                                   b[M], 0.3) ;
 R[I90]=          PAN             -hv-> C2O3    + NO2                          @ j[PAN_to_NO2] ;

NAMES
 PhotoRateIDs += { PACD_to_OH, ALDX_to_HO2, PANX_to_NO2,
                   MGLY_to_HO2, ACRO_to_RO2 };

 R[I91] = C2O3 + HO2             ----> 0.80*PACD + 0.20*AACD + 0.20*O3     @ 4.3E-13*EXP(1040./TK) ;
 R[I92] = C2O3 + MEO2             ----> 0.90*MEO2 + 0.90*HO2
                                         + FORM + 0.10*AACD                    @ 2.0E-12*EXP( 500./TK) ;
 R[I93] = C2O3 + XO2             ----> 0.90*MEO2 + 0.10*AACD                 @ 4.4E-13*EXP(1070./TK) ;
```

```
  R[I94] = C2O3 + C2O3        ----> 2.00*MEO2                                  @ 2.9E-12*EXP( 500./TK) ;
  R[I95] = PACD + OH          ----> C2O3                                       @ 4.0E-13*EXP( 200./TK) ;
  R[I96] = PACD               -hv-> MEO2          + OH                         @ 0.0E+0*j[ROOH_to_OH] ;
  R[I97] = AACD + OH          ----> MEO2                                       @ 4.0E-13*EXP( 200./TK) ;
  R[I98] = ALDX + O3P         ----> CXO3          + OH                         @ 1.3E-11*EXP(-870./TK) ;
  R[I99] = ALDX + OH          ----> CXO3                                       @ 5.1E-12*EXP( 405./TK) ;
 R[I100] = ALDX + NO3         ----> CXO3          + HNO3                       @ 6.5E-15 ;
 R[I101] = ALDX               -hv-> MEO2          + CO          + HO2          @ j[ALDX_to_HO2] ;
 R[I102] = CXO3 + NO          ----> ALD2 + NO2 + HO2 + XO2                     @ 6.7E-12*EXP( 340./TK) ;
 R[I103] = CXO3 + NO2         -M--> PANX                                       @ TROE(2.7E-28*T_300^-7.1,
                                                                                       1.2E-11*T_300^-0.9,
                                                                                       b[M], 0.3) ;
 R[I104] = PANX               -M--> CXO3 + NO2                                 @ TROE(4.9E-3*EXP(-12100./TK),
                                                                                       5.4E16*EXP(-13830./TK),
                                                                                       b[M], 0.3) ;
 R[I105] = PANX               -hv-> CXO3 + NO2                                 @ j[PAN_to_NO2] ;
 R[I106] = PANX + OH          ----> ALD2 + NO2                                 @ 3.0E-13 ;
 R[I107] = CXO3 + HO2         ----> 0.80*PACD + 0.20*AACD + 0.20*O3            @ 4.3E-13*EXP(1040./TK) ;
 R[I108] = CXO3 + MEO2        ----> 0.90*ALD2 + 0.90*XO2    + HO2
                                    + 0.10*AACD + 0.10*FORM                    @ 2.0E-12*EXP( 500./TK) ;
 R[I109] = CXO3 + XO2         ----> 0.90*ALD2 + 0.10*AACD                      @ 4.4E-13*EXP(1070./TK) ;
 R[I110] = CXO3 + CXO3        ----> 2.00*ALD2 + 2.00*XO2    + 2.00*HO2         @ 2.9E-12*EXP( 500./TK) ;
 R[I111] = CXO3 + C2O3        ----> MEO2 + XO2 + HO2    + ALD2                 @ 2.9E-12*EXP( 500./TK) ;
 R[I112] = PAR    + OH        ----> 0.87*XO2    + 0.13*XO2N + 0.11*HO2 +
                                    0.06*ALD2 + s_p1*PAR    + 0.76*ROR +
                                    0.05*ALDX                                  @ 8.1E-13 ;
 R[I113] = ROR                ----> 0.96*XO2    + 0.60*ALD2 + 0.94*HO2 +
                                    s_p2*PAR    + 0.04*XO2N + 0.02*ROR +
                                    0.50*ALDX                                  @ 1.0E+15*EXP(-8000./TK) ;
 R[I114] = ROR                ----->          HO2                              @ 1.6E+03 ;
 R[I115] = ROR    + NO2       ----->          NTR                              @ 1.5E-11 ;
 R[I116] = O3P    + OLE       ----> 0.20*ALD2 + 0.30*ALDX + 0.30*HO2 +
                                    0.20*XO2    + 0.20*CO     + 0.20*FORM +
                                    0.01*XO2N + 0.20*PAR    + 0.10*OH     @ 1.0E-11*EXP( -280./TK) ;
 R[I117] = OH     + OLE       ----> 0.80*FORM + 0.33*ALD2 + 0.62*ALDX +
                                    0.80*XO2    + 0.95*HO2    + s_p3*PAR    @ 3.2E-11 ;
 R[I118] = O3     + OLE       ----> 0.18*ALD2 + 0.74*FORM + 0.32*ALDX +
                                    0.22*XO2    + 0.10*OH     + 0.33*CO +
                                    0.44*HO2 + s_p4*PAR                        @ 6.5E-15*EXP(-1900./TK) ;
 R[I119] = NO3    + OLE       ----> NO2 + FORM + 0.91*XO2 + 0.09*XO2N +
                                    0.56*ALDX    + 0.35*ALD2 + s_p4*PAR @ 7.0E-13*EXP(-2160./TK) ;
 R[I120] = O3P    + ETH       ----> FORM + 1.70*HO2 + CO + 0.70*XO2 +
                                    0.30*OH                                    @ 1.04E-11*EXP(-792./TK) ;
 R[I121] = OH     + ETH       -M--> XO2 + 1.56*FORM + 0.22*ALDX + HO2 @ TROE(1.0E-28*T_300^-0.8,
                                                                                   8.8E-12*T_300^0.0,
                                                                                   b[M], 0.6) ;
 R[I122] = O3     + ETH       ----> FORM + 0.63*CO    + 0.13*HO2
                                        + 0.13*OH    + 0.37*FACD               @ 1.2E-14*EXP(-2630./TK) ;
 R[I123] = NO3    + ETH       ----> NO2 + XO2 + 2.0*FORM                       @ 3.3E-12*EXP(-2880./TK) ;
 R[I124] = IOLE + O3P         ----> 1.24*ALD2 + 0.66*ALDX + 0.10*HO2 +
                                    0.10*XO2    + 0.10*CO     + 0.10*PAR    @ 2.3E-11 ;
 R[I125] = IOLE + OH          ----> 1.30*ALD2 + 0.70*ALDX + HO2 + XO2 @ 1.0E-11*EXP(    550./TK) ;
 R[I126] = IOLE + O3          ----> 0.65*ALD2 + 0.35*ALDX + 0.25*FORM +
                                    0.25*CO     + 0.50*O3P    + 0.50*OH +
                                    0.50*HO2                                   @ 8.4E-15*EXP(-1100./TK) ;
 R[I127] = IOLE + NO3         ----> 1.18*ALD2 + 0.64*ALDX + HO2 + NO2 @ 9.6E-13*EXP( -270./TK) ;
 R[I128] = TOL    + OH        ----> 0.44*HO2    + 0.08*XO2    + 0.36*CRES +
                                    0.56*TO2                                   @ 1.8E-12*EXP(    355./TK) ;
 R[I129] = TO2    + NO        ----> 0.90*NO2    + 0.90*HO2    + 0.90*OPEN +
                                    0.10*NTR                                   @ 8.1E-12 ;
```

```
R[I130] = TO2                  ---->          CRES +          HO2                        @ 4.2 ;
R[I131] = OH     + CRES         ----> 0.40*CRO    + 0.60*XO2     + 0.60*HO2 +
                                      0.30*OPEN                                       @ 4.1E-11 ;
R[I132] = CRES + NO3           ---->          CRO    +          HNO3                    @ 2.2E-11 ;
R[I133] = CRO    + NO2         ---->          NTR                                    @ 1.4E-11 ;
R[I134] = CRO    + HO2         ---->          CRES                                   @ 5.5E-12 ;
R[I135] = OPEN                 -hv->          C2O3 + HO2 + CO                        @ j[FORM_to_HO2]*kOPEN_R ;
R[I136] = OPEN + OH            ----> XO2 + 2*CO + 2*HO2 + C2O3 + FORM    @ 3.0E-11 ;
R[I137] = OPEN + O3            ----> 0.03*ALDX + 0.62*C2O3 + 0.70*FORM +
                                      0.03*XO2    + 0.69*CO     + 0.08*OH +
                                      0.76*HO2    + 0.20*MGLY                        @ 5.4E-17*EXP( -500./TK) ;
R[I138] = OH     + XYL         ----> 0.70*HO2    + 0.50*XO2    + 0.20*CRES +
                                      0.80*MGLY + 1.10*PAR    + 0.30*TO2    @ 1.7E-11*EXP(    116./TK) ;
R[I139] = OH     + MGLY          ---->          XO2    +          C2O3                   @ 1.7E-11 ;
R[I140] = MGLY                   -hv->          C2O3 +          HO2    +          CO     @ j[MGLY_to_HO2] ;
R[I141] = O3P    + ISOP        ----> 0.75*ISPD + 0.50*FORM + 0.25*XO2 +
                                      0.25*HO2    + 0.25*CXO3 + 0.25*PAR    @ 3.6E-11 ;
R[I142] = OH     + ISOP         ----> 0.991*XO2 + 0.912*ISPD + 0.629*FORM +
                                      0.912*HO2 + 0.088*XO2N                         @ 2.54E-11*EXP(407.6/TK);
R[I143] = O3     + ISOP        ----> 0.65*ISPD + 0.60*FORM + 0.20*XO2 +
                                     0.066*HO2    + 0.266*OH    + 0.20*CXO3 +
                                      0.15*ALDX + 0.35*PAR    + 0.066*CO    @ 7.86E-15*EXP(-1912./TK);
R[I144] = NO3    + ISOP         ----> 0.20*ISPD + 0.80*NTR    + XO2 +
                                      0.80*HO2    + 0.20*NO2    + 0.80*ALDX +
                                      2.40*PAR                                       @ 3.03E-12*EXP( -448./TK);
R[I145] = OH     + ISPD         ----> 1.565*PAR + 0.167*FORM + 0.713*XO2 +
                                     0.503*HO2    + 0.334*CO     + 0.168*MGLY +
                                      0.252*ALD2 + 0.21*C2O3    + 0.25*CXO3 +
                                      0.12*ALDX                                      @ 3.36E-11 ;
R[I146] = O3     + ISPD        ----> 0.114*C2O3 + 0.15*FORM + 0.85*MGLY +
                                      0.154*HO2 + 0.268*OH     + 0.064*XO2 +
                                      0.02*ALD2 + 0.36*PAR     + 0.225*CO @ 7.1E-18 ;
R[I147] = NO3    + ISPD         ----> 0.357*ALDX + 0.282*FORM + 1.282*PAR +
                                     0.925*HO2    + 0.643*CO     + 0.85*NTR +
                                      0.075*CXO3 + 0.15*HNO3 + 0.075*XO2 @ 1.0E-15 ;
R[I148] = ISPD                 -hv-> 0.333*CO    + 0.067*ALD2 + 0.90*FORM +
                                     0.832*PAR    + 1.033*HO2    + 0.70*XO2 +
                                      0.967*C2O3                                     @ 3.6E-3*j[ACRO_to_RO2];
R[I149] = TERP + O3P           ----> 0.15*ALDX + 5.12*PAR                  @ 3.6E-11 ;
R[I150] = TERP + OH            ----> 0.75*HO2    + 1.25*XO2     + 0.25*XO2N +
                                      0.28*FORM + 0.47*ALDX    + 1.66*PAR @ 1.5E-11*EXP(    449./TK) ;
R[I151] = TERP + O3            ----> 0.57*OH     + 0.07*HO2     + 0.76*XO2 +
                                     0.18*XO2N + 0.24*FORM    + 0.39*CXO3 +
                                      7.00*PAR    + 0.21*ALDX    + 0.001*CO @ 1.2E-15*EXP( -821./TK) ;
R[I152] = TERP + NO3           ----> 0.47*NO2    + 0.28*HO2     + 1.03*XO2 +
                                      0.25*XO2N + 0.47*ALDX    + 0.53*NTR @ 3.7E-12*EXP(    175./TK) ;
R[I153] = SO2    + OH           -M--->          SULF +          HO2                    @ TROE(3.0E-31*T_300^-3.3,
                                                                                             1.5E-12*T_300^0.0,
                                                                                             b[M], 0.6) ;
R[I154] = OH     + ETOH          ---->          HO2    + 0.90*ALD2    + 0.05*ALDX
                                      + 0.10*FORM + 0.10*XO2                         @ 6.9E-12*EXP( -230./TK) ;
R[I155] = OH     + ETHA          ----> 0.991*ALD2 + 0.991*XO2 + 0.009*XO2N
                                      + HO2                                          @ 8.7E-12*EXP(-1070./TK) ;
R[I156] = NO2    + ISOP         ----> 0.80*NTR + 0.80*HO2 + 0.20*NO + XO2
                                      + 0.80*ALDX + 2.40*PAR + 0.20*ISPD    @ 1.5E-19 ;

R[I157] = NR                   ---->          NR                                     @ 0.0001 ;


#end
```

```
// end of principle mechanism file.
```

==========

CB05-Ua:

Note: The reactions other than R128, R129 and R130 are the same as in CB05-Base.

```
R[I128] = TOL    + OH              ----> 0.44*HO2    + 0.08*XO2    + 0.36*CRES +
                                         0.56*TO2                                    @ 1.8E-12*EXP(    355./TK) ;
                 //[Update in I129] rate constant = 8.1E-12 => 2.7E-12*EXP(    360./TK)
R[I129] = TO2    + NO              ----> 0.90*NO2    + 0.90*HO2    + 0.90*OPEN +
                                         0.10*NTR                                    @ 2.7E-12*EXP(    360./TK) ;
                 //[Update in I130] {TO2 => CRES + HO2 @ 4.2} to {TO2 + HO2 => @ 1.9E-13*EXP( 1300./TK) }
R[I130] = TO2    + HO2             ----> TO2HO2                                      @ 1.9E-13*EXP( 1300./TK)
;
```

==========

CB05-Ub:

Note: The reactions other than R128, R129 and R130 are the same as in CB05-Base.

```
R[I128] = TOL    + OH              ----> 0.26*HO2    + 0.08*XO2    + 0.18*CRES +
                                         0.74*TO2                                    @ 1.8E-12*EXP(    355./TK) ;
                 //[Update in I129] rate constant: 8.1E-12 => 2.7E-12*EXP(    360./TK)
R[I129] = TO2    + NO              ----> 0.90*NO2    + 0.90*HO2    + 0.90*OPEN +
                                         0.10*NTR                                    @ 2.7E-12*EXP(    360./TK) ;
                 //[Update in I130] {TO2 => CRES + HO2 @ 4.2} to {TO2 + HO2 => @ 0.0 }
R[I130] = TO2    + HO2             ----> TO2HO2                                    @ 0.0*EXP( 1300./TK) ;
```

==========

CB05-UNClite:

Note: The reactions of CB05-Base other than Reactions R128 – R137 are also used in CB05-UNClite and will not be repeated here.

```
//              Start: Proposed update [UNClite]
R[TL1] = TOL + OH ----> 0.280*HO2 + 0.10*XO2 + 0.180*CRES +
                        0.650*TO2 + 0.072*OH                    @ 1.80E-12*EXP(355./TK) ;
 R[TL2] = TO2 + NO ----> 0.860*NO2 + 1.200*HO2 + 0.860*OPEN +
                        0.140*NTR + 0.520*MGLY + 0.336*FORM +
                        0.336*CO                                 @ 2.70E-12*EXP(360./TK) ;
 R[TL3] = TO2 + HO2 ---->                                       @ 1.90E-13*EXP(1300./TK) ;
 R[TL4] = OH + CRES ----> 0.060*CRO + 0.120*XO2 + 1.120*HO2 +
                        0.130*OPEN + 0.732*CAT1 + 0.06*CO +
                        0.06*XO2N + 0.06*FORM                    @ 1.70E-12*EXP(950./TK) ;
 R[TL5] = CRES + NO3 ----> 0.300*CRO + HNO3 + 0.600*XO2 +
                        0.360*HO2 + 0.48*ALDX + 0.24*FORM + 0.24*MGLY +
                        0.12*OPEN + 0.10*XO2N + 0.24*CO          @ 1.40E-11 ;
 R[TL6] = CRO + NO2 ----> CRON                  @ 2.10E-12 ;
 R[TL7] = CRO + HO2 ----> CRES                  @ 5.50E-12 ;
 R[TL8] = CRON + OH ----> CRNO                  @ 1.53E-12 ;

//TL9: UNClite uses 3.80E-12 instead of 3.13E-13 of Hu et al. (2007) but from SAPRC-99.
```

```
//Communication with Dr. Gary Z. Whitten on 21 August 2008.
  R[TL9] = CRON + NO3 ----> CRNO + HNO3        @ 3.80E-12 ;
R[TL10] = CRNO + NO2 ----> 2.000*NTR           @ 2.10E-12 ;
R[TL11] = CRNO + O3 ----> CRN2                 @ 2.86E-13 ;
R[TL12] = CRN2 + NO ----> CRNO + NO2           @ 2.54E-12*EXP(360./TK) ;
R[TL13] = CRN2 + HO2 ----> CRPX                @ 2.40E-13*EXP(1300./TK);
R[TL14] = CRPX      ----> CRNO + OH              @ 0.01*j[NO2_to_O3P] ;

//TL15: UNClite used 3.00E-12*Exp(190/T) instead of 1.9E-12*Exp(190/T) in Hu et al. (2007)
// 3.00E-12*Exp(190/T) => 1.9E-12*Exp(190/T)
R[TL15] = CRPX + OH ----> CRN2                 @ 1.90E-12*EXP(190./TK) ;
R[TL16] = OPEN      -hv-> OPO3 + HO2 + CO      @ 0.04*j[NO2_to_O3P] ;
R[TL17] = OPEN + OH ----> 0.6*OPO3 + 0.4*CAO2  @ 4.40E-11 ;
R[TL18] = OPEN + O3 ----> 0.03*ALDX + 0.62*OPO3 + 0.70*FORM +
                          0.76*HO2 + 0.69*CO + 0.20*MGLY +
                          0.08*OH + 0.03*XO2   @ 5.40E-17*EXP(-500./TK) ;
R[TL19] = OPEN + NO3 ----> OPO3 + HNO3         @ 3.80E-12 ;

//TL20: UNClite used 7.00E-11 instead of 6.98E-10; 7.00E-11 => 6.98E-10 (21 Aug 08)
// Return to 7.00E-11 according to Dr. Gary Z. Whitten's comment      (7 Sep 08)
R[TL20] = CAT1 + OH ----> CAO2                 @ 7.00E-11 ;
R[TL21] = CAT1 + NO3 ----> CRO + HNO3          @ 1.70E-10 ;
R[TL22] = CAO2 + NO ----> 0.86*NO2 + 1.2*HO2 + 0.344*FORM +
                          0.344*CO + 0.14*NTR  @ 2.54E-12*EXP(360./TK) ;
R[TL23] = CAO2 + HO2 ----> CRPX                @ 2.40E-13*EXP(1300./TK) ;

//TL24: Add HO2 as a product in TL24 (7 Sep 08)
// OPO3 + NO = NO2 + XO2 + ALDX => OPO3 + NO = NO2 + XO2 + HO2 + ALDX (7 Sep 08)
R[TL24] = OPO3 + NO ----> NO2 + XO2 + HO2 + ALDX   @ 1.00E-11 ;
R[TL25] = OPO3 + NO2 ----> OPAN                @ 1.00E-11 ;
R[TL26] = OPAN      ----> OPO3 + NO2           @ 1.00E-04 ;
//            End: Proposed update [UNClite]
```

==========

CB05-Dinitro:

Note: The reactions of CB05-Base other than Reactions R128 – R134 are also used in CB05-Dinitro and will not be repeated here.

```
//            Start: Proposed update [Dinitro]
  R[TL1] = TOL + OH ----> 0.260*HO2 + 0.080*XO2 + 0.180*CRES +
                          0.740*TO2                                  @ 1.80E-12*EXP(355./TK) ;
  R[TL2] = TO2 + NO ----> 0.900*NO2 + 0.900*HO2 + 0.900*OPEN +
                          0.100*NTR                                  @ 2.70E-12*EXP(360./TK) ;
  R[TL3] = TO2 + HO2 ---->                                           @ 1.90E-13*EXP(1300./TK) ;
  R[TL4] = OH + CRES ----> 0.800*CRO + 0.200*XO2 + 0.200*HO2 + 0.100*OPEN @ 4.10E-11 ;
  R[TL5] = CRES + NO3 ----> CRO + HNO3                               @ 2.20E-11 ;
  R[TL6] = CRO + NO2 ----> CRON                                      @ 2.10E-12 ;
  R[TL7] = CRO + HO2 ----> CRES                                      @ 5.50E-12 ;
  R[TL8] = CRON + OH ----> 0.800*CRNO + 0.200*XO2 + 0.200*HO2 + 0.100*OPEN @ 1.53E-12 ;
  R[TL9] = CRON + NO3 ----> CRNO + HNO3                              @ 3.80E-12 ;
R[TL10] = CRNO + NO2 ----> 2.000*NTR                                 @ 2.10E-12 ;
R[TL11] = CRNO + HO2 ----> CRON                                      @ 5.50E-12 ;
//            End: Proposed update [Dinitro]
```

A3. AUXILIARY MECHANISMS USED IN ENVIRONMENTAL CHAMBER SIMULATIONS

A3.1. Auxiliary Mechanism Used in the SAPRC Software

Carter and Lurmann (1991) argued that *using wall parameters best describing all relevant chamber characterization experiments without tuning the parameters to make fits better for individual experiments* is a consistent and practicable approach. On the other hand, there is *chamber run-to-run variability* (Carter et al., 2005). Therefore, the 31 UCR chamber experiments in the SAPRC dataset are classified into multiple groups, and each group is assigned a characterization file which defines parameters in the auxiliary mechanism (Carter, 2000 and 2009). In this way, a limited number of characterization files (around 10) served those 31 experiments used in this study (Table S2). Different values of parameters were used for some reactions in the auxiliary mechanism in simulating the 31 toluene experiments in the SARPC dataset. Those different sets of parameter values were defined in their characterization files (*.CHR or *.IN) and INP-type input files (*.INP).

References:

Carter, W.P.L., 2000. Documentation of the SAPRC-99 chemical mechanism for VOC reactivity assessment, Report to the California Air Resources Board, Contracts 92-329 and 95-308. (http://www.engr.ucr.edu/~carter/absts.htm#saprc99)

Carter, W.P.L., 2009. Development of the SAPRC-07 chemical mechanism and updated ozone reactivity scales. Final Report to the California Air Resources Board Contract No. 03-318. (http://www.engr.ucr.edu/~carter/SAPRC/)

Carter, W.P.L., Cocker, D.R., Fitz, D.R., Malkina, I.L., Bumiller, K., Sauer, C.G., Pisano, J.T., Bufalino, C., and Song, C., 2005. A new environmental chamber for evaluation of gas-phase chemical mechanisms and secondary aerosol formation. Atmospheric Environment, 39, 7768-7788.

Carter, W.P.L., Lurmann, F.W., 1991. Evaluation of a detailed gas-phase atmospheric reaction mechanism using environmental chamber data. Atmospheric Environment 25A, 2771-2806.

Codes for the auxiliary mechanism in the format compatible with the SAPRC software*:

*Source: CB05WALL.RXN in the SAPFC software package

Summary of the auxiliary mechanism without information about the rate constants and other rate-related parameters

```
REACTIONS)     K          (         A          EA        B     )
 O3W )    0.000E+00 (    0.000E+00    0.00    0.000)    O3 =
 HPW )    0.000E+00 (    0.000E+00    0.00    0.000)    H2O2 =
 N25I)    0.000E+00 (    0.000E+00    0.00    0.000)    N2O5 = #2 NOX-WALL
 N25S)    0.000E+00 (    0.000E+00    0.00    0.000)    N2O5 + H2O = #2 NOX-WALL
 NAW )    0.000E+00 (    0.000E+00    0.00    0.000)    HNO3 = NOX-WALL
 NO2W)    0.000E+00 (    0.000E+00    0.00    0.000)    NO2 = #YHONO HONO + #1-YHONO NOX-WALL
 NONO)    0.000E+00 (    0.000E+00    0.00    0.000)    NO + NO2 + H2O = #2 HONO
 RSS )                      K SAME AS RXN 1              NO2 + HV + #RS-S = #.5 HONO + #.5 NOX-WALL
 RS    )  0.000E+00 (    0.000E+00    0.00    0.000)    HV + #NO2 + #RS-FAC = OH
 RSI )                             K SAME AS RXN 1              HV + #RS-I + #RS-FAC = OH
 RSI1)                      K SAME AS RXN 1              HV + #T290 + #RS-I1F = OH
 RSI2)                      K SAME AS RXN 1              HV + #T300 + #RS-I2F = OH
 RSI3)                      K SAME AS RXN 1              HV + #T310 + #RS-I3F = OH
 RSI4)                      K SAME AS RXN 1              HV + #T320 + #RS-I4F = OH
 RN    )  0.000E+00 (    0.000E+00    0.00    0.000)    HV + #NO2 + #RS-FAC = HONO + #-1 NOX-WALL
 RNI )                      K SAME AS RXN 1              HV + #RN-I + #RS-FAC = HONO + #-1 NOX-WALL
 RNI1)                      K SAME AS RXN 1              HV + #T290 + #RN-I1F = HONO + #-1 NOX-WALL
 RNI2)                      K SAME AS RXN 1              HV + #T300 + #RN-I2F = HONO + #-1 NOX-WALL
 RNI3)                      K SAME AS RXN 1              HV + #T310 + #RN-I3F = HONO + #-1 NOX-WALL
 RNI4)                      K SAME AS RXN 1              HV + #T320 + #RN-I4F = HONO + #-1 NOX-WALL
 RS2 )    0.000E+00 (    0.000E+00    0.00    0.000)    NO2 + NO2 + HV = HONO + NOX-WALL
 ONO2)                      K SAME AS RXN 1              HV + #E-NO2/K1 = NO2 + #-1 NOX-WALL
 1NO2)                      K SAME AS RXN 1              HV + #T290 + #E1NO2/K1 = NO2 + #-1 NOX-WALL
 2NO2)                      K SAME AS RXN 1              HV + #T300 + #E2NO2/K1 = NO2 + #-1 NOX-WALL
 3NO2)                      K SAME AS RXN 1              HV + #T310 + #E3NO2/K1 = NO2 + #-1 NOX-WALL
 4NO2)                      K SAME AS RXN 1              HV + #T320 + #E4NO2/K1 = NO2 + #-1 NOX-WALL
 OALD)                      K SAME AS RXN 1              HV + #E-ALD/K1 = FORM
 OHON)                      K SAME AS RXN 1              HV + #EHONO/K1 = HONO + #-1 NOX-WALL
 XSHC)    0.000E+00 (    0.000E+00    0.00    0.000)    OH = HO2
 WVOC)                        K SAME AS RXN 1                    HV + #EVOC/K1 = WALLVOC
 WVOH) 0.000E+00 (    0.000E+00    0.00    0.000)    WALLVOC + OH = HO2 + #WVA1 FORM
 EVW )    1.000E+00 (    1.000E+00    0.00    0.000)       E.WVOC = WALLVOC
 EA1 )    1.000E+00 (    1.000E+00    0.00    0.000)    E.HCHO = FORM
 OHW )    0.000E+00 (    0.000E+00    0.00    0.000)    OH =
 HO2W)    0.000E+00 (    0.000E+00    0.00    0.000)     HO2 =
```

CB05WALL.RXN:

```
! ========================Start: CB05WALL.RXN
!-------------------------------------------------------------------------------
```

```
!       CHAMBER DEPENDENT REACTIONS, WITHOUT ADJUSTABLE RADICAL SOURCE
!       FOR CMAQ CB4
!
!       Similar to standard SAPRC-90 version except that option to
!       represent both radical source and NOx offgasing as HONO offgasing
!       is added.
!
!       Default:    No wall effects
!
!
!       Coefficients and Rate Constants Used to Define Chamber Effects:
!
!               RS=FAC              ...     (Coefficient.)    Factor to multiply RS, RS-I,
!                                   and RS-N parameters to adjust radical source
!                                   for all chambers.
!                                   DEFAULT OF 1.5 REMOVES BIAS IN RS SIMULATIONS
!                                   FOR RUNS WHERE RS PARAMETERS ADJUSTED TO FIT
SAPRC99
.COE
RS-FAC 1.5
!
!               RS-I        ...   (Coefficient.)    Intersept of the "radical
!                                   source" regression of OH input rate vs NO2.
!                                   Ratio of Radical input rate to NO2 photolysis
!                                   rate when NO2 not present.    Default = 0.
!
!               RS-I1, RS-I2, RS-I3 ... Values of RS-I at 290, 300, 310
!
!               RN-I        ...   (Coefficient.)    Ratio of HONO input rate
!                                   to NO2 photolysis rate.
!
!               RN-I1, RN-I2, RN-I3 ... Values of RN-I at 290, 300, 310
!
!               RS-S        ...     (Coefficent.)    Slope of the "radical source"
!                                   regression of the ratio of OH input rate to
!                                   the NO2 photolysis rate vs NO2.    Default = 0.
!
!               HONO-F              ...    Ratio of initial HONO to initial NO2.    Default
!                                   = 0.
!
!               E-NO2/K1    ...  Ratio of NO2 offgasing rate to the NO2
!                                   photolysis rate.    Default = 0.
!
!               E-ALD/K1    ...  Ratio of HCHO offgasing rate to the NO2
!                                   photolysis rate.    Default = 0.
!
!               EHONO/K1    ...    Ratio of HONO offgasing rate to the NO2
!                                   photolysis rate.    Default = 0.
!
!               EVOC/K1             ...     Ratio of offgasing of reactive VOCs to the NO2
!                                   photolysis rate.    Default = 0.
!                                   (Offgased VOC parameters: K(WVOH) = OH rate
!                                   constant, WVA1 = formaldehyde yield in OH rxn.
!
```

```
!                   O3W         ...   Ozone wall loss rate constant.
!
!                   HPW         ...   H2O2 wall loss rate constant.
!
!                   N25I        ...   Intercept of regression of N2O5 wall loss
!                                     rate.  Unimolecular loss of N2O5 to the
!                                     walls in the absense of H2O.
!
!                   N25S        ...   Slope of regression of N2O5 wall loss
!                                     rate.  Bimolecular rate constant for
!                                     N2O5 + H2O -> loss of N2O5 to wall.
!
!                   NAW         ...   Unimolecular rate constant for HNO3 going
!                                     to the walls.  Doesn't affect any of the
!                                     chemistry except the HNO3 concentration.
!
!                   NO2W        ...   Unimolecular rate constant for NO2
!                                     wall hydrolysis and loss.
!
!                   YHONO       ...   Yield of HONO in the unimolecular reaction
!                                     (or hydrolysis) of NO2 on the walls.  Default
!                                     = 0.
!
!                   XSHC        ...   "Excess" hydrocarbon reactivity (units of
!                                     min-1).  [HC] x k(OH+HC) for "contaminant"
!                                     organics.  Unimolecular rate constant
!                                     converting HO to HO2.
!
!         Buildup Species Used for Accounting Purposes:
!
!                   NOX-WALL    ...   NOx absorbed on walls.  Used in part to keep
!                                     track of N-balance.  Can be negative if wall
!                                     off-gasing occurs at a greater rate than NOx
!                                     going to wall.
!
!         Dark Reactions.
!
.UNITS=OK
.RXN
O3W)    0.0             ;O3 =
HPW)    0.0             ;H2O2 =
N25I)   0.0             ;N2O5 = #2 NOX-WALL
N25S)   0.0             ;N2O5 + H2O = #2 NOX-WALL
NAW)    0.0             ;HNO3 = NOX-WALL
NO2W)           0.0             ;NO2 = #YHONO HONO + #1-YHONO NOX-WALL
NONO2W)         0.0             ;NO + NO2 + H2O = #2 HONO
.COE
YHONO           0.0
!
!         This code defines NOX-WALL as the sink for Nitrogen which does not
!         appear as HONO when NO2 goes to the walls.
!
.INS INIT
'1-YHONO' = 1.0-'YHONO'
```

```
!
!       Light Reactions
.COE
RS-I    0.0
RS-S    0.0
RS-I1   0.0
RS-I2   0.0
RS-I3   0.0
RS-I4   0.0
!
RN-I    0.0
RN-I1   0.0
RN-I2   0.0
RN-I3   0.0
RN-I4   0.0
.VTEMP 4
        290.0, 300.0, 310.0, 320.0
.VTCO
T290    1.0     0.0     0.0     0.0
T300    0.0     1.0     0.0     0.0
T310    0.0     0.0     1.0     0.0
T320    0.0     0.0     0.0     1.0
.RXN
!
RSS)    SAMEK 1                 ;NO2 + HV + #RS-S = #.5 HONO + #.5 NOX-WALL
!
RS)     0.0             ;HV + #NO2 + #RS-FAC = OH
RSI)    SAMEK 1                 ;HV + #RS-I + #RS-FAC = OH
RSI1)   SAMEK 1                 ;HV + #T290 + #RS-I1F = OH
RSI2)   SAMEK 1                 ;HV + #T300 + #RS-I2F = OH
RSI3)   SAMEK 1                 ;HV + #T310 + #RS-I3F = OH
RSI4)   SAMEK 1                 ;HV + #T320 + #RS-I4F = OH
!
RN)     0.0             ;HV + #NO2 + #RS-FAC = HONO + #-1 NOX-WALL
RNI)    SAMEK 1                 ;HV + #RN-I + #RS-FAC = HONO + #-1 NOX-WALL
RNI1)   SAMEK 1                 ;HV + #T290 + #RN-I1F = HONO + #-1 NOX-WALL
RNI2)   SAMEK 1                 ;HV + #T300 + #RN-I2F = HONO + #-1 NOX-WALL
RNI3)   SAMEK 1                 ;HV + #T310 + #RN-I3F = HONO + #-1 NOX-WALL
RNI4)   SAMEK 1                 ;HV + #T320 + #RN-I4F = HONO + #-1 NOX-WALL
!
RS2)    0.0             ;NO2 + NO2 + HV = HONO + NOX-WALL
!
.INS DIFF
'RS-I1F' = 'RS-I1' * 'RS-FAC'
'RS-I2F' = 'RS-I2' * 'RS-FAC'
'RS-I3F' = 'RS-I3' * 'RS-FAC'
'RS-I4F' = 'RS-I4' * 'RS-FAC'
'RS-I1F' = 'RN-I1' * 'RS-FAC'
'RN-I2F' = 'RN-I2' * 'RS-FAC'
'RN-I3F' = 'RN-I3' * 'RS-FAC'
'RN-I4F' = 'RN-I4' * 'RS-FAC'
!
!       Wall Off-Gasing
.COE
```

```
E-NO2/K1 0.0
E1NO2/K1 0.0
E2NO2/K1 0.0
E3NO2/K1 0.0
E4NO2/K1 0.0
!
E-ALD/K1 0.0
EHONO/K1 0.0
.RXN
ONO2)  SAMEK 1                  ;HV + #E-NO2/K1 = NO2 + #-1 NOX-WALL
1NO2)  SAMEK 1                  ;HV + #T290 + #E1NO2/K1 = NO2 + #-1 NOX-WALL
2NO2)  SAMEK 1                  ;HV + #T300 + #E2NO2/K1 = NO2 + #-1 NOX-WALL
3NO2)  SAMEK 1                  ;HV + #T310 + #E3NO2/K1 = NO2 + #-1 NOX-WALL
4NO2)  SAMEK 1                  ;HV + #T320 + #E4NO2/K1 = NO2 + #-1 NOX-WALL
!
OALD)  SAMEK 1                  ;HV + #E-ALD/K1 = FORM
OHON)  SAMEK 1                  ;HV + #EHONO/K1 = HONO + #-1 NOX-WALL
!
!       Define initial HONO as fraction of initial NO2, or as absolute HONO
.COE
HONO-F          0.0
HONO-I0.0
!
!       This code multiplies the initial concentration of NO2 by HONO-F
!       and adds it to the initial concentration of HONO.    Subtracted
!       from initial NO2 (HONO interference on NOx analyzer).
!
.INS INIT
"C HONO" = "C HONO" + ("C NO2"*'HONO-F')
"C NO2" = AMAX1("C NO2" - ("C NO2"*'HONO-F'),0.0)
IF ("C NO2".GT.'HONO-I') THEN
        "C NO2" = "C NO2" - 'HONO-I'
        "C HONO" = "C HONO" + 'HONO-I'
ELSE
        "C HONO" = "C HONO" + "C NO2"
        "C NO2" = 0.0
ENDIF
!
!       Background HC contaminants.
.RXN
XSHC)  0.0              ;OH = HO2
WVOC) SAMEK 1                   ;HV + #EVOC/K1 = WALLVOC
WVOH) 0.0               ;WALLVOC + OH = HO2 + #WVA1 FORM
EVW)   1.0              ;E.WVOC = WALLVOC
EA1)   1.0              ;E.HCHO = FORM
.CON
E.WVOC          0.0
E.HCHO          0.0
.COE
WVA1   0.0
!
!       Radical Wall Loss
.RXN
OHW)   0.0              ;OH =
```

```
HO2W)  0.0                    ;HO2 =
!
!           END OF FILE
! ========================End: CB05WALL.RXN
```

Table A-6. A summary of auxiliary mechanism reactions actually used for 31 toluene experiments in the SAPRC dataset.*

Class	No.	Rxn ID	O3W	N25I	N25S	NAW	NO2W	RSS	RSI2	RSI3	RSI4	RN	RNI	ONO2	1NO2	2NO2	3NO2	4NO2	OALD	XSHC
Low -NOx	1	EPA066B	X	X			X						X						X	
	2	EPA074A	X	X			X						X						X	
	3	EPA077A	X	X			X						X						X	
	4	EPA210A	X	X			X						X						X	
	5	EPA210B	X	X			X						X						X	
	6	EPA443A	X	X			X						X						X	
	7	EPA443B	X	X			X						X						X	
	8	EPA066A	X	X			X						X						X	
	9	EPA072A	X	X			X						X						X	
	10	EPA072B	X	X			X						X						X	
	11	EAP074B	X	X			X						X						X	
	12	EPA077B	X	X			X						X						X	
Mid -NOx	1	CTC026	X	X	X		X						X							X
	2	CTC034	X	X	X		X						X							X
	3	CTC048	X	X	X		X						X							X
	4	XTC106	X	X	X		X					X								X
	5	EC264	X	X	X		X	X					X	X						
	6	EC266	X	X	X		X	X					X	X						
	7	EC271	X	X	X		X	X					X	X						
	8	EC273	X	X	X		X	X					X	X						
	9	EC293	X	X	X		X	X					X	X						
	10	OTC299A	X	X	X		X					X								X
	11	OTC300B	X	X	X		X					X								X
High -NOx	1	EC269	X	X	X		X	X					X	X						
	2	EC270	X	X	X		X	X					X	X						
	3	EC327	X	X	X		X	X					X	X						
	4	EC340	X	X	X		X	X					X	X						
	5	OTC300A	X	X	X		X					X								X

Low O_3/NOx	1	CTC065	X	X	X	X		X		X
	2	CTC079	X	X	X	X		X		X
	3	OTC299B	X	X	X	X	X			X

*Note: reactions having non-zero reaction rates are marked with "x; the reaction rate constants are set to be equal to the photolysis frequency of NO_2 ($J(NO_2)$) in the auxiliary mechanism used in the SAPRC software for following reactions whose reaction ID's are RSS, RSI, RSI1, RSI2, RSI3, RSI4, RNI, RNI1, RNI2, RSI3, RNI4, ONO2, 1NO2, 2NO2, 3NO2, 4NO2, OALD, OHON, WVOC.

Table A-7. Reaction rate parameters in the auxiliary mechanism used for 12 low-NOx toluene experiments in the SAPRC dataset.

No.	1	2	3	4	5	6	7	8	9	10	11	12
Exp ID	EPA066B	EPA074A	EPA077A	EPA210A	EPA210B	EPA443A	EPA443B	EPA066A	EPA072A	EPA072B	EAP074B	EPA077B
Reaction rate constants (k(rxn ID))												
k(O3W)	1.08E-04	1.08E-04	1.08E-04	1.08E-04	1.08E-04	1.08E-04	1.08E-04	1.08E-04	1.08E-04	1.08E-04	1.08E-04	1.08E-04
k(N25I)	2.80E-03	2.80E-03	2.80E-03	2.80E-03	2.80E-03	2.80E-03	2.80E-03	2.80E-03	2.80E-03	2.80E-03	2.80E-03	2.80E-03
k(NO2W)	1.60E-04	1.60E-04	1.60E-04	1.60E-04	1.60E-04	1.60E-04	1.60E-04	1.60E-04	1.60E-04	1.60E-04	1.60E-04	1.60E-04
Other parameters												
RS-FAC	1.5	1.5	1.5	1.5	1.5	1.5	1.5	1.5	1.5	1.5	1.5	1.5
HV	1	1	1	1	1	1	1	1	1 or 0	1 or 0	1	1
RN-I	5.00E-06	5.00E-06	5.00E-06	1.28E-05	8.50E-06	5.00E-06	5.00E-06	5.00E-06	5.00E-06	5.00E-06	5.00E-06	5.00E-06
E-ALD/K1	1.00E-05	1.00E-05	1.00E-05	1.00E-05	1.00E-05	1.00E-05	1.00E-05	1.00E-05	1.00E-05	1.00E-05	1.00E-05	1.00E-05
HONO-I	5.00E-05	5.00E-05	5.00E-05	5.00E-05	5.00E-05	5.00E-05	5.00E-05	5.00E-05	5.00E-05	5.00E-05	5.00E-05	5.00E-05
YHONO	0.2	0.2	0.2	0.2	0.2	0.2	0.2	0.2	0.2	0.2	0.2	0.2
DIL	0.0	0.0	0.0	0.0	0.0	0.0	0.0	0.0	0.0	0.0	0.0	0.0
H2O	3.44E+02	3.44E+02	3.44E+02	3.44E+02	3.44E+02	3.44E+02	3.44E+02	3.44E+02	3.45E+02	3.46E+02	3.47E+02	3.48E+02
Measured photolysis frequencies of NO_2 (P(1)) [units: 1/min]												
P(1)	0.26	0.26	0.26	0.26	0.26	0.26	0.26	0.26	0.26	0.26	0.26	0.26

Table A-8. Reaction rate parameters in the auxiliary mechanism used for 11 mid-NOx toluene experiments in the SAPRC dataset.

No.	1	2	3	4	5	6	7	8	9	10	11
Exp ID	CTC026	CTC034	CTC048	XTC106	EC264	EC266	EC271	EC273	EC293	OTC299A	OTC300B
Reaction rate constants (k(rxn ID))											
k(O3W)	8.50E-05	8.50E-05	8.50E-05	1.50E-04	1.10E-03	1.10E-03	1.10E-03	1.10E-03	1.10E-03	1.67E-04	1.67E-04
k(N25I)	2.80E-03	2.80E-03	2.80E-03	2.80E-03	4.65E-03	4.65E-03	4.65E-03	4.65E-03	4.65E-03	2.80E-03	2.80E-03
k(N25S)	1.10E-06	1.10E-06	1.10E-06	1.10E-06	1.82E-06	1.82E-06	1.82E-06	1.82E-06	1.82E-06	1.10E-06	1.10E-06
k(NAW)	0	0	0	0	0	0	0	0	0	0	0
k(NO2W)	1.60E-04	1.60E-04	1.60E-04	1.60E-04	2.80E-04	2.80E-04	2.80E-04	2.80E-04	2.80E-04	1.60E-04	1.60E-04
k(RN)*	0	0	0	**	0	0	0	0	0	***	***
k(XSHC)	2.50E+02	2.50E+02	2.50E+02	2.50E+02	0	0	0	0	0	2.50E+02	2.50E+02
Other parameters											
RS-FAC	1.5	1.5	1.5	1.5	1.5	1.5	1.5	1.5	1.5	1.5	1.5
HV	1	1	1	1	1	1	1	1	1	1.07	1.07
RN-I	6.41E-05	6.41E-05	6.41E-05	0	3.08E-04	3.08E-04	3.08E-04	3.08E-04	3.08E-04	0	0
E-NO2/K1	0.00E+00	0.00E+00	0.00E+00	0	1.00E-04	1.00E-04	1.00E-04	1.00E-04	1.00E-04	0	0
E1NO2/K1	0	0	0	0	0	0	0	0	0	0	0
E2NO2/K1	0	0	0	0	0	0	0	0	0	0	0
E3NO2/K1	0	0	0	0	0	0	0	0	0	0	0
E4NO2/K1	0	0	0	0	0	0	0	0	0	0	0
HONO-F	0.008	0.008	0.008	0.012	0.070	0.070	0.070	0.070	0.070	0.000	0.000
YHONO	0.2	0.2	0.2	0.2	0.5	0.5	0.5	0.5	0.5	0.2	0.2
RS-S	0	0	0	0	1.70E-03	1.70E-03	1.70E-03	1.70E-03	1.70E-03	0	0
RS-I1	0	0	0	0	0	0	0	0	0	0	0
RS-I2	0	0	0	0	0	0	0	0	0	0	0
RS-I3	0	0	0	0	0	0	0	0	0	0	0
RS-I4	0	0	0	0	0	0	0	0	0	0	0
DIL	3.67E-05	6.70E-05	6.70E-05	2.61E-05	3.00E-04	3.00E-04	3.00E-04	3.00E-04	3.00E-04	6.67E-05	6.67E-05
H2O	1.00E+03	1.00E+03	1.00E+03	1.00E+03	1.51E+04	1.48E+04	1.57E+04	1.51E+04	1.54E+04	1.00E+03	1.00E+03
Measured photolysis frequencies of NO_2 (P(1)) [units: 1/min]											

P(1)	0.199	0.198	0.196	0.248	0.339	0.34	0.351	0.395	0.4	variable	variable

*: k (RN) = KP1·Exp(-KP2/(R·Temperature)) where R is the ideal gas constant, R = 0.0019872 kcal·mol^{-1}·K^{-1}. **: KP1 = 5.25E+9, KP2 = 19.3. ***: KP1 = 6.04E+9, KP2 = 19.3

Table A-9. Reaction rate parameters in the auxiliary mechanism used for 5 high-NOx and 3 low O_3/NOx toluene experiments in the SAPRC dataset.

	High-NOx Experiments					Low O_3/NOx Experiments		
No.	1	2	3	4	5	1	2	3
Exp ID	EC269	EC270	EC327	EC340	OTC300A	CTC065	CTC079	OTC299B
Reaction rate conatants (k(rxn ID))								
k(O3W)	1.10E-03	1.10E-03	1.10E-03	1.10E-03	1.67E-04	8.50E-05	8.50E-05	1.67E-04
k(N25I)	4.65E-03	4.65E-03	4.65E-03	4.65E-03	2.80E-03	2.80E-03	2.80E-03	2.80E-03
k(N25S)	1.82E-06	1.82E-06	1.82E-06	1.82E-06	1.10E-06	1.10E-06	1.10E-06	1.10E-06
k(NAW)	0	0	0	0	0	0	0	0
k(NO2W)	2.80E-04	2.80E-04	2.80E-04	2.80E-04	1.60E-04	1.60E-04	1.60E-04	1.60E-04
k(RN)*	0	0	0	0	**	0	0	**
k(XSHC)	0	0	0	0	2.50E+02	2.50E+02	2.50E+02	2.50E+02
Other parameters								
RS-FAC	1.5	1.5	1.5	1.5	1.5	1.5	1.5	1.5
HV	1	1	1	1	1	1	1	1.07
RN-I	3.08E-04	3.08E-04	3.08E-04	3.08E-04	0	6.41E-05	6.41E-05	0
E-NO2/K1	1.00E-04	1.00E-04	1.00E-04	1.00E-04	0	0	0	0
HONO-F	0.070	0.070	0.070	0.070	0.000	0.008	0.000	0.000
YHONO	0.5	0.5	0.5	0.5	0	0.2	0	0
RS-S	1.70E-03	1.70E-03	1.70E-03	1.70E-03	0	0	0	0
RS-I1	0	0	0	0	0	0	0	0
RS-I2	0	0	0	0	0	0	0	0
RS-I3	0	0	0	0	0	0	0	0
RS-I4	0	0	0	0	0	0	0	0

DIL	3.00E-04	3.00E-04	3.00E-04	3.00E-04	2.00E-04	6.70E-05	6.70E-05	6.67E-05
H2O	1.51E+04	1.57E+04	1.51E+04	1.48E+04	variable	1.00E+03	1.00E+03	1.00E+03
Measured photolysis frequencies of NO_2 (P(1)) [units: 1/min]								
P(1)	0.344	0.347	0.414	0.364	variable	0.193	0.191	variable

*: k (RN) = KP1·Exp(-KP2/(R·Temperature)) where R is the ideal gas constant, R = 0.0019872 kcal·mol^{-1}·K^{-1}. **: KP1 = 6.04E+9, KP2 = 19.3.

A3.2. Auxiliary Mechanism Used in the Morpho Software

The same values of reaction parameters were used in the auxiliary mechanism in simulating 7 toluene experiments and 2 experiments for quality assurance (QA) in the Morpho software.

Codes for the auxiliary mechanism in the format compatible with the Morpho software*:

*Source: (1) CB05_UNC.mec, (2) UNCAuxMechGZW.rxn, (3) SampleLine.rxn, (4) UNCAuxPhysStd.rxn, (5), UNCAuxOrgStd.rxn, (6) UNCAuxInorgStd.rxn, (7) UNCAuxNOxWallsGZW.rxn, (8) UNCAuxO3Inj.rxn

Summary of the auxiliary mechanism without information about the rate constants

```
R[entrain1]          ----
>amb_CO*CO+amb_O3*O3+amb_H2*H2+amb_CH4*CH4+amb_BVOC*BVOC+amb_CCl4*CCl4
R[entrain2]          ---->amb_HCHO*FORM
R[BVOC]              OH+BVOC---->0.667*MEO2+0.167*C2O3+0.001*PAR
R[DepoH2O2]          H2O2---->
R[DepoO3]            O3---->
R[DepoN2O5]          N2O5+WH2O---->2.0*WHNO3
R[DepoHNO3f]         HNO3+WH2O---->WHNO3
R[DepoHNO3r]         WHNO3---->HNO3
R[DepoHNO3l]         WHNO3---->
R[DepoHONOf]         HONO+WH2O---->WHONO
R[DepoHONOr]         WHONO---->HONO+WH2O
R[DepoNO2f]          NO2---->WNO2
R[DepoNO2r]          WNO2---->NO2
R[DepoNOf ]          NO---->WNO
R[DepoNOr]           WNO---->NO
R[PNApWH2O]                  PNA+WH2O---->WHNO3
R[WNOpWNO2]                  WNO+WNO2---->2.0*WHONO
R[WH2ON2O5]                  WH2O+N2O5---->2.0*HNO3
R[WHNO3toNO2]                WHNO3---->NO2
```

7 files related to the auxiliary mechanism in the Morpho software:

(1) UNCAuxMechGZW.rxn
(2) UNCAuxPhysStd.rxn
(3) SampleLine.rxn
(4) UNCAuxOrgStd.rxn
(5) UNCAuxInorgStd.rxn
(6) UNCAuxNOxWallsGZW.rxn
(7) UNCAuxO3Inj.rxn

```
//================================Start: (1) UNCAuxMechGZW.rxn
#ifnot    UNCAUXMECHGZW_RXN_
```

```
#define UNCAUXMECHGZW_RXN_

/* Made from
  * $Log: /MorphoModel/Mechanisms/Sources/stdinclude/UNCAuxMech0301.rxn $
  *
  * 1         4/02/01 10:53a Jeffries
  * First version added
  *
  */

/*****************************************************************
*                                                                *
*     UNC Chamber Dependent Reactions                            *
*     Units are molecules/cc/secs ( 3/3/01, HEJ )                *
*                                                                *
*****************************************************************/


// Include the standard chamber Physical Reactions
#include "%STDINC%UNCAuxPhysStd.rxn"


// Include the standard chamber Organic Reactions
#include "%STDINC%UNCAuxOrgStd.rxn"

// Include the standard chamber Inorganic Reactions
#include "%STDINC%UNCAuxInorgStd.rxn"

// Include the current version of NOx + Walls Reactions
#include "%STDINC%UNCAuxNOxWallsGZW.rxn"

#if _DARK_O3_INJ_
// Include the current version of NOx + Walls Reactions
#include "%STDINC%UNCAuxO3Inj.rxn"
#end



#end    // UNCAUXMECHGZW_RXN_
//==================================End: (1) UNCAuxMechGZW.rxn

//==================================Start: (2) UNCAuxPhysStd.rxn
#ifnot    UNCAUXPHYSSTD_RXN_
#define UNCAUXPHYSSTD_RXN_

/*
  * $Log: /MorphoModel/Mechanisms/Sources/stdinclude/UNCAuxPhysStd.rxn $
  *
  * 1         4/02/01 10:53a Jeffries
  * First version added
  *
  */

/*****************************************************************
*                                                                *
*     UNC Chamber Dependent Physical Reactions (Standard)        *
*     Units are molecules/cc/secs ( 3/2/01, HEJ )                *
*                                                                *
*****************************************************************/
```

```
//---------------------------------------------------------------
//                                                        P a r t   O n e
//
// reactants added to chamber via dilution entrainment.
//      Stoichiometric factors are ambient concentrations
//      in ppm; change to mppc via total number density and factors.
SCALARS
  DL,
  mpcc_ppm,
  amb_CO, amb_O3, amb_H2, amb_CH4, amb_BVOC, amb_CCl4;

start DL             = 1.0;                    // used to adjust entrainment
withk mpcc_ppm = 1.0E-06 * b[M];
withk amb_CO      = 0.500 * mpcc_ppm; // i.e., 0.500 ppm CO in ambient air
withk amb_O3      = 0.085 * mpcc_ppm;
withk amb_H2      = 0.580 * mpcc_ppm;
withk amb_CH4     = 1.790 * mpcc_ppm;
withk amb_BVOC = 0.085 * mpcc_ppm;
withk amb_CCl4 = 0.000 * mpcc_ppm;

R[entrain1] = ----> amb_CO      * CO      + amb_O3      * O3      + amb_H2      * H2      +
                              amb_CH4    * CH4    + amb_BVOC * BVOC + amb_CCl4 * CCl4
                                                                    @ DL * p[k1st] ;


//---------------------------------------------------------------
//                                                        P a r t   T w o
//
// add reactions that correct for the sampleline reaction
//      O3 + NO --> NO2 dark titration

#include "%STDINC%SampleLine.rxn"
//==================================End: (2) UNCAuxPhysStd.rxn

//==================================Start: (3) SampleLine.rxn
#ifnot    SAMPLELINE_RXN_
#define SAMPLELINE_RXN_

/*
  * $Log:    $
  *
  */

// ============================================================================
//                                              correct O3, NO, NO2 for sampleline rxns
/*
  * O3 and NO react rapidly enough with each other that the time spend
  * in the chamber sample line (about 16-18 seconds) is sufficient to
  * cause significant changes in the measured concentrations.    This is
  * simulated here as a plug flow reactor between the chamber and the
  * monitors, with a residence time of 18 seconds.    The second order
  * reaction can be solved analytically for the end of the sample line
  * concentrations using
  *    ( 1/(a-b) ) * ln( (b*(a-x))/(a*(b-x)) ) = kt
  */

NAMES
```

```
  BlkSpcIDs += { mO3, mNO, mNO2 }; // these are the measured quantities

start b[mO3]    = n[O3] ;
start b[mNO]    = n[NO] ;
start b[mNO2] = n[NO2];

SCALAR
  X_Rxn       =    0.0,
  E_Loss      =    0.0,
  T_Line      = 18.0,    // SEC == residence time in sample line
  k_T_O3NO =    0.0;


after k_T_O3NO = 2.0E-12*EXP(-1400.0/TK) * T_Line; // NASA97, T1

after E_Loss = EXP(k_T_O3NO * (n[O3]-n[NO]));

after X_Rxn    = n[O3]*n[NO]*(1.0-E_Loss)/(n[NO]-n[O3]*E_Loss);

after b[mO3]    = n[O3]    - X_Rxn;
after b[mNO]    = n[NO]    - X_Rxn;
after b[mNO2] = n[NO2] + X_Rxn;

/*
  * NB::User should plot mO3, mNO, and mNO2 to compare with monitor readings.
  * For example:
  *
  *    OUTPUT FILE conc, HHMMSS
  *    {
  *       CONC, PPM { mO3:"n[O3]"    mNO2:"n[NO2]" mNO:"n[NO]" }
  *    }
  *
  */

// end of file
#end
```

//==========End: (3) SampleLine.rxn

//==========Start: (4) UNCAuxOrgStd.rxn

```
#ifnot    UNCAUXORGSTD_RXN_
#define UNCAUXORGSTD_RXN_

/*
  * $Log: /MorphoModel/Mechanisms/Sources/stdinclude/UNCAuxOrgStd.rxn $
  *
  * 1         4/02/01 10:53a Jeffries
  * First version added
  * 2         July 29, 2007 GH: Change "HCHO" to "FORM" for CB4 and CB4_CAMx
  */

/*****************************************************************
*                                                                *
*      UNC Chamber Dependent Organic Reactions (STD)                    *
*      Units are molecules/cc/secs ( 3/2/01, HEJ )                *
*                                                                *
*****************************************************************/

/* NOTE WELL::
  *    This file provides for mechanism specific species for
```

```
 *    _XPT_    UNC's explicit species mechanism
 *    _MRF_    UNC's explicit allomorph mechanism
 *    _CB4_    Carbon Bond Four 1999 mechanism
 *    _MCM_    Jenkins and Saunders mechanism
 *    _CB05_
 *
 * Other mechanism may require the file be modified.
 */

/* NOTE WELL::
 *    This file must follow the UNCAuxPhysStd.rxn file.
 */


//-----------------------------------------------------------------
//                                                          P a r t   O n e
// organic entrainment
SCALAR
  amb_HCHO;

  withk amb_HCHO = 0.002 * mpcc_ppm;

R[entrain2] = ---->

#select
  #case _XPT_
                        amb_HCHO * 'H-CO-H'
  #case _MRF_
                        amb_HCHO * 'H-CO-H'
  #case _CB4_
                        amb_HCHO *    FORM
  #case _MCM_
                        amb_HCHO *    HCHO
  #case _CB05_
                        amb_HCHO *    FORM
  #case _S99_CAMx_
                        amb_HCHO *    HCHO
  #case _CB4_CAMx_
                        amb_HCHO *    FORM

  #else
     #message "ERROR::You did not define which model to simulate, ie, missing -D _???_ check
UNCAuxOrgStd.rxn".
#end
                                                                  @ DL * p[k1st] ;


//-----------------------------------------------------------------
//                                                          P a r t   T w o
//
// reactants to represent the "background VOC" reactivity

#if _MRF_
VECTOR
  sv_BVOCa['ALK-O2.'],
  sv_BVOCb['ALK-CO-O2.'];

withk sv_BVOCa[Me]      = 0.667;
withk sv_BVOCb[Acet] = 0.167;
#end
```

```
// oxidation of background VOC
// methyl peroxy 66.7%
// acetyl peroxy 16.7%
R[BVOC]     = OH + BVOC ---->
#select
#case   _XPT_
                                0.667*'CH3-OO.'     +
                                0.167*'CH3-CO-OO.'
#case   _MRF_
                                sv_BVOCa*'ALK-O2.' +
                                sv_BVOCb*'ALK-CO-O2.'
#case   _MCM_
                                0.667*CH3O2     +
                                0.167*CH3CO3
#case   _CB4_
                                0.667*(XO2 + FORM + HO2) +
                                0.167*C2O3 + 0.001*PAR
#case _CB05_
                                0.667*MEO2 +
                                0.167*C2O3 + 0.001*PAR
#case _S99_CAMx_
                                0.667*CXO2    +
                                0.167*CCO3
#case   _CB4_CAMx_
                                0.667*(XO2 + FORM + HO2) +
                                0.167*C2O3 + 0.001*PAR

#else
    #message "ERROR::You did not define which model to simulate, ie, missing -D _???_ check
UNCAuxOrgStd.rxn".
#end
                                                                @ 3.0E-12;


#end     // UNCAUXORGSTD_RXN_
//==================================End: (4) UNCAuxOrgStd.rxn

//==================================Start: (5) UNCAuxNOxWallsGZW.rxn
#ifnot   UNCAUXINORSTD_RXN_
#define UNCAUXINORSTD_RXN_

/*
 * $Log: /MorphoModel/Mechanisms/Sources/stdinclude/UNCAuxInorgStd.rxn $
 *
 * 1         4/02/01 10:53a Jeffries
 * First version added
 *
 */

/*****************************************************************
*                                                                *
*     UNC Chamber Dependent Inorganic Reactions (Std)            *
*     Units are molecules/cc/secs ( 3/10/99, HEJ )               *
*                                                                *
*****************************************************************/


// ===============================================================
```

```
//                                                    H2O2 and O3 wall deposition
//
SCALAR
  k_depo_H2O2 = 6.7E-4, // measured    loss rate, 1/sec
  k_depo_O3   = 2.3E-6; // measured    loss rate, 1/sec (EUPHORE 3.0E-6 /sec)

#select
#case _CB05_
  R[DepoH2O2] =          H2O2 ---->                    @ k_depo_H2O2 ;
#case _S99_CAMx_
  R[DepoH2O2] =          HO2H ---->                    @ k_depo_H2O2 ;
#case _CB4_CAMx_
  R[DepoH2O2] =          H2O2 ---->                    @ k_depo_H2O2 ;
#else
#message "check if mechanism is listed in UNCAuxInorgStd, for H2O2"
#end

  R[DepoO3    ] =          O3     ---->                 @ k_depo_O3     ;


// ===================================================================
//                                                N2O5 wall deposition and hydrolysis
// rate is 1.4E-5 /s at WH2O middle of day
SCALARS
  sf_WH2OpN2O5 = 1.0;

  R[DepoN2O5] =    N2O5 + WH2O    ----> 2.0 * WHNO3    @ sf_WH2OpN2O5 * 2.6E-18 ;

// ===================================================================
//                                                  HNO3 wall deposition and emission
// EUPHORE first order dry rate was 8.2E-5 /sec
SCALAR
  sf_depo_HNO3f = 1.0,
  sf_depo_HNO3r = 1.0,
  sf_depo_HNO3l = 1.0;

  R[DepoHNO3f] =      HNO3 + WH2O     ----> WHNO3     @ 2.6E-18 * sf_depo_HNO3f ;
  R[DepoHNO3r] =             WHNO3    ----> HNO3      @ 6.6E-6    * sf_depo_HNO3r ;
  R[DepoHNO3l] =             WHNO3    ---->           @ 3.0E-6    * sf_depo_HNO3l ;


// ===================================================================
//                                                  HONO wall deposition and emission
//
SCALAR
  sf_depo_HONOf = 1.0,
  sf_depo_HONOr = 1.0;


  R[DepoHONOf] =      HONO    + WH2O    ----> WHONO           @ 8.9E-21 * sf_depo_HONOf ;
  R[DepoHONOr] =             WHONO    ----> HONO    + WH2O    @ 9.0E-3    * sf_depo_HONOr ;


#end     // UNCAUXINORSTD_RXN_
```

//==========End: (5) UNCAuxInorgStd.rxn

//==========Start: (6) UNCAuxNOxWallsGZW.rxn

```
#ifnot    UNCAUXNOXWALLSGZW_RXN_
#define UNCAUXNOXWALLSGZW_RXN_
```

```
/* Based on
  * $Log: /MorphoModel/Mechanisms/Sources/stdinclude/UNCAuxNOxWalls01.rxn $
  *
  * Version by GZW for UT comparison study between CB4, CB05, and SAPRC99
  * Completed on 13 July, 2007
  *
  */

/*****************************************************************
*                                                                *
*     UNC Chamber Dependent Inorganic Reactions (Walls)          *
*     Units are molecules/cc/secs ( 13 July, 2007, GZW)          *
*                                                                *
*****************************************************************/


/* ------------------------P a r t   O n e ----------------------- */


// ================================================================================
//                                                    NO2 wall reactions
//
SCALAR
  sf_depoNO2f    = 1.0,
  sf_depoNO2r    = 1.0,

#select
#case _S99_CAMx_
  sf_depoNO2f = 1.0,
#end

sf_WNO2WNO     = 1.0;

  R[DepoNO2f ] =                NO2          ---->   WNO2          @ 4.0E-06 * sf_depoNO2f ;
  R[DepoNO2r ] =                WNO2          ---->   NO2          @ 3.5E-05 * sf_depoNO2r ;

  R[DepoNOf ]   =                NO          ---->   WNO          @ 1.0E-05 * sf_depoNO2f ;
  R[DepoNOr ]   =                WNO          ---->   NO          @ 3.5E-05 * sf_depoNO2r ;

#select
#case _S99_CAMx_
  R[HNO4pWH2O] =        HNO4      +   WH2O        ---->   WHNO3                  @ 3.0E-17*
sf_WNO2WNO ;
#case _CB05_
  R[PNApWH2O]   =       PNA       +   WH2O        ---->   WHNO3                  @ 3.0E-17*
sf_WNO2WNO ;
#case _CB4_CAMx_
  R[PNApWH2O]   =       PNA       +   WH2O        ---->   WHNO3                  @ 3.0E-17*
sf_WNO2WNO ;
#else
#message "check if mechanism is listed in UNCAuxNOxWallGZW, for PNA"
#end

  R[WNOpWNO2]=          WNO       +   WNO2        ---->   2.0*WHONO              @ 1.0E-13*
sf_WNO2WNO ;

//   Chamber wall water loss of N2O5
SCALARS
  sf_WH2OpN2O5 = 1.0;
```

```
 R[WH2ON2O5] = WH2O + N2O5        ----> 2.0*HNO3      @ 2.0E-17 * sf_WH2OpN2O5 ;

// Chamber wall NOx production
// 1.0E-6 used before
 SCALARS
   sf_wall_NOx_src = 0.0;    // "scale factor", not rate

 R[WHNO3toNO2] =                 WHNO3    -hv-> NO2                                  @ sf_wall_NOx_src *
                                                                                    j[NO2_to_O3P];

//#end


#end     // UNCAUXNOXWALLS01_RXN_
```

//==========End: (6) UNCAuxNOxWallsGZW.rxn

//==========Start: (7) UNCAuxO3Inj.rxn

```
#ifnot    UNCAuxO3INJ_RXN
#define UNCAuxO3INJ_RXN

/*
 * $Log: /MorphoModel/Mechanisms/Sources/stdinclude/UNCAuxO3Inj.rxn $
 *
 * 1         4/02/01 10:53a Jeffries
 * First version added
 *
 */
/*****************************************************************
*                                                                *
*     UNC Chamber Dependent Inorganic Reactions (Std)            *
*     Units are molecules/cc/secs ( 3/30/01, HEJ )               *
*                                                                *
*****************************************************************/

/*
 * NOTE WELL:
 *      define "DARK_O3_INJ" before including UNCAuxMechxx01.rxn
 *
 */
// ===========================================================================
//                                                  H2O2 and O3 wall deposition
//
// O3 injection rate for night run experiments


NAMES
 PhotoRateIDs += { O3TOCHAM };       // 0.0 or 1.0 to signal constant inj rate

SCALAR
            kO3inj;         // used to set the actual rate in mpcc

 R[O3inj_1]=                          ----> O3                        @ kO3inj*j[O3TOCHAM];


// end include UNCAuxO3INJ_RXN
#end
```

//==========End: (7) UNCAuxO3Inj.rxn

A4. BOX MODELING RESULTS WITH CB05-BASE AND CB05-UNCLITE

This section is based on Heo et al. (2009) presented at the 102nd Annual Conference of the Air and Waste Management Association, June 16-19, 2009. The box modeling part of Heo et al. (2009) is described here.

Box modeling:

Box modeling simulations with two versions of CB05, containing Base or UNClite as its toluene mechanism (CB05-Base, CB05-UNClite) were performed to compare CB05-Base and CB05-UNClite under simulated ambient conditions. In this work, the SAPRC software (Carter, 1994 and 2009) was also used as a box modeling tool, however, with settings for the "airshed" simulation instead of settings for the environmental chamber simulation. Two modeling cases, "LaPorte2000" and "39-City Average", were used:

- *LaPorte2000*: Speciation of volatile organic compounds (VOCs) and initial conditions (Table 2) are based on Baylor University's aircraft measurements near surface in southeast Texas in August and September of 2000. For details such as meteorological conditions used in this study, refer to Faraji et al. (2008).
- *39-City Average*: Initial conditions were based on the averages of 39 different U.S. cities, originally developed by EPA (1985) and used by Carter (1994).

Comparison of CB05-Base and CB05-UNClite Using Box Modeling:

CB05-UNClite showed higher maximum O_3 than CB05-Base in the two cases: LaPorte2000 ([VOC]/[NOx] = 10 ppmC/ppm at the start) and 39-City Average (Figures 2 and 3). The higher Max(O_3) can be explained by relatively higher OH and HO_2 in

CB05-UNClite. When the VOC/NOx ratio was increased from 10 to 15, the difference in Max(O_3) decreased from 15 ppb to 4 ppb (Figure 2), which indicates that the effect on Max(O_3) of the updates in the toluene mechanism of CB05 depends on specific atmospheric conditions such as VOC/NOx ratios and emissions. Comparisons of CB05-Base and CB05-UNClite under simulated ambient conditions using box modeling indicate that using CB05-UNClite instead of CB05-Base will probably result in increased maximum O_3.

Table A-10. Split factors and initial concentrations for the LaPorte2000 case ([VOC]/[NOx] = 10 ppmC/ppm at start).

Model species	Split factor (ppm/ppmC)	Initial concentration (ppb)	Number of carbons	Initial concentration (ppbC)
PAR	0.5353	240.9	1	240.9
OLE	0.0083	3.7	2	7.5
TOL	0.0076	3.4	7	23.8
XYL	0.0073	3.3	8	26.4
FORM	0.0018	0.8	1	0.8
ALD2	0.0069	3.1	2	6.2
ETH	0.0237	10.7	2	21.3
ISOP	0.0003	0.1	5	0.7
MEOH	0.0177	8.0	1	8.0
ETOH	0.0000	0.0	2	0.0
ETHA	0.0385	17.3	2	34.6
IOLE	0.0026	1.2	4	4.7
ALDX	0.0048	2.2	2	4.3
TERP	0.0002	0.1	10	0.9
UNR	0.1552	69.8	1	69.8
Sum	-	-	-	450.0

Figure A-1. Comparison of O_3, NO, NO_2 simulated by CB05-Base and CB05-UNClite for LaPorte2000 cases where [VOC]/[NOx]t=t0 (ppmC/ppm) = 10 (left), 15 (right).

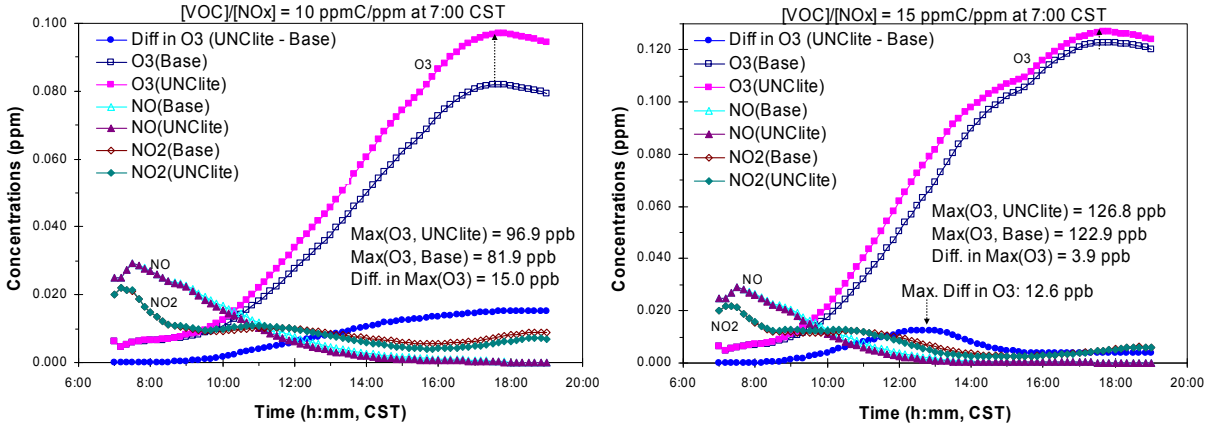

Figure A-2. Comparison of O_3 concentrations simulated by CB05-Base and CB05-UNClite for the 39-City Average case.

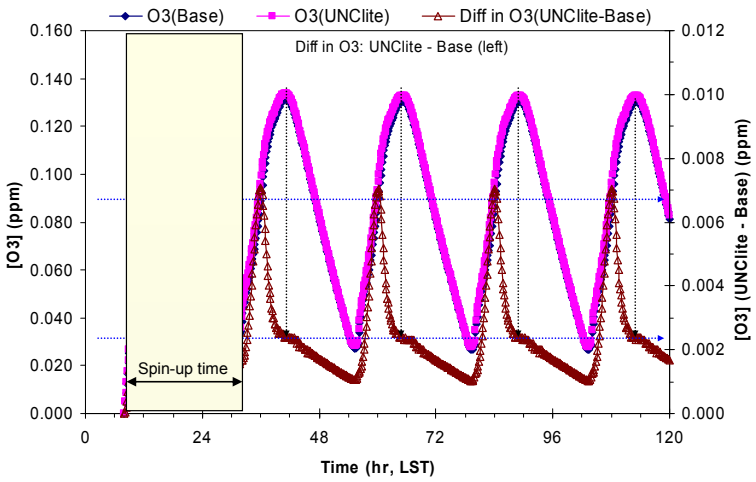

References:

Carter, W.P.L., 1994. Development of ozone reactivity scales for volatile organic compounds. Journal of the Air & Waste Management Association 44, 881-899.

Carter, W.P.L., 2009. Development of the SAPRC-07 chemical mechanism and updated ozone reactivity scales. Final Report to the California Air Resources Board Contract No. 03-318, March 20. (http://www.engr.ucr.edu/~carter/SAPRC/)

Faraji, M., Kimura, Y., McDonald-Buller, E., Allen, D., 2008. Comparison of the carbon bond and SAPRC photochemical mechanisms under conditions relevant to southeast Texas. Atmospheric Environment 42, 5821-5836.

Heo, G., Kimura, Y., McDonald-Buller, E., Allen, D.T., Yarwood, G., Whitten, G.Z., 2009. Evaluation of a new toluene mechanism for Carbon Bond 05 using environmental chamber data and ambient data. Presented at the 102nd Annual Conference of the Air & Waste Management Association, June 16-19, 2009, Detroit, MI. (Abstract of this paper (Paper AB-2b.154) is available at http://www.conferencearchives.com/awma/2009/abstracts/AB-2b.154_a.html).

U.S. EPA. Guideline for using the Carbon Bond mechanism in city-specific EKMA. EPA-450/4-84-005, February 1984.

Appendix B: Further Information for Chapter 4

This Appendix consists of four sections as follows:

- B1. Graphical representation of major pathways leading to radical formation in the ozonolysis of 1-alkenes.
- B2. Listings of explicit reactions of 18 additional alkenes added to the Fixed version of SAPRC-07 (SAPRC07B.RXN).
- B3. Implementation of the reaction of 1-butene and O_3 for the mechanisms listed in Table 4-9.
- B4. Additional information regarding box model simulations.

B1. GRAPHICAL REPRESENTATION OF MAJOR PATHWAYS LEADING TO RADICAL FORMATION IN THE OZONOLYSIS OF 1-ALKENES

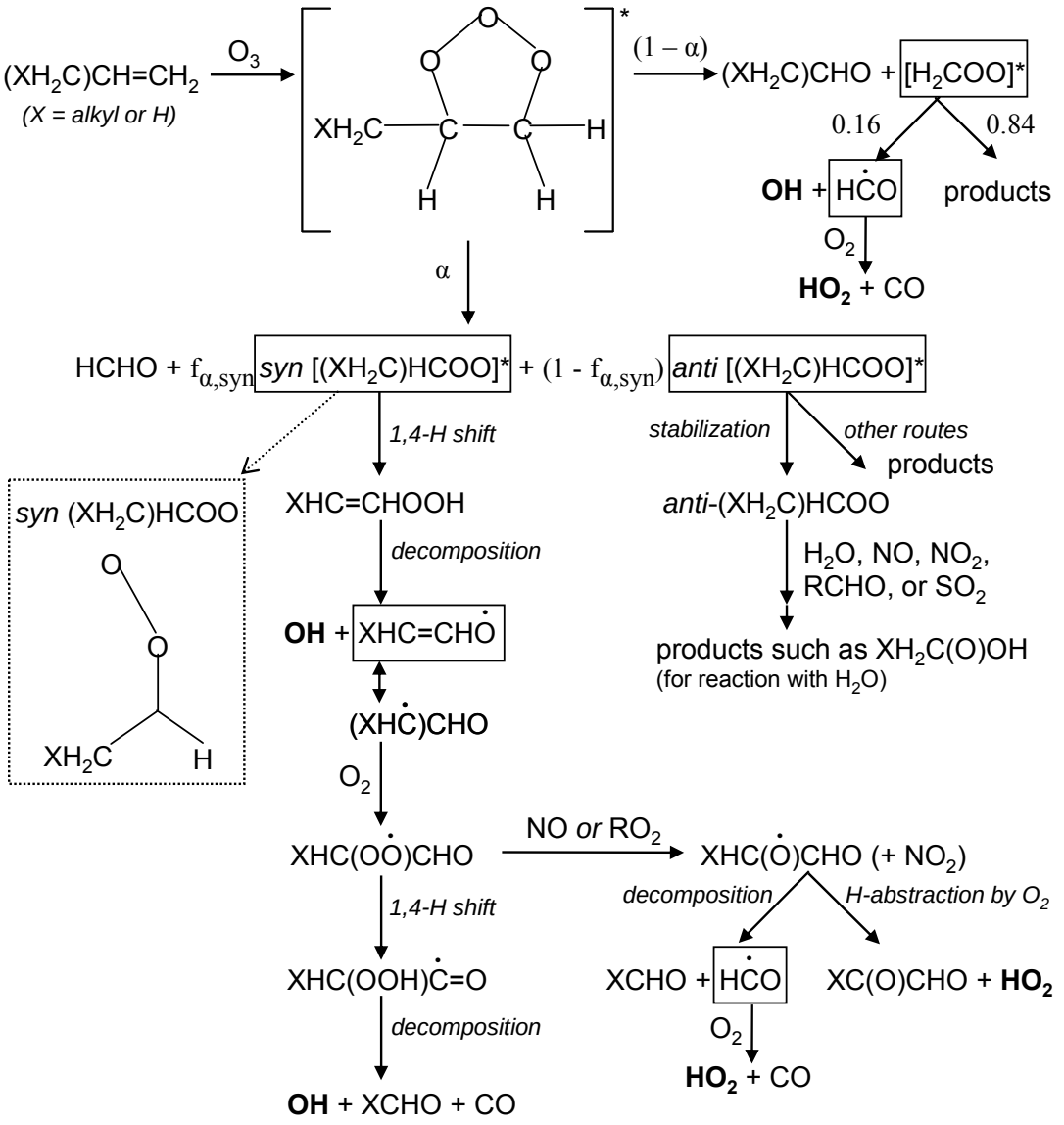

Figure B-1. Major pathways leading to radical formation in the ozonolysis of 1-alkenes.

References: Atkinson et al., 2006; Calvert et al., 2000; Kuwata et al., 2003, 2005; Paulson et al., 1999). Note: for 1-butene, X = CH_3 in this figure. For the references cited here, refer to the References section of Chapter 4.

B2. LISTINGS OF EXPLICIT REACTIONS OF 18 ADDITIONAL ALKENES ADDED TO THE FIXED VERSION OF SAPRC-07 (SAPRC07B.RXN)

*File SAPRC07B.RXN written by Dr. William P. L. Carter at UC-Riverside (http://www.engr.ucr.edu/~carter/SAPRC/files.htm) was used for SAPRC-07F which is described in Chapter 4.

```
!START: Explicit alkene mechanisms ============================================
!measured alkenes during the TexAQS-2000:
! compound                                    k(O3) at 298K/OH Yield at 1 bar (Atkinson et al., 2006)
! ethene                                       1.6E-18 / 0.18
! tetrachloroethylene (Perchloroethylene)
! propene                                      1.0E-17 / 0.34
! methylpropene (isobutene, 2-methylpropene) 1.1E-17 / 0.62
! 1-butene
! 2-methyl-1-butene
! 3-methyl-1-butene
! Trans-2-butene (E-2-butene)                 1.9E-16 / 0.64
! Cis-2-butene (Z-2-butene)                   1.3E-16 / 0.33
! 2-methyl-2-butene                          4.1E-16 / 0.88
! 1-pentene
! Trans-2-pentene (E-2-pentene)
! Cis-2-penetene (Z-2-pentene)
! Cyclopentene
! 1-hexene
! 1,3-butadiene
! isoprene                                    1.27E-17 / 0.25
! alpha-pinene                                9.0E-17    / 0.80
! limonene
! 2,3-dimethyl-2-butene (not measured)        1.1E-16 / 0.90
! =====[summary of added explicit reactions for alkenes with OH/O3/NO3/O3P]
! 1. ethene and isoprene have been already expressed as explicit species in SAPRC07B.RXN.
! 2. 17 additional alkenes were expressed explicitly:
!       propene, isobutene (2-methylpropene), 1-butene, 2-methyl-1-butene, 3-methyl-1-butene,
!       trans-2-butene (E-2-butene), cis-2-butene (Z-2-butene), 2-methyl-2-butene,
!       trans-2-pentene (E-2-pentene), cis-2-pentene (Z-2-pentene), cyclopentene,
!       1-hexene, 1,3-butadiene, alpha-pinene, limonene (D-limonene), 2,3-dimethyl-2-butene
! 3. tetrachloroethylene (Perchloroethylene) was not added because the focus is on alkene + O3 reaction
! 4. D-limonene's reactions are used for limonene
! 5. References: Worksheet B-2 of SAPRC07.XLS of Dr. William P. L. Carter at UC-Riverside.
!                                File SAPRC07B.RXN of Dr. William P. L. Carter at UC-Riverside. (for SAPRC-07F).
!================================================================================
.RXN
! PROPENE: PROPENE + OH/O3/NO3: Atkinson and Arey (2003)
!               PROPENE + O3P: Calvert et al. (2002)
AL01) 4.85E-12 -1.002              ;PROPENE + OH = #.984 RO2C + #.016 RO2XC +
                                       #.016 zRNO3 + #.984 xHO2 + #.984 xHCHO +
                                       #.984 xCCHO + yROOH + #-.048 XC
AL02) 5.51E-15 3.732               ;PROPENE + O3 = #.35 OH + #.165 HO2 +
                                       #.355 MEO2 + #.525 CO + #.215 CO2 + #.5 HCHO +
```

```
                                    #.5 CCHO + #.185 HCOOH + #.075 CCOOH + #.07 XC
AL03) 4.59E-13 2.297          ;PROPENE + NO3 = #.949 RO2C + #.051 RO2XC +
                                    #.051 zRNO3 + #.949 xHO2 + yROOH +
                                    #2.693 XC + XN
AL04) 1.02E-11 0.556          ;PROPENE + O3P = #.45 RCHO + #.55 MEK + #-.55 XC
! 1-BUTENE: 1-BUTENE + OH/O3/NO3: Atkinson and Arey (2003)
!             1-BUTENE + O3P: Calvert et al. (2002)
AL05) 6.55E-12 -0.928         ;1-BUTENE + OH = #.986 RO2C + #.027 RO2XC +
                                    #.027 zRNO3 + #.973 xHO2 + #.948 xHCHO +
                                    #.946 xRCHO + #.007 xMACR + #.015 xMVK +
                                    #.005 xIPRD + yROOH + #-.06 XC
AL06) 3.36E-15 3.525          ;1-BUTENE + O3 = #.128 OH + #.095 HO2 +
                                    #.063 RO2C + #.303 CO + #.088 CO2 + #.5 HCHO +
                                    #.5 RCHO + #.185 HCOOH + #.425 RCOOH +
                                    #.063 xHO2 + #.063 xCCHO + #.063 yROOH +
                                    #.025 XC
AL07) 3.14E-13 1.864          ;1-BUTENE + NO3 = #.995 RO2C + #.08 RO2XC +
                                    #.08 zRNO3 + #.92 xHO2 + #.075 xCCHO +
                                    #.92 xRNO3 + yROOH + #-2.15 XC + #.08 XN
AL08) 1.34E-11 0.696          ;1-BUTENE + O3P = #.45 RCHO + #.55 MEK + #.45 XC
! 1-PENTENE: 1-PENTENE + OH/O3/NO3: Atkinson and Arey (2003)
!             1-PENTENE + O3P: Calvert et al. (2002)
AL09) 3.14E-11                 ;1-PENTEN + OH = #1.093 RO2C + #.076 RO2XC +
                                    #.076 zRNO3 + #.924 xHO2 + #.767 xHCHO +
                                    #.047 xCCHO + #.845 xRCHO + #.019 xPROD2 +
                                    #.047 xMACR + #.005 xMVK + #.009 xIPRD +
                                    yR6OOH + #.785 XC
AL10) 2.13E-15 3.140          ;1-PENTEN + O3 = #.128 OH + #.095 HO2 +
                                    #.061 RO2C + #.001 RO2XC + #.001 zRNO3 +
                                    #.303 CO + #.088 CO2 + #.5 HCHO + #.5 RCHO +
                                    #.013 MEK + #.185 HCOOH + #.425 RCOOH +
                                    #.061 xHO2 + #.061 xRCHO + #.063 yR6OOH +
                                    #.909 XC
AL11) 1.50E-14                 ;1-PENTEN + NO3 = #1.615 RO2C + #.166 RO2XC +
                                    #.166 zRNO3 + #.834 xHO2 + #.016 xRCHO +
                                    #.834 xRNO3 + yR6OOH + #-1.051 XC + #.166 XN
AL12) 1.78E-11 0.795          ;1-PENTEN + O3P = #.45 RCHO + #.55 MEK + #1.45 XC
! 1-HEXENE: 1-HEXENE + OH/O3/NO3: Atkinson and Arey (2003)
!             1-HEXENE + O3P: Calvert et al. (2002)
AL13) 3.70E-11                 ;1-HEXENE + OH = #1.342 RO2C + #.104 RO2XC +
                                    #.104 zRNO3 + #.896 xHO2 + #.483 xHCHO +
                                    #.005 xCCHO + #.612 xRCHO + #.263 xPROD2 +
                                    #.048 xMACR + #.009 xMVK + #.008 xIPRD +
                                    yR6OOH + #1.201 XC
AL14) 1.62E-15 2.941          ;1-HEXENE + O3 = #.128 OH + #.095 HO2 +
                                    #.105 RO2C + #.004 RO2XC + #.004 zRNO3 +
                                    #.303 CO + #.088 CO2 + #.5 HCHO + #.5 RCHO +
                                    #.013 MEK + #.425 PROD2 + #.185 HCOOH +
                                    #.058 xHO2 + #.058 xRCHO + #.063 yR6OOH +
                                    #.625 XC
AL15) 1.80E-14                 ;1-HEXENE + NO3 = #1.608 RO2C + #.237 RO2XC +
                                    #.237 zRNO3 + #.763 xHO2 + #.763 xRNO3 +
                                    yR6OOH + #.237 XN
AL16) 1.51E-11 0.656          ;1-HEXENE + O3P = #.45 RCHO + #.55 MEK + #2.45 XC
! methylpropene (isobutene): ISOBUTENE + OH/O3/NO3: Atkinson and Arey (2003)
!             ISOBUTENE + O3P: Calvert et al. (2002)
AL17) 9.47E-12 -1.002         ;ISOBUTEN + OH = #.9 RO2C + #.1 RO2XC +
                                    #.1 zRNO3 + #.9 xHO2 + #.9 xHCHO + #.9 xACET +
                                    yROOH + #-.2 XC
AL18) 2.70E-15 3.243          ;ISOBUTEN + O3 = #.72 OH + #.053 HO2 +
```

```
                                    #.667 RO2C + #.17 CO + #.04 CO2 + #.667 HCHO +
                                    #.333 ACET + #.123 HCOOH + #.667 xMECO3 +
                                    #.667 xHCHO + #.667 yROOH
AL19) 3.44E-13                      ;ISOBUTEN + NO3 = #.961 RO2C + #.039 RO2XC +
                                    #.039 zRNO3 + #.644 xNO2 + #.316 xMEO2 +
                                    #.644 xHCHO + #.644 xACET + yROOH + #.87 XC +
                                    #.356 XN
AL20) 1.14E-11 -0.233               ;ISOBUTEN + O3P = #.4 RCHO + #.6 MEK + #.4 XC
! 2-methyl-1-butene: OH/O3: Atkinson and Arey (2003),
!                          NO3 (Estimated;Carter, 2000), O3P (Calvert et al., 2002)
AL21) 6.10E-11                      ;2M-1-BUT + OH = #.939 RO2C + #.066 RO2XC +
                                    #.066 zRNO3 + #.934 xHO2 + #.924 xHCHO +
                                    #.92 xMEK + #.004 xMVK + #.011 xIPRD + yR6OOH +
                                    #-.066 XC
AL22) 4.90E-15 3.460                ;2M-1-BUT + O3 = #.72 OH + #.053 HO2 +
                                    #.64 RO2C + #.026 RO2XC + #.026 zRNO3 +
                                    #.17 CO + #.04 CO2 + #.667 HCHO + #.333 MEK +
                                    #.123 HCOOH + #.558 xMECO3 + #.082 xRCO3 +
                                    #.082 xHCHO + #.558 xCCHO + #.667 yR6OOH +
                                    #-.053 XC
AL23) 3.32E-13                      ;2M-1-BUT + NO3 = #1.851 RO2C + #.065 RO2XC +
                                    #.065 zRNO3 + #.019 xNO2 + #.916 xHO2 +
                                    #.019 xHCHO + #.916 xCCHO + #.019 xMEK +
                                    yR6OOH + #2.682 XC + #.981 XN
AL24) 1.80E-11                      ;2M-1-BUT + O3P = #.4 RCHO + #.6 MEK + #1.4 XC
! 3-methyl-1-butene: O3 (Atkinson and Arey, 2003;
! Temperature-dependency using A factor from 1-butene)
AL25) 5.32E-12 -1.059               ;3M-1-BUT + OH = #1.132 RO2C + #.075 RO2XC +
                                    #.075 zRNO3 + #.9 xHO2 + #.025 xMEO2 +
                                    #.719 xHCHO + #.162 xCCHO + #.698 xRCHO +
                                    #.156 xACET + #.011 xPROD2 + #.021 xMACR +
                                    #.03 xMVK + #.009 xIPRD + yR6OOH + #.603 XC
AL26) 3.36E-15 3.476                ;3M-1-BUT + O3 = #.128 OH + #.095 HO2 +
                                    #.06 RO2C + #.003 RO2XC + #.003 zRNO3 +
                                    #.303 CO + #.088 CO2 + #.5 HCHO + #.5 RCHO +
                                    #.013 MEK + #.185 HCOOH + #.425 RCOOH +
                                    #.06 xHO2 + #.06 xACET + #.063 yR6OOH + #.905 XC
AL27) 1.39E-14                      ;3M-1-BUT + NO3 = #1.678 RO2C + #.149 RO2XC +
                                    #.149 zRNO3 + #.851 xHO2 + #.794 xACET +
                                    #.884 xRNO3 + yR6OOH + #-3.58 XC + #.116 XN
AL28) 1.03E-11 0.537                ;3M-1-BUT + O3P = #.45 RCHO + #.55 MEK + #1.45 XC
! Trans-2-butene (E-2-butene)                    1.9E-16 / 0.64    (IUPAC, 2005)
! Trans-2-butene + O3: Atkinson and Arey, 2003: 1.95E-16 / 0.54
AL29) 1.01E-11 -1.093               ;T-2-BUTE + OH = #.965 RO2C + #.035 RO2XC +
                                    #.035 zRNO3 + #.965 xHO2 + #1.93 xCCHO +
                                    yROOH + #-.07 XC
AL30) 6.64E-15 2.104                ;T-2-BUTE + O3 = #.54 OH + #.17 HO2 + #.71 MEO2 +
                                    #.54 CO + #.31 CO2 + CCHO + #.15 CCOOH + #.14 XC
AL31) 1.10E-13 -0.759 2.0           ;T-2-BUTE + NO3 = #.92 RO2C + #.08 RO2XC +
                                    #.08 zRNO3 + #.705 xNO2 + #.215 xHO2 +
                                    #1.41 xCCHO + #.215 xRNO3 + yROOH + #-.59 XC +
                                    #.08 XN
AL32) 1.09E-11 -0.358               ;T-2-BUTE + O3P = MEK
! Cis-2-butene (Z-2-butene)                      1.3E-16 / 0.33 (IUPAC, 2005)
! Cis-2-butene + O3: Atkinson and Arey, 2003: 1.28E-16 / 0.54
AL33) 1.10E-11 -0.968               ;C-2-BUTE + OH = #.965 RO2C + #.035 RO2XC +
                                    #.035 zRNO3 + #.965 xHO2 + #1.93 xCCHO + yROOH +
                                    #-.07 XC
AL34) 3.22E-15 1.924                ;C-2-BUTE + O3 = #.54 OH + #.17 HO2 + #.71 MEO2 +
                                    #.54 CO + #.31 CO2 + CCHO + #.15 CCOOH + #.14 XC
```

```
AL35) 3.52E-13                ;C-2-BUTE + NO3 = #.92 RO2C + #.08 RO2XC +
                                 #.08 zRNO3 + #.705 xNO2 + #.215 xHO2 +
                                 #1.41 xCCHO + #.215 xRNO3 + yROOH + #-.59 XC +
                                 #.08 XN
AL36) 1.10E-11 -0.278         ;C-2-BUTE + O3P = MEK
! 2-methyl-2-butene                          4.1E-16 / 0.88 (IUPAC, 2005)
! 2-methyl-2-butene + O3: Atkinson and Arey, 2003: 4.11E-16 / 0.862
AL37) 1.92E-11 -0.894         ;2M-2-BUT + OH = #.935 RO2C + #.065 RO2XC +
                                 #.065 zRNO3 + #.935 xHO2 + #.935 xCCHO +
                                 #.935 xACET + yR6OOH + #-.065 XC
AL38) 6.51E-15 1.647          ;2M-2-BUT + O3 = #.862 OH + #.051 HO2 +
                                 #.213 MEO2 + #.7 RO2C + #.162 CO + #.093 CO2 +
                                 #.7 CCHO + #.3 ACET + #.045 CCOOH + #.7 xMECO3 +
                                 #.7 xHCHO + #.7 yR6OOH + #.042 XC
AL39) 9.37E-12                ;2M-2-BUT + NO3 = #.935 RO2C + #.065 RO2XC +
                                 #.065 zRNO3 + #.935 xNO2 + #.935 xCCHO +
                                 #.935 xACET + yR6OOH + #-.065 XC + #.065 XN
AL40) 2.44E-11 -0.437         ;2M-2-BUT + O3P = MEK + XC
! Trans-2-pentene (E-2-pentene): T-2-pentene + O3: 1.63E-16 / 0.318 (Atkinson and Arey, 2003)
AL41) 6.70E-11                ;T-2-PENT + OH = #.939 RO2C + #.066 RO2XC +
                                 #.066 zRNO3 + #.934 xHO2 + #.926 xCCHO +
                                 #.921 xRCHO + #.013 xIPRD + yR6OOH + #-.076 XC
AL42) 7.10E-15 2.250          ;T-2-PENT + O3 = #.318 OH + #.1 HO2 +
                                 #.355 MEO2 + #.063 RO2C + #.318 CO +
                                 #.183 CO2 + #.5 CCHO + #.5 RCHO + #.075 CCOOH +
                                 #.425 RCOOH + #.063 xHO2 + #.063 xCCHO +
                                 #.063 yR6OOH + #.095 XC
AL43) 3.70E-13                ;T-2-PENT + NO3 = #1.148 RO2C + #.134 RO2XC +
                                 #.134 zRNO3 + #.471 xNO2 + #.395 xHO2 +
                                 #.481 xCCHO + #.471 xRCHO + #.395 xRNO3 +
                                 yR6OOH + #-.548 XC + #.134 XN
AL44) 1.15E-11 -0.358         ;T-2-PENT + O3P = MEK + XC
! Cis-2-penetene (Z-2-pentene): C-2-pentene + O3: 1.31E-16 / 0.318 (Atkinson and Arey, 2003)
AL45) 6.50E-11                ;C-2-PENT + OH = #.944 RO2C + #.066 RO2XC +
                                 #.066 zRNO3 + #.934 xHO2 + #.931 xCCHO +
                                 #.921 xRCHO + #.012 xIPRD + yR6OOH + #-.086 XC
AL46) 3.70E-15 1.991          ;C-2-PENT + O3 = #.318 OH + #.1 HO2 +
                                 #.355 MEO2 + #.063 RO2C + #.318 CO + #.183 CO2 +
                                 #.5 CCHO + #.5 RCHO + #.075 CCOOH +
                                 #.425 RCOOH + #.063 xHO2 + #.063 xCCHO +
                                 #.063 yR6OOH + #.095 XC
AL47) 3.70E-13                ;C-2-PENT + NO3 = #1.148 RO2C + #.134 RO2XC +
                                 #.134 zRNO3 + #.471 xNO2 + #.395 xHO2 +
                                 #.481 xCCHO + #.471 xRCHO + #.395 xRNO3 +
                                 yR6OOH + #-.548 XC + #.134 XN
AL48) 1.14E-11 -0.238         ;C-2-PENT + O3P = MEK + XC
! Cyclopentene: Cyclopetene + O3: 5.61E-16 / 0.095 (Aktinson and Arey, 2003)
AL49) 6.70E-11                ;CYC-PNTE + OH = #.99 RO2C + #.071 RO2XC +
                                 #.071 zRNO3 + #.921 xHO2 + #.009 xMACO3 +
                                 #.018 xCO + #.028 xHCHO + #.901 xRCHO +
                                 #.018 xMACR + #.001 xMVK + yR6OOH + #1.713 XC
AL50) 1.80E-15 0.696          ;CYC-PNTE + O3 = #.095 OH + #.03 HO2 +
                                 #.12 RO2C + #.005 RO2XC + #.005 zRNO3 +
                                 #.095 CO + #.055 CO2 + #.875 RCHO + #.12 xRCO3 +
                                 #.125 yR6OOH + #1.835 XC
AL51) 4.20E-13                ;CYC-PNTE + NO3 = #1.013 RO2C + #.125 RO2XC +
                                 #.125 zRNO3 + #.812 xNO2 + #.064 xHO2 +
                                 #.735 xRCHO + #.077 xMGLY + #.064 xRNO3 +
                                 yR6OOH + #1.435 XC + #.125 XN
AL52) 2.40E-11 0.079          ;CYC-PNTE + O3P = #.24 MEK + #.76 PROD2 +
```

```
                                    #-.52 XC
! 1,3-butadiene: + O3: 6.64E-18 / 0.08 (Aktinson and Arey, 2003)
AL53) 1.48E-11 -0.890          ;13-BUTDE + OH = #1.189 RO2C + #.049 RO2XC +
                                    #.049 zRNO3 + #.951 xHO2 + #.708 xHCHO +
                                    #.48 xMACR + #.471 xIPRD + yROOH + #-1.277 XC
AL54) 1.34E-14 4.537           ;13-BUTDE + O3 = #.08 OH + #.08 HO2 + #.255 CO +
                                    #.185 CO2 + #.5 HCHO + #.125 PROD2 + #.5 MACR +
                                    #.375 MVK + #.185 HCOOH + #-1.375 XC
AL55) 1.00E-13                 ;13-BUTDE + NO3 = #1.055 RO2C + #.065 RO2XC +
                                    #.065 zRNO3 + #.12 xNO2 + #.815 xHO2 +
                                    #.115 xHCHO + #.46 xMVK + #.12 xIPRD +
                                    #.355 xRNO3 + yROOH + #-1.076 XC + #.524 XN
AL56) 2.26E-11 0.079           ;13-BUTDE + O3P = #.25 HO2 + #.235 RO2C +
                                    #.015 RO2XC + #.015 zRNO3 + #.75 PROD2 +
                                    #.117 xHO2 + #.118 xMACO3 + #.115 xCO +
                                    #.001 xAFG1 + #.001 xAFG2 + #.115 xMACR +
                                    #.25 yROOH + #-1.647 XC
! isoprene                          1.27E-17 / 0.25 (IUPAC, 2005)
! isoprene in the basemech.rxn:  1.34E-17 / 0.266 (Atkinson and Arey, 2003)
! alpha-pinene                       9.0E-17    / 0.80 (IUPAC, 2005)
!                                     8.55E-17 / 0.728 (Atkinson and Arey, 2003)
AL57) 1.21E-11 -0.866          ;A-PINENE + OH = #1.042 RO2C + #.197 RO2XC +
                                    #.197 zRNO3 + #.799 xHO2 + #.004 xRCO3 +
                                    #.002 xCO + #.022 xHCHO + #.776 xRCHO +
                                    #.034 xACET + #.02 xMGLY + #.023 xBACL +
                                    yR6OOH + #6.195 XC
AL58) 5.00E-16 1.053           ;A-PINENE + O3 = #.728 OH + #.009 HO2 +
                                    #1.511 RO2C + #.337 RO2XC + #.337 zRNO3 +
                                    #.029 CO + #.017 CO2 + #.008 MEK + #.255 PROD2 +
                                    #.102 xHO2 + #.001 xMECO3 + #.297 xRCO3 +
                                    #.051 xCO + #.344 xHCHO + #.24 xRCHO +
                                    #.345 xACET + #.002 xGLY + #.081 xBACL +
                                    #.737 yR6OOH + #3.004 XC
AL59) 1.19E-12 -0.974          ;A-PINENE + NO3 = #1.05 RO2C + #.293 RO2XC +
                                    #.293 zRNO3 + #.643 xNO2 + #.056 xHO2 +
                                    #.007 xRCO3 + #.005 xCO + #.007 xHCHO +
                                    #.684 xRCHO + #.069 xACET + #.002 xMGLY +
                                    #.056 xRNO3 + yR6OOH + #5.608 XC + #.301 XN
AL60) 3.20E-11                 ;A-PINENE + O3P = PROD2 + #4 XC
! limonene
! d-limonene (assume all limonene molecules are d-limonene)
! d-limonene: + O3: 2.17E-16 / 0.729 (Atkinson and Arey, 2003)
AL61) 4.28E-11 -0.797          ;D-LIMONE + OH = #.972 RO2C + #.17 RO2XC +
                                    #.17 zRNO3 + #.827 xHO2 + #.003 xRCO3 +
                                    #.288 xHCHO + #.539 xRCHO + #.053 xMEK +
                                    #.287 xPROD2 + #.019 xMVK + #.012 xIPRD +
                                    yR6OOH + #5.001 XC
AL62) 2.95E-15 1.556           ;D-LIMONE + O3 = #.729 OH + #.009 HO2 +
                                    #.619 RO2C + #.177 RO2XC + #.177 zRNO3 +
                                    #.029 CO + #.017 CO2 + #.263 PROD2 +
                                    #.021 xHO2 + #.482 xMECO3 + #.058 xRCO3 +
                                    #.089 xHCHO + #.5 xRCHO + #.015 xMACR +
                                    #.007 xIPRD + #.738 yR6OOH + #4.497 XC
AL63) 1.22E-11                 ;D-LIMONE + NO3 = #1.11 RO2C + #.296 RO2XC +
                                    #.296 zRNO3 + #.626 xNO2 + #.076 xHO2 +
                                    #.002 xRCO3 + #.078 xHCHO + #.009 xCCHO +
                                    #.641 xRCHO + #.039 xMACR + #.009 xMVK +
                                    #.028 xIPRD + #.069 xRNO3 + yR6OOH +
                                    #5.452 XC + #.304 XN
AL64) 7.20E-11                 ;D-LIMONE + O3P = PROD2 + #4 XC
```

```
! 2,3-dimethyl-2-butene (not measured) 1.1E-16 / 0.90 (IUPAC, 2005)
! 2,3-dimethyl-2-butene: + O3:          1.14E-15 / 1.0 (Atkinson and Arey, 2003)
AL65) 1.10E-10                  ;23M2-BUT + OH = #.902 RO2C + #.098 RO2XC +
                                   #.098 zRNO3 + #.902 xHO2 + #1.805 xACET + yR6OOH
AL66) 3.03E-15 0.584            ;23M2-BUT + O3 = OH + RO2C + ACET + xMECO3 +
                                   xHCHO + yR6OOH
AL67) 5.72E-11                  ;23M2-BUT + NO3 = #.902 RO2C + #.098 RO2XC +
                                   #.098 zRNO3 + #.902 xNO2 + #1.805 xACET +
                                   yR6OOH + #.098 XN
AL68) 2.81E-11 -0.596           ;23M2-BUT + O3P = MEK + #2 XC

! Explicit mechanisms of reactions of Cyclohexene
! Written by Gookyoung Heo at CEER, UT-Austin on March 12, 2009.
! Rate constants are in units of cm3 molec-1 s-1. Temperature dependence is
! given by k(T) = A exp(-Ea/RT) (T/300)^B, where T is the temperature
! in degrees k and R = 0.0019872.
! Reference: Worksheet B-2 of SAPRC07.XLS of Dr. William P. L. Carter at UC-Riverside.
! Original references: CYC-HEXE + OH/O3/NO3: Atkinson and Arey (2003)
!                      CYC_HEXE + O3P: As recommended or tabulated by Calvert et al (2002)
!=========================================================================
.UNITS=PPM
.RXN
! Cyclohexene (CYC-HEXE)
AL69) 6.77E-11                  ;CYC-HEXE + OH = #.966 RO2C + #.111 RO2XC +
                                   #.111 zRNO3 + #.87 xHO2 + #.019 xRCO3 +
                                   #.001 xHCHO + #.843 xRCHO + #.001 xMACR +
                                   #.034 xIPRD + yR6OOH + #2.572 XC
AL70) 2.87E-15 2.112            ;CYC-HEXE + O3 = #.095 OH + #.03 HO2 +
                                   #.225 RO2C + #.016 RO2XC + #.016 zRNO3 +
                                   #.095 CO + #.055 CO2 + #.875 RCHO +
                                   #.109 xHO2 + #.008 xCO + #.109 xRCHO +
                                   #.125 yR6OOH + #2.795 XC
AL71) 5.10E-13                  ;CYC-HEXE + NO3 = #.941 RO2C + #.165 RO2XC +
                                   #.165 zRNO3 + #.296 xNO2 + #.539 xHO2 +
                                   #.296 xRCHO + #.539 xRNO3 + yR6OOH + #.888 XC +
                                   #.165 XN
AL72) 2.21E-11 0.060            ;CYC-HEXE + O3P = PROD2


!The four reaction below were not actually used in this study,
!but can be used to extend the SAPRC-07E mechanism to separately !simulate beta-pinene as well.

! Explicit mechanisms of reactions of beta-pinene (B-PINENE)
! Written by Gookyoung Heo at CEER, UT-Austin on April 1, 2009.
! Rate constants are in units of cm3 molec-1 s-1. Temperature dependence is
! given by k(T) = A exp(-Ea/RT) (T/300)^B, where T is the temperature
! in degrees k and R = 0.0019872.
! Reference: Worksheet B-2 of SAPRC07.XLS of Dr. William P. L. Carter at UC-Riverside.
! Original references: B-PINENE + OH/O3/NO3: Atkinson and Arey (2003)
!                      B-PINENE + O3P: As recommended or tabulated by Calvert et al (2000*)
!                      *:Originally, Carter attributed this to Calvert et al. (2002).
!                        However, Calvert et al. (2002) is for aromatics
!                        and Calvert et al. (2000) is for alkenes
!=========================================================================
.UNITS=PPM
.RXN
! Beta-pinene (B-PINENE)
! Reaction number starts at AL73 because AL72 is the last reaction number
! already used for explicit reactions for alkenes
AL73) 1.55E-11 -0.928           ;B-PINENE + OH = #.999 RO2C + #.184 RO2XC +
```

```
                    #.184 zRNO3 + #.811 xHO2 + #.005 xRCO3 +
                    #.002 xCO + #.784 xHCHO + #.046 xRCHO +
                    #.035 xACET + #.781 xPROD2 + #.007 xMGLY +
                    yR6OOH + #3.144 XC
AL74) 1.20E-15 2.583 ;B-PINENE + O3 = #.353 OH + #.123 HO2 +
                    #.458 RO2C + #.093 RO2XC + #.093 zRNO3 +
                    #.393 CO + #.092 CO2 + #.23 HCHO + #.77 PROD2 +
                    #.285 HCOOH + #.07 xHO2 + #.067 xRCO3 +
                    #.011 xHCHO + #.006 xRCHO + #.104 xACET +
                    #.007 xMGLY + #.063 xBACL + #.23 yR6OOH +
                    #3.009 XC
AL75) 2.51E-12      ;B-PINENE + NO3 = #2.435 RO2C + #.611 RO2XC +
                    #.611 zRNO3 + #.33 xHO2 + #.059 xRCO3 +
                    #.027 xCO + #.027 xHCHO + #.258 xRCHO +
                    #.393 xACET + #.001 xGLY + #.33 xRNO3 +
                    yR6OOH + #2.169 XC + #.67 XN
AL76) 2.70E-11      ;B-PINENE + O3P = #.4 RCHO + #.6 PROD2 + #5.2 XC
```

B3. IMPLEMENTATION OF THE REACTION OF 1-BUTENE AND O_3 FOR THE MECHANISMS LISTED IN TABLE 4-9

SAPRC-07F (The Fixed version)

```
! Reference: SAPRC07B.RXN of Dr. William P. L. Carter at UC-Riverside
! (http://www.engr.ucr.edu/~carter/SAPRC/files.htm).
! OLE1 + O3 represents the reaction of 1-butene and O3 in the Fixed version.
BL07) 3.15e-15 3.379          ;OLE1 + O3 = #.116 HO2 + #.04 xHO2 + #.193 OH +
                                  #.104 MEO2 + #.063 RO2C + #.004 RO2XC +
                                  #.004 zRNO3 + #.368 CO + #.125 CO2 + #.5 HCHO +
                                  #.147 CCHO + #.007 xCCHO + #.353 RCHO +
                                  #.031 xRCHO + #.002 xACET + #.006 MEK +
                                  #.185 HCOOH + #.022 CCOOH + #.112 RCOOH +
                                  #.189 PROD2 + #.007 yROOH + #.037 yR6OOH +
                                  #.69 XC
```

SAPRC-07A/E (The Adjustable and Extended versions)

```
! Reference: Worksheet B-2 of SAPRC07.XLS of Dr. William P. L. Carter at UC-Riverside
! (http://www.engr.ucr.edu/~carter/SAPRC/files.htm).
AL06) 3.36E-15 3.525          ;1-BUTENE + O3 = #.128 OH + #.095 HO2 +
                                  #.063 RO2C + #.303 CO + #.088 CO2 + #.5 HCHO +
                                  #.5 RCHO + #.185 HCOOH + #.425 RCOOH +
                                  #.063 xHO2 + #.063 xCCHO + #.063 yROOH +
                                  #.025 XC
```

X[1-butene + O_3 killed]

No reaction included for 1-BUTENE + O3

A1 [alpha (0.5), OH (0.33)]

```
! Y(OH) = 0.33; alpha=0.5; x=0.50; y=0.0.
! References: Carter, 2000 and 2009 (the SAPRC-99 and SAPRC-07 documents),
! Table 9 and Fig. S1.
! CH2=CH-CH2-CH3 + O3 = 0.5(CH2OO* + CHO-CH2-CH3) +
!                       0.5 (HCHO + 0.5 syn-*OOCH-CH2-CH3 + 0.5 anti-*OOCH-CH2-
CH3)
! CH2OO* = 0.37 CH2OO + 0.16 (HCO + OH) + 0.12 (H2 + CO2) + 0.35 (CO + H2O)
!        = 0.37 CH2OO [HCOOH] + 0.16 OH + (0.16) HO2 + (0.16 + 0.35) CO + 0.12 CO2
!        = 0.37 HCOOH + 0.16 OH + 0.16 HO2 + 0.51 CO + 0.12 CO2
! syn-*OOCH-CH2-CH3 = OH + CH3-CH2. + CO
! anti-*OOCH-CH2-CH3 = HOC(O)-CH2-CH3 [RCOOH]
AL06) 3.36E-15 3.525          ;1-BUTENE + O3 = #.33 OH + #.08 HO2 + #.25 RO2C +
                                  #.505 CO + #.06 CO2 +
                                  #.5 HCHO + #.5 RCHO + #.185 HCOOH + #.5
RCOOH +
                                  #.25 {RO2C + xHO2 + xCCHO + yROOH}
```

A2 [alpha (0.5), OH (0.29)]
! Y(OH) = 0.29; alpha=0.5; x=0.42; y=0.0.
! References: Carter, 2000 and 2009 (the SAPRC-99 and SAPRC-07 documents),
! Tables 4 and 9 and Fig. S1.
! CH2=CH-CH2-CH3 + O3 = 0.5 (CH2OO* + CHO-CH2-CH3) + 0.5 (HCHO + CH3CH2CHOO*)
! = 0.5 (0.37 HCOOH [CH2OO] + 0.16 (OH + HO2) + 0.51 CO + 0.12 CO2
! + 0.5 [0.58 RCOOH (CH3CH2CHOO and others)
! + 0.42 {(OH) + (xCCHO + xCO + xHO2 + ROC2 + yROOH)}]
AL06) 3.36E-15 3.525 ;1-BUTENE + O3 = #.29 OH + #.08 HO2 +
#.255 CO + #.06 CO2 + #.5 HCHO + #.5 RCHO +
#.185 HCOOH + #.29 RCOOH +
#.21 {xCCHO + xCO + xHO2 + RO2C + yROOH}

A3 [alpha (0.5), OH (0.16)]
! Y(OH) = 0.16; alpha=0.5; x=0.16; y=0.0.
! References: Carter, 2000 and 2009 (the SAPRC-99 and SAPRC-07 documents),
! Table 9 and Fig. S1.
AL06) 3.36E-15 3.525 ;1-BUTENE + O3 = #.20 OH + #.08 HO2 +
#.255 CO + #.06 CO2 + #.5 HCHO + #.5 RCHO +
#.185 HCOOH + #.38 RCOOH +
#.12 {xCCHO + xCO + xHO2 + RO2C + yROOH}

B [alpha (0.5), OH (0.29)]
! Y(OH) = 0.29; alpha=0.5; x=0.28; y=0.5.
! References: Carter, 2000 and 2009 (the SAPRC-99 and SAPRC-07 documents);
! Tables 4 and 9 and Fig. S1.
AL06) 3.36E-15 3.525 ;1-BUTENE + O3 = #.29 OH + #.08 HO2 +
#.325 CO + #.06 CO2 + #.5 HCHO + #.5 RCHO +
#.185 HCOOH + #.36 RCOOH +
#.07 {CCHO + xCCHO + xCO + xHO2 + RO2C + yROOH}

C [alpha (0.65), OH (0.29)]
! Y(OH) = 0.29; alpha=0.65, x=0.360, y=0.0.
! References: Carter, 2000 and 2009 (the SAPRC-99 and SAPRC-07 documents);
! Rickard et al., 1999 for alpha = 0.65; Tables 4 and 9 and Fig. S1.
AL06) 3.36E-15 3.525 ;1-BUTENE + O3 = #.29 OH + #.056 HO2 +
#.234 {xHO2 + xCCHO + RO2C + yROOH + xCO} +
#.10 ALK1 + #.06 ETOH + #.239 CO + #.142 CO2 +
#.163 H2O + #.65 HCHO + #.35 RCHO +
#.13 HCOOH + #.256 RCOOH

D [alpha (0.65), OH (0.29)]
! Y(OH) = 0.29; alpha=0.65, x=0.288, y=0.25.
! References: Carter, 2000 and 2009 (the SAPRC-99 and SAPRC-07 documents),
! Rickard et al., 1999 for alpha = 0.65; Tables 4 and 9 and Fig. S1.
AL06) 3.36E-15 3.525 ;1-BUTENE + O3 = #.29 OH + #.056 HO2 +
#.140 {xHO2 + xCCHO + RO2C + yROOH + xCO} +

#.10 ALK1 + #.06 ETOH + #.285 CO + #.142 CO2 +
#.163 H2O + #.65 HCHO + #.35 RCHO +
#.13 HCOOH + #.303 RCOOH + #0.047 CCHO

B4. ADDITIONAL INFORMATION REGARDING BOX MODEL SIMULATIONS

In this study, the SAPRC software which allows users to modify their chemical mechanisms relatively conveniently was used as a box modeling tool, however, with settings for the "airshed" simulation instead of settings for the environmental chamber simulation (Carter, 2000 and 2009). Simulations were done by using measured inorganic and organic concentrations at 7:30 AM CST as initial conditions, estimated temperatures, water vapor pressures and mixing heights based on measurements, and no additional emissions (Tables B-1 and B-2).

Table B-1. Initial concentrations of hydrocarbons and inorganics used in box modeling[a]

Alkenes	Fixed	Extended	Other organics	Fixed/Extended
ethene	103.229	103.229	ACET	5.196
isoprene	0.385	0.385	ACETYLEN	4.695
OLE1[b]	95.635	0.166[f]	ALK1	39.183
Propene	-	90.468	ALK2	79.769
1-butene	-	3.513	ALK3	29.930
1-pentene	-	0.977	ALK4	42.381
1-hexene	-	0.310	ALK5	2.937
3-methyl-1-butene	-	0.201	ARO1	4.490
Sum (OLE1 alkenes)	95.635	95.635	ARO2	2.964
OLE2[c]	5.619	0.322[g]	BENZENE	1.896
2-methyl propene	-	0.658	HCHO	23.611
2-methyl-1-butene	-	0.466	CCHO	7.853
E-2-butene	-	0.206	RCHO	2.195
Z-2-butene	-	0.187	MEK	1.448
E-2-pentene	-	1.233	INERT	0.051
Z-2-pentene	-	0.662	Inorganics	Fixed/Extended
2-methyl-2-butene	-	1.100	O_3	10.000
2,3-dimethyl-2-butene	-	0.000	NO	38.170
cyclopentene	-	0.061	NO_2	53.755
Cyclohexene	-	0.000	CO	619.757
1,3-butadiene	-	0.725	PAN	0.373

Sum (OLE2 alkenes)	5.619	5.619	PAN2	0.070
TERP[d]	0.174	-	Constant species	Fixed/Extended
α-pinene	-	0.117	CH_4	1850[h]
d-limonene[e]	-	0.057	H_2	530[i]
Sum (terpenes)	0.174	0.174		

[a]For explanations of the SAPRC-07 model species names listed in this table, refer to Carter (2009). [b]OLE1 is a model species in SAPRC-07 representing alkenes (other than ethene) with their OH reaction rate constant (k(OH)) less than 4.74×10^{-11} molecule$^{-1}\cdot$cm$^3\cdot$sec^{-1} (7.0×10^4 ppm^{-1} min^{-1}). [C]OLE2 is a model species in SAPRC-07 representing alkenes with their k(OH) equal to or higher than 4.74×10^{-11} molecule$^{-1}\cdot$cm$^3\cdot$sec^{-1}. [d]TERP is a model species for terpenes such as α- and β-pinene. [e]The measured concentration of limonene was assumed to be the concentration of *d*-limonene. [f]Methyl acetylene was speciated as OLE1 according to the speciation rule defined in File SAPRC07L.LCC prepared Carter (http://www.engr.ucr.edu/~carter/SAPRC/files.htm). [g]Styrene was speciated as OLE2 according to the speciation rule defined in File SAPRC07L.LCC. [h]1.85 ppm CH_4 was used as in CAMx/CB-IV implemented in CAMx, (ENVIRON, 2008. Comprehensive Air Quality Model with Extensions (CAMx) User's Guide, Version 4.50, http://www.camx.com/files/CAMxUsersGuide_v4.5.pdf). [i]530 ppb H_2 was used according to a global average H_2 concentration of 530 ppb (P.C. Novelli et al., Journal of Geophysical Research 104 (D23), 30,427-30,444, 1999).

Table B-2. Meteorological conditions used in box modeling[a]

Time (CST)	Mixing height (meters)	Time (CST)	Temperature (Kelvin)
6:00	250	6:00	296.55
6:30	250	9:00	295.29
7:00	250	12:00	297.77
7:30	270	15:00	300.23
8:00	450	18:00	300.19
8:30	580		
9:00	660	Time (CST)	$[H_2O]$[b] (ppm)
9:30	740	6:00	27760
10:00	820	9:00	29757
10:30	900	12:00	23052
11:00	980	15:00	17034
11:30	1080	18:00	24558
12:00	1180		

[a]For details, refer to Chapter 9 of Faraji et al. (2007): Faraji, M., Heo, G., Kimura, Y., McDonald-Buller, E., Allen, D., Yarwood, G., Whitten, G., Carter, W., 2007. Comparison of the Carbon Bond and SAPRC photochemical mechanisms. Report to the Texas Commission on Environmental Quality, Work Order No. 582-04-65588-07, August, 2007. [b]Water vapor concentration.

Appendix C: Further Information for Chapter 5

- Appendix C1. Modification of CB05 to incorporate the chlorine mechanism of Tanaka et al. (2003).
- Appendix C2. Modification of SAPRC-07 to incorporate chlorine chemistry.

APPENDIX C1. MODIFICATION OF CB05 TO INCORPORATE THE CHLORINE MECHANISM OF TANAKA ET AL. (2003A)

Several modifications were made in the chlorine mechanism of Tanaka et al. (2003a) originally developed for use with CB-IV to be compatible with CB05. Additional 15 reactions were added to CB05-Base and CB05-UNClite and implemented in the SAPRC software. For CB05-Base and CB05-UNClite, refer to Chapter 3 and Appendix A.

Implementation of 15 additional reactions in the SAPRC software:

```
.UNITS=PPM
.UNITS=EA:DEGK
.RXN
!.................
! Original Chlorine mechanism in CB4 (Tanaka et al., 2003a; Mechanism 1 in CAMx)
!I97) PF=no2 FAC=.264       ;CL2              = #2.000 CL
!I98) PF=ispd FAC=143.      ;HOCL             = OH + CL
!I99) 2.8815e-11 260.       ;CL + O3        = CLO + O2
!I100) 6.1605e-12 -295.     ;CLO + NO     = CL + NO2
!I101) 4.5706e-13 -710.     ;CLO + HO2 = HOCL + O2
!I102) 6.3516e-11             ;CL + PAR    = HCL +    #0.870 XO2 +    #0.130 XO2N +    &
!                                 #0.110 RCHO + #0.760    ROR + #-0.110 PAR
!I103) 1.0478e-10 -504.     ;CL + OLE    = FMCL + RCHO + #2.000 XO2 + HO2 + &
!                                 #-1.000 PAR
!I104) 3.0100e+02 1240.     ;CL = HCL + XO2 + HCHO + HO2
!I105) 2.5597e-11 -411.     ;CL + ETH    = HCHO + #2.000 XO2 + FMCL + HO2
!I106) 4.4960e-10             ;CL + ISOP = #0.150 HCL + XO2 + HO2 + #0.280 ICL1
!I107) 1.8983e-11             ;OH + ICL1 = ICL2
!I108) 4.1962e-10             ;CL + BUTA = XO2 + HO2 + #0.700 BCL1
!I109) 3.5968e-11             ;OH + BCL1 = BCL2
!I110) 1.3405e-11 2000.     ;CLO + CLO = #0.300 CL2 + #1.400 CL
!.................
! Incorporation into CB05
I157) PF=NO2 FAC=.264       ;CL2              = #2.000 CL
! PF=ispd FAC=143 (in CB4-CL mechanism)
! PF=ACROX QY=3.60e-3 for ISPD + HV (rxn 148 in CB05UL3.RXN) as follows
!148) PF=ACROX QY=3.60e-3 ;ISPD + HV = #0.333 CO + #0.067 ALD2 + #0.9 FORM +
!                                 #0.832 PAR + #1.033 HO2 + #0.7 XO2 + #0.967 C2O3
! Therefore, PF=ACROX QY=3.60E-3*143 = 0.515
! (In CB4-CL) I158) PF=ispd FAC=143.      ;HOCL             = OH + CL
```

```
I158) PF=ACROX QY=.515      ;HOCL             = OH + CL
I159) 2.8815e-11 260.       ;CL + O3        = CLO + O2
I160) 6.1605e-12 -295.    ;CLO + NO    = CL + NO2
I161) 4.5706e-13 -710.    ;CLO + HO2 = HOCL + O2
! RCHO in Reaction CL + PAR and CL + OLE was renamed as ALD2
! (a model species for aldehydes in CB4)
I162) 6.3516e-11              ;CL + PAR    = HCL +    #0.870 XO2 +    #0.130 XO2N +    &
                                    #0.110 ALD2 + #0.760    ROR + #-0.110 PAR
I163) 1.0478e-10 -504.    ;CL + OLE    = FMCL + ALD2 + #2.000 XO2 + HO2 + &
                                    #-1.000 PAR
! HCHO in Reaction I164 and I165 was replaced by FORM.
I164) 3.0100e+02 1240.    ;CL = HCL + XO2 + FORM + HO2
I165) 2.5597e-11 -411.    ;CL + ETH    = FORM + #2.000 XO2 + FMCL + HO2
I166) 4.4960e-10              ;CL + ISOP = #0.150 HCL + XO2 + HO2 + #0.280 ICL1
I167) 1.8983e-11              ;OH + ICL1 = ICL2
I168) 4.1962e-10              ;CL + BUTA = XO2 + HO2 + #0.700 BCL1
I169) 3.5968e-11              ;OH + BCL1 = BCL2
I170) 1.3405e-11 2000.    ;CLO + CLO = #0.300 CL2 + #1.400 CL
! Reaction of IOLE with CL is approximated by reaction of OLE with CL:
I171) 1.0478e-10 -504.    ;CL + IOLE    = FMCL + ALD2 + #2.000 XO2 + HO2 + &
                                    #-1.000 PAR
.
```

APPENDIX C2. MODIFICATION OF SAPRC-07 TO INCORPORATE CHLORINE CHEMISTRY

18 reactions were added to SAPRC-07E described in Chapter 3 and Appendix B so that 18 additional alkenes could be modeled separately instead of being lumped as OLE1, OLE2 or TERP. Except for propene, the reactions of 17 alkenes with atomic chlorine (CL) were described by using (1) reaction OLE1 + CL for OLE1 alkenes, reaction OLE2 + CL for OLE2 alkenes, and (3) reaction TERP + CL for terpenes. One reaction for describing the reaction of isoprene with atomic chlorine was also slightly modified both in SAPRC-07F and SAPRC-07E to produce CMBO and CMBA separately from IPRD (a lumped model species in SAPRC-07). Then, additional reactions for describing decay of CMBO and CMBA were added. Details of the modifications are given below.

Implementation of 18 additional reactions in the SAPRC software:

```
!OLEnCL01 contains reaction of CL with 18 separately modeled alkenes
!(5 OLE1, 11 OLE2,2 TERP; for details, refer to Chapter 4; July 9, 2009 by G. Heo)
!Reactions of alkenes (OLE1, OLE2 and TERP alkenes) with CL
!Just used three reactions in SAPRC07B.RXN for all 17 alkenes except PROPENE
! : OLE1 + CL, OLE2 + CL, TERP + CL.
!For PROPENE + CL, reaction CH15 in CLCHMECH.RXN for PROPENE + CL was used.
!========================================================================
!OLE1 alkenes:
!1. PROPENE, 2. 1-BUTENE, 3. 1-PENTEN, 4. 1-HEXENE, 5. 3M-1-BUT,
!OLE2 alkenes:
!6. ISOBUTEN, 7. 2M-1-BUT, 8. T-2-BUTE, 9. C-2-BUTE, 10. 2M-2-BUT, 11. T-2-PENT, 12. C-2-PENT,
!13. CYC-PNTE, 14. 13-BUTDE, 15. 23M2-BUT, 16. CYC-HEXE
! TERP alkenes:
!17. A-PINENE, 18. D-LIMONE.
! Source: \CLCHMECH.RXN of Carter (http://www.engr.ucr.edu/~carter/SAPRC/files.htm) for PROPENE + CL
!CH15) 2.67e-10 0.000 0.00       ;PROPENE + CL = #.124 HCL + #.971 RO2C +
!                                    #.029 RO2XC + #.029 zRNO3 + #.971 xHO2 +
!                                    #.124 xMACR + #.306 xCLCCHO + #.540 xCLACET +
!                                    yROOH + #.098 XC
! Source: SAPRC07B.RXN
!CL06) 3.55e-10                  ;OLE1 + CL = #.902 xHO2 + #1.42 RO2C +
!                                    #.098 RO2XC + #.098 zRNO3 + #.308 HCL +
```

```
!                                  #.025 xHCHO + #.146 xCCHO + #.051 xRCHO +
!                                  #.188 xMACR + #.014 xMVK + #.027 xIPRD +
!                                  #.225 xCLCCHO + #.396 xCLACET + #.413 yROOH +
!                                  #.587 yR6OOH + #1.361 XC
!CL07) 3.83e-10                   ;OLE2 + CL = #.447 xHO2 + #.448 xCL + #.001 xMEO2 +
!                                  #1.514 RO2C + #.104 RO2XC + #.104 zRNO3 +
!                                  #.263 HCL + #.228 xHCHO + #.361 xCCHO +
!                                  #.3 xRCHO + #.081 xACET + #.04 xMEK +
!                                  #.049 xMACR + #.055 xMVK + #.179 xIPRD +
!                                  #.012 xCLCCHO + #.18 xCLACET + #.357 yROOH +
!                                  #.643 yR6OOH + #.247 XC
!CL10) 5.46e-10                   ;TERP + CL = #.252 xHO2 + #.068 xCL +
!                                  #.034 xMECO3 + #.05 xRCO3 + #.016 xMACO3 +
!                                  #2.258 RO2C + #.582 RO2XC + #.582 zRNO3 +
!                                  #.548 HCL + #.035 xCO + #.158 xHCHO +
!                                  #.185 xRCHO + #.274 xACET + #.007 xGLY +
!                                  #.003 xBACL + #.003 xMVK + #.158 xIPRD +
!                                  #.006 xAFG1 + #.006 xAFG2 + #.001 xAFG3 +
!                                  #.109 xCLCCHO + yR6OOH + #3.543 XC
!
.UNITS=PPM
.RXN
!------------------
!OLE1 alkenes:
!1. PROPENE,
CL21) 2.67e-10 0.000 0.00         ;PROPENE + CL = #.124 HCL + #.971 RO2C +
                                   #.029 RO2XC + #.029 zRNO3 + #.971 xHO2 +
                                   #.124 xMACR + #.306 xCLCCHO + #.540 xCLACET +
                                   yROOH + #.098 XC
!2. 1-BUTENE,
CL22) 3.55e-10                    ;1-BUTENE + CL = #.902 xHO2 + #1.42 RO2C +
                                   #.098 RO2XC + #.098 zRNO3 + #.308 HCL +
                                   #.025 xHCHO + #.146 xCCHO + #.051 xRCHO +
                                   #.188 xMACR + #.014 xMVK + #.027 xIPRD +
                                   #.225 xCLCCHO + #.396 xCLACET + #.413 yROOH +
                                   #.587 yR6OOH + #1.361 XC
!3. 1-PENTEN,
CL23) 3.55e-10                    ;1-PENTEN + CL = #.902 xHO2 + #1.42 RO2C +
                                   #.098 RO2XC + #.098 zRNO3 + #.308 HCL +
                                   #.025 xHCHO + #.146 xCCHO + #.051 xRCHO +
                                   #.188 xMACR + #.014 xMVK + #.027 xIPRD +
                                   #.225 xCLCCHO + #.396 xCLACET + #.413 yROOH +
                                   #.587 yR6OOH + #1.361 XC
!4. 1-HEXENE,
CL24) 3.55e-10                    ;1-HEXENE + CL = #.902 xHO2 + #1.42 RO2C +
                                   #.098 RO2XC + #.098 zRNO3 + #.308 HCL +
                                   #.025 xHCHO + #.146 xCCHO + #.051 xRCHO +
                                   #.188 xMACR + #.014 xMVK + #.027 xIPRD +
                                   #.225 xCLCCHO + #.396 xCLACET + #.413 yROOH +
                                   #.587 yR6OOH + #1.361 XC
!5. 3M-1-BUT,
CL25) 3.55e-10                    ;3M-1-BUT + CL = #.902 xHO2 + #1.42 RO2C +
                                   #.098 RO2XC + #.098 zRNO3 + #.308 HCL +
                                   #.025 xHCHO + #.146 xCCHO + #.051 xRCHO +
                                   #.188 xMACR + #.014 xMVK + #.027 xIPRD +
                                   #.225 xCLCCHO + #.396 xCLACET + #.413 yROOH +
                                   #.587 yR6OOH + #1.361 XC
!OLE2 alkenes:
!6. ISOBUTEN,
CL26) 3.83e-10                    ;ISOBUTEN + CL = #.447 xHO2 + #.448 xCL +
```

```
                    #.001 xMEO2 +
                    #1.514 RO2C + #.104 RO2XC + #.104 zRNO3 +
                    #.263 HCL + #.228 xHCHO + #.361 xCCHO +
                    #.3 xRCHO + #.081 xACET + #.04 xMEK +
                    #.049 xMACR + #.055 xMVK + #.179 xIPRD +
                    #.012 xCLCCHO + #.18 xCLACET + #.357 yROOH +
                    #.643 yR6OOH + #.247 XC
!7. 2M-1-BUT,
CL27) 3.83e-10      ;2M-1-BUT + CL = #.447 xHO2 + #.448 xCL +
                    #.001 xMEO2 +
                    #1.514 RO2C + #.104 RO2XC + #.104 zRNO3 +
                    #.263 HCL + #.228 xHCHO + #.361 xCCHO +
                    #.3 xRCHO + #.081 xACET + #.04 xMEK +
                    #.049 xMACR + #.055 xMVK + #.179 xIPRD +
                    #.012 xCLCCHO + #.18 xCLACET + #.357 yROOH +
                    #.643 yR6OOH + #.247 XC
!8. T-2-BUTE,
CL28) 3.83e-10      ;T-2-BUTE + CL = #.447 xHO2 + #.448 xCL +
                    #.001 xMEO2 +
                    #1.514 RO2C + #.104 RO2XC + #.104 zRNO3 +
                    #.263 HCL + #.228 xHCHO + #.361 xCCHO +
                    #.3 xRCHO + #.081 xACET + #.04 xMEK +
                    #.049 xMACR + #.055 xMVK + #.179 xIPRD +
                    #.012 xCLCCHO + #.18 xCLACET + #.357 yROOH +
                    #.643 yR6OOH + #.247 XC
!9. C-2-BUTE,
CL29) 3.83e-10      ;C-2-BUTE + CL = #.447 xHO2 + #.448 xCL +
                    #.001 xMEO2 +
                    #1.514 RO2C + #.104 RO2XC + #.104 zRNO3 +
                    #.263 HCL + #.228 xHCHO + #.361 xCCHO +
                    #.3 xRCHO + #.081 xACET + #.04 xMEK +
                    #.049 xMACR + #.055 xMVK + #.179 xIPRD +
                    #.012 xCLCCHO + #.18 xCLACET + #.357 yROOH +
                    #.643 yR6OOH + #.247 XC
!10. 2M-2-BUT,
CL30) 3.83e-10      ;2M-2-BUT + CL = #.447 xHO2 + #.448 xCL +
                    #.001 xMEO2 +
                    #1.514 RO2C + #.104 RO2XC + #.104 zRNO3 +
                    #.263 HCL + #.228 xHCHO + #.361 xCCHO +
                    #.3 xRCHO + #.081 xACET + #.04 xMEK +
                    #.049 xMACR + #.055 xMVK + #.179 xIPRD +
                    #.012 xCLCCHO + #.18 xCLACET + #.357 yROOH +
                    #.643 yR6OOH + #.247 XC
!11. T-2-PENT,
CL31) 3.83e-10      ;T-2-PENT + CL = #.447 xHO2 + #.448 xCL +
                    #.001 xMEO2 +
                    #1.514 RO2C + #.104 RO2XC + #.104 zRNO3 +
                    #.263 HCL + #.228 xHCHO + #.361 xCCHO +
                    #.3 xRCHO + #.081 xACET + #.04 xMEK +
                    #.049 xMACR + #.055 xMVK + #.179 xIPRD +
                    #.012 xCLCCHO + #.18 xCLACET + #.357 yROOH +
                    #.643 yR6OOH + #.247 XC
!12. C-2-PENT,
CL32) 3.83e-10      ;C-2-PENT + CL = #.447 xHO2 + #.448 xCL +
                    #.001 xMEO2 +
                    #1.514 RO2C + #.104 RO2XC + #.104 zRNO3 +
                    #.263 HCL + #.228 xHCHO + #.361 xCCHO +
                    #.3 xRCHO + #.081 xACET + #.04 xMEK +
                    #.049 xMACR + #.055 xMVK + #.179 xIPRD +
                    #.012 xCLCCHO + #.18 xCLACET + #.357 yROOH +
```

```
                    #.643 yR6OOH + #.247 XC
!13. CYC-PNTE,
CL33) 3.83e-10      ;CYC-PNTE + CL = #.447 xHO2 + #.448 xCL +
                    #.001 xMEO2 +
                    #1.514 RO2C + #.104 RO2XC + #.104 zRNO3 +
                    #.263 HCL + #.228 xHCHO + #.361 xCCHO +
                    #.3 xRCHO + #.081 xACET + #.04 xMEK +
                    #.049 xMACR + #.055 xMVK + #.179 xIPRD +
                    #.012 xCLCCHO + #.18 xCLACET + #.357 yROOH +
                    #.643 yR6OOH + #.247 XC
!14. 13-BUTDE,
CL34) 3.83e-10      ;13-BUTDE + CL = #.447 xHO2 + #.448 xCL +
                    #.001 xMEO2 +
                    #1.514 RO2C + #.104 RO2XC + #.104 zRNO3 +
                    #.263 HCL + #.228 xHCHO + #.361 xCCHO +
                    #.3 xRCHO + #.081 xACET + #.04 xMEK +
                    #.049 xMACR + #.055 xMVK + #.179 xIPRD +
                    #.012 xCLCCHO + #.18 xCLACET + #.357 yROOH +
                    #.643 yR6OOH + #.247 XC
!15. 23M2-BUT
CL35) 3.83e-10      ;23M2-BUT + CL = #.447 xHO2 + #.448 xCL +
                    #.001 xMEO2 +
                    #1.514 RO2C + #.104 RO2XC + #.104 zRNO3 +
                    #.263 HCL + #.228 xHCHO + #.361 xCCHO +
                    #.3 xRCHO + #.081 xACET + #.04 xMEK +
                    #.049 xMACR + #.055 xMVK + #.179 xIPRD +
                    #.012 xCLCCHO + #.18 xCLACET + #.357 yROOH +
                    #.643 yR6OOH + #.247 XC
!16. CYC-HEXE
CL36) 3.83e-10      ;CYC-HEXE + CL = #.447 xHO2 + #.448 xCL +
                    #.001 xMEO2 +
                    #1.514 RO2C + #.104 RO2XC + #.104 zRNO3 +
                    #.263 HCL + #.228 xHCHO + #.361 xCCHO +
                    #.3 xRCHO + #.081 xACET + #.04 xMEK +
                    #.049 xMACR + #.055 xMVK + #.179 xIPRD +
                    #.012 xCLCCHO + #.18 xCLACET + #.357 yROOH +
                    #.643 yR6OOH + #.247 XC
! TERP alkenes:
!17. A-PINENE,
CL37) 5.46e-10      ;A-PINENE + CL = #.252 xHO2 + #.068 xCL +
                    #.034 xMECO3 + #.05 xRCO3 + #.016 xMACO3 +
                    #2.258 RO2C + #.582 RO2XC + #.582 zRNO3 +
                    #.548 HCL + #.035 xCO + #.158 xHCHO +
                    #.185 xRCHO + #.274 xACET + #.007 xGLY +
                    #.003 xBACL + #.003 xMVK + #.158 xIPRD +
                    #.006 xAFG1 + #.006 xAFG2 + #.001 xAFG3 +
                    #.109 xCLCCHO + yR6OOH + #3.543 XC
!18. D-LIMONE,
CL38) 5.46e-10      ;D-LIMONE + CL = #.252 xHO2 + #.068 xCL +
                    #.034 xMECO3 + #.05 xRCO3 + #.016 xMACO3 +
                    #2.258 RO2C + #.582 RO2XC + #.582 zRNO3 +
                    #.548 HCL + #.035 xCO + #.158 xHCHO +
                    #.185 xRCHO + #.274 xACET + #.007 xGLY +
                    #.003 xBACL + #.003 xMVK + #.158 xIPRD +
                    #.006 xAFG1 + #.006 xAFG2 + #.001 xAFG3 +
                    #.109 xCLCCHO + yR6OOH + #3.543 XC

.
```

Modifications related to CMBO and CMBA and implementation in the SAPRC software:

```
!==========Reactions for CMBO and CMBA
! CBMO and CMBA are approxmiated by IPRD
!1. following footnote 19 of Table A-5 of Carter (2009),
! replace 0.671 xIRPD by 0.272 xIPRD + 0.221 CMBO + 0.178 CMBA in SAPRC07B.RXN of Carter
! (http://www.engr.ucr.edu/~carter/SAPRC/files.htm).
! I am not sure if I have to use xIPRD or IPRD,
!but in presence of significant NOx, either would be ok.
!2. to model the decay of CMBO and CMBA,
!    use the four reactions of IPRD (BP64 - BP67 in Table A-2 of Carter (2009).
!CE03) 4.80e-10                  ;ISOPRENE + CL = #.15 HCL + #1.168 RO2C +
!                                   #.085 RO2XC + #.085 zRNO3 + #.738 xHO2 +
!                                   #.177 xCL + #.275 xHCHO + #.177 xMVK +
!                                   #.671 xIPRD + #.067 xCLCCHO + yR6OOH + #.018 XC
CE03) 4.80e-10                  ;ISOPRENE + CL = #.15 HCL + #1.168 RO2C +
                                   #.085 RO2XC + #.085 zRNO3 + #.738 xHO2 +
                                   #.177 xCL + #.275 xHCHO + #.177 xMVK +
                                   #.272 xIPRD + #.221 CMBO + #.178 CMBA +
                                   #.067 xCLCCHO + yR6OOH + #.018 XC
!==========addition of reactions for CMBO and CMBA
CL11) 6.19e-11                  ;CMBO + OH = #.289 MACO3 + #.67 {RO2C + xHO2} +
                                   #.041 {RO2XC + zRNO3} + #.336 xCO + #.055 xHCHO +
                                   #.129 xCCHO + #.013 xRCHO + #.15 xMEK +
                                   #.332 xPROD2 + #.15 xGLY + #.174 xMGLY +
                                   #-0.504 XC + #.711 yR6OOH
CL12) 4.18e-18                  ;CMBO + O3 = #.285 OH + #.4 HO2 + #.048 {RO2C +
                                   xRCO3} + #.498 CO + #.14 CO2 + #.124 HCHO +
                                   #.21 MEK + #.023 GLY + #.742 MGLY + #.1 HCOOH +
                                   #.372 RCOOH + #.047 xCCHO + #.001 xHCHO +
                                   #.048 yR6OOH + #-.329 XC
CL13) 1.00e-13                  ;CMBO + NO3 = #.15 {MACO3 + HNO3} + #.799 {RO2C +
                                   xHO2} + #.051 {RO2XC + zRNO3} + #.572 xCO +
                                   #.227 xHCHO + #.218 xRCHO + #.008 xMGLY +
                                   #.572 xRNO3 + #.85 yR6OOH + #.278 XN + #-.815 XC
CL14) PF=MACR-06                 ;CMBA + HV = #1.233 HO2 + #.467 MECO3 + #.3 RCO3 +
                                   #1.233 CO + #.3 HCHO + #.467 CCHO + #.233 MEK +
                                   #-.233 XC
CL15) 6.19e-11                  ;CMBA + OH = #.289 MACO3 + #.67 {RO2C + xHO2} +
                                   #.041 {RO2XC + zRNO3} + #.336 xCO + #.055 xHCHO +
                                   #.129 xCCHO + #.013 xRCHO + #.15 xMEK +
                                   #.332 xPROD2 + #.15 xGLY + #.174 xMGLY +
                                   #-0.504 XC + #.711 yR6OOH
CL16) 4.18e-18                  ;CMBA + O3 = #.285 OH + #.4 HO2 + #.048 {RO2C +
                                   xRCO3} + #.498 CO + #.14 CO2 + #.124 HCHO +
                                   #.21 MEK + #.023 GLY + #.742 MGLY + #.1 HCOOH +
                                   #.372 RCOOH + #.047 xCCHO + #.001 xHCHO +
                                   #.048 yR6OOH + #-.329 XC
CL17) 1.00e-13                  ;CMBA + NO3 = #.15 {MACO3 + HNO3} + #.799 {RO2C +
                                   xHO2} + #.051 {RO2XC + zRNO3} + #.572 xCO +
                                   #.227 xHCHO + #.218 xRCHO + #.008 xMGLY +
                                   #.572 xRNO3 + #.85 yR6OOH + #.278 XN + #-.815 XC
CL18) PF=MACR-06                 ;CMBA + HV = #1.233 HO2 + #.467 MECO3 + #.3 RCO3 +
                                   #1.233 CO + #.3 HCHO + #.467 CCHO + #.233 MEK +
                                   #-.233 XC
.
```

Bibliography

Alicke, B., Geyer, A., Hofzumahaus, A., Holland, F., Konrad, S., Pätz, H.W., Schäfer, J., Stutz, J., Volz-Thomas, A., Platt, U., 2003. OH formation by HONO photolysis during the BERLIOZ experiment. Journal of Geophysical Research 108(D4), 8247, doi:10.1029/2001JD000579.

Alicke, B., Platt, U., Stutz, J., 2002. Impact of nitrous acid photolysis on the total hydroxyl radical budget during the Limitation of Oxidant Production/Pianura Padana Produzione di Ozono study in Milan. Journal of Geophysical Research 107(D22), 8196, doi:10.1029/2000JD000075.

Anderson, R.S., Huang, L., Iannone, R., Rudolph, J. 2007a. Laboratory measurements of the $^{12}C/^{13}C$ kinetic isotope effects in the gas-phase reactions of unsaturated hydrocarbons with Cl atoms at 298±3 K. Journal of Atmospheric Chemistry 56, 275-291.

Anderson, R.S., Huang, L., Iannone, R., Rudolph, J. 2007b. Measurements of the $^{12}C/^{13}C$ kinetic isotope effects in the gas-phase reactions of light alkanes with chlorine atoms. Journal of Physical Chemistry A 111, 495-504.

Andino, J. M., Smith, J. N., Flagan, R. C., Goddard III, W. A., and Seinfeld, J. H.: Mechanism of atmospheric photooxidation of aromatics: A theoretical study, Journal of Physical Chemistry 100, 10 967–10 980, 1996.

Andino J.M., Vivier-Bunge, A., 2008. Tropospheric chemistry of aromatic compounds emitted from anthropogenic sources. Advances in Quantum Chemistry: Applications of Theoretical Methods to Atmospheric Science 55, 297-310.

Arey, J., Obermeyer, G., Aschmann, S.M., Chattopadhyay, S., Cusick, R.D., Atkinson, R., 2009. Dicarbonyl products of the OH radical-initiated reaction of a series of aromatic hydrocarbons. Environmental Science & Technology 43, 683-689.

Ariya, P.A., Sander, R., Crutzen, P.J., 2000. Significance of HOx and peroxides production due to alkene ozonolysis during fall and winter: A modeling study. Journal of Geophysical Research-Atmospheres 105(D14), 17,721-17,738.

Aschmann, S.M., Arey, J., Atkinson, R., 2002. OH radical formation from the gas-phase reactions of O_3 with a series of terpenes. Atmospheric Environment 36, 4347-4355.

Atkinson, R., 1997. Gas-phase tropospheric chemistry of volatile organic compounds: 1. Alkanes and alkenes. Journal of Physical and Chemical Reference Data 26, 215-290.

Atkinson, R., 2000. Atmospheric chemistry of VOCs and NOx. Atmospheric Environment 34, 2063-2101.

Atkinson, R., Arey, J., 2003. Atmospheric degradation of volatile organic compounds. Chemical Reviews 103, 4605-4638.

Atkinson, R., Aschmann, S.M., Arey, J., Shorees, B., 1992. Formation of OH radicals in the gas phase reactions of O_3 with a series of terpenes. Journal of Geophysical Research-Atmospheres 97(D5), 6065-6073.

Atkinson, R., Baulch, D.L., Cox, R.A., Crowley, J.N., Hampson, R.F., Hynes, R.G., Jenkin, M.E., Rossi, M.J., Troe, J., 2006. Evaluated kinetic and photochemical data for atmospheric chemistry: Volume II – gas phase reactions of organic species. Atmospheric Chemistry and Physics 6, 3625-4055. (http://www.atmos-chem-phys.net/6/3625/2006/)

Bierbach, A., Barnes, I., Becker, K.H., Wiesen, E., 1994. Atmospheric chemistry of unsaturated carbonyls: Butendial, 4-oxo-2-pentenal, 3-hexene-2,5-dione, maleic anhydride, 3*H*-furan-2-one, and 5-methyl-3H-furan-2-one. Environmental Science & Technology 28, 715-729.

Bloss, C., Wagner, V., Bonzanini, A., Jenkin, M.E., Wirtz, K., Martin-Reviejo, M., Pilling, M.J., 2005a. Evaluation of detailed aromatic mechanisms (MCMv3 and MCMv3.1) against environmental chamber data. Atmospheric Chemistry and Physics 5, 623-639. (http://www.atmos-chem-phys.net/5/623/2005/acp-5-623-2005.pdf)

Bloss, C., Wagner, V., Jenkin, M.E., Volkamer, R., Bloss, W.J., Lee, J.D., Heard, D.E., Wirtz, K., Martin-Reviejo, M., Rea, G., Wenger, J.C., Pilling, M.J., 2005b. Developments of a detailed chemical mechanism (MCMv3.1) for the atmospheric oxidation of aromatic hydrocarbons. Atmospheric Chemistry and Physics 5, 641-664. (http://www.atmos-chem-phys.net/5/641/2005/acp-5-641-2005.pdf)

Bohn, B., 2001. Formation of peroxy radicals from OH-toluene adducts and O_2. Journal of Physical Chemistry A 105, 6092-6101.

Calvert, J. G., Atkinson, R., Becker, K.H., Kamens, R.M., Seinfeld, J.H., Wallington, T.J., Yarwood, G., 2002. The Mechanisms of Atmospheric Oxidation of Aromatic Hydrocarbons, Oxford University Press, New York, 566p.

Calvert, J. G., R. Atkinson, R., J. A. Kerr, J.A., S. Madronich, S., G. K. Moortgat, G.K., T. J. Wallington, T.J., Yarwood, G., 2000. The Mechanisms of Atmospheric Oxidation of Alkenes, Oxford University Press, New York, 552p.

Carter, W.P.L., 2000. Documentation of the SAPRC-99 chemical mechanism for VOC reactivity assessment, Report to the California Air Resources Board, Contracts 92-329 and 95-308. (http://www.engr.ucr.edu/~carter/absts.htm#saprc99)

Carter, W.P.L., 2004. Evaluation of a gas-phase atmospheric reaction mechanism for low NOx conditions. Final Report to California Air Resources Board Contract No. 01-305, May 5. (http://www.engr.ucr.edu/~carter/absts.htm#lnoxrpt).

Carter, W.P.L., 2009. Development of the SAPRC-07 chemical mechanism and updated ozone reactivity scales. Final Report to the California Air Resources Board Contract No. 03-318, March 20. (http://www.engr.ucr.edu/~carter/SAPRC/)

Carter, W.P.L., Atkinson, R., 1987. An experimental study of incremental hydrocarbon reactivity. Environmental Science & Technology 21, 670-679.

Carter, W.P.L., Atkinson, R., Winer, A.M., Pitts, J.N., 1982. Experimental investigation of chamber-dependent radical sources. International Journal of Chemical Kinetics 14, 1071-1103.

Carter, W.P.L., Cocker, D.R., Fitz, D.R., Malkina, I.L., Bumiller, K., Sauer, C.G., Pisano, J.T., Bufalino, C., and Song, C., 2005. A new environmental chamber for evaluation of gas-phase chemical mechanisms and secondary aerosol formation. Atmospheric Environment, 39, 7768-7788.

Carter, W.P.L., Luo, D., Malkina, I.L., Fitz, D., 1995a. The University of California, Riverside Environmental Chamber Data Base for Evaluating Oxidant Mechanism. Indoor Chamber Experiments through 1993. Report submitted to the U. S. Environmental Protection Agency, EPA/AREAL, Research Triangle Park, NC, March 20. Available at http://www.engr.ucr.edu/~carter/pubs/.

Carter, W.P.L., Luo, D., Malkina, I.L., Pierce, J.A., 1995b. Environmental chamber studies of atmospheric reactivities of volatile organic compounds. Effects of varying chamber and light source. Final Report to National Renewable Energy Laboratory, Contract XZ-2-12075, Coordinating Research Council, Inc., Project M-9, California Air Resources Board, Contract A032-0692, and South Coast Air Quality Management District, Contract C91323, March 26. Available at http://www.cert.ucr.edu/~carter/absts.htm#explrept.

Carter, W.P.L., Lurmann, F.W., 1991. Evaluation of a detailed gas-phase atmospheric reaction mechanism using environmental chamber data. Atmospheric Environment 25A, 2771-2806.

Carter, W.P.L., Pierce, J.A., Luo, D., Malkina, I.L., 1995. Environmental chamber study of maximum incremental reactivities of volatile organic compounds. Atmospheric Environment 29, 2499-2511.

Carter, W.P.L., Winer, A.M., Pitts, J.N., 1981a. Major atmospheric sink for phenol and the cresols: Reaction with the nitrate radical. Environmental Science & Technology 15(7), 829-831.

Carter, W. P. L., Winer, A. M., Pitts Jr., J. N., 1981b. Effect of peroxy acetyl nitrate on the initiation of photochemical smog. Environmental Science & Technology 15(7), 831-834.

Chang, S., McDonald-Buller, E., Kimura, Y., Yarwood, G., Neece, J., Russell, M., Tanaka, P., Allen, D., 2002. Sensitivity of urban ozone formation to chlorine emission estimates. Atmospheric Environment 36, 4991-5003.

Chen, S., Ren, X., Mao, J., Chen, Z., Brune, W.H., Lefer, B., Rappenglück, B., Flynn, J., Olson, J., Crawford, J.H., 2009. A comparison of chemical mechanisms based on TRAMP-2006 field data, Atmospheric Environment (2009), doi: 10.1016/j.atmosenv.2009.05.027.

Clemitshaw, K. C., 2003. Hydroxyl Radical, in: Holton, J.R., Pyle, J.A., Curry, J.A., (Eds.), Encyclopedia of Atmospheric Sciences, Elsevier, Amsterdam, 2403-2411.

Coquet, S., Ariya, P.A., 2000. Kinetics of the gas-phase reactions of Cl atom with selected C_2–C_5 unsaturated hydrocarbons at 283 < T < 323 K. International Journal of Chemical Kinetics 32, 478-484.

Darnall, K.R., Atkinson, R., Pitts, J.N., 1979. Observation of biacetyl from the reaction of OH radicals with o-xylene. Evidence for ring cleavage. Journal of Physical Chemistry 83(15), 1943-1946.

Dasgupta, P.K., Li., J., Zhang, G., Luke, W.T., McClenny, W. A., Stutz, J., Fried, A., 2005. Summertime ambient formaldehyde in five U.S. metropolitan areas: Nashville, Atlanta, Houston, Philadelphia, and Tampa. Environmental Science & Technology 39, 4767-4783.

Daum, P. H., Kleinman, L.I., Springston, S.R., Nunnermacker, L.J., Lee, Y.-N., Weinstein-Lloyd, J., Zheng, J., Berkowitz, C.M., 2003. A comparative study of O_3 formation in the Houston urban and industrial plumes during the 2000 Texas Air Quality Study. Journal of Geophysical Research-Atmospheres 108(D23), 4715, doi:10.1029/2003JD003552.

Daum, P. H., Kleinman, L.I., Springston, S.R., Nunnermacker, L.J., Lee, Y.-N., Weinstein-Lloyd, J., Zheng, J., Berkowitz, C.M., 2003. Origin and properties of plumes of high ozone observed during the Texas 2000 Air Quality Study

(TexAQS 2000). Journal of Geophysical Research-Atmospheres 109, D17306, doi:10.1029/2003JD004311.

Dodge, M.C., 2000. Chemical oxidant mechanisms for air quality modeling: critical review. Atmospheric Environment 34, 2103-2130.

Donahue, N.M., Kroll, J.H., Anderson, J.G., Demerjian, K.L., 1998. Direct observation of OH production from the ozonolysis of olefins. Geophysical Research Letters 25(1), 59-62.

Ehhalt, D.H., 1999. Photooxidation of trace gases in the troposphere. Physical Chemistry Chemical Physics 1, 5401-5408.

ENVIRON, 2008. Comprehensive Air Quality Model with Extensions (CAMx) User's Guide, Version 4.50, http://www.camx.com/files/CAMxUsersGuide_v4.5.pdf.

Eom, I.-Y., Li, Q., Li, J., Dasgupta, P.K., 2008. Robust hybrid flow analyzer for Formaldehyde. Environmental Science & Technology 42, 1221-1226.

Ezell, M.J., Wang, W., Ezell, A.A., Soskin, G., Finlayson-Pitts, B.J., 2002. Kinetics of reactions of chlorine atoms with a series of alkenes at 1 atm and 298 K: Structure and reactivity. Physical Chemistry Chemical Physics 4, 5813-5820.

Faloona, I., Tan, D., Brune, W., Hurst, J., Barket, D., Couch, T.L., Shepson, P., Apel, E., Riemer, D., Thornberry, T., Carroll, M.A., Sillman, S., Keeler, G.J., Sagady, J., Hooper, D., Paterson, K., 2001. Nighttime observations of anomalously high levels of hydroxyl radicals above a deciduous forest canopy. Journal of Geophysical Research-Atmospheres 106(D20), 24,315-24,333.

Faloona, I.C., Tan, D., Lesher, R.L., Hazen, N.L., Frame, C.L., Simpas, J.B., Harder, H., Martinez,M., Di Carlo, P., Ren, X., Brune, W.H., 2004. A laser induced fluorescence instrument for detecting tropospheric OH and HO_2: characteristics and calibration. Journal of Atmospheric Chemistry 47, 139–167.

Faraji, M., Heo, G., Kimura, Y., McDonald-Buller, E., Allen, D., Yarwood, G., Whitten, G., Carter, W. 2007. Comparison of the Carbon Bond and SAPRC photochemical mechanisms. Report to the Texas Commission on Environmental Quality, Work Order No. 582-04-65588-07.

Faraji, M., Kimura, Y., McDonald-Buller, E., Allen, D., 2008. Comparison of the carbon bond and SAPRC photochemical mechanisms under conditions relevant to southeast Texas. Atmospheric Environment 42, 5821-5836.

Fenske, J.D., Kuwata, K.T., Houk, K.N., Paulson, S.E., 2000. OH radical yields from the ozone reaction with cycloalkenes. Journal of Physical Chemistry A 1004, 7246-7254.

Finlayson-Pitts, B. J., Keoshian, C.J., Buehler, B., Ezell, A.A., 1999. Kinetics of reaction of chlorine atoms with some biogenic organics. International Journal of Chemical Kinetics 31, 491-499.

Finlayson-Pitts, B.J., Pitts, J.N., 1997. Tropospheric air pollution: Ozone, airborne toxics, polycyclic aromatic hydrocarbons, and particles. Science 276 (May 16), 1045-1052.

Finlayson-Pitts, B.J., Pitts, J.N., 2000. Chemistry of the Upper and Lower Atmosphere: Theory, Experiments, and Applications, Academic Press, San Diego, 969p.

Forstner, H.J.L., Flagan, R.C., Seinfeld, J.H., 1997. Secondary organic aerosol from the photooxidation of aromatic hydrocarbons: Molecular composition. Environmental Science & Technology 31, 1345-1358.

Gery, M.W., Whitten, G.Z., and Killus, J.P., Dodge, M.C., 1989. A photochemical kinetics mechanism for urban and regional scale computer modeling. Journal of Geophysical Research 94(D10), 12,925-12,956.

Geyer, A., Alike, B., Ackermann, R., Martinez, M., Harder, H., Brune, W., Di Carlo, P., Williams, E., Jobson, T., Hall, S., Shetter, R., Stutz, J., 2003. Direct observations of daytime NO_3: Implications for urban boundary layer chemistry. Journal of Geophysical Research 108(D12), 4368, doi:10.1029/2002JD002967.

Gilman, J.B., Kuster, W.C., Goldan, P.D., Herndon, S.C., Zahniser, M.S., Tucker, S.C., Brewer, W.A., Lerner, B.M., Williams, E.J., Harley, R.A., Fehsenfeld, F.C., Warneke, C., de Gouw, J.A., 2009. Measurements of volatile organic compounds during the 2006 TexAQS/GoMACCS campaign: Industrial influences, regional characteristics, and diurnal dependencies of the OH reactivity. Journal of Geophysical Research-Atmospheres 114, D00F06, doi:10.1029/2008JD011525.

Goldstein, A.H., McKay, M., Kurpius, M.R., Schade, G.W., Lee, A., Holzinger, R., Rasmussen, R.A., 2004. Forest thinning experiment confirms ozone deposition to forest canopy is dominated by reaction with biogenic VOCs. Geophysical Research Letters 31, L22106, doi:10.1029/2004GL021259.

Gómez Alvarez, E., Viidanoja, J., Muñoz, A., Wirtz, K., Hjorth, J., 2007. Experimental confirmation of the dicarbonyl route in the photo-oxidation of toluene and benzene. Environmental Science & Technology 41, 8362-8369.

Heard, D.E., Carpenter, L.J., Creasey, D.J., Hopkins, J.R., Lee, J.D., Lewis, A.C., Pilling, M.J., Seakins, P.W., 2004. High levels of the hydroxyl radical in the winter urban troposphere. Geophysical Research Letters 31, L18112, doi:10.1029/2004GL020544.

Heo, G., Kimura, Y., McDonald-Buller, E., Allen, D.T., Yarwood, G., Whitten, G.Z., 2009. Evaluation of a new toluene mechanism for Carbon Bond 05 using environmental chamber data and ambient data. Presented at the 102nd Annual Conference of the Air and Waste Management Association, June 16-19, 2009, Detroit, MI. (Abstract of this paper (Paper AB-2b.154) is available at http://www.conferencearchives.com/awma/2009/abstracts/AB-2b.154_a.html).

Hess, G.D., Carnovale, F., Cope, M.E., Johnson, G.M., 1992. The evaluation of some photochemical smog reaction mechanisms - I. Initial composition effects. Atmospheric Environment 26A, 625-641.

Hov, O., 1985. The effect of chlorine on the formation of photochemical oxidants in southern Telemark, Norway. Atmospheric Environment 19, 471–485.

Hu, D., Tolocka, M., Li, Q., Kamens, R.M., 2007. A kinetic mechanism for predicting secondary organic aerosol formation from toluene oxidation in the presence of NOx and natural sunlight. Atmospheric Environment 41, 6478–6496

Jeffries, H., Kessler, M., 1999. A User's Guide to MEval Solver Program for Morphoecule Mechanisms, a Part of Morpho, University of North Carolina, Chapel Hill, NC. (A short description on Morpho is available at http://airchem.sph.unc.edu/Research/Products/Software/Morpho/default.htm.)

Jenkin, M.E., Clemitshaw, K.C., 2000. Ozone and other secondary photochemical pollutants: chemical processes governing their formation in the planetary boundary layer. Atmospheric Environment 34, 2499-2527.

Jobson, B. T., Berkowitz, C. M., Kuster, W. C., Goldan, P. D., Williams, E. J., Fesenfeld, F. C., Apel, E. C., Karl, T., Lonneman, W. A., Riemer, D., 2004. Hydrocarbon source signatures in Houston, Texas: Influence of the petrochemical industry. Journal of Geophysical Research 109, D24305, doi:10.1029/2004JD004887.

Johnson, D., Marston, G., 2008. The gas-phase ozonolysis of unsaturated volatile organic compounds in the troposphere. Chemical Society Reviews 37, 699-716.

Johnson, D., Raoult, S., Lesclaux, R., Krasnoperov, L.N., 2005. UV absorption spectra of methyl-substituted hydroxyl-cyclohexadienyl radicals in the gas phase. Journal of Photochemistry and Photobiology A: Chemistry 176, 98-106.

Karl, T., Jobson, T., Kuster, W.C., Williams, E., Stutz, J., Shetter, R., Hall, S.R., Goldan, P., Fehsenfeld, F., W. Lindinger, W., 2003. Use of proton transfer-reaction mass spectrometry to characterize volatile organic compound sources at the La Porte super site during the Texas Air Quality Study. Journal of Geophysical Research 108(D16), 4508, doi:10.1029/2002JD003333.

Kenley, R.A., Davenport, J.E., Hendry, D.G., 1981. Products and pathways for the reaction of OH with aromatic hydrocarbons. Journal of Physical Chemistry 85(19), 2740-2746.

Killus, J.P., Whitten, G.Z., 1982. A mechanism describing the photochemical oxidation of toluene in smog. Atmospheric Environment 16(8), 1973-1988.

Killus, J. P., Whitten, G. Z., 1990. Background reactivity in smog chambers. International Journal of Chemical Kinetics, 22, 547-575.

Kimura, Y., Allen, D.T., 2008. Application of mechanism-independent photochemical cycles analysis tool (pyIrr) to evaluate the effect of changes in temperature, isoprene concentrations and insolation on regional photochemistry using CB05, SAPRC99 and SAPRC07 mechanisms. Presented at the second International Conference on Atmospheric Chemical Mechanisms, Unversity of California at Davis, December 10 – 12, 2008.

Klotz, B.G., Bierbach, A., Barnes, I., Becker, K.H., 1995. Kinetic and mechanistic study of atmospheric chemistry of muconaldehydes. Environmental Science & Technology 29, 2322-2332.

Klotz, B., Sørensen, S., Barnes, I., Becker, K.H., Etzkorn, T., Volkamer, R., Platt, U., Wirtz, K., Martín-Reviejo, M., 1998. Atmospheric oxidation of toluene in a large-volume outdoor photoreactor: In situ determination of ring-retaining product yields. Journal of Physical Chemistry A 102, 10289-10299.

Knispel, R., Koch, R., Siese, M., Zetzsch, C., 1990. Adduct formation of OH radicals with benzene, toluene, and phenol and consecutive reactions of the adducts with NOx and O_2. Berichte Der Bunsen-Gesellschaft-Physical Chemistry Chemical Physics 94(11), 1375-1379.

Koch, R., Knispel, R., Elend, M., Siese, M., Zetzsch, C., 2007. Consecutive reactions of aromatic-OH adducts with NO, NO_2 and O_2: benzene, naphthalene, toluene, m- and p-xylene, hexamethylbenzene, phenol, m-cresol and aniline. Atmospheric Chemistry and Physics 7, 2057-2071. (http://www.atmos-chem-phys.net/7/2057/2007/)

Kovacs, T.A., Brune, W.H., Harder, H., Martinez, M., Simpas, J.B., Frost, G.J., Williams, E., Jobson, T., Stroud, C., Young, V., Fried, A., Wert, B., 2003. Direct measurements of urban OH reactivity during Nashville SOS in summer 1999. Journal of Environmental Monitoring 5, 68–74, doi:10.1039/b204339d.

Kukui, A., Le Bras, G., 2001. Theoretical study of the thermal decomposition of several β-chloroalkoxy radicals. Physical Chemistry and Chemical Physics 3, 175-178.

Kuster, W.C., Jobson, B.T., Karl, T., Riemer, D., Apel, E., Goldan, P.D., Fehsenfeld, F.C., 2004. Intercomparison of volatile organic carbon measurement techniques and data at La Porte during the TexAQS2000 Air Quality study. Environmental Science & Technology, 38, 221-228.

Li, J., Dasgupta, P.K., Luke, W., 2004. Measurement of gaseous and aqueous trace formaldehyde: Revisiting the pentanedione reaction and field applications. Analytica Chimica Acta 531, 51-68.

Lindinger, W., Hansel, A., Jordan, A., 1998. On-line monitoring of volatile organic compounds at pptv levels by means of Proton-Transfer-Reaction Mass Spectrometry (PTR-MS): Medical applications, food control and environmental research. International Journal of Mass Spectrometry and Ion Processes, 173, 191-241.

Liu, X., Jeffries, H.E., Sexton, K.G., 1999. Atmospheric photochemical degradation of 1,4-unsaturated dicarbonyls. Environmental Science & Technology 33, 4212-4220.

Luecken, D.J., Phillips, S., Sarwar, G., Jang, C., 2008. Effects of using the CB05 vs. SAPRC99 vs. CB4 chemical mechanism on model predictions: Ozone and gas-phase photochemical precursor concentrations. Atmospheric Environment 42, 5805-5820.

Kuwata, K.T., Hasson, A.S., Dickinson, R.V., Peterson, E.B., Valin, L.C., 2005. Quantum chemical and master equation simulations of the oxidation and isomerization of vinoxy radicals. Journal of Physical Chemistry A 109, 2514-2524.

Kuwata, K.T., Templeton, K.L., Hasson, A.S., 2003. Computational studies of the chemistry of syn acetaldehyde oxide. Journal of Physical Chemistry A 107, 11,525-11,532.

Mao, J., Ren, X., Chen, S., Brune, W.H., Chen, Z., Martinez, M., Harder, H., Lefer, B., Rappenglück, Flynn, J., Leuchner, M., 2009. Atmospheric oxidation capacity in the summer of Houston 2006: Comparison with summer measurements in other metropolitan studies. Atmospheric Environment (2009), doi:10.1016/j.atmosenv.2009.01.013.

Markert, F., Pagsberg, P., 1993. UV spectra and kinetics of radicals produced in the gas phase reactions of Cl, F and OH with toluene. Chemical Physics Letters 209, 445-454.

Martinez, M., Harder, H., DiCarlo, P., Brune, W.H., Hall, S.R., Shetter, R.E., Williams, E.J., Kuster, W., Jobson, B.T., 2002. OH and HO_2 concentrations, production and loss rates at the La Porte site during TexAQS 2000. Presented at the fourth

Conference on Atmospheric Chemistry of the American Meteorological Society, Orlando, January 2002. Available at http://ams.confex.com/ams/annual2002/techprogram/paper_32451.htm.

Martinez, M., Harder, H., Kovacs, T.A., Simpas, J.B., Bassis, J., Lesher, R., Brune, W.H., Frost, G.J., Williams, E.J., Stroud, C.A., Jobson, B.T., Roberts, J.M., Hall, S.R., Shetter, R.E., Wert, B., Fried, A., Alicke, B., Stutz, J., Young, V.L., White, A.B., Zamora, R.J., 2003. OH and HO_2 concentrations, sources, and loss rates during the Southern Oxidants Study in Nashiville, Tennessee, summer 1999. Journal of Geophysical Research 108(D19), 4617, doi:10.1029/2003JD003551.

Meng, Z., Dabdub, D., Seinfeld, J.H., 1997. Chemical coupling between atmospheric ozone and particulate matter. Science 277 (July 4), 116-119.

Molina, M.J., Zhang, R., Broekhuizen, K., Lei, W., Navarro, R., Molina, L.T., 1999. Journal of American Chemical Society 121, 10,225-10,226.

Murphy, C. F., Allen, D.T., 2005. Hydrocarbon emissions from industrial release events in the Houston-Galveston area and their impact on ozone formation. Atmospheric Environment 39, 3785-3798.

Nakayama, T., Takahashi, K., Matsumi, Y., Toft, A., Anderson, M.P.S., Nielsen, O.J., Waterland, R.L., Buck, R.C., Hurley, M.D., Wallington, T.J., 2007. Atmospheric chemistry of $CF_3CH{=}CH_2$ and $C_4F_9CH{=}CH_2$: Products of the gas-phase reactions with Cl atoms and OH radicals. Journal of Physical Chemistry A 111, 909-915.

Neeb, P., Moortgat, G.K., 1999. Formation of OH radicals in the gas-phase reaction of propene, isobutene, and isoprene with O_3: Yields and mechanistic implications. Journal of Physical Chemistry A 103, 9003-9012.

Niki, H., Maker, P.D., Savage, C.M., Breitenbach, L.P., Hurley, M.D., 1987. FTIR spectroscopic study of the mechanism for the gas-phase reaction between ozone and tetramethylethylene. Journal of Physical Chemistry 91, 941-946.

Nordmeyer, T., W. Wang, M. L. Ragains, B. J. Finlayson-Pitts, C. W. Spicer, and R. A. Plastridge, 1997. Unique products of the reaction of isoprene with atomic chlorine: Potential markers of chlorine atom chemistry. Geophysical Research Letters 24(13), 1615-1618.

Orlando, J.J., Tyndall, G.S., Apel, E.C., Riemer, D.D., Paulson, S.E., 2003. Rate coefficients and mechanisms of the reaction of Cl-atoms with a series of unsaturated hydrocarbons under atmospheric conditions. International Journal of Chemical Kinetics 35(8), 334-353.

Orlando, J.J., Tyndall, G.S., Bilde, M., Ferronato, C., Wallington, T.J., Vereecken, L., Peeters, J., 1998. Laboratory and theoretical study of the oxy radicals in the OH-

and Cl-initiated oxidation of ethene. Journal of Physical Chemistry A 102, 8116-8123.

Orzechowska, G.E., Paulson, S.E., 2002. Production of OH radicals from the reactions of C_4-C_6 internal alkenes and styrenes with ozone in the gas phase. Atmospheric Environment 36, 571-581.

Osthoff, H.D., Roberts, J.M., Ravishankara, A.R., Williams, E.J., Lerner, B.M., Sommariva, R., Bates, T.S., Coffman, D., Quinn, P.K., Dibb, J.E., Stark, H., Burkholder, J.B., Talukdar, R.K., Meagher, J., Fehsenfeld, F.C., Brown, S.S., 2008. High levels of nitryl chloride in the polluted subtropical marine boundary layer. Nature Goescience 1, 324-328.

Oum, K.W., Lakin, M.J., DeHaan, D.O., Brauers, T., Finlayson-Pitts, B.J., 1998. Formation of molecular chlorine from the photolysis of ozone and aqueous sea-salt particles. Science 297, 74-77.

Paulson, S.E., Chung, M.Y., Hasson, A.S., 1999. OH radical formation from the gas-phase reaction of ozone with terminal alkenes and the relationship between structure and mechanism. Journal of Physical Chemistry A 103, 8125-8138.

Paulson, S.E., Flagan, R.C., Seinfeld, J.H., 1992a. Atmospheric photo-oxidation of isoprene: part I. The hydroxyl radical and ground state atomic oxygen reactions. International Journal of Chemical Kinetics 24, 79–101.

Paulson, S.E., Flagan, R.C., Seinfeld, J.H., 1992b. Atmospheric photooxidation of isoprene. 2. The ozone-isoprene reaction. International Journal of Chemical Kinetics 24(1), 103-125.

Paulson, S.E., Orlando, J.J., 1996. The reactions of ozone with alkenes: An important source of HOx in the boundary layer. Geophysical Research Letters 23, 3727-3730.

Perry, R.A., Atkinson, R., Pitts, J.N., 1977. Kinetics and mechanism of the gas phase reaction of hydroxyl radicals with aromatic hydrocarbons over the temperature range 296-473 K. Journal of Physical Chemistry 81(4), 296-304.

Platt, U., Perner, D., Harris, G.W., Winer, A.M., Pitts, J.N., Jr, 1980. Observations of nitrous acid in an urban atmosphere by differential optical absorption. Nature (London) 285, 312-314.

Ragains, M.L.; Finlayson-Pitts, B.J., 1997. Kinetics and mechanism of the reaction of Cl atoms with 2-methyl-1,3-butadiene (isoprene). Journal of Physical Chemistry A 101, 1509-1517.

Rappenglück, B., Lefer, B., 2007. TRAMP data analysis and radical chemistry study, final report to Houston Advanced Research Center (HARC), TERC project H86, December 2007. (Available at http://files.harc.edu/Projects/AirQuality/Projects/H086/H086FinalReport.pdf)

Ren, X., Harder, H., Martinez, M., Lesher, R.L., Oliger, A., Shirley, T., Adams, J., Simpas, J.B., Brune, W.H., 2003a. HOx concentrations and OH reactivity observations during the PMTACS-NY 2001 campaign in New York City. Atmospheric Environment 37, 3627–3637.

Ren, X., Harder, H., Martinez, M., Lesher, R.L., Oliger, A., Simpas, J.B., Brune, W.H., Schwab, J.J., Demerjian, K.L., He, Y., Zhou, X., Gao, H., 2003b. OH and HO_2 chemistry in the urban atmosphere of New York City. Atmospheric Environment 37, 3639-3651.

Ren, X., Mao, J., Kang, E., Metcalf, A.R., Mitchell, M., Lesher, R.L., Shirley, T., Brune, W.H., Carter, W.P., Tonnesen, G., Chien, C., Fitz, D., Malkina, I., Sauer, C., Bumiller, K., Bufalino, C., 2004. Behavior of the hydroxyl and hydroperoxy radicals in a smog chamber study, EOS Trans. AGU, 85(47), Fall Meet. Suppl., Abstract A53C-0908. (http://www.agu.org/meetings/fm04/fm04-sessions/fm04_A53C.html)

Rickard, A.R., Johnson, D., McGill, C.D., Marston, G., 1999. OH yields in the gas-phase reactions of ozone with alkenes. Journal of Physical Chemistry A 103, 7656–7664.

Riemer, D. D.; Apel, E. C.,2001. Confirming the presence and extent of oxidation by Cl in the Houston, Texas urban area using specific isoprene oxidation products as tracers. Final report to the Texas Natural Resource Conservation Commission, Contract 582034743, University of Miami, FL. (Available at http://www.tceq.state.tx.us/assets/public/implementation/air/am/contracts/reports/oth/ConfirmingPresenceandExtentOfOxidationByCI.pdf)

Roberts, J. M., Flocke, F., Stroud, C.A., Hereid, D., Williams, E.J., Fehsenfeld, F.C., Brune, W., Martinez, M., Harder, H., 2002. Ground-based measurements of PANs during the 1999 Southern Oxidants Study Nashville intensive. Journal of Geophysical Research 107(D21), 4554, doi:10.1029/2001JD000947.

Roberts, J.M., Jobson, B.T., Kuster, W., Goldan, P., Murphy, P., Williams, E., Frost, G., Riemer, D., Apel, E., Stroud, C., Wiedinmyer, C., Fehsenfeld, F., 2003. An examination of the chemistry of peroxycarboxylic nitric anhydrides and related volatile organic compounds during Texas Air Quality Study 2000 using ground-based measurements. Journal of Geophysical Research 108(D16), 4495, doi:10.1029/2003JD003383.

Rohrer, F., Bohn, B., Brauers, T., Brüning, D., Johnen, F.-J., Wahner, A., Kleffmann, J., 2005. Characterisation of the photolytic HONO-source in the atmosphere simulation chamber SAPHIR. Atmospheric Chemistry and Physics 5, 2189–2201.

Russell, A., Dennis, R., 2000. NARSTO critical review of photochemical models and modeling. Atmospheric Environment 34, 2283-2324.

Ryerson, T.B., Trainer, M., Angevine, W.M., Brock, C.A., Dissly, R.W., Fehsenfeld, F.C., Frost, G.J., Goldan, P.D., Holloway, J.S., Hubler, G., Jakoubek, R.O., Kuster, W.C., Neuman, J.A., Nicks Jr., D. K., Parrish, D.D., Roberts, J.M., Sueper, D.T., Atlas, E.L., Donnelly, S.G., Flocke, F., Fried, A., Plotter, W.T., Schauffler, S., Stroud, V., Weinheimer, A.J., Wert, B.P., Wiedinmyer, C., 2003. Effect of petrochemical industrial emissions of reactive alkenes and NOx on tropospheric ozone formation in Houston, Texas. Journal of Geophysical Research-Atmospheres 108(D8), 4249, doi:10.1029/2002JD003070.

Sander, S.P., Orkin, V.L., Kurylo, M.J., Golden, D.M., Huie, R.E., Kolb, C.E., Finlayson-Pitts, B.J., Molina, M.J., Friedl, R.R., Ravishankara, A.R., Moortgat, G. K., Keller-Rudek, H., Wine, P.H., 2006. Chemical Kinetics and Photochemical Data for Use in Atmospheric Studies, Evaluation Number 15. NASA Jet Propulsion Laboratory. February. Available at http://jpldataeval.jpl.nasa.gov/download.html.

Seinfeld, J.H., Pandis, S.N., 1998. Atmospheric Chemistry and Physics: From Air Pollution to Climate Change, Wiley-Interscience, New York, 1326p.

Shetter, R.E., Müller, M., 1999. Photolysis frequency measurements using actinic flux spectroradiometry during the PEM-Tropics mission: Instrumentation description and some results. Journal of Geophysical Research 104(D5), 5647-5661.

Shi, J.C., Bernhard, M.J.,1997. Kinetic studies of Cl-atom reactions with selected aromatic compounds using the photochemical reactor-FTIR spectroscopy technique. International Journal of Chemical Kinetics 29, 349-358.

Siese, M., Becker, K.H., Brockmann, K.J., Geiger, H., Hofzumahaus, A., Holland, F., Mihelcic, D., Wirtz, K., 2001. Direct measurement of OH radicals from ozonolysis of selected alkenes: A EUPHORE simulation chamber study. Environmental Science & Technology 35, 4660-4667.

Simonaitis, R., Meagher, J., Bailey, E.M., 1997. Evaluation of the condensed Carbon Bond Mechanism against smog chamber data at low VOC and NOx Concentrations. Atmospheric Environment 31, 27–43.

Smith, D.F., McIver, C.D., Kleindienst, T.E., 1998. Primary product distribution from the reaction of hydroxyl radicals with toluene at ppb NOx mixing ratios. Journal of Atmospheric Chemistry 30, 209-228.

Sokolov, O.; Hurley, M. D.; Wallington, T. J.; Kaiser, E. W.; Platz, J.; Nielsen. O. J.; Berho, F.; Rayez, M.-T.; Lesclaux, R., 1998. Kinetics and mechanism of the gas-phase reaction of Cl atoms with benzene. Journal of Physical Chemistry A 102, 10671-10681.

Stutz, J., Alicke, B., Ackermann, R., Geyer, A., Wang, S., White, A.B., Williams, E.J., Spicer, C.W., Fast, J.D., 2004a. Relative humidity dependence of HONO chemistry in urban areas. Journal of Geophysical Research 109, D03307, doi:10.1029/2003JD004135.

Stutz, J., Alicke, B., Ackermann, R., Geyer, A., White, A., Williams, E., 2004b. Vertical profiles of NO_3, N_2O_5, O_3, and NOx in the nocturnal boundary layer: 1. Observations during the Texas Air Quality Study 2000, Journal of Geophysical Research 109, D12306, doi:10.1029/2003JD004209.

Suh, I., Zhang, D., Zhang, R.Molina, L.T., Molina, M.J., 2002. Theoretical study of OH addition reaction to toluene. Chemical Physics Letters 364, 454-462.

Suh, I., Zhang, R., Molina, L.T., Molina, M.J., 2003. Oxidation mechanism of aromatic peroxy and bicyclic radicals from OH-toluene reactions. Journal of American Chemical Society 125, 12,655-12,665.

Suh, I., Zhao, J., Zhang, R., 2006. Unimolecular decomposition of aromatic bicylic alkoxy radicals and their acyclic radicals. Chemical Physics Letters 432, 313-320.

Tanaka, P.L., Oldfield, S., Neece, J.D., Mullins, C.B., Allen, D.T., 2000. Anthropogenic sources of chlorine and ozone formation in urban atmospheres. Environmental Science & Technology 34, 4470-4473.

Tanaka, P. L., D. T. Allen, and C. B. Mullins, 2003a. An environmental chamber investigation of chlorine-enhanced ozone formation in Houston, Texas. Journal of Geophysical Research, 108(D18), 4576, doi:10.1029/2002JD003314.

Tanaka, P.L.; Riemer, D.D.; Chang, S.; Yarwood, G.; McDonald-Buller, E.C.; Apel, E.C.; Orlando, J.J.; Silva, P.J.; Jimenez, J.L.; Canagaratna, M.R.; Neece, J.D.; Mullins, C.B.; Allen, D.T., 2003b. Direct evidence for chlorine-enhanced urban ozone formation in Houston, Texas. Atmospheric Environment 37, 1393-1400.

Tang, Y., Zhu, L., 2005. Photolysis of butenedial at 193, 248, 280, 308, 351, 400, and 450 nm. Chemical Physics Letters 409, 151-156.

Thomas, R., Smith, J., Jones, M., MacKay, J., Jarvie, J., 2008. Emissions modeling of specific highly reactive volatile organic compounds (HRVOC) in the Houston-Galveston-Brazoria ozone nonattainment area. Presented at the 17th Annual International Emission Inventory Conference: Inventory Evolution – Portal to

Improved Air Quality, Portland, Oregon, June 2-5, 2008. Available at http://www.epa.gov/ttn/chief/conference/ei17/session6/thomas.pdf.

Ullerstam, M., Evert Ljungström and Langer, S., 2000. Reactions of acrolein, crotonaldehyde and pivalaldehyde with Cl atoms: structure-activity relationship and comparison with OH and NO_3 reactions. Physical Chemistry Chemical Physics 3, 986-992.

Volkamer, R., Platt, U., Wirtz, K., 2001. Primary and secondary glyoxal formation from aromatics: Experimental evidence for the bicycloalkyl-radical pathway from benzene, toluene, and p-xylene. Journal of Physical Chemistry A 105, 7865-7874.

Volkamer, R., Spietz, P., Burrows, J., Platt, U., 2005. High-resolution absorption cross-section of glyoxal in the UV-vis and IR spectral ranges. Journal of Photochemistry and Photobiology A: Chemistry 172, 35-46.

Wang, L., Arey, J., Atkinson, R., 2005. Reactions of chlorine atoms with a series of aromatic hydrocarbons. Environmental Science & Technology 39, 5302-5310.

Wang, W., Finlayson-Pitts, B.J., 2000. 4-Chlorocrotonaldehyde as a unique chlorine-containing compound from the reaction of atomic chlorine with 1,3-butadiene in air at room temperature. Geophysical Research Letters 27(7), 947– 950.

Wert, B.P., Trainer, M., Fried, A., Ryerson, T.B., Henry, B., Potter, W., Angevine, W.M., Atlas, E., Donnelly, S.G., Fehsenfeld, F.C., Frost, G.J., Goldan, P.D., Hansel, A., Holloway, J.S., Hubler, G., Kuster, W.C., Nicks Jr., D.K., Neuman, J.A., Parrish, D.D., Schauffler, S., Stutz, J., Sueper, D.T., Wiedinmyer, C., Wisthaler, A., 2003. Signatures of terminal alkene oxidation in airborne formaldehyde measurements during TexAQS 2000, Journal of Geophysical Research 108(D3), 4104, doi:10.1029/2002JD002502.

Whitten, G. Z., 1983. The chemistry of smog formation: A review of current knowledge. Environmental International 9, 447-463.

Whitten, G.Z., Heo, G., Kimura, Y., McDonald-Buller, E., Allen, D.T., Yarwood, G., 2009. A new condensed toluene mechanism for Carbon Bond. Submitted for publication in *Atmospheric Environment*.

Whitten, G.Z., Hogo, H., Killus, J.P., 1980. The carbon-bond mechanism: A condensed kinetic mechanism for photochemical smog. Environmental Science & Technology 14, 690-700.

Williams, E.J., Fehsenfeld, F.C., Jobson, B.T., Kuster, W.C., Goldan, P.D., Stutz, J., McClenny, W.A., 2006. Comparison of Ultraviolet Absorbance, Chemiluminescence, and DOAS Instruments for Ambient Ozone Monitoring. Environmental Science & Technology 40(18), 5755 – 5762.

Xiang, B., Zhu, L., Tang, Y., 2007. Photolysis of 4-oxo-2-pentenal in the 190-460 nm region. Journal of Physical Chemistry A 111(37), 9025-9033.

Yarwood, G., Peng, N., Niki, H., 1992. FTIR spectroscopic study of the Cl-atom and Br-atom initiated oxidation of ethene. International Journal of Chemical Kinetics 24(4), 369-383.

Yarwood, G., Rao, S., Yocke, M., Whitten, G.Z., 2005. Updates to the Carbon Bond mechanism: CB05. Report to the U.S. Environmental Protection Agency, December 2005. (http://www.camx.com/publ/pdfs/CB05_Final_Report_120805.pdf)

Yu, J., Jeffries, H.E., Sexton, K.G., 1997. Atmospheric photooxidation of alkylbenzenes-I. Carbonyl product analyses. Atmospheric Environment 31(5), 2261-2280.

Zádor, J., Turányi, T., Wirtz, K., Pilling, M.J. (2006). Measurement and investigation of chamber radical sources in the European Photoreactor (EUPHORE). Journal of Atmospheric Chemistry 55, 147-166.

Vita

Gookyoung Heo was born as the youngest of his parents in a small town in the southern region of The Republic of Korea (South Korea) where his father was a teacher. He attended the GyeongSang National University High School in Jinju. In 1992, he started his college studies at the Seoul National University (SNU) in Seoul and completed his obligatory military service after serving 26 months before he obtained his Bachelor of Science degree in Chemistry in 1999 and his Master's degree in City Planning (specialty in Environmental Planning) under supervision of Prof. Jung Wk Kim in 2001 from SNU. He also worked with Prof. Dong Soo Lee and Prof. Dowon Lee at SNU. In 2001, he worked with Dr. Byoung-Cheol Choi at the Applied Meteorological Research Lab, the Meteorological Research Institute where he modified the HYSPLIT model of ARL, NOAA for prediction of Asian dust events in Korea. In 2003, he started his Ph.D. studies under supervision of Prof. David T. Allen in the Environmental and Water Resources Engineering program, the University of Texas at Austin. He worked with Dr. Greg Yarwood, Dr. Gary Z. Whitten and Dr. William P.L. Carter while evaluating chemical mechanisms used in air quality models.

Permanent address: 33-1 CheongWon-ri, Jisu-myeon, Jinju, GyeongSangNam-do
660-892, The Republic of Korea

This dissertation was typed by the author.